

# **Delineation of Molecular Mechanisms Underlying the Pathobiology of ALK- positive Anaplastic Large-cell Lymphoma**

by

Chengsheng Wu

A thesis submitted in partial fulfillment of the requirements for the degree of

Doctor of Philosophy

Medical Sciences - Laboratory Medicine and Pathology  
University of Alberta

© Chengsheng Wu, 2017

## **Abstract**

ALK-positive anaplastic large-cell lymphoma (ALK+ALCL) is a rare type non-Hodgkin lymphoma of null/T cell origin, preferentially occurs in children and young adults. Approximately 85% of ALK+ALCL patients carry the gene translocation  $t(2;5)(p23;q35)$ , which results in the generation of the chimeric protein — NPM-ALK, a key oncogenic driver of this disease. NPM-ALK interacts and activates a wide range of molecules, including STAT3, ERK1/2, and PI3K, thus triggering the cell proliferation and anti-apoptotic effects. In this thesis, I further explored the molecular mechanisms of the pathobiology of ALK+ALCL from different perspectives, and hypothesized that the pathobiology of ALK+ALCL, such as tumorigenicity, chemoresistance and cancer stemness, can be attributed to novel NPM-ALK—regulated biochemical defects as well as signaling pathways that are not directly linked to NPM-ALK.

STAT1 is generally considered as a tumor suppressor and reported to antagonize STAT3 transcriptional activity in some cell models. However, the biological function of STAT1 has not been studied in ALK+ALCL. This study firstly reported that STAT1 expression is decreased in ALK+ALCL cell lines and patient samples; and NPM-ALK is directly responsible for the downregulation of STAT1, as it promotes STAT1 phosphorylation at Y701 and, thereby, downregulates STAT1 in a STAT3-dependent proteasome pathway. Furthermore, results showed that STAT1, if overexpressed to a

relatively high level, functions as a potent tumor suppressor in ALK+ALCL by attenuating STAT3 transcriptional activity and inducing the expression of IFN $\gamma$  which further activates the STAT1 signaling.

The Lai lab previously unearthed two distinct cell populations in ALK+ALCL cell lines that are differentially responding to a Sox2 reporter, with cells responsive to the reporter (RR) being more tumorigenic and chemoresistant than cells unresponsive to the reporter (RU). Although Sox2 is implicated in the RU/RR dichotomy, the expression level of Sox2 is not different between RU and RR cells, suggesting the involvement of other factor(s). This study reported that MYC is one of the key factors in the RU/RR dichotomy, as it is highly expressed in RR cells as compared to RU cells. The high level of MYC was firstly reported to promote Sox2 DNA binding and its transcriptional activity in RR cells. More evidence suggested that it is the highly active Wnt/ $\beta$ -catenin pathway in RR cells that confers to the high expression of MYC. The transcriptionally active Sox2 in RR cells in return upregulates the Wnt/ $\beta$ -catenin pathway, which thereafter promotes the expression of MYC, thus forming a positive forward loop. In conclusion, the positive forward loop involving the Wnt/ $\beta$ -catenin/MYC/Sox2 axis defines a highly tumorigenic small cell population in ALK+ALCL.

The molecular mechanisms underlining tumor plasticity, especially in hematological malignance, is not fully understood. This study reported that H<sub>2</sub>O<sub>2</sub>, a potent oxidative

stress inducer, can convert a fraction of RU cells derived from ALK+ALCL cells to RR cells (converted RR cells), supporting the existence of tumor plasticity in hematological malignancy. The converted RR cells have adopted the RR cells' phenotypes ( including chemoresistance to doxorubicin, a widely used chemotherapeutic drug for ALK+ALCL patients, clonogenicity and sphere-forming ability) and biochemical features (the increased expression of Wnt/ $\beta$ -catenin/MYC and Sox2 downstream targets). Similar biological changes were observed in RR cells upon oxidative challenge. Furthermore, more evidence showed that the activated Wnt/ $\beta$ -catenin/MYC/Sox2 axis upon oxidative stress is required for the RU to RR cells conversion since pharmacological inhibition of  $\beta$ -catenin/MYC or siRNA knockdown of Sox2 significantly abrogated the conversion. In conclusion, this study has demonstrated a novel experimental model in which acquisition of tumorigenicity and cancer stem-like features can be induced by oxidative stress in ALK+ALCL, a hematologic malignancy, through the activation of Wnt/ $\beta$ -catenin/MYC/Sox2 axis.

Overall, characterization of these molecular mechanisms underlying the tumorigenesis of ALK+ALCL has furthered the understanding of the pathobiology of this disease and also provided potential therapeutic targets for ALK+ALCL patients that are less responsive or resistance to conventional chemotherapy.

## **Preface**

This thesis represents collaborative work, led by Dr. Raymond Lai at the University of Alberta. The patient samples were obtained and diagnosed at Cross Cancer Institute, University of Alberta, Edmonton, Alberta, Canada, and the use of these patient samples for research has received research ethics approval at Feb 17<sup>th</sup> of 2016, by the Human Research Ethics Board at the University of Alberta (Study title: Study of biology of ALK in human ALK+ cancers, with approval number: Pro00062737). The animal studies in this thesis have also received ethical approval by the Animal Care and Use Committee (ACUC) at Dec 10<sup>th</sup> of 2015 (Study title: Mouse models for development of antitumor therapies, approval number: AUP00000782).

### **Chapter 2 of this thesis has been published as:**

Wu C, Molavi O, Zhang H, Gupta N, Alshareef A, Bone K, Gopal K, Wu F, Lewis J, Douglas D, Kneteman N, and Lai R. STAT1 is phosphorylated and down-regulated by the oncogenic tyrosine kinase NPM-ALK in ALK-positive anaplastic large-cell lymphoma. *Blood*. 2015.126:336-345. I was first author of this paper. I prepared the first draft and revisions based on the suggestions and comments of the co-authors. I designed and performed most of the experiments described herein, except for the following: O.M. performed some studies, data shown in Figure 2.1A and Figure 2.4F-G; H.Z., N.G., A.A., and F.W. performed portions of the experiments and provided technical support and intellectual input. K.B. provided SupM2 and Karpas 299 cell lines that were stably transfected with Tet on system. N.G., K.G., J.L, D.D., and N.K. were responsible for the animal study design, conducting euthanization of the SCID mouse and data analysis. R.L. provided numerous comments and final review of the manuscript before it was submitted for publication.

**Chapter 3 of this thesis has been published as:**

Wu C, Zhang H, Gupta N, Alshareef A, Wang Q, Huang Y, Lewis JT, Douglas DN, Kneteman NM, and Lai R. A positive feedback involving the Wnt/ $\beta$ -catenin/MYC/Sox2 axis defines a highly tumorigenic cell subpopulation in ALK-positive anaplastic large-cell lymphoma. *Journal of Hematology and Oncology*, 2016.9(1):120. I was first author of this paper. I prepared the first draft and revisions based on the suggestions and comments of the co-authors. I designed and performed most of the experiments described herein, except for the following: N.G. performed the CHIP-qPCR experiment and data analysis, shown in Figure 3.4E; A.A. performed the Wnt signaling pathway PCR array and data analysis, shown in Figure 3.6; H.Z., Q.W. and Y.H. have contribution to the Figure 3.3C and Figure 3.11A. H.Z., N.G. and A.A. also provided significant intellectual input. J.L., D.D., and N.K. were responsible for the animal study design, conducting euthanization of the SCID mouse and data analysis. R.L. provided numerous comments and final review of the manuscript before it was submitted for publication.

**Chapter 4 of this thesis has been prepared for submission as:**

Wu C, Gupta N, Zhang H, Huang Y, and Lai R. Oxidative stress promotes the tumorigenicity in ALK-positive anaplastic large-cell lymphoma by activating the Wnt/ $\beta$ -catenin/MYC/Sox2 axis. In preparation. I was first author of this paper, I prepared the first draft and revisions based on the suggestions and comments of the co-authors. I designed and performed all the experiments in this study. N.G., H.Z., and Y.H. contributed to Figure 4.3A, provided technical assistance and intellectual input. R.L. provided numerous comments and final review of the manuscript.

## **Acknowledgements**

I wish to express my sincere gratitude to the following individuals without whom this thesis would not be possible.

Foremost, my sincerest thanks to my supervisor, Dr. Raymond Lai, for his scientific training and guidance throughout the PhD program. He taught me how to critical think and also, most importantly, ignited my passion for science. Without his supervision, I would not have gotten this work done or have current achievements.

I would like to thank my committee members Dr. Yangxin Fu and Dr. Robert Ingham for their constant mentorship, support and comments throughout my whole doctoral program, as well as their suggestions with respect to the content of this thesis. Here I would like again to express my sincere thanks to Dr. Robert Ingham for his kindness to allow me to use the electroporator in his lab in the past 4 years.

I would like to thank Dr. Monika Keelan, who is in charge of the graduate studies program in the Department of Laboratory Medicine and Pathology, for her assistance and guidance throughout my PhD study. I also would like to express my sincere thanks to Ms. Cheryl Titus, the graduate program advisor, for her kindness and constant assistance in my whole PhD study.

I would also like to thank Dr. Roger Leng and Dr. Ing Swie Goping for serving as examiners for my candidacy examination. I appreciate their time, questions and comments for my study. I also would like to thank Dr. Jelena Holovati for chairing my candidacy examination and her support during the examination. I would also like to

appreciate Dr. Suzanne Kresta for her time to attend my candidacy examination and her supports to me as well.

I would like to thank Dr. Roger Leng and Dr. Shirin Bonni for serving as external examiners for my final PhD defense. I do appreciate your time and valuable comments. I also would like to thank Dr. Jelena Holovati for chairing my final PhD defense. I really do appreciate your time and support.

I would like to thank all present and past members of Dr.Lai's lab, who gave me their support and help throughout my PhD study. Specifically, I would like to give thanks to Dr. Hai-feng Zhang, Mr. Alshareef Abdulraheem, Dr. Gupta Nidhi, Mr.Yung-Hsing Huang, Dr. Fang Wu, and Dr. Peng Wang for their constant help and invaluable friendship. Thanks to Ms. Yuen Morrissey as well for her help in my PhD study.

I would like to acknowledge the technical assistance of Jingzhou Huang and Dr. Xue-Jun Sun in the Flow Cytometry lab at the Department of Experimental Oncology, Cross Cancer Institute, University of Alberta.

I would like to express my sincere gratitude to the Chinese Scholar Council (CSC) for supporting me with a graduate scholarship for the past 4 years. Without the generous support from CSC, I do not even have any chance to stand here. I would like to thank the Canadian Institutes of Health Research (CIHR) for funding the research projects.

Last but not the least; I would like to give my sincere thanks and gratitude to my family and my wife Lois Luo for all their endless loves and supports. Without your selfless loves and support, I would never have reached this stage.



## Table of contents

Title Page.....	i
Abstract.....	ii
Preface.....	v
Acknowledgments.....	vii
Table of Contents.....	ix
List of Abbreviations.....	xviii
List of Tables.....	xxiv
List of Figures.....	xxv
Bibliography.....	xvii

<b>CHAPTER 1: General Introduction.....</b>	<b>1</b>
1.1 Introduction.....	2
1.2 ALK-positive anaplastic Large Cell Lymphoma .....	3
1.2.1 Morphology .....	3
1.2.2 Immunophenotype.....	6
1.2.3 Survival analysis.....	7
1.2.4 Genotype.....	8
1.2.4.1 ALK.....	8
1.2.4.2 NPM.....	10
1.2.4.3 NPM-ALK .....	11

1.2.4.4 Other ALK fusion proteins.....	12
1.2.5 NPM-ALK-mediated transformation.....	15
1.2.6 NPM-ALK – interacting substrates and activated signaling pathways.....	16
1.2.6.1 JAK/STATs.....	18
A) JAKs and STAT3 in ALK+ALCL.....	18
B) STAT1.....	22
1.2.6.2 PLC- $\gamma$ .....	26
1.2.6.3 PI3K/AKT.....	26
1.2.6.4 RAS/MEK/ERK.....	29
1.2.6.5 mTOR.....	30
1.2.7 Therapeutic strategy for ALK+ALCL patients.....	30
1.3 Wnt/ $\beta$ -catenin.....	32
1.3.1 Wnt/ $\beta$ -catenin signaling.....	32
1.3.2 Wnt/ $\beta$ -catenin in cancer and ALK+ALCL.....	34
1.4 Cancer Stem Cells (CSCs).....	35
1.4.1 Identification and isolation of CSCs.....	35
1.4.2 Molecular features of CSCs.....	37
1.4.3 Signaling pathways in CSCs.....	38
1.4.4 CSCs in ALK+ALCL .....	39
1.5 Inducible pluripotent stem cells (iPS) factors.....	40

1.5.1 Sox2.....	41
1.5.1.1 Sox2 in cancer.....	41
1.5.1.2 Post-translational modification of Sox2.....	43
1.5.2 MYC in cancer.....	44
1.6 Reactive oxygen species (ROS) in cancer.....	48
1.7 Thesis overview.....	52
1.7.1 Rationale.....	52
1.7.2 Objectives.....	54
1.8 References.....	55

**CHAPTER 2: STAT1 is phosphorylated and downregulated by the oncogenic tyrosine kinase NPM-ALK in ALK-positive anaplastic large-cell**

<b>lymphoma.....</b>	<b>94</b>
2.1 Introduction.....	95
2.2 Methods and materials.....	97
2.2.1 Primary tumors and cell lines.....	97
2.2.2 Chemical treatments.....	98
2.2.3 Immunohistochemistry.....	99
2.2.4 Short interfering RNA and transfections.....	99
2.2.5 Plasmid constructs and transfection.....	100
2.2.6 Generation of Tet-on inducible stable cell lines.....	100

2.2.7 Cell-cycle assay.....	101
2.2.8 Western blotting and co-immunoprecipitation.....	102
2.2.9 Methylcellulose colony formation assay.....	104
2.2.10 Dual luciferase assay.....	104
2.2.11 STAT3 DNA probe binding assay.....	105
2.2.12 Trypan blue exclusion assay and MTS assay.....	106
2.2.13 RNA extraction, cDNA synthesis, and quantitative reverse transcriptase PCR (quantitative RT-PCR).....	106
2.2.14 SCID mouse xenograft studies.....	107
2.2.15 Statistical analysis.....	108
2.3 Results.....	108
2.3.1 STAT1 is expressed at a low level in ALK+ALCL tumors and cell lines.....	108
2.3.2 The ubiquitin-proteasome pathway is involved in the downregulation of STAT1 in ALK+ALCL cells.....	110
2.3.3 NPM-ALK promotes STAT1 phosphorylation at Y701 and downregulates STAT1.....	113
2.3.4 STAT3 is necessary for the downregulation of STAT1 mediated by NPM-ALK.....	116
2.3.5 STAT1 signaling is functionally intact in ALK+ALCL.....	117
2.3.6 The STAT1-IFN $\gamma$ positive feedback loop.....	124

2.3.7 STAT1C is a tumor suppressor in ALK+ALCL <i>in vitro</i> and <i>in vivo</i> ...	125
2.3.8 STAT1C significantly decreases STAT3 transcriptional activity .....	127
2.3.9 siRNA knockdown of STAT1 confers resistance to STAT3 inhibition-induced cell death.....	129
2.4 Discussion.....	131
2.5 References.....	136

**CHAPTER 3: A positive feedback involving the Wnt/ $\beta$ -catenin/MYC/Sxo2 axis defines a highly tumorigenic cell subpopulation in ALK-positive anaplastic**

<b>large-cell lymphoma.....</b>	<b>145</b>
3.1 Introduction.....	146
3.2 Methods and materials.....	148
3.2.1 Primary tumors, cell lines and treatments.....	148
3.2.2 Short interfering RNA and transfections.....	149
3.2.3 RNA extraction, cDNA synthesis, quantitative reverse transcriptase PCR (quantitative RT-PCR) and chromatin-immunoprecipitation PCR.....	149
3.2.4 Immunohistochemistry and immunofluorescence studies.....	152
3.2.5 Plasmid constructs and transfection.....	153
3.2.6 Western blotting.....	153
3.2.7 Luciferase assay .....	154
3.2.8 Transwell assay .....	154

3.2.9 Cell-cycle and MTS assay.....	155
3.2.10 SRR2 probe binding assay.....	155
3.2.11 Nuclear cytoplasm fractionation assay.....	156
3.2.12 Methylcellulose colony formation assay.....	156
3.2.13 SCID mouse xenograft studies.....	156
3.2.14 Side population assay.....	157
3.2.15 Statistical analysis.....	157
3.3 Results.....	158
3.3.1 The identification of MYC as a key regulator of the RU/RR dichotomy.....	158
3.3.2 MYC promotes Sox2-SRR2 binding and the transcriptional activity of Sox2.....	166
3.3.3 The high level of MYC in RR cells is attributed to the Wnt/ $\beta$ -catenin pathway.....	171
3.3.4 The positive regulatory loop involving Sox2, Wnt/ $\beta$ -catenin and MYC in RR cells.....	180
3.3.5 MYC is heterogeneously expressed in primary tumor samples, and it co-localizes with active $\beta$ -catenin.....	182
3.3.6 RU cells stably transfected with MYC are biochemically and phenotypically similar to RR cells.....	185
3.3.7 Side population cells are not detectable in RU and RR cells and ABCG2 is	

not significantly differentially expressed in mRNA level between RU and RR cells.....	187
3.4 Discussion.....	190
3.5 References.....	197

**CHAPTER 4: Oxidative stress promotes the tumorigenicity in ALK-positive anaplastic large-cell lymphoma by activating the Wnt/ $\beta$ -catenin/MYC/Sox2**

<b>axis.....</b>	<b>204</b>
4.1 Introduction.....	205
4.2 Methods and materials.....	207
4.2.1 Cell lines and chemicals.....	207
4.2.2 H <sub>2</sub> O <sub>2</sub> , NAC, 10074-G5 and quercetin treatment.....	207
4.2.3 Luciferase assay and flow cytometry.....	208
4.2.4 Trypan blue exclusion and MTS assay.....	209
4.2.5 Short interfering RNA and transfections.....	209
4.2.6 RNA extraction, cDNA synthesis, and quantitative reverse transcriptase PCR (quantitative RT-PCR).....	209
4.2.7 Western blotting.....	210
4.2.8 Nuclear cytoplasm fractionation assay.....	210
4.2.9 SRR2 probe binding assay.....	210
4.2.10 Methylcellulose colony formation assay.....	210

4.2.11 Limiting dilution assay.....	211
4.2.12 Statistical analysis.....	211
4.3 Results.....	211
4.3.1 Oxidative stress induces a conversion from RU to RR cells.....	211
4.3.2 The converted RR cells share the similar biological functions with RR cells.....	218
4.3.3 The converted RR cells share the similar biochemical characteristics with RR cells.....	222
4.3.4 Inhibition of $\beta$ -catenin/MYC or siRNA knockdown of Sox2 dramatically abrogates the conversion of RU cells to RR cells induced by oxidative stress.....	224
4.3.5 ERK1/2 is activated in both RU and RR cells upon H <sub>2</sub> O <sub>2</sub> re-challenge.....	226
4.3.6 STAT1 is activated in both RU and RR cells upon oxidative stress.....	228
4.4 Discussion.....	230
4.5 References.....	236
<b>CHAPTER 5: General Discussion and Conclusions.....</b>	<b>244</b>
5.1 Thesis overview.....	245
5.2 STAT1 in ALK+ALCL.....	246
5.3 The RU/RR dichotomy in ALK+ALCL.....	248
5.4 Oxidative stress-induced RU/RR conversion in ALK+ALCL.....	251



5.5 STAT1 and the RU/RR dichotomy.....	253
5.6 Conclusions and future directions.....	254
5.7 References.....	256
<b>Bibliography.....</b>	<b>257</b>

## List of Abbreviations

$^1\text{O}_2$  – singlet oxygen

ABC transporters – ATP-binding cassette transporters

ALCL – anaplastic large-cell lymphoma

ALDH – Aldehyde dehydrogenase

ALK – anaplastic lymphoma kinase

AML – acute myeloid leukemia

AP-1 – Activator Protein-1

APC – adenomatous polyposis coli

ATM – ataxia telangiectasia mutated

BAD – Bcl2-associated death promoter

Bcl-2 – B-cell lymphoma-2

Bcl-X<sub>L</sub> – B-cell lymphoma-extra large

BCR-ABL – breakpoint cluster region- Abelson

bHLH – helix-loop-helix

BRCA1 – breast cancer susceptibility 1

CA-CTNNB1 – constitutive catenin beta 1

CD – cytoplasmic tyrosine kinase domain

CDC25A – cell division cycle 25 homolog A

Cdk2 – cyclin-dependent kinase 2

ChIP – chromatin-immunoprecipitation

CHOP – Cyclophosphamide, hydroxydaunorubicin (doxorubicin), oncovin (vincristine),  
and prednisone

CK1 $\alpha$  – casein kinase 1 $\alpha$

CML – chronic myeloid leukemia

CRC – colon-rectal cancer

CSC – cancer stem cells

DAG – diacylglycerol

DMSO – dimethyl sulfoxide

DNMTs – DNA methyltransferases

DVI – disheveled

ECD – extracellular domain

eIF2A – eukaryotic translation initiation factor 2A

EMA – epithelial membrane antigen

EMT – epithelia-mesenchymal transition

ER – endoplasmic reticulum

ER – estrogen receptor

ERK – extracellular signal-related kinase

ETS-1 – E26 transformation-specific-1

EV – empty vector

FOXO3a – forkhead family of transcription factors 3a

FZD – Frizzled

GAS – IFN--activated-site

GSK3 $\beta$  – glycogen synthase kinase-3 $\beta$

H<sub>2</sub>O<sub>2</sub> – hydrogen peroxide

HGFR –Hepatocyte growth factor receptor

HHAT – Hedgehog acyltransferase

HMG – high mobility group DNA binding domain

HOXA5 – homeobox A5

IFN – interferon

IFNAR1/2 – IFN alpha receptor

IGF – insulin growth factor

IP3 – inositol triphosphate

iPS – pluripotent stem cells

IRF-1 – Interferon regulatory factor -1

ISGF3 – IFN-stimulated gene factor 3

ISRE – IFN-stimulated response element

I $\kappa$ B – inhibitors of  $\kappa$ B

JAK – Janus activated kinase

Jeb – Jelly belly

LRP5/6 – Low density lipoprotein receptor-related protein 5/6

MAPK- Mitogen-activated protein kinase

Max – MYC-associated factor X

Mcl-1 – myeloid cell leukemia sequence 1

MEFs – mouse embryonic fibroblasts

mESCs – mouse embryonic stem cells

miRNA – microRNA

MK – midkine

mTOR – mammalian target of rapamycin

MTS-3-(4,5-dimethylthiazol-2-yl)-5-(3-carboxymethoxyphenyl)-2-(4-sulfophenyl)-2H-tetrazolium

MYC: V-myc avian myelocytomatosis viral oncogene homolog

NAC – N-acetyl-L-cysteine

NADPH – nicotinamide adenine dinucleotide phosphate

NF- $\kappa$ B – nuclear factor kappa-light-chain-enhancer of activated B cells

NHL – non-Hodgkin lymphoma

NKLAM – Natural Killer Lytic-Associated Molecule

NKLAM – natural killer lytic-associated molecule

NPM – nucleophosmin

Nrf2 – nuclear factor erythroid 2-related factor 2

NSCLC – non-small-cell lung cancer

O<sub>2</sub><sup>-</sup> – superoxide anions

O<sub>3</sub> – ozone

OH<sup>-</sup> – hydrogen radical

PI3K – phosphatidylinositol 3 kinase

PIP2 – phosphatidylinositol

PKC – protein kinase C

PLC- $\gamma$  – phospholipase C  $\gamma$

PTEN – phosphatase and tensin homolog

PTN – pleiotrophin

qRT-PCR – quantitative reverse transcriptase-polymerase chain reaction

ROS – reactive oxygen species

ROS1 – c-ros oncogene 1

RPS6 – ribosomal protein S6

RR – reporter responsive

RTK – receptor tyrosine kinase

RU – reporter unresponsive

SCID – severe combined immune deficiency

SHH – Sonic Hedgehog

SHP1 – Src homology region 2 domain-containing phosphatase-1

shRNA – small hairpin RNA

siRNA – small interfering RNA

Smurf1 – smad ubiquitination regulation factor 1

Sox2 – sex determining region Y- box 2

SRR2 – Sox2 regulatory region 2

STAT – signal transducer and activator of transcription

STAT1C – constitutively active STAT1

TCF/LEF – T-cell factor/lymphoid enhancer factor

TICs – tumor-initiating cells

TM – transmembrane domain

TNF – tumor necrosis factor

TPM4 – tropomyosin

TSCs – tumor stem cells

TYK2 – tyrosine kinase 2

VEGF – vascular endothelia growth factor

WHO – World Health Organization

## List of Tables

Table 1.1 Chromosomal translocations involving ALK in ALK+ALCL and other malignancies.....	14
Table 3.1 Primers used for quantitative RT-PCR.....	151
Table 3.2 The top putative factors that are predicated to bind to SRR2 sequence by JASPAR motif matches analysis at $P < 0.001$ .....	160
Table 4.1 Primers used for quantitative RT-PCR.....	209



## List of Figures

Figure 1.1 The common pattern of ALK+ALCL.....	4
Figure 1.2 Variant morphological patterns in ALK+ALCL.....	5
Figure 1.3 Immunohistochemical stainings of CD30 and ALK in ALCL.....	7
Figure 1.4 The functional domains of ALK, NPM, and NPM-ALK.....	10
Figure 1.5 Representative signaling pathways activated by NPM-ALK.....	17
Figure 1.6 NPM-ALK activates STATs signaling pathway in ALK+ALCL.....	21
Figure 1.7 Signal transduction of the IFN/STATs.....	23
Figure 1.8 NPM-ALK activates the PI3K/AKT pathway in ALK+ALCL.....	28
Figure 1.9 Overview of the Wnt/ $\beta$ -catenin pathway.....	33
Figure 1.10 The biological processes regulated by MYC in cancer cells.....	47
Figure 1.11 Phosphorylation and stabilization of MYC by ERK and GSK3 $\beta$ .....	48
Figure 1.12 Determination of cellular redox status by a balance between levels of ROS inducers and ROS scavengers.....	51
Figure 2.1 Expression of STAT1 in ALK+ALCL cell lines and patient samples.....	109
Figure 2.2 The ubiquitin-proteasome pathway is involved in the downregulation of STAT1 in ALK+ALCL cells.....	111
Figure 2.3 NPM-ALK promotes STAT1 phosphorylation at Y701 and downregulates STAT1.....	114
Figure 2.4 STAT1 signaling is functionally intact in ALK+ALCL.....	118

Figure 2.5 STAT1 provides tumor suppressor function in ALK+ALCL <i>in vitro</i> .....	122
Figure 2.6 Overexpression of STAT1 induces the expression of IFN $\gamma$ in ALK+ALCL and suppresses the tumor cell growth <i>in vivo</i> .....	124
Figure 2.7 STAT1C significantly decreases STAT3 transcriptional activity.....	128
Figure 2.8 siRNA knockdown of STAT1 confers resistance to STAT3 inhibition-induced cell death.....	130
Figure 2.9 Schematic model of STAT1 in ALK+ ALCL.....	136
Figure 3.1 Knockdown of Sox2 by siRNA significantly downregulates the SRR2 luciferase activity in RR cells.....	159
Figure 3.2 RR cells express a substantially higher level of MYC than RU cells.....	161
Figure 3.3 The high MYC expression contributes to the RR phenotype.....	162
Figure 3.4 MYC promotes the SRR2 probe binding and the transcriptional activity of Sox2.....	168
Figure 3.5 NPM-ALK/STAT3 is not differentially activated or expressed between RU and RR cells.....	172
Figure 3.6 The Wnt signaling is more active in SupM2-RR cells in comparison to SupM2-RU cells.....	174
Figure 3.7 The Wnt/ $\beta$ -catenin pathway contributes to the high MYC expression in RR cells.....	175
Figure 3.8 RU cells transfected with the constitutively active <i>CTNNB1</i> (CA- <i>CTNNB1</i> ) acquire the RR phenotype.....	179

Figure 3.9 The positive regulatory loop of Sox2–Wnt/β-catenin–MYC in RR cells.....	181
Figure 3.10 MYC is heterogeneously expressed and its expression is co-localized with active β-catenin in ALK+ALCL tumor cells.....	184
Figure 3.11 RU cells stably transfected with <i>MYC</i> are biochemically and phenotypically similar with RR cells.....	186
Figure 3.12 Identification of side populations cells by Hoechst-efflux assay and the expression of ABC transporters in RU and RR cells derived from ALK+ALCL.....	189
Figure 4.1 Oxidative challenge induces the conversion of RU to RR cells.....	213
Figure 4.2 RU and RR cells upon H <sub>2</sub> O <sub>2</sub> re-challenge treatment are more doxorubicin-resistant and clonogenic, and have captured enhanced sphere-forming ability as compared to cells without treatment.....	221
Figure 4.3 The converted RR cells induced by oxidative stress share the biochemical features with RR cells.....	223
Figure 4.4 Pharmacological inhibition of MYC or β-catenin, or siRNA knockdown of Sox2 in RU cells significantly abrogates the conversion of RU cells to RR cells.....	225
Figure 4.5 Inhibition of ERK1/2 activity .in RR cells dramatically decreases the expression level of MYC and Sox2, as well as the SRR2 luciferase activity.....	227
Figure 4.6 STAT1 is activated in RU and RR cells upon oxidative stress.....	229

## **CHAPTER 1**

### **General Introduction**

---

## 1.1 Introduction

Anaplastic large-cell lymphoma (ALCL), first described by Stein and colleagues in 1985, is a rare type of peripheral null or T-cell non-Hodgkin lymphoma (NHL), consisting of approximately 2-3% of all lymphoid malignancies, ~3% of all adult NHLs, and ~10-20% of childhood lymphomas (1, 2). The subtype of this lymphoma cells strongly express an antigen named CD30, a member of the tumor necrosis factor receptor family (3, 4). CD30 was initially detected and recognized by antibody generated in Kiel, West Germany, and therefore termed as Ki-1 (3). In the early 1990s, Morris *et al* found that a group of ALCL cases carry a recurrent chromosome translocation involving the anaplastic lymphoma kinase (ALK) gene on chromosome 2p23 and the nucleophosmin (NPM) gene on chromosome 5q35, and this chromosome translocation results in the generation of a fusion protein – NPM-ALK (5). In 2008, the World Health Organization (WHO) classified ALCL into 3 entities including primary cutaneous ALCL, ALK-negative ALCL (ALK-ALCL) and ALK-positive ALCL (ALK+ALCL) (6). Primary cutaneous ALCL preferentially presents in the skin; while ALK- and ALK+ ALCL usually present in systemic forms (7), therefore, they are also classified as systemic ALCL. Primary systemic ALCL preferentially occurs in childhood and young adults, and accounts for approximately 40% of pediatric patients with NHL (7). However, primary systemic ALCL only accounts for less than 5% of adult patients with NHL, with male predominance (7). Patients diagnosed with systemic ALCL are often found in an advanced stage of disease; specifically, involvements of lymph nodes and multiple extranodal sites are usually presented in these patients (1).

## 1.2 ALK-positive anaplastic large-cell lymphoma

### 1.2.1 Morphology

The WHO classification has described at least 5 histologic variants or patterns of ALK+ALCL cases, including common pattern, lymphohisocytic variant, the small-cell variant, Hodgkin-like, and a “composite” type containing more than one variant (6).

The common pattern constitutes of ~70% of all ALK+ALCL cases (7), and it refers to that a small number of tumor cells typically infiltrate the lymphatic sinusoids and these tumor cells usually present a pattern of sheet-like in the lymph node (**Figure 1.1**) (6). In some cases, immunohistochemistry stainings, such as anti-ALK staining, are required to recognize the tumor cells, as a relatively small number of tumor cells are infiltrated in the lymph node (6). Approximately 10% of all ALK+ALCL cases are lymphohistiocytic variant in which the infiltrated reactive histiocytes can be easily observed (**Figure 1.2A-B**) (8). Sometimes, the ALK+ALCL tumor cells are difficult to find because of erythrophagocytosis in situ (9). The small-cell variant consists of ~5-10% of all cases and it, namely, presents the smaller size of tumor cells, in which the perivascular clustering can be occasionally observed (**Figure 1.2C-D**) (10). A Hodgkin-like pattern, representing ~1-3% of all cases, resembles the nodular sclerosis variant of classical Hodgkin lymphoma with a polymorphous cellular background (**Figure 1.2E-F**) (11, 12). However, not all cases of ALK+ALCL present only one of above patterns (13), in other words, multiple patterns are always observed in a single case. A “composite” type containing more than one variant can be seen in a small number of cases (13). Note that the histologic pattern may vary in sequential biopsies of ALK+ALCL tumors from

the same patient (14), indicating the existence of multiple histologic patterns in a single case.

Nevertheless, the representative ALK+ALCL cells or hallmark cells can be identified in all patterns of cases (3). The hallmark cells are featured with irregular large size of cell, with “horse or kidney-shaped” nucleus and abundant cytoplasm, along with an evidently central Golgi apparatus (**Figure 1.1C and 1.2B**) (14)

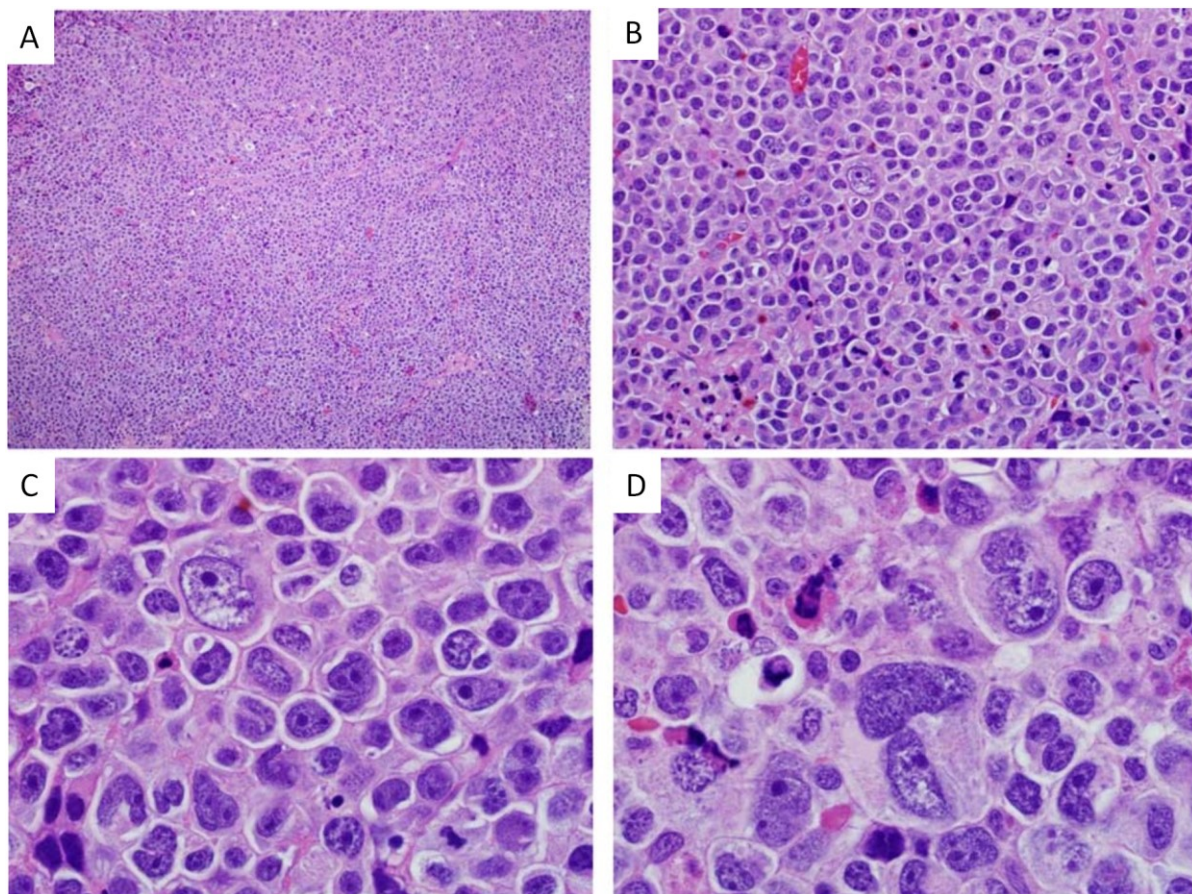


**Figure 1.1 The common pattern of ALK+ALCL.** A, B) The lymph node architecture is effaced by sheets of neoplastic lymphoid cell (A:H&E, X100; B:H&E, X400). C, D) Two high-power images taken at the same magnification from the same case demonstrate a wide spectrum of cytologic features and cell sizes, including characteristic hallmark cells (C:H&E, X1000) and very large, sometimes multinucleated cells (D:H&E, X1000).

Reprinted with consent from “Xing X and Feldman AL. Anaplastic Large Cell Lymphoma: ALK Positive, ALK Negative, and Primary Cutaneous. *Adv Anat Pathol.* 2015; 22(1):29-49.” Licence number: 3976891276365.

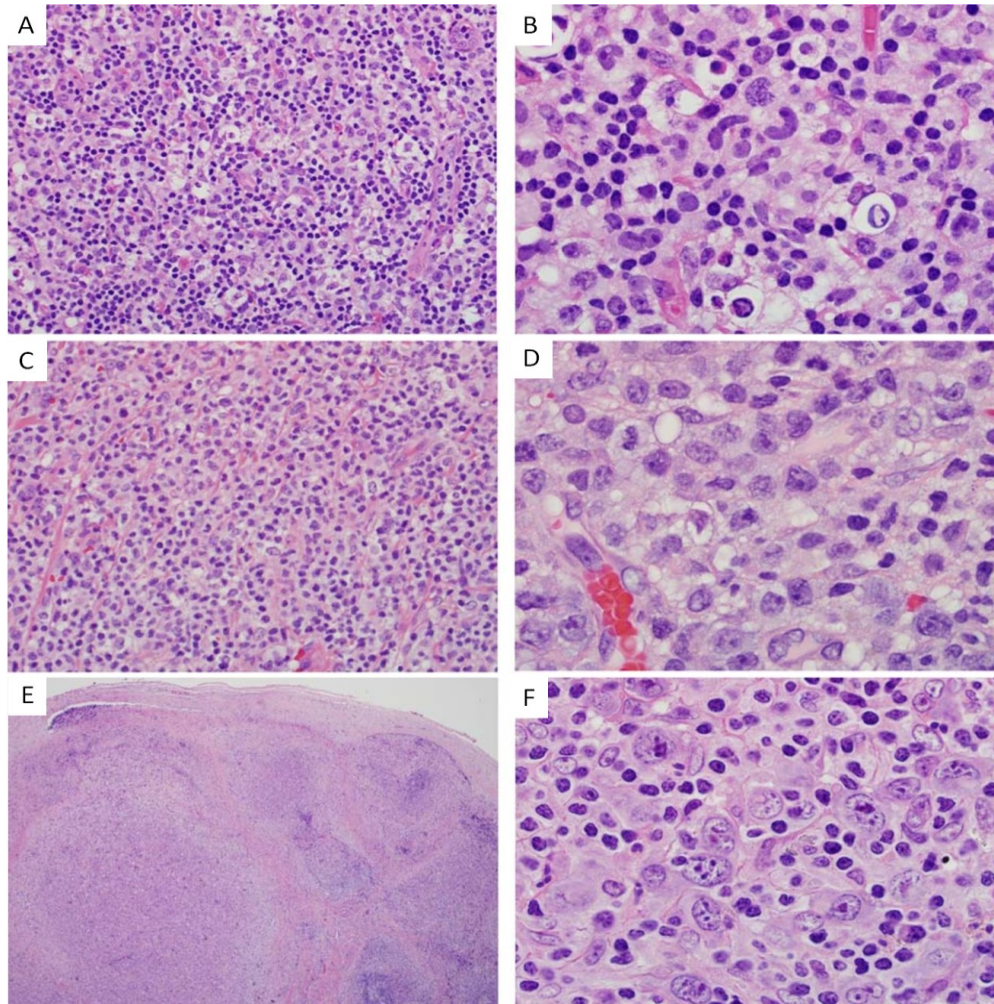


**Figure 1.2 Variant morphologic patterns in ALK+ALCL.** In the lymphohistiocytic pattern, the tumor cells mix with histiocytes and small lymphocytes (A: H&E, X400); hallmark cells can be seen (B: H&E, X1000). The small-cell pattern contains predominantly small-sized to medium-sized cells, often with pale cytoplasm (C: H&E, 400), but hallmark cells also can be found, often adjacent to blood vessels (D: H&E, 1000). The Hodgkin-like pattern shows the architectural features of the nodular sclerosis type of classical Hodgkin lymphoma (E: X40), although the neoplastic cells within the nodules typically resemble hallmark cells more than classic Reed-Sternberg cells (F: X1000).



Reprinted with consent from “Xing X and Feldman AL. Anaplastic Large Cell Lymphoma: ALK Positive, ALK Negative, and Primary Cutaneous. *Adv Anat Pathol*. 2015; 22(1):29-49.” Licence number: 3976891276365.

### 1.2.2 Immunophenotype

Nearly all ALK+ALCL cases exhibit the positive staining of CD30 on the cell surface and within the Golgi area (**Figure 1.3**) (9, 10). CD30, as a member of the tumor necrosis factor (TNF) receptor superfamily, is generally expressed on activated lymphocyte cells (15). Most of ALK+ALCL cases also present the positive staining of epithelial membrane antigen (EMA, or Mucin 1) (16), which is a glycoprotein generally expressed on the surface of epithelia cells in the lungs, intestines, *etc* (17). Besides, the cytotoxic cell antigen T-cell restricted intracellular antigen 1 (TIA-1), granzyme B and perforin are also detectable in most of ALK+ALCL cases (18-21).

As a type of T-cell lymphoma, most of ALK+ALCL cells have gene rearrangement of T-cell receptor (TCR) and the expressions of one or more T-cell/nature killer cells antigens (20, 22). For instance, CD2 and CD4 are widely expressed on ALK+ALCL cells, and CD8 is also detectable in some cases (20). However, ALK+ALCL cells are deficient in normal T-cell signaling pathways because of lack of or decreased expressions of T-cell antigens including the pan T-cell marker CD3 and the  $\alpha\beta$  T-cell receptor complex (22). An early study revealed that the expression of CD3 was lost in 23 of 24 ALK+ALCL cases (22), and the expressions of CD5 and CD7 are always undetectable on ALK+ALCL cells (23). While some ALK+ALCL cells are diagnosed as “Null” cell type, as they lack T-cell phenotype (13). Due to the lack of both T-cell and B-

cell surface markers, the “Null” cell type ALK+ALCL cells are thereby deficient in some specific T or B-cell signaling pathways (13).

The most evident immunophenotype for ALK+ALCL is the expression of chimeric ALK proteins (**Figure 1.3**) (24). In general, the immunohistochemical stainings for both ALK and CD30 has been widely applied as a diagnostic tool in clinical for diagnosing ALK+ALCL cases (8).

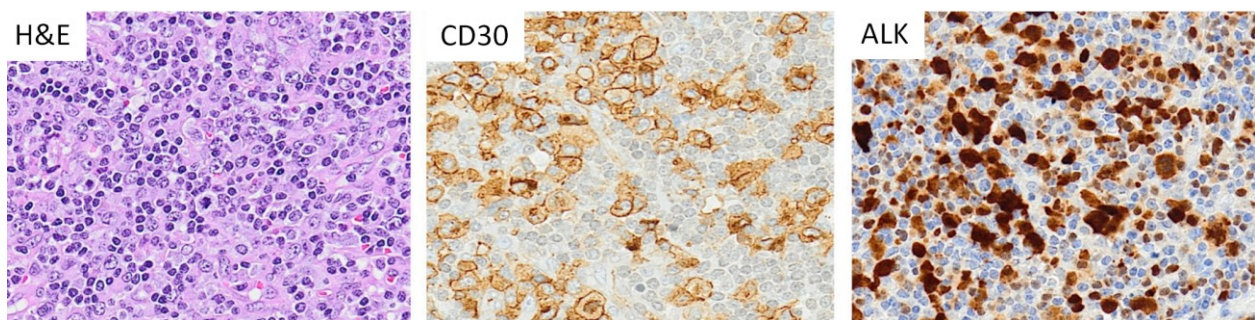


**Figure 1.3 Immunohistochemical stainings of CD30 and ALK in ALCL.** The ALCL cells show a broad spectrum of morphologic features, and virtually all cases display a variable proportion of “hallmark cells”. Positive immunohistochemical staining of CD30 and ALK on an ALCL case are shown here.

Modified with consent from “Tobbo F, *et al.* ALK signaling and target therapy in anaplastic large cell lymphoma. *Front Oncol.* 2012; 2(41).” *Frontiers in Oncology* is an Open-access journal, which permits non-commercial use, distribution, and reproduction in other forums, provided the original authors and source are credited.

### 1.2.3 Survival analysis

Overall, patients with ALK+ALCL have a favourable prognosis, except for the CD56-positive cell variant (3). Patients with ALK+ALCL usually have a good response to conventional chemotherapy (7). Complete remission occurs in up to 90% of pediatric

patients upon conventional chemotherapy (8). The 3-year and 5-year disease-free survival for pediatric patients range from 60% to 85%, and the 5-year overall survival for young adult patients is ~85% with conventional chemotherapy (3). A recent clinical study has indicated that patients with ALK+ALCL have a significantly higher 5-year overall survival rate than ALK-ALCL patients (70% versus 49%) (3, 25). Of note, no significant difference is observed when comparing the 5-year survival rates between ALK+ALCL and ALK-ALCL patients of over 40 years old (2), this indicates that the younger ages of patients might help explain the favourable diagnosis of ALK+ALCL versus ALK-ALCL (3).

## **1.2.4 Genotype**

### **1.2.4.1 ALK**

ALK is a receptor tyrosine kinase (RTK), belonging to the superfamily of insulin growth factor (IGF) receptor (26). ALK contains 3 domains including an extracellular domain (ECD) for ligand binding, a transmembrane domain (TM), and a cytoplasmic tyrosine kinase domain (CD) (**Figure 1.4**) (26).

The ligands of ALK signaling in vertebrates remain poorly studied (27). In *D melanogaster*, Jelly belly (Jeb) protein has been shown as a ligand and activator of ALK (28). The small heparin-binding growth factors pleiotrophin (PTN) and midkine (MK) have been found to activate the ALK downstream targets by physically binding the extracellular domain of ALK in some cell models (29, 30). However, PTN or MK, as ligand and activator of ALK, is controversial due to lack of reproducibility (31, 32). More

recently, Murray *et al* reported that heparin specifically binds to ALK and induces ALK dimerization and activation in the neuroblastoma cell line – NB1 independent of PTN or MK (33). Two independent research groups have recently identified that augmentor- $\alpha$  (also known as FAM150B) specifically binds to the extracellular domain of ALK and robustly stimulates ALK signaling (34, 35). However, the two groups had conflicting conclusion on augmentor- $\beta$  (also named FAM150A) being as a potent ALK ligand. Guan *et al* reported that augmentor- $\beta$  activates ALK signaling as potently as augmentor- $\alpha$  (34), but Andrey *et al* suggested that augmentor- $\beta$  only weakly binds to and activates ALK (35).

The expression of ALK is typically restricted to the cells of neural system, such as the thalamus, mid-brain, olfactory bulb and ganglia, thus it is considered that ALK may play key roles in the development of neural system (36). *ALK* gene-double knockout mice exhibit abnormal behaviours (37), thus supporting the idea that ALK is involved in the development of mammalian brain system, despite its exact physiological roles being unidentified (37). Intriguingly, the aberrant expression of ALK has been detected in certain types of cancer, such as neuroblastoma (38) and glioblastoma (39), which are both of neural origin. Further studies have demonstrated that the aberrant ALK expression, either by gene amplification or mutation, is implicated in the pathogenesis of these types of cancer (40, 41). Nevertheless, the oncogenic role of ALK remains poorly understood, since the majority of studies on the oncogenic role of ALK has been performed in ALK+ALCL cells in which ALK mostly exists as a NPM-ALK fusion protein (26).

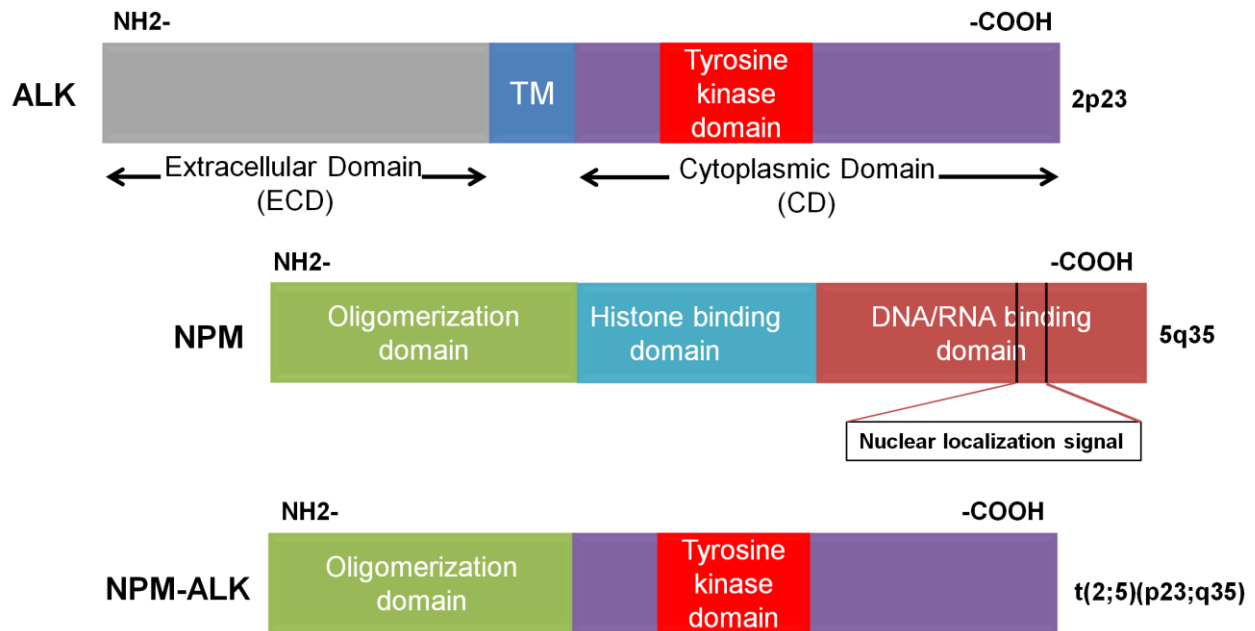


**Figure 1.4 The functional domains of ALK, NPM, and NPM-ALK.** Anaplastic lymphoma kinase (ALK) kinase contains three domains, including extracellular domain (ECD), transmembrane domain (TM), and cytoplasmic domain (CD) where the tyrosine kinase domain is localized. As for nucleophosmin (NPM), it consists of oligomerization domain, histone binding domain, and DNA/RNA binding domain. The chromosomal translocation involving ALK and NPM leads to the fusion kinase NPM-ALK which is comprised of oligomerization domain from NPM and tyrosine kinase domain derived from ALK. The oligomerization domain of NPM-ALK confers its ability to form dimerization.

#### 1.2.4.2 NPM

Nucleophosmin (NPM, also known as nucleolar phosphoprotein B23) is ubiquitously expressed in human cells (42). NPM protein consists of 3 functional domains including oligomerization domain, histone-binding domain, and DNA/RNA binding domain (**Figure 1.4**) (42). NPM usually functions as a shuttle transferring cytoplasmic proteins to the nucleolus via the oligomerization domain and the nuclear localization signal in

DNA/RNA binding domain (43). Intriguingly, studies have indicated that NPM is involved in genomic stability and DNA repair in cancer cells (42-45). The *NPM* gene is found aberrantly expressed including overexpression, mutation, and chromosome translocation, in various types of cancer (42). For instance, chromosomal translocations involving *NPM* have been detected in non-Hodgkin T-cell lymphoma (46), acute myelogenous leukemia (47), and acute promyelocytic leukemia (48). The aberrant NPM expression has been shown to exert oncogenic functions in tumor cells (42, 43).

#### **1.2.4.3 NPM-ALK**

Approximate 80% of ALK+ALCL cases harbor the chromosome translocation involving  $t(2;5)(p23;q35)$ , which results in the generation of the fusion tyrosine kinase – NPM-ALK (3). The chimeric protein NPM-ALK fuses the oligomerization domain of NPM to the entire cytoplasmic domain of the ALK (**Figure 1.4**) (49). As a result of this chromosomal translocation, *ALK* gene expression is driven by the ubiquitous *NPM* promoter, thus it is constitutively expressed in ALK+ALCL (49, 50). The NPM-ALK protein oligomerizes with other NPM-ALK proteins or NPM proteins via the NPM oligomerization domain to form homodimers or heterodimers, respectively (51). NPM-ALK homodimers are usually localized in the cytoplasm because the truncated NPM lacks nuclear localization signal; while NPM-ALK/NPM heterodimers can be found in both cytoplasm and nucleus, as wild-type NPM contains nuclear localization signal (52). Taken together, NPM-ALK can be detected in ALK+ALCL cells in both cytoplasm and nucleus by using anti-ALK antibody in immunohistochemistry assay (52).

The dimerization of NPM-ALK results in the autophosphorylation and constitutive activation of ALK kinase in the absence of ligands, and subsequently, NPM-ALK exerts as a potent oncogenic tyrosine kinase by interacting and activating a wide range of proteins or signaling pathways, such as Janus activated kinase/signal transducer and activator of transcription (JAK/STAT) (53), phosphatidylinositol 3 kinase (PI3K)/AKT (54), RAS/ERK kinase (MEK)/extracellular signal-related kinase (ERK) (51, 55, 56), all of which are related with important biological processes such as cell proliferation, survival, invasiveness, *etc* (51, 55, 56). The oncogenic role of NPM-ALK *in vitro* and *in vivo* has been well documented in a number of studies using cell lines and transgenic mouse models (50).

#### **1.2.4.4 Other ALK fusion proteins**

Other than NPM-ALK fusion protein, numerous other ALK fusion proteins have been detected in ALK+ALCL (**Table 1**) (57). All these ALK fusion proteins, including NPM-ALK, share common characteristics, as demonstrated below: 1) The ALK partner gene drives ALK gene expression (3, 26, 52). 2) The ALK partner protein contains oligomerization domain through which ALK fusion protein dimerizes with each other (3, 26, 52). 3) The ALK fusion proteins can be automatically phosphorylated and constitutively activated by themselves (3, 26, 52). 4) The ALK partner protein determines the subcellular localization of the ALK fusion protein (3, 26, 52). In the case of NPM-ALK, as mentioned above, it can be detected in both cytoplasm and nucleus (55). To be specific, it is the NPM-ALK/NPM heterodimers that are localized in cytoplasm and nucleus (52). As for most of other types of ALK fusion proteins, they are

only detectable in cytoplasm (26, 57). This differential subcellular localization of NPM-ALK and other ALK fusion proteins can be ascribed to the wild-type NPM which contains nuclear localization signals to assist in shuttling the NPM-ALK/NPM heterodimers to the nucleus (8, 57). However, other truncated ALK partner proteins lack of this nuclear localization signal; therefore, these ALK fusion proteins cannot migrate to the nucleus (8, 57). For instance, as TPM4 lacks nuclear localization signal, TPM4-ALK homodimers and TPM4/TPM4-ALK heterodimers are both localized in cytoplasm (**Table 1**) (57).

Notably, chromosomal translocations involving ALK are detected not only in ALK+ALCL but also in other types of malignancies, such as non-small-cell lung cancer (NSCLC) (58) and colorectal cancer (CRC) (59) (**Table 1.1**).



**Table 1.1 Chromosomal translocations involving ALK in ALK+ALCL and other malignancies.**

Disease	Chromosomal abnormalities	Fusion protein (kDa)	Partner	Frequency (%)	ALK IHC staining	Reference
ALCL	t(2;5)(p23;q35)	NPM-ALK (80)	<i>NPM1</i>	75–80	Cyto/nuclear	Morris et al. (1994), Shiota et al. (1994)
ALCL	t(2;17)(p23;q25)	ALO17-ALK (ND)	<i>ALO17</i>	<1	Cyto	Cools et al. (2002)
ALCL	t(2;3)(p23;q21)	TFG-ALK (113)	<i>TFG</i>	2	Cyto	Hernandez et al. (1999, 2002)
ALCL	t(2;X)(p32;q11–12)	MSN-ALK (125)	<i>MSN</i>	<1	Cyto	Tort et al. (2001, 2004)
ALCL	t(1;2)(q25;p23)	TPM3-ALK (104)	<i>TPM3</i>	12–18	Cyto	Lamant et al. (1999), Siebert et al. (1999)
ALCL	t(2;19)(p23;p13)	TPM4-ALK (95)	<i>TPM4</i>	<1	Cyto	Meech et al. (2001)
ALCL	inv(2)(p23;q35)	ATIC-ALK (96)	<i>ATIC</i>	2	Cyto	Ma et al. (2000), Trinei et al. (2000), Colleoni et al. (2000)
ALCL	t(2;22)(p23;q11.2)	MYH9-ALK (220)	<i>MYH9</i>	<1	Cyto	Lamant et al. (2003)
ALCL	t(2;17)(p23;q23)	CLTC1-ALK (250)	<i>CLTC1</i>	2	Cyto	Touriol et al. (2000)
DLBCL	t(2;5)(p23;q35)	NPM-ALK (80)	<i>NPM1</i>	N/A	Cyto/nuclear	Adam et al. (2003), Onciu et al. (2003)
DLBCL	t(2;17)(p23;q23)	CLTC1-ALK (250)	<i>CLTC1</i>	N/A	Granular cyto	De Paepe et al. (2003)
DLBCL	t(2;5)(p23.1;q35.3)	SQSTM1-ALK (ND)	<i>SQSTM1</i>	N/A	Cyto	Takeuchi et al. (2011)
DLBCL	ins(4)(2,4)(?,q21)	SEC31A-ALK (ND)	<i>SEC31A</i>	N/A	Cyto	Bedwell et al. (2011), Van Roosbroeck et al. (2010)
IMT	t(1;2)(q25;p23)	TPM3-ALK (104)	<i>TPM3</i>	50	Cyto	Lawrence et al. (2000)
IMT	t(2;19)(p23;p13)	TPM4-ALK (95)	<i>TPM4</i>	<5	Cyto	Lawrence et al. (2000)
IMT	t(2;17)(p23;q23)	CTLC-ALK (250)	<i>CLTL</i>	<5	Cyto	Bridge et al. (2001), Patel et al. (2007)
IMT	inv(2)(p23;q35)	ATIC-ALK (96)	<i>ATIC</i>	<5	Cyto	Debiec-Rychter et al. (2003)
IMT	t(2;11;2)(p23;p15;q31)	CARS-ALK (ND)	<i>CARS</i>	<5	Cyto	Cools et al. (2002), Debelenko et al. (2003)
IMT	t(2;2)(p23;q13)	RANBP2-ALK (ND)	<i>RANBP2</i>	<5	N/M	Ma et al. (2003), Marino-Enriquez et al. (2011)
IMT	inv(2)(p23;p15;q31)	SEC31L1-ALK (ND)	<i>SEC31L1</i>	<5	Cyto	Panagopoulos et al. (2006)
ESCC	t(2;19)(p23;p13)	TPM4-ALK (110)	<i>TPM4</i>	N/A	Cyto	Jazii et al. (2006), Du et al. (2007)
RCC	t(2;10)(p23;q22)	VCL-ALK (117)	<i>VCL</i>	N/A	Cyto	Debelenko et al. (2011)
NSCLC	inv(2)(p21;p23)	EML4-ALK (120)	<i>EML4</i>	2–5	Cyto	Rikova et al. (2007), Soda et al. (2007)
NSCLC	t(2;3)(p23;q21)	TFG-ALK (113)	<i>TFG</i>	2	Cyto	Rikova et al. (2007)
NSCLC	t(2;10)(p23;p11)	KIF5B-ALK (ND)	<i>KIF5B</i>	<1	Cyto	Takeuchi et al. (2009), Wong et al. (2011)
NSCLC	t(2;14)(p23;q32)	KLC1-ALK (ND)	<i>KCL1</i>	<5%	Cyto	Togashi et al. (2012)
NSCLC	t(2;9)(p23;q31)	PTPN3-ALK (ND)	<i>PTPN3</i>	N/A	Cyto	Jung et al. (2012)
CRC	inv(2)(p21;p23)	EML4-ALK (120)	<i>EML4</i>	<5%	Cyto	Lin et al. (2009)
CRC	t(2;2)(p23.3)	C2orf44-ALK (ND)	<i>C2orf44</i>	N/A	Cyto	Lipson et al. (2012)
BC	inv(2)(p21;p23)	EML4-ALK (120)	<i>EML4</i>	<5%	Cyto	Lin et al. (2009)

ND, not determined; Cyto, cytoplasmic; N/M, nuclear/membrane; N/A, non-assessed; ALCL, anaplastic large cell lymphoma; DLBCL, diffuse large B-cell lymphoma; IMT, inflammatory myofibroblastic tumor; ESCC, esophageal squamous cell cancer; RCC, renal cell cancer; NSCLC, non-small-cell lung cancer; CRC, colon-rectal cancer; BC, breast cancer.

Reprinted with consent from “Tobbo F, *et al.* ALK signaling and target therapy in anaplastic large cell lymphoma. *Front Oncol.* 2012; 2(41).” Frontiers in Oncology is an open-access journal, which permits non-commercial use, distribution, and reproduction in other forums, provided the original authors and source are credited.

### 1.2.5 NPM-ALK–mediated transformation

ALK+ALCL cells are highly ALK-addicted (56). Since ~85% of ALK+ALCL cases express NPM-ALK chimeric kinase, NPM-ALK is the most well studied ALK fusion kinase in ALK+ALCL (3). The oncogenic potential of NPM-ALK fusion kinase has been well established both *in vitro* and *in vivo* (50). The transformative ability of NPM-ALK was first validated in mice transplanted with NPM-ALK–transduced bone marrow progenitors (60). In a recent study, Zhang *et al* showed that NPM-ALK is able to transform human CD4+ T lymphocytes, and the transformed T cells were morphologically and immunophenotypically similar to patient-derived ALK+ALCL cells (61). These transformed T cells implanted into immunodeficient mice developed tumors that are indistinguishable from human ALK+ALCL tumors (61). However, it is still controversial in terms of the cell lineage of NPM-ALK–induced hematopoietic lymphoma in NPM-ALK transgenic mice (50). Some studies have revealed that NPM-ALK transgenic mice develop T-cell lymphoma (60-63); while evidence from other studies have supported that NPM-ALK transgenic mice develop B-cell lineage lymphoma (60, 64-66), even when NPM-ALK expression was driven by a T-cell specific promoter (63, 65). Of note, Malcolm *et al* recently reported that CD4-driven NPM-ALK transgenic mice with RAG2<sup>-/-</sup> develops peripheral T cell lymphoma where the malignance arises in early thymic precursors, and more importantly, these murine tumors histologically resemble human ALK+ALCL (67). In this study, the authors also reported that NPM-ALK signaling mimics T-cell receptor (TCR)  $\beta$  signaling and induces the maturation of thymic T cell lymphomas (67). This study has provided a novel insight

on how NPM-ALK initiates peripheral T cell lymphoma in a mouse transgenic model that histologically resembles human ALK+ALCL.

Given that NPM-ALK transgenic mice do not develop classic ALK+ALCL tumors, it is reasonable to speculate that other factors, in addition to NPM-ALK, are required to fully drive ALK+ALCL pathogenesis (50). This notion has also been supported by the observation that a relatively high frequency of NPM-ALK transcripts can be detected in non-malignant cells (68).

### **1.2.6 NPM-ALK—interacting substrates and activated oncogenic signaling pathways**

A few studies have revealed a number of substrates of NPM-ALK by mass spectrometry-based proteomic approach. An study published in 2004 suggested that a total of 46 proteins were identified as substrates of NPM-ALK by co-immunoprecipitation with anti-ALK antibody, followed by electrospray ionization and tandem mass spectrometry, and these proteins include Jak2, Jak3, Stat3, PI3K, some adaptor molecules (such as Rho-GTPase activating protein), heat shock proteins (such as Hsp60 precursor), and phosphatases (protein phosphatase 2 subunit) (69). Voena *et al* used tandem mass spectrometry and found that NPM-ALK directly interacts and phosphorylates Shp2, also named protein-tyrosine phosphatase 2C (PTP-2C), in the tyrosine residues Y542 and Y580, thus promoting ALK+ALCL cell proliferation (70). More importantly, the authors unearthed that only the active form of NPM-ALK, but not the kinase dead NPM-ALK<sup>K210R</sup>, is able to bind and activate Shp2 (70). In parallel with this study, another group reported that NPM-ALK interacts and phosphorylates

protein-associated splicing factor (PSF) at Tyr293, resulting in its subcellular delocalization and dysfunction (71). In addition, the interaction between NPM-ALK and PSF depends on the active ALK kinase domain, as PSF does not bind kinase-dead NPM-ALK (71). More recent studies using advanced tandem mass spectrometry have revealed novel substrates of NPM-ALK, such as DNA mismatch repair protein MSH2 (72), and Wiskott-Aldrich syndrome protein (WASp), thus contributing to the tumorigenesis of ALK+ALCL cells (73).

In general, NPM-ALK, along with other ALK fusion kinases, exerts its oncogenic roles mainly by directly or indirectly interacting and activating a number of molecules involved in multiple oncogenic signaling pathways (56), including JAK/STATs (53), PI3K/AKT (54), RAS/MEK/ERK (74), and phospholipase C- $\gamma$  (PLC- $\gamma$ ) (75) (**Figure 1.5**).

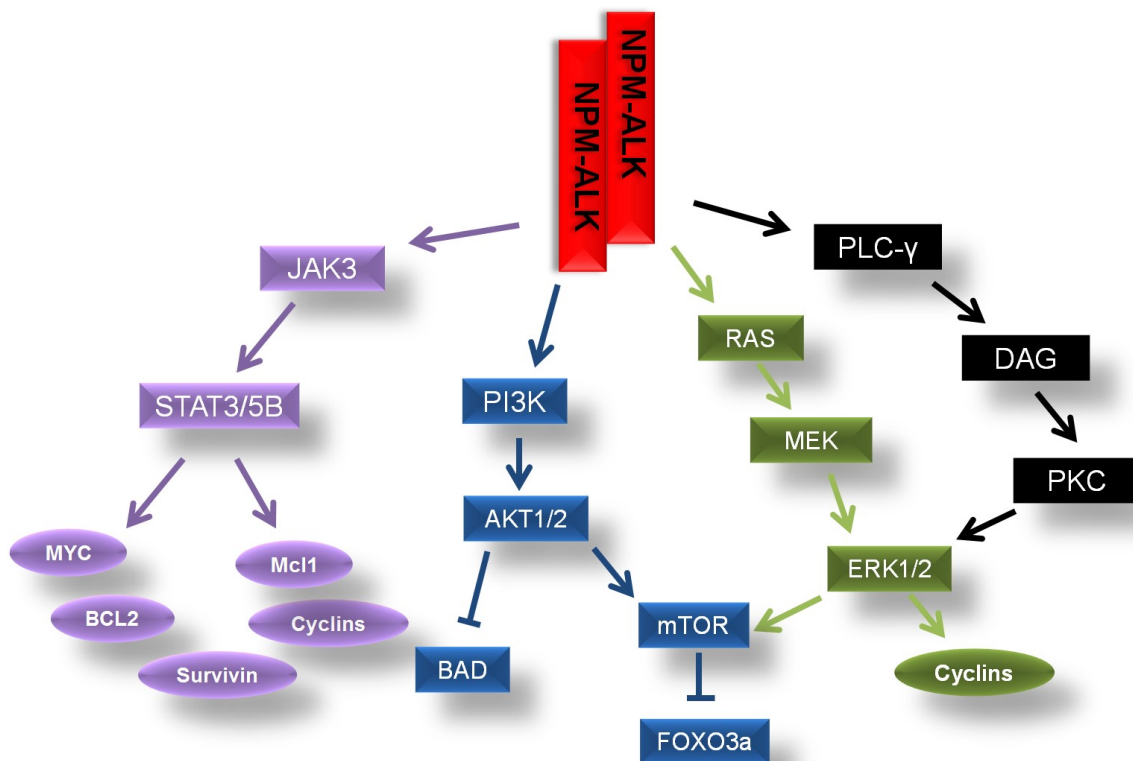


**Figure 1.5 Representative signaling pathways activated by NPM-ALK.** In ALK+ anaplastic large-cell lymphoma (ALK+ALCL), NPM-ALK interacts and activates many essential adaptors involved in multiple signaling pathways, including JAK/STATs, PI3K, RAS/MEK/ERK and PLC- $\gamma$ . Four representative signaling pathways are shown here.

NPM-ALK: Nucleophosphomin–anaplastic lymphoma kinase; STATs: Signal transducer and activator of transcription; PI3K: phosphatidylinositol 3 kinase; MAPK: Mitogen-activated protein kinase; ERK: extracellular signal-related kinase; PLC- $\gamma$ : phospholipase C  $\gamma$ . JAK3: Janus kinase 3; Bcl2: B-cell lymphoma 2; Mcl1: Myeloid cell lymphoma 1; BAD: Bcl-2-associated death promoter; mTOR: mammalian target of rapamycin; FOXO3a: Forkhead box protein O 3a; DAG: diacylglycerol; PKC: protein kinase C.

#### 1.2.6.1 JAK/STATs

##### A) JAKs and STAT3 in ALK+ALCL

The JAK/STAT pathway is one of the most studied pathways that are activated by NPM-ALK in ALK+ALCL (55). NPM-ALK fusion tyrosine kinase interacts and phosphorylates STAT3 at tyrosine 705 (pSTAT3<sup>Y705</sup>) (76), a critical residue for STAT3 activation and dimerization (77). Then the phosphorylated STAT3 forms homo or heterodimers with phosphorylated STAT3 or other family members of STATs, followed by translocation to the nucleus to execute as a transcription factor regulating a wide range of genes involved in cell proliferation, survival, and anti-apoptosis, such as *MYC*, *CCNDs*, *BCL2*, and *Survivin* (78). Indeed, high level of pSTAT3<sup>Y705</sup> and the nuclear localized pSTAT3<sup>Y705</sup> are always detected in ALK+ALCL primary tumor cells and cell lines (76, 79). Multiple factors contribute to the constitutive activation of STAT3 in ALK+ALCL (56). For instance, Han *et al* reported that JAK3, which can be activated by cellular cytokines such as interleukin 2 (IL2), IL4, IL9, IL13, IL15, and IL21 (80-85),

phosphorylates STAT3 at tyrosine 705 in ALK+ALCL (86). In keeping with this, two other studies have demonstrated that ALK+ALCL cells express IL9 and IL21, both of which are JAK3 activators (82, 85), to activate the JAK3/STAT3 axis (84, 87). In addition, JAK3 is directly phosphorylated and activated by NPM-ALK in ALK+ALCL (26). The significance of JAK3 for STAT3 activity is underscored by the finding that pharmaceutical inhibitor or siRNA knockdown of JAK3 downregulates the pSTAT3<sup>Y705</sup> level in ALK+ALCL (86, 88). Amin *et al* used co-immunoprecipitation assay and found that NPM-ALK, STAT3 and JAK3 physically interact with each other in ALK+ALCL cells, indirectly suggesting the close interaction between them (88). Further studies have demonstrated that the level of active JAK3 strongly correlates with the level of NPM-ALK and pSTAT3<sup>Y705</sup> in ALK+ALCL primary tumors (86). Intriguingly, one study reported that NPM-ALK induces the expression of IL22 and its receptor IL22R in ALK+ALCL, thus forming an autocrine stimulatory loop for JAK3/STAT3 activation (89).

STAT3 is a well-known potent oncogenic protein (90). Aberrant expression or activation of STAT3 has been widely observed in solid human tumors and haematological malignancies, including ALK+ALCL (91-95). STAT3 is known to be a key mediator of the NPM-ALK–induced transformation in ALK+ALCL (91). Inhibition of STAT3 activity by STAT3 dominant negative construct (96) or pharmaceutical reagent (97) induces significant cell-cycle arrest and cell apoptosis in ALK+ALCL cell lines. One study showed that siRNA knockdown of STAT3 in SupM2 cells, an ALK+ALCL cell line, modulates the expression of around 1500 genes, with approximately 900 of them downregulated (98). In addition, STAT3 transcriptionally induces the expression of DNA methyltransferases 1 (DNMT1) which thereafter physically interacts with STAT3 and

histone deacetylase 1 (HDAC-1) and binds to the promoter of the tumor-suppressor gene – Src homology region 2 domain-containing phosphatase-1 (*SHP1*), leading to the epigenetically silence of *SHP1* (99, 100). SHP1 is known as a tyrosine phosphatase that physically interacts with NPM-ALK, JAK3 and STAT3 in ALK+ALCL, subsequently resulting in the dephosphorylation of both NPM-ALK and JAK3/STAT3 and degradation of NPM-ALK and JAK3 in a proteasomal pathway (101, 102). Similarly, *STAT5A* is also epigenetically silenced by STAT3-induced DNA methylation (103). As a member of the STAT family, *STAT5A* functions as a negative regulator of NPM-ALK expression in ALK+ALCL, evidenced by that restoration of *STAT5A* expression transcriptionally downregulates the expression of NPM-ALK and decreases the level of pSTAT3<sup>Y705</sup> (103). In contrast, *STAT5B* functions as an oncogenic protein to promote cell proliferation and growth upon NPM-ALK phosphorylation and activation (104). The relationship between NPM-ALK, JAKs, STAT3, *STAT5A* and *STAT5B* has been briefly illustrated in **Figure 1.6**.

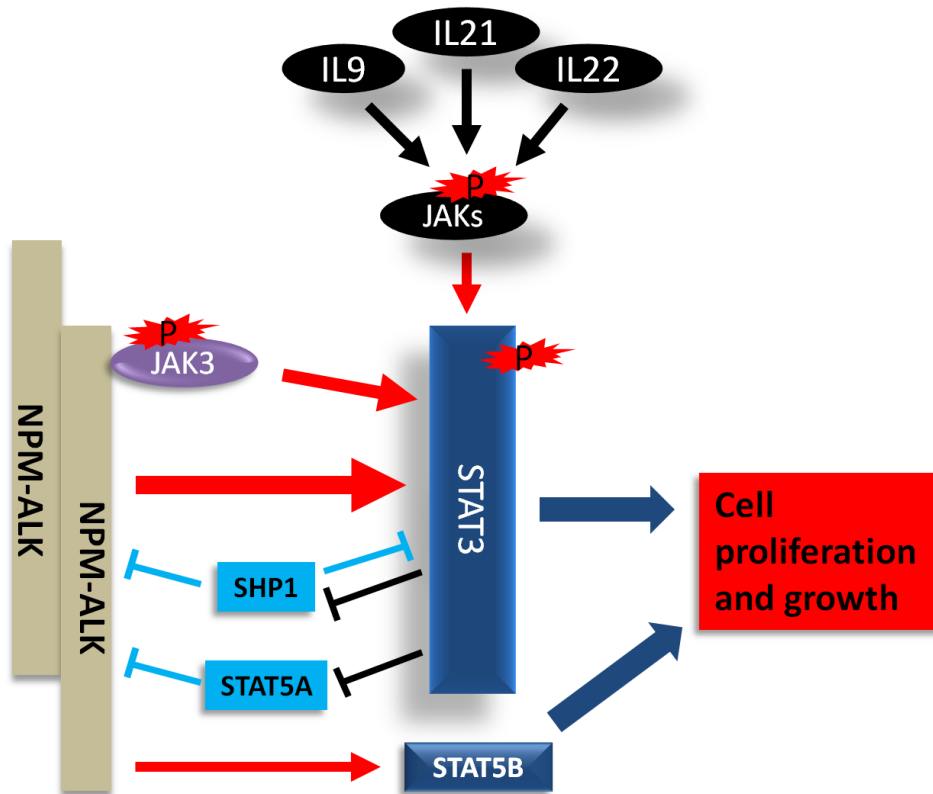


**Figure 1.6 NPM-ALK activates STATs signaling pathway in ALK+ALCL.** Signal transducer and activator of transcription 3 (STAT3) can be directly activated by NPM-ALK, or indirectly through Janus kinase 3 (JAK3). Besides, ALK+ALCL cells express interleukin 9 (IL9), IL21 and IL22, which are JAKs' activator, to activate STAT3 as well. The activated STAT3 signaling potently promotes cell proliferation and growth by regulating a number of genes, such as *Survivin*, *B-cell lymphoma 2 (BCL2)* and *BCL-X<sub>L</sub>*. Src homology region 2 domain-containing phosphatase-1 (*SHP1*) and *STAT5A* are reported to be methylated and silenced in ALK+ALCL because of STAT3. If their expressions are restored, both SHP1 and STAT5A act as negative regulators of NPM-ALK/STAT3 axis by transcriptionally downregulating the expression of NPM-ALK and decreasing the level of pSTAT3<sup>Y705</sup>. In addition, STAT5B, another family member of STATs, is also phosphorylated and activated by NPM-ALK, thus promoting cell growth and proliferation.



## B) STAT1

### IFNs/STAT1 signaling

STAT1 is the first-discovered member of STATs family (90). Induction of STAT1 activation occurs through cytokines, growth factors, and hormones (105). STAT1 is well-known as the main mediator of both type I interferon (IFN $\alpha/\beta$ ) and type II interferon (IFN $\gamma$ ) signaling pathway in immune responses, thus it is regarded as an important component in immune system (106, 107). Upon type I IFN binding with cellular receptor IFN alpha receptor (IFNAR1/2), the endogenous kinase JAK1 and tyrosine kinase 2 (TYK2) are recruited to the cytoplasmic domain of IFNAR1/2, followed by phosphorylation and activation; and the activated JAK1 and TYK2 reversely phosphorylate IFNAR1/2 (105, 106). The phosphorylated IFNAR1/2 thus create docking sites for STAT1 and STAT2, another member of STATs family, and then the phosphorylated JAK1 and TYK2 that bound to the cytoplasmic domain of IFNAR1/2 phosphorylate STAT1 and STAT2, then the phosphorylated STAT1 and STAT2 form homodimers or heterodimers and subsequently migrate to the nucleus to regulate a number of IFN-related genes (**Figure 1.7**) (105, 106). Specifically, STAT1/STAT2 heterodimers or STAT1 homodimers bind to the IFN-stimulated response element (ISRE) promoter sequence or the IFN--activated-site (GAS) promoter sequences, respectively, to stimulate IFN-stimulated gene transcription (105, 106). As for type II IFN signaling pathway, the binding of IFN $\gamma$  and its receptor IFN $\gamma$  receptor 1/2 (IFNGR1/2) phosphorylates and activates JAK1 and JAK2, following by the phosphorylation of IFNGR1/2 (105, 106). The phosphorylated IFNGR1/2 thus create docking sites for STAT1 which subsequently is phosphorylated by JAK1 and

JAK2, and consequently the phosphorylated STAT1 homodimerizes with itself and migrate to the nucleus to bind to GAS promoter sequence to function as transcription factors (**Figure 1.7**) (106).

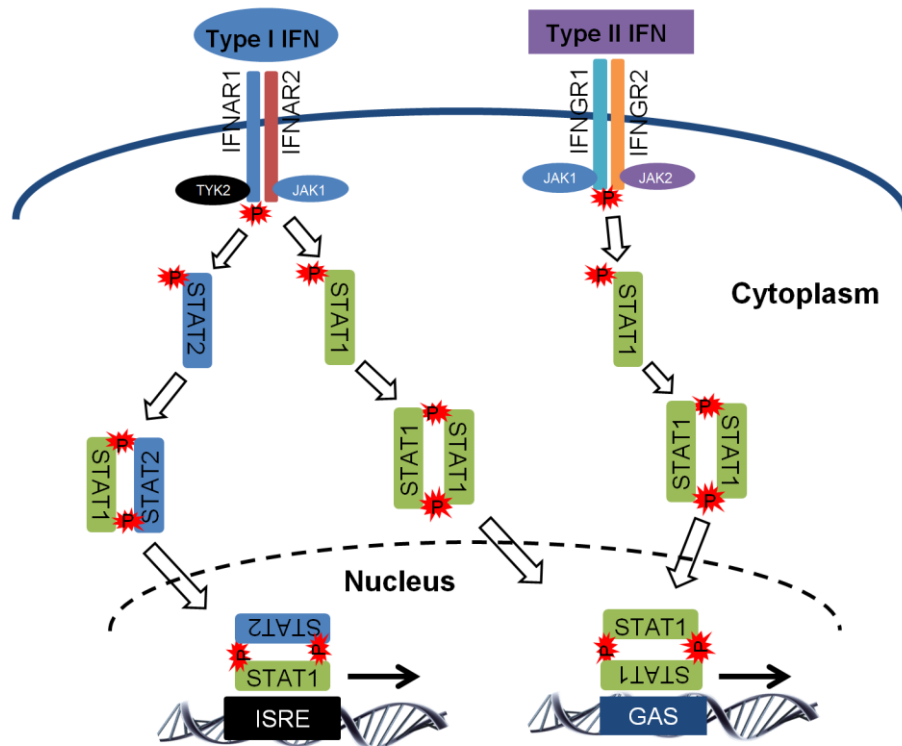


**Figure 1.7 Signal transduction of the IFN/STATs.** Binding of type I and type II IFNs to their respective receptors (IFNAR1/2 for type I and IFNGR1/2 for type II) leads to the activations of Janus kinases 1 (JAK1) and tyrosine kinase 2 (TYK2) for IFNAR1/2, and JAK1 and JAK2 for IFNGR1/2. The activated JAKs and TYK2 subsequently phosphorylate the respective receptors, which thereby create docking sites for signal transducer and activator of transcription 1 (STAT1) or STAT2. STAT1 and STAT2 are phosphorylated on tyrosine residues by JAKs and TYK2 once they bound to the docking sites of the IFNs receptors. Phosphorylated STATs form STAT1 homodimers and STAT1/STAT2 heterodimers which move to the nucleus to function as transcription factors. STAT1 homodimers bind to IFN--activated-site (GAS) promoter sequences and

STAT1/STAT2 heterodimers bind to the IFN-stimulated response element (ISRE) promoter sequence, respectively, to stimulate IFN-stimulated gene transcription.

### **STAT1 is degraded in ubiquitin-dependent proteasome pathway**

Ubiquitin-dependent proteasome pathway is an important biological process that regulates the degradation of cellular proteins by ubiquitinating substrate proteins, followed by protein degradation in 26S multisubunit proteasome system (108). This biological process requires the involvement of a sequential of ubiquitin-related enzymes including ubiquitin-activating enzymes (E1), ubiquitin-conjugating enzymes (E2), and ubiquitin ligases (E3) (108). In brief, the E1 enzyme activates ubiquitin, which is subsequently transferred to ubiquitin-conjugating enzymes E2; then the ubiquitin is transferred to the substrate protein with the assist of specific E3 ligase (109). Consequently, the ubiquitin-tagged substrate protein is degraded in the 26S proteasome (109). Mounting studies have suggested that STAT1 is degraded in ubiquitin-dependent proteasome pathway (110-115). In a study published in 2008, the authors reported that ERK1/2 phosphorylates STAT1 at serine 727 and downregulates its expression in ubiquitin-dependent proteasome pathway in mouse embryonic fibroblasts model, in which the F-box E3 ligase  $\beta$ TRCP promotes STAT1 ubiquitination (112). In a recent study, an E3 ligase smad ubiquitination regulation factor 1 (Smurf1) is reported to ubiquitinate and degrade STAT1 in human embryonic kidney 293 cells (113). More recently, one study revealed that pSTAT1<sup>Y701</sup>, the active form of STAT1, is the primary form of ubiquitinated STAT1 induced by IFN $\gamma$  in 293T cells, and it is rapidly degraded in K48-linked ubiquitin-proteasome pathway (111). Moreover, the authors of

the study also demonstrated that the deubiquitinase USP2a interacts with pSTAT1<sup>Y701</sup> in the nucleus and abrogates the ubiquitination and degradation of pSTAT1<sup>Y701</sup> (111). Surprisingly, Lawrence and Kornbluth recently reported that an E3 ubiquitin ligase – Natural Killer Lytic-Associated Molecule (NKLAM) ubiquitinates STAT1, but positively regulates STAT1 transcriptional activity and its DNA binding ability in mice macrophage cells (110).

### **The biological function of STAT1**

STAT1 has been reported to be a tumor suppressor by transcriptionally regulating the expression of a host of pro-apoptotic and anti-proliferative genes, such as Interferon response factor -1 (*IRF-1*) (116), caspases (117), members of the death receptor family (118), *BCL-X<sub>L</sub>* and *BCL-2* (119, 120). A number of studies have suggested that STAT1 antagonizes the transcriptional activity of the oncogenic protein STAT3 in some models (90, 120-122). The tumor suppressor function of STAT1 is also indicated in an *in vivo* study showing STAT1<sup>-/-</sup> double knockout mice are more vulnerable to virus and bacterial infections and also prone to develop tumors upon exposure to cancer-inducing chemicals (123, 124). STAT1-deficient female mice also spontaneously develop mammary adenocarcinomas (125). In keeping with its tumor suppressor function, STAT1 expression is frequently absent or decreased in various types of cancer, including oral squamous cell carcinoma (126), melanoma (127, 128), cutaneous T-cell lymphoma (129), breast cancer (130) and esophagus squamous cancer (131, 132). How STAT1 is downregulated in cancer remains poorly understood. There is one relevant report, in which *STAT1* gene promoter was found methylated in human head

and neck squamous cancer (133). Nevertheless, a few studies have concluded that STAT1 is a tumor promoter in some cancer models, such as breast cancer (134), T-cell acute lymphoblastic leukemia (135) and late-stage melanoma (136). These contradictory findings indicate the dilemma functions of STAT1 in cancer in a cellular context-dependent manner (90).

#### **1.2.6.2 PLC- $\gamma$**

PLC- $\gamma$  is an enzyme that cleaves phospholipids (137). The activation of PLC- $\gamma$  by cell receptor tyrosine kinases (RTKs) results in the hydrolysis of phosphatidylinositol (PIP2) into two secondary messages, inositol triphosphate (IP3) and diacylglycerol (DAG) (137). IP3 stimulates the release of  $\text{Ca}^{2+}$  from the endoplasmic reticulum, and DAG interacts and activates the serine/threonine protein kinase C (PKC) (137, 138). NPM-ALK tyrosine residue 664 (Y664) directly interacts with PLC- $\gamma$  and leads to the activation of PLC- $\gamma$  (75). The significance of PLC- $\gamma$  to the NPM-ALK-induced transformation is underscored by the finding that mutant NPM-ALK<sup>Y664F</sup> cannot bind or activate PLC- $\gamma$  and demonstrated attenuated transforming ability in Ba/F3 and Rat-1 cells, which can be partially rescued by the overexpression of PLC- $\gamma$  (75).

#### **1.2.6.3 PI3K/AKT**

NPM-ALK also activates the PI3K/AKT pathway in ALK+ALCL (54). Activation of the PI3K/AKT pathway promotes cell growth of ALK+ALCL cells (54, 139). Inhibition of PI3K/AKT pathway by either pharmacologic inhibitors, or dominant-negative *PI3K*, or

*AKT* mutants suppress cell growth or induce cell apoptosis in multiple types of cells transfected with *NPM-ALK* (54, 139).

PI3K contains two subunits including a catalytic subunit p110 and a regulatory subunit p85 (140, 141). *NPM-ALK* fusion kinase binds to p85 and phosphorylates PI3K, which subsequently phosphorylates and activates the serine/threonine kinase *AKT* (also known as protein kinase B) at threonine 308 (54, 56). However, the maximal activation of *AKT* requires additional phosphorylation at serine 473 (141). The fully activated *AKT* regulates diverse cellular processes, such as protein synthesis, cell anti-apoptosis/survival, cell growth and proliferation, cell metabolism, and cell migration/invasion (141, 142). Specifically, activated *AKT* suppresses the pro-apoptotic protein Bcl2-associated death promoter (BAD), and thus leads to the increase of anti-apoptotic protein Bcl-X<sub>L</sub> (143). On the other hand, activated *AKT* promotes cell survival by increasing the activity of nuclear factor kappa-light-chain-enhancer of activated B cells (NF-κB) and promoting the degradation of inhibitors of κB (IκB), which sequesters the nuclear translocation of NF-κB (144). The activated PI3K/*AKT*-promoted cell growth of ALK+ALCL is also partially dependent on the activated Sonic Hedgehog (SHH) pathway, which is downstream of *AKT* signaling (145, 146). In addition, activated *AKT* suppresses cell apoptosis by inhibiting the activity of caspase 9 and decreasing the expression of FAS ligand (147, 148). *NPM-ALK*-induced activation of PI3K/*AKT* pathway phosphorylates Forkhead family of transcription factors 3a (FOXO3a) and prevents its nuclear translocation, consequently leading to the degradation of FOXO3a in a proteasome pathway (149-151). The degraded FOXO3a links to the downregulation of the negative regulator of cell cycle progression p27<sup>Kip1</sup> and Bim 1, as

well as the upregulation of cyclin D2 (150, 151). A brief interaction between NPM-ALK and PI3K/AKT has been illustrated in **Figure 1.8**.

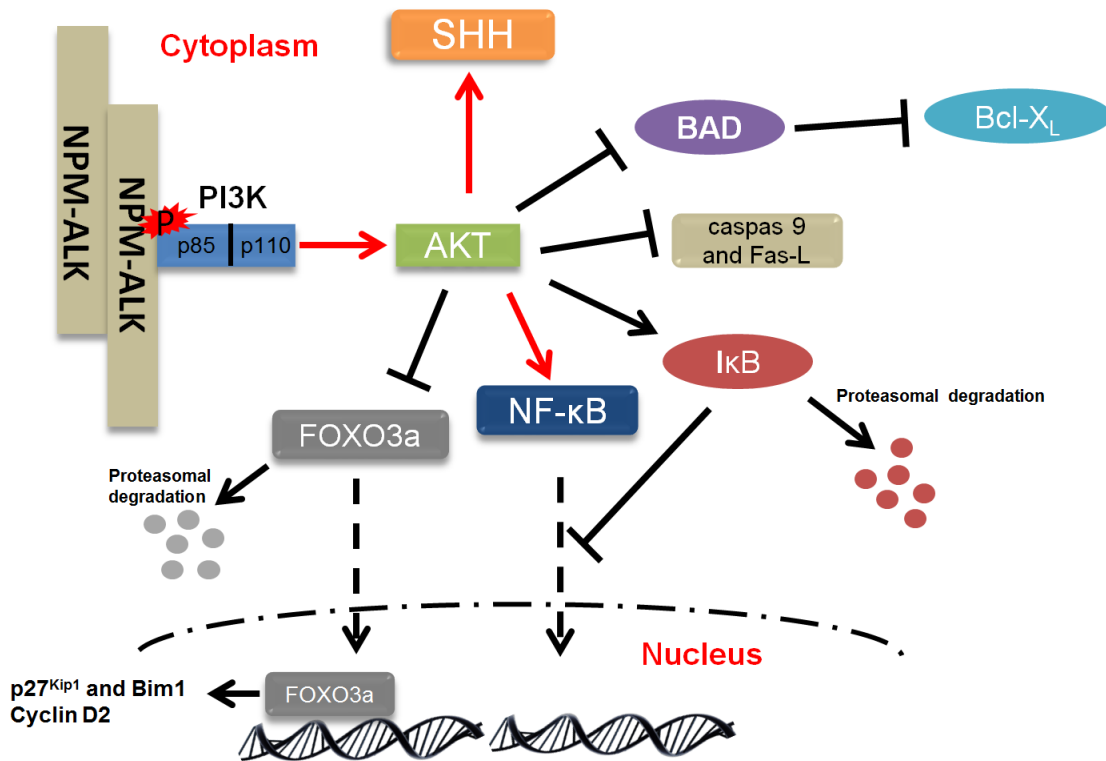


**Figure 1.8 NPM-ALK activates the PI3K/AKT pathway in ALK+ALCL.** NPM-ALK phosphorylates and activates PI3K at p85 subunit, which subsequently activates the serine/threonine kinase AKT. The activated AKT phosphorylates Forkhead family of transcription factors 3a (FOXO3a) and promotes FOXO3a degradation in a proteasome pathway. Phosphorylation of the FOXO3a sequesters its nuclear translocator to upregulate the negative regulator of cell cycle progression p27<sup>Kip1</sup> and Bim1 and downregulate cyclin D2. Activated AKT also promotes the activity of nuclear factor-κB (NF- κB) by degrading inhibitor of κB (IκB) in a proteasomal pathway. IκB inhibits the activity of NF- κB by preventing the nucleus translocation of NF- κB. The phosphorylated AKT also suppresses the activity of caspases 9 and the expression of Fas ligands (FAS-L), as well as the activity of Bcl 2-associated death promoter (BAD) which

suppresses the expression of anti-apoptotic protein Bcl-X<sub>L</sub>. In addition, AKT signalling also promotes the expression of sonic hedgehog (SHH), which also contributes to the cell proliferation of ALK+ALCL.

#### **1.2.6.4 RAS/MEK/ERK**

The serine/threonine kinase ERK1/2-mediated pathway is known to promote cell growth, survival, differentiation, and migration (152). ERK1/2 can be activated by many growth factors and some kinases through the activation of the Ras GTPase following by the phosphorylation and activation of Raf1 (153). While the NPM-ALK-induced activation of MEK/ERK appears to be independent of Raf-1, as inhibition of Raf-1 with pharmacological inhibitors or siRNA knockdown of Raf-1 have no effects on ERK1/2 phosphorylation induced by NPM-ALK (154). The activated RAS/MEK/ERK pathway can be found in both ALK+ALCL cell lines and primary tumor samples (154). Inhibition of ERK1/2 by MEK1/2 inhibitor U0126 or siRNA knockdown of ERK1 suppresses cell growth and induces cell apoptosis in ALK+ALCL cell lines, supporting the role of the ERK1/2 pathway in promoting the cell growth of ALK+ALCL cells (154). NPM-ALK-mediated activation of ERK1/2 activates E26 transformation-specific-1 (ETS-1) in ALK+ALCL (155). Interestingly, the transcriptional active ETS-1 enhances the gene promoter activation of JunB, which is reported to promote CD30 expression; and the upregulated expression of CD30 in turn activates ERK1/2 in ALK+ALCL, thus creating a positive forward loop in ALK+ALCL (155, 156).



#### **1.2.6.5 mTOR**

In ALK+ALCL, the serine/threonine kinase mTOR is also activated by NPM-ALK mediated by PI3K/AKT and RAS/MEK/ERK (155, 157). The biological significance of mTOR is underlined by the fact that inhibition of mTOR by pharmaceutical inhibitor rapamycin induced significant cell apoptosis in ALK+ALCL cell lines (158). mTOR regulates a number of genes associated with protein translation, cell proliferation, and survival (159, 160). For instance, mTOR phosphorylates and activates p70S6K (also known as ribosomal protein S6 kinase beta-1), which thereafter phosphorylates and activates ribosomal protein S6 (RPS6) to regulate protein synthesis and enhance cell growth (161).

#### **1.2.7 Therapeutic strategy for ALK+ALCL patients**

As indicated above, ALK+ALCL generally have a better prognosis in comparison to ALK-ALCL (7). Cyclophosphamide, hydroxydaunorubicin (doxorubicin), oncovin (vincristine), and prednisone (CHOP)—based therapeutic regimen is the standard treatment for aggressive lymphomas, including ALK+ALCL (1). Brentuximab vedotin has also showed encouraging clinical outcomes when it was applied to treat CD30+ peripheral T-cell lymphomas (including ALK+ALCL), either as a follow-up treatment with CHOP or a combination with CHP (due to the overlapped neurotoxicity between vincristine and Brentuximab vedotin) as the front-line treatment (1, 162). CHOP-based standard treatment induces complete remission in most of ALK+ALCL patients, but up to 40% of patients still develop tumor relapses and chemoresistance (55). Patients with

relapsed or refractory disease usually benefit from high-dose of chemotherapy or autologous stem cell transplantation (8).

Although stem cell transplantation is an effective therapeutic regimen for relapsed ALK+ALCL patients, novel therapy based on the pathobiology of ALK+ALCL is warranted (55). As ALK+ALCL cells are very much NPM-ALK addicted, this chimeric protein has become an obvious and easy therapeutic target for this disease, supported by a number of *in vitro* and *in vivo* studies (50, 163-165). As the discovery of full length, translocated, or mutated ALK contributing to the tumorigenesis of neuroblastoma or non-small-cell lung cancer, a number of small molecular inhibitors targeting ALK have been developed (166-168). For instance, crizotinib is a small molecule inhibitor developed for targeting ALK, c-Met/Hepatocyte growth factor receptor (HGFR) and c-ros oncogene 1 (ROS1), and it specifically binds within the ATP-binding pocket of target kinases (168). In 2011, the U.S. Food and Drug Administration (FDA) approved crizotinib (PF-02341066; Trade name: Xalkori, Pfizer) for the treatment of late-stage ALK-positive non-small-cell lung cancers (169). Currently, crizotinib is also undergoing clinical trials for treating patients with ALK+ALCL and neuroblastoma (170, 171). Results from a small number of clinical trials have shown the effectiveness of crizotinib in pediatric ALK+ALCL patients and the relapsed/refractory patients (170). Despite the success of crizotinib, crizotinib-resistance still could happen in ALK+ALCL patients and other ALK-positive malignancies (172, 173). The novel therapeutic strategies overcoming the potential crizotinib-resistance to this type of malignancy generally involve targeting NPM-ALK downstream molecules in combination with ALK inhibitors (1, 8, 174).

## 1.3 Wnt/ $\beta$ -catenin

### 1.3.1 Wnt/ $\beta$ -catenin signaling

One of the most extensively studied and important cellular signaling pathways in cancer is the Wnt/ $\beta$ -catenin pathway, also known as the Wnt canonical pathway (175). The Wnt/ $\beta$ -catenin pathway is highly conserved among different species (175). Wnt ligand family has 19 members in *Homo sapiens*, while only portions of them, such as Wnt1, Wnt2B, Wnt3 and Wnt5, can activate Wnt/ $\beta$ -catenin pathway (175). In the absence of Wnt ligands,  $\beta$ -catenin remains in a cytoplasmic destruction complex containing adenomatous polyposis coli (APC), Axin, casein kinase 1 $\alpha$  (CK1 $\alpha$ ), and glycogen synthase kinase-3 $\beta$  (GSK3 $\beta$ ), and then  $\beta$ -catenin is phosphorylated by CK1 $\alpha$  and GSK3 $\beta$ , following by degradation in ubiquitin-dependent proteasome pathway (176, 177) (**Figure 1.10**). In the presence of canonical Wnt ligands, the interaction between Wnt ligands with their cell-surface receptor complex consisting of LRP5/6 and Frizzled (FZD) breaks the destruction box by phosphorylating the cytoplasmic protein disheveled (Dvl) and GSK3 $\beta$  (176, 177). The phosphorylated GSK3 $\beta$  leaves  $\beta$ -catenin in the destruction box dephosphorylated, resulting in  $\beta$ -catenin stabilization and accumulation in cytoplasm, following by its translocation into nucleus as a transcription factor (176, 177). The nuclear  $\beta$ -catenin enhances the activity of the transcription factor T-cell factor (TCF)/lymphoid enhancer factor (LEF) and stimulates the expression of their downstream targets (e.g. *CCND1*, *MYC* and *TWIST*) that are involved in some critical biological processes such as cell growth, proliferation, migration, metastasis, etc (176, 177) (**Figure 1.9**). The Wnt/ $\beta$ -catenin pathway is known to be critical for homeostatic maintenance of tissues and organs, and thus its activity is stringently regulated during

normal development (178). Deregulation of the Wnt/ $\beta$ -catenin pathway is implicated in various diseases, including cancers (178).

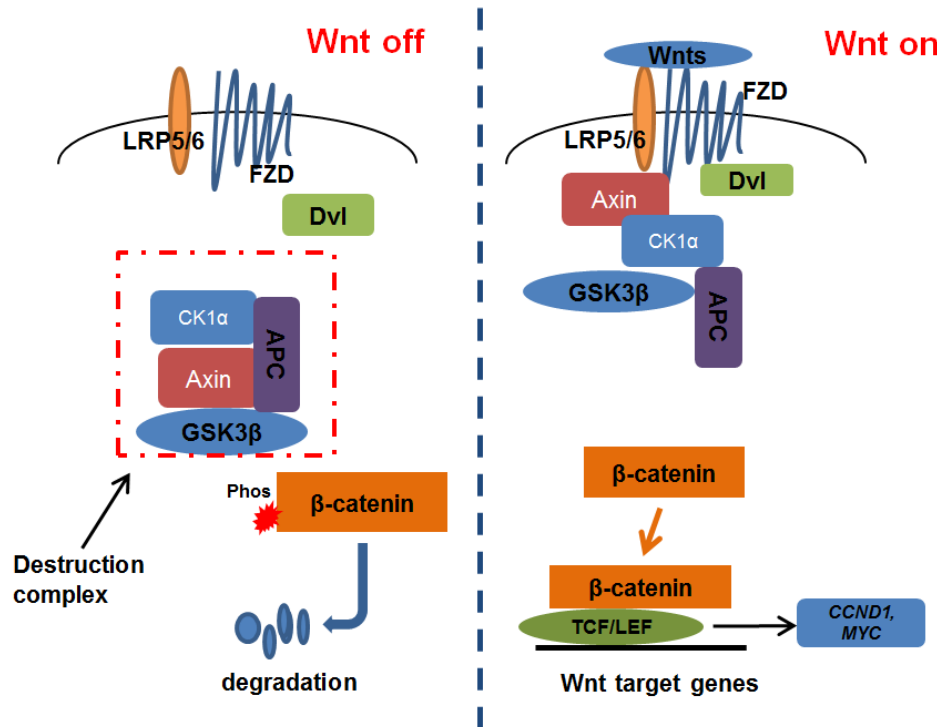


**Figure 1.9 Overview of the Wnt/ $\beta$ -catenin pathway.** In the absence of Wnt ligands,  $\beta$ -catenin remains in the destruction complex containing adenomatous polyposis coli (APC), Axin, casein kinase 1 $\alpha$  (CK1 $\alpha$ ), and glycogen synthase kinase-3 $\beta$  (GSK3 $\beta$ ), where it is phosphorylated by CK1 $\alpha$  and GSK3 $\beta$ , following by degradation in ubiquitin-dependent proteasome pathway (**Left panel**). In the presence of Wnt ligands, the interaction between Wnt ligands with their cell-surface receptor complex consisting of LRP5/6 and Frizzled (FZD) interrupt the destruction box by phosphorylating disheveled (Dvl) and GSK3 $\beta$ , and inhibiting GSK3 $\beta$ -mediated phosphorylation of  $\beta$ -catenin. The dephosphorylation of  $\beta$ -catenin leads to its stabilization and accumulation and translocation into nucleus where it exerts as a transcription factor. The nuclear  $\beta$ -catenin cooperates with the transcription factor T-cell factor (TCF)/lymphoid enhancer factor (LEF) to promote the expression of their downstream targets, including *CCND1* and *MYC* (**Right panel**).

### 1.3.2 Wnt/ $\beta$ -catenin in cancer and ALK+ALCL

Upregulated Wnt/ $\beta$ -catenin activity has been widely observed in human cancers (177). For example,  $\beta$ -catenin is deregulated in 21% of cases of primary cutaneous B-cell lymphomas and 42% of cases of cutaneous T-cell lymphoma (179). The constitutive activation of the Wnt/ $\beta$ -catenin pathway is also reported in mantle cell lymphoma and ALK+ALCL (180-182). Lai lab previously described that  $\beta$ -catenin is constitutively active in ALK+ALCL cells, and knockdown of this pathway by  $\beta$ -catenin siRNA transfection results in significant cell death in ALK+ALCL cell lines (182). Strikingly, Lai group also found that siRNA knockdown of  $\beta$ -catenin dramatically decreases the levels of pSTAT3<sup>Y705</sup> and STAT3, representing yet another mechanism by which STAT3 in ALK+ALCL (182). Of note, unlike the relationship between Break Point Cluster-Abelson (BCR-ABL) tyrosine kinase and  $\beta$ -catenin in chronic myeloid leukemia (CML), NPM-ALK does not regulate the protein level, nuclear localization or tyrosine phosphorylation of  $\beta$ -catenin but the transcriptional activity of Wnt/ $\beta$ -catenin in ALK+ALCL (182, 183). In normal cells,  $\beta$ -catenin is phosphorylated at multiple serine/threonine residues by GSK3 $\beta$  and therefore downregulated in ubiquitin-proteasome pathway (175). One recent report suggested that NPM-ALK phosphorylates GSK3 $\beta$  on Serine 9 through the PI3K/AKT pathway (184). Considering the negative role of active GSK3 $\beta$  on the protein level of  $\beta$ -catenin, this report correlates well with the findings of constitutively active  $\beta$ -catenin in ALK+ALCL cells (168, 170).

## **1.4 Cancer stem cells (CSCs)**

The CSCs are a small fraction of cells within tumor bulks that have the ability to initiate the whole tumor bulks and are also capable to self-renew to maintain the small population (185). This small cell population is also called tumor-initiating cells (TICs) or tumor stem cells (TSCs) (186). Like normal stem cells, CSCs are not only capable to self-renew to maintain the CSCs population, but also able to differentiate into non-CSCs, resulting in the heterogeneity of tumor cells (186, 187). It is widely accepted that CSCs are responsible for chemoresistance and tumor relapses in cancer patients, as it is believed that conventional chemotherapy only eliminates the major population of tumor cells but leave CSCs untouched (188).

### **1.4.1 Identification and Isolation of CSCs**

CSCs population was firstly described in human acute myeloid leukemia (AML) in 1997 (189). Since then, the CSCs have been identified in various types of cancers including breast cancer, colon cancer, prostate, esophagus squamous cancer, lung cancer (185). Up to date, multiple assays and approaches have been developed to identify the CSCs population, such as side population assay (using Hoechst 33343 dye efflux assay), specific cell surface markers detection, tumorsphere formation assay and serial transplantation assay (188).

The side population assay is a flow cytometric approach based on the dye efflux properties of ATP-binding cassette (ABC) transporters (190). This assay has been performed in multiple studies to identify the CSC population derived from a number of

cancers including ovarian cancer (191, 192), breast cancer (193, 194), head and neck cancer (195), renal cell carcinoma (196), as well as ALK+ALCL (197). Nevertheless, there are two major limitations of this assay (198). Firstly, the side population cells contain both CSCs and non-CSCs, and they do not represent all CSCs (198). Secondly, Hoechst 33342, used in this assay for isolating side population cells, cannot be applied to many types of cells because of its cellular toxicity (198). Furthermore, the side population assay has also received many criticisms because of its relatively high technical challenges, poor consistency and low reproducibility (190). As for specific cell surface markers' staining, it has also been widely deployed to identify the CSC population. For instance, CD44<sup>High</sup>/CD24<sup>Low</sup> and Aldehyde dehydrogenase<sup>High</sup> (ALDH<sup>high</sup>) have been considered as stem cell markers for both breast cancer and esophagus squamous cells (199-203). The CD133 has also been reported to be a CSCs marker for both colon cancer and brain cancer (204, 205). Like side population cells, stem cell markers positive cells do not represent all the CSCs, which also include non-CSCs. As for tumorsphere formation assay, it is a valuable tool to identify CSCs *in vitro*, as cells with high ability of self-renewal and differentiation are expected to grow into colonies in serum-free medium or in soft agar/methylcellulose medium (188). However, this *in vitro* assay has many limitations. For instance, this assay only measures *ex vivo* cell proliferation but not tumor propagating ability *in vivo* (188). Therefore, *in vivo* study is always required to confirm the results of this *in vitro* assay (188). Last but not the least, serial transplantation assay is regarded as the gold standard assay to identify CSCs because this assay fulfills two criteria of CSCs including the ability to self-renew and initiate the tumor bulks (188). This assay has been widely used in a number of studies of identifying CSCs (185, 186, 188, 197, 206). Briefly, in this assay, tumor cells are

transplanted into the immunodeficient mice, then the xenograft tumors formed by the tumor cells are isolated, diluted and implanted into the new immunodeficient mice, if applicable, the newly formed xenograft tumors are again isolated, diluted and implanted into new immunodeficient mice to test the tumor cells' self-renewal and tumor-initiating ability.

#### **1.4.2 Molecular features of CSCs**

Mounting studies have suggested that CSCs carry elevated expression of some embryonic stem cells markers (e.g. MYC, Sox2, and Nanog) in comparison to tumor bulk cells (186). Two recent reports have showed that the tomaxifen-resistant triple-negative and estrogen receptor-positive (ER+) breast cancer cell lines have enriched breast CSCs which are characterized by elevated expression of Nanog, Oct3/4, and Sox2, as compared to their major cell populations (207, 208). MYC is also found highly expressed in glioma stem cells and CD34+ AML cells (considered as leukemia stem cells), as compared to their non-stem cells counterparts (209, 210). Importantly, the high level of MYC expression is critical for maintaining the CSC population, as inhibition of MYC in glioma stem cells and leukemia stem cells significantly decreases the CSC populations (209, 210). In addition to these embryonic stem cell markers, CSCs also overexpress ABC transporters, a cell surface protein family responsible for drug transportations. Among the family of ABC transporters, ABCG2 is the one that has been widely studied, and it is also the one that mainly confers to the side population cell phenotype by pumping out Hoechst 33342 dye efflux (198). Enriched expression of ABCG2 has been reported in a number of CSCs from various types of cancer, such as



lung cancer (211), hepatocellular carcinoma (212), retinoblastoma (213), and ALK+ALCL (197). Of note, ABCG2 may even serve as a potential biomarker for CSCs in some types of tumors (198).

### **1.4.3 Signaling pathways in CSCs**

Accumulated evidence have demonstrated that certain signaling pathways (e.g. Notch, SHH, Wnt/ $\beta$ -catenin and fibroblast growth factor-2), that are known to regulate the differentiation and self-renewal of normal embryonic stem cells (214), are specially more active in CSCs (186). These embryonic signaling pathways contribute to the self-renewal and tumor-initiating ability in CSCs (185, 186, 215). For instance, Jang *et al* reported that breast CSCs have enhanced Wnt/ $\beta$ -catenin activity, and inhibition of Wnt/ $\beta$ -catenin signaling suppresses breast cancer cells growth, tumorigenicity, metastasis and the expression of CSCs-related genes (216). The Wnt/ $\beta$ -catenin signaling is also found more active in leukemia-initiating cells (217, 218), and depletion of  $\beta$ -catenin results in impaired leukemogenesis in a BCR-ABL-induced CML mouse model (219, 220). Lai lab also recently reported that the PI3K/AKT/MYC pathway is elevated in cancer stem-like cells of esophagus squamous cancer cell lines, pharmacological inhibition of PI3K/AKT/MYC dramatically attenuates the cancer stemness features including chemoresistance and tumor formation ability (221). In a recent study, Justilien *et al* showed that the SHH pathway is elevated by phosphorylated Sox2 at threonine 118 in lung cancer stem-like cells, and the SHH pathway is essential for maintaining the CSC phenotype, as inhibition of this pathway diminishes the CSC phenotype (222).

#### 1.4.4 CSCs in ALK+ALCL

NHL is a heterogeneous malignance comprising more than 40 different entities classified by various parameters including morphology and immunophenotype (223). Most of NHLs are believed to originate from mature peripheral lymphocytes, such as many B-cell NHLs arise from germinal center cells (223, 224). However, evidence shows that T-cell lymphoblastic lymphoma cells originate from immature precursor lymphocytes in the thymus (223). Three recent studies have unearthed that ALK+ALCL tumor cells may originate from early thymic progenitor cells (67, 197, 225). Moti *et al* has reported that ALK+ anaplastic large-cell lymphoma-propagating cells isolated by side population assay share gene expression signatures with early thymic progenitors, indicating these tumor-propagating cells being of a primitive origin (197). The same research group further reported that the murine peripheral T cell lymphoma in CD4-driven NPM-ALK transgenic mouse arises in early thymocytes (67). In addition, Hassler *et al* recently compared the DNA methylation patterns of ALK+ALCL cells with T cells of different differentiation stages and found that the DNA methylation patterns of ALK+ALCL highly resemble progenitor thymic T cells, suggesting that ALK+ALCL occurs in progenitor thymic T cells rather than mature T cells (225). Notably, there is a single study to date that has unearthed the biology of CSCs in ALK+ALCL (197). In this report, Moti *et al* declared that they were able to use side population technique to find CSCs in ALK+ALCL cell lines and patient samples, and these CSCs not only give rise to the bulk population but also maintain the growth of entire cell population (197). Biochemically, ALK+ALCL CSCs are featured with relatively high expression of some embryonic stem cell or CSC markers including Sox2, Oct4, Klf4, and ABCG2, as

compared to the main cell population (197). Of note, these CSC cells also harbor elevated expression of NPM-ALK, and these CSCs cells show sensitivity to crizotinib due to the high level of NPM-ALK in this subset of cells, indicating that NPM-ALK may be a promising therapeutic target in these CSCs (197).

### **1.5 Inducible pluripotent stem cells (iPS) factors**

The iPS factors are those transcription factors being crucial for maintaining and promoting cell pluripotency (226). The biological significance of these factors including Oct4, MYC, Sox2, and Klf4 is highlighted by their ability to reprogramming fully differentiated somatic cells to iPS cells in certain conditions (227, 228). The expressions of these iPS factors usually are restricted to embryonic stem cells and some somatic stem cells (228). However, recent studies have reported that these iPS factors also have been detected in various types of cancer cells (229). Emerging evidence has suggested that these iPS factors contribute to the tumor cell growth and progression (230). For example, Klf4 is shown aberrantly expressed in pancreatic cancer cell lines and primary tumor samples (231), and it promotes cell-cycle progression by downregulating cell-cycle inhibitors p27<sup>Kip1</sup> and p21<sup>CIP1</sup> (231). For another instance, Sox2 and MYC are both aberrantly expressed in breast cancer cell lines and patients samples (232, 233), and the two proteins orchestrate to promote the tumorigenesis and cancer stemness of breast cancer cells (207, 232). Of the four iPS factors, Sox2 and MYC will be focused and discussed in my thesis.

### **1.5.1 Sox2**

The Sox (Sex determining region Y-Box) family members are a group of transcription factors containing a highly conserved DNA binding domain, namely, High Mobility Group DNA binding domain (HMG box domain) (234). The Sox family proteins are known to be involved in the regulation of embryonic development and determination of cell fate (234, 235). Sox2, as one of the Sox family members, is one of the four master iPS factors involved in reprogramming fibroblasts to iPS cells (227). In embryonic stem cells, Sox2 orchestrates with other factors, particularly Oct3/4, to maintain the cell pluripotency and self-renewal ability (236). Further studies have shown that Sox2 transcriptionally regulated genes often share a common DNA element Sox2-Oct cis-regulatory element where Sox2 and Oct3/4 can both bind synergistically, indicating these two factors cooperatively regulating target genes(236).

#### **1.5.1.1 Sox2 in cancer**

Although Sox2 expression is strictly existed in embryonic stem cells and some somatic stem cells, it is aberrantly expressed in various types of tumors, including breast cancer (232, 237), colon cancer (237), small-cell-lung cancer (238), and ALK+ALCL (239). The biological significance of Sox2 in cancer has been underlined by the fact that Sox2 regulates tumor metastasis (240), migration (241), and CSC populations in various cancer models (207, 232). Sox2 expression in some cancers is correlated with cancer stemness properties, such as chemoresistance (207), tumor initiation (242) and self-renewal ability (242). Indeed, as mentioned above, Sox2 expression is found enriched

in CSCs derived from multiple types of cancer cells, and knockdown of Sox2 using siRNA results in sensitization of cells to chemotherapy and the decreased CSCs population (242-244).

Sox2 has been shown to facilitate the G1/S transition and upregulate the cyclin D1 expression in breast cancer cells (245). In addition, Sox2 is reported to co-operate with  $\beta$ -catenin to promote Sox2 downstream targets expression, thus promoting cell proliferation and tumorigenesis (245). Besides, Sox2 is found to promote the expression of pluripotency-promoting signaling pathways or stem cell markers or proteins, such as Wnt/ $\beta$ -catenin, Notch, AKT/mTOR, and Hedgehog, as well as CD44, ALDH1 and MYC in some cancer cell models (222, 241, 246-249). Intriguingly, there is one study showing that Sox2 upregulates the Wnt/ $\beta$ -catenin pathway, which in turn upregulates Sox2 expression, thus forming a positive forward loop in breast cancer cells (207). Moreover, Sox2 is also reported to promote cell migration and invasion by promoting the epithelia-mesenchymal transition (EMT) through upregulating Slug expression and the Wnt/ $\beta$ -catenin pathway (250, 251). Our current understanding of Sox2 biological function in cancer is mostly based on the studies performed in solid tumor models, while the biological role of Sox2 in haematological malignance remains elusive (252). Lai lab previously determined that Sox2 is aberrantly expressed in ALK+ALCL, in which NPM-ALK/STAT3 axis is the main driver of Sox2 expression (239). Interestingly, Lai lab also revealed that Sox2 transcriptional activity is heterogeneous in ALK+ALCL cell lines (239); this phenomenon is not restricted to ALK+ALCL cells, as it is also observed in ER+ breast cancer cells (253).

### 1.5.1.2 Post-translational modifications of Sox2

The post-translational modifications of Sox2 and their regulations are poorly understood either in embryonic stem cells or cancer cells (235). Most of the studies on the Sox2 post-translational regulation are performed in mouse embryonic stem cells (mESCs) (254). In mESCs, AKT1 is reported to phosphorylate Sox2 at threonine 118 (T118) and stabilize it, and thereafter promote its transcriptional activity (255). The biological significance of phosphorylation of Sox2 at T118 is underscored by that mouse embryonic fibroblasts (MEFs) with phosphorylated Sox2 T118 enabling more efficient induction of iPS cells (255). In concert with this report, Fang *et al* reported the same findings in another study (256). Interestingly, Fang *et al* also reported that Sox2 protein and its transcriptional activity are regulated by a balanced methylation and phosphorylation switch in ESCs (256). Specifically, the authors suggested that Set7 monomethylates Sox2 at lysine 119 (K119), resulting in the decreased Sox2 transcriptional activity and degradation of Sox2 in ubiquitin-dependent proteasome pathway; on the other hand, AKT1 phosphorylates Sox2 at threonine 118 (T118) and stabilizes Sox2 protein by antagonizing K119me by Set7 (256). Furthermore, the increased Set7 expression correlates with decreased Sox2 expression and appropriate differentiation in their cultured embryoid bodies (EBs), which are in parallel with early embryonic developments (256). In addition, Ouyang *et al* reported that cyclin-dependent kinase 2 (Cdk2) physically interacts and phosphorylates Sox2 at two other phosphorylation sites, Ser 39 and Ser 253, both of which are required for establishing the pluripotent state but not for maintenance of ESC. Notably, a recent study has demonstrated that Sox2 transcriptional activity can be positively regulated by O-GlcNAc

(257). In this study, Sox2 is found to be O-GluNAcylated during reprogramming in mESCs, and Sox2 loses O-GlcNAcylation at Ser 248 upon induction of differentiation in mESCs (257). In the same study, authors also provided evidence that MEFs with an O-GlcNAc-deficient Sox2 (S248A) show increased somatic cell reprogramming efficiency (257).

However, post-translational regulation of Sox2 in human cancer remains poorly studied. Only two studies of Sox2 phosphorylation in cancer have been reported to date (222, 258). In one literature, the authors have demonstrated that protein kinase C $\gamma$  (PKC $\gamma$ ) phosphorylates Sox2 at T118, which then promotes the SHH signaling pathway by upregulating the SHH ligands, thus maintaining a cancer stem-like phenotype in lung squamous carcinoma cancer stem-like cell (222). In the other study, Sox2 is phosphorylated by aurora kinase A, which is a crucial process for maintaining the stem cell-like cell population in ovarian teratocarcinoma cell line PA-1 (258). Overall, our understanding of post-translational regulation of Sox2 in cancer is very limited.

### **1.5.2 MYC in cancer**

MYC family of protein comprises three members, c-MYC (also known as MYC), L-MYC, and N-MYC, and they all share the basic helix-loop-helix (bHLH) domain (259). The biological role of L-MYC is poorly understood (260). As for N-MYC, its expression is tissue specific and can be found in some mouse tissues of an early stage of development, such as kidney and forebrain (261). The overexpression of N-MYC is observed in some cancer, such as neuroblastoma and human small-cell lung cancer

(262, 263), and the high expression of N-MYC in cancer is correlated with worse clinical outcome (262-264). MYC, as a proto-oncogene, is generally expressed in a broad spectrum of tissues in both newborn and adult mice (259). As a transcription factor, MYC usually heterodimerizes with MYC-associated factor X (Max) and regulates their downstream targets (259). Like Sox2, MYC is also one of the four iPS factors which are indispensable for reprogramming and induction of iPSs (228). The biological significance of MYC has been highlighted by the fact that ~15% of human genes are the downstream targets of MYC (265).

It is necessary to stress that the expression of MYC is generally low in adult tissues (259). Due to the critical biological functions of MYC, the expression of MYC in normal circumstances is stringently regulated (266). In general, the half-life of MYC in normal cells is approximately 20 to 30 minutes (267). Deregulation of MYC expression lead to various disorders, including cancer (268). The overexpression of MYC is indeed observed in a wide range of (~70%) human cancers (268). As indicated above, the relatively high level of MYC is observed in CSCs derived from multiple types of cancer cells, in comparison with bulk tumor cells (209, 221, 266, 269).

Mounting studies have indicated that the overexpressed MYC in cancer cells plays pivotal roles in various biological processes, including cell cycle, cell growth, apoptosis, energy metabolism, chromatin modification, angiogenesis, genome stability, *etc* (**Figure 1.10**) (268-270). For instance, Perna *et al* used chromatin immunoprecipitation (ChIP)-Seq and mRNA profiling in mouse fibroblasts cells with MYC overexpression and identified close to 300 MYC-dependent serum responses genes that are involved in a variety of biological processes including nucleotide biosynthesis, ribosome biogenesis,



DNA replication and RNA processing (271). Another interesting study published recently has shown that MYC induces the expression of PD-L1 and CD47, two immune checkpoint proteins on the tumor cell surface, thereby assisting tumor cells evading immune surveillance (272). A number of studies have concluded that inhibition of MYC can lead to tumor regression and cell differentiation through both tumor cell-intrinsic and host-dependent manner (273).

It has been revealed that multiple factors account for the upregulated expression of MYC in cancer cells (268). For example, chromosomal translocations involving *MYC* and *BCL2* or immunoglobulin heavy chain locus *Ig H* have been detected in diffuse large B-cell lymphoma and Burkitt's lymphoma (274-276). *MYC* gene amplification has been frequently found in many human malignancies including breast cancer, lung cancer, and ovarian cancer (233, 277-279). In addition, a number of oncogenic signaling pathways contribute to the upregulation of MYC mRNA or stabilization of MYC protein, such as JAK/STAT (280), Wnt/ $\beta$ -catenin (281), Notch (282), MEK/ERK (283), and PI3K/AKT (284). For example, ERK1/2 kinase is frequently activated in human cancer (285, 286), and it is reported that ERK phosphorylates MYC at serine 62 (p-MYC<sup>S62</sup>), which is an active form of MYC (287, 288). The p-MYC<sup>S62</sup> is subsequently phosphorylated at another residue threonine 58 (T58) by GSK3 $\beta$ , which results in the binding of p-MYC<sup>S62/S58</sup> with the ubiquitin ligase Fbw7-SCF, followed by the degradation of MYC protein in proteasome pathway (**Figure 1.11**) (289, 290). The ratio of MYC phosphorylation at S62 and T58 determinates the protein level and transcriptional activity of MYC in cancer (283, 288) .

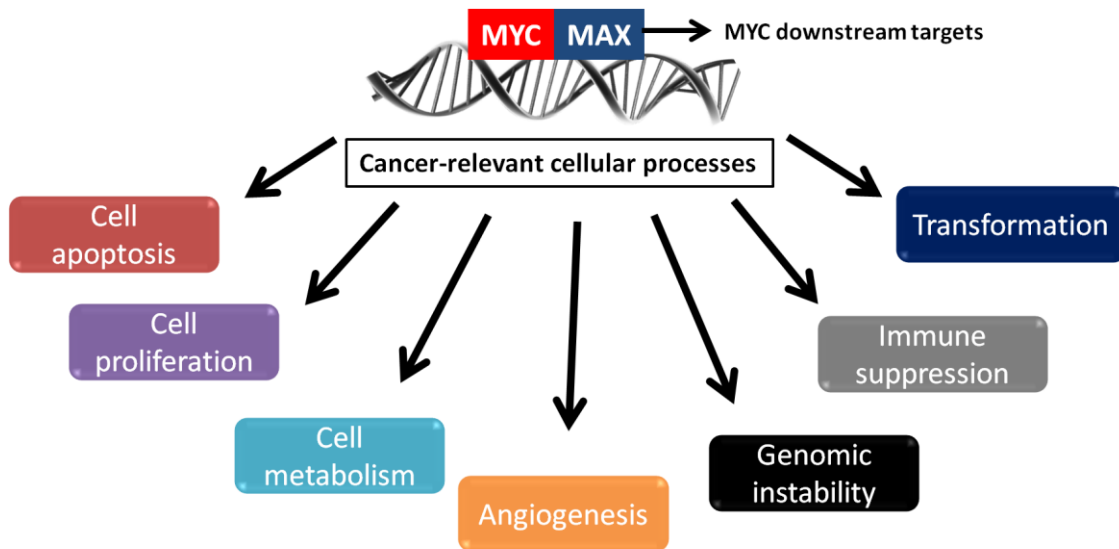


**Figure 1.10 The biological processes regulated by MYC in cancer cells.**

The main cellular processes regulated by MYC/MAX includes but not limits to cell apoptosis, cell proliferation, metabolism, angiogenesis, genomic instability, immune suppression, and cell transformation.

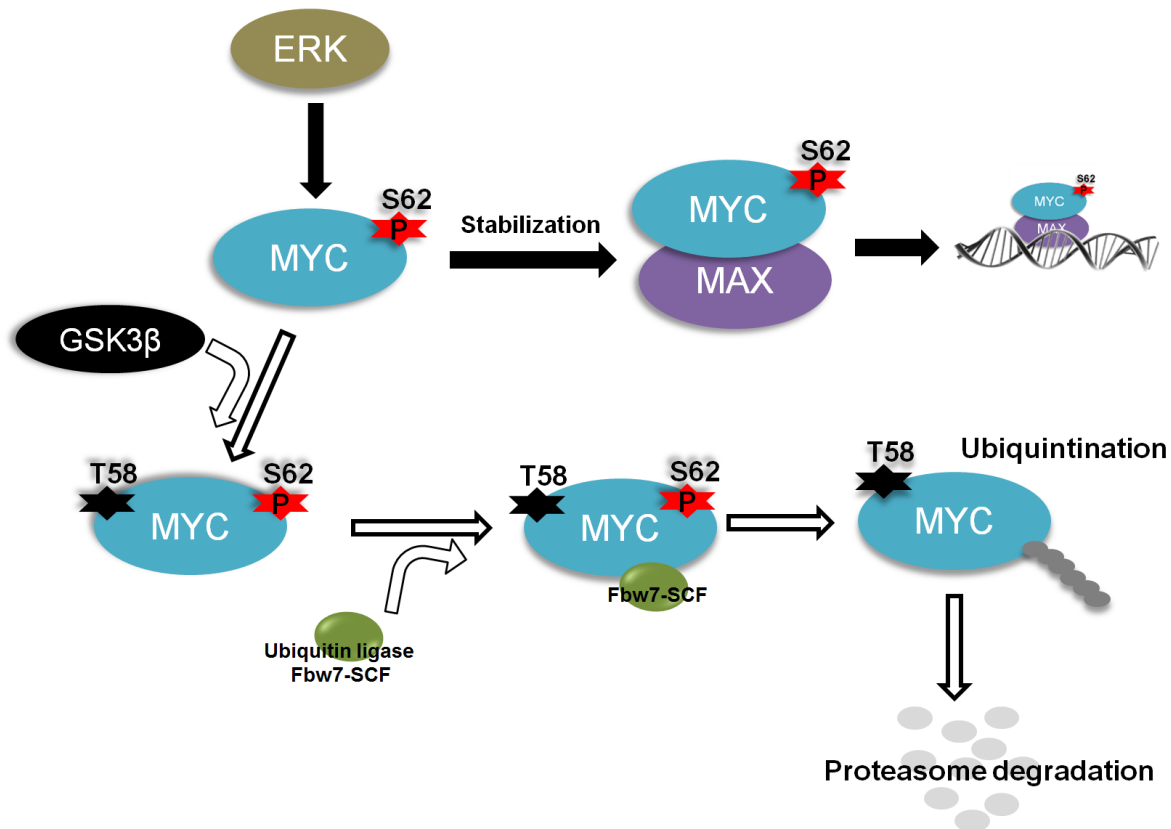


**Figure 1.11 Phosphorylation and stabilization of MYC by ERK and GSK3 $\beta$ .** Extracellular signal-regulated kinase (ERK) phosphorylates MYC at Serine 62 (p-MYC<sup>S62</sup>) and stabilizes MYC protein, which then heterodimerizes with MYC-associated factor X (MAX) and acts as transcription factor. The p-MYC<sup>S62</sup> can also be further phosphorylated by glycogen synthase kinase 3 $\beta$  (GSK3 $\beta$ ) at Threonine 58 (p-MYC<sup>S62/T58</sup>). Upon binding of p-MYCS62/T58 with the ubiquitin ligase Fbw7-SCF, MYC protein is subsequently ubiquitinated and degraded in proteasome pathway.

This figure has been modified from “Chang F, *et al.* Signaling transduction mediated by the Ras/Raf/MEK/ERK pathway from cytokine receptors to transcription factors: potential targeting for therapeutic interventions. *Leukemia*. 2013(7):1263-1293.”

## 1.6 Reactive oxygen species (ROS) in cancer

Reactive species, mainly consisting of ROS, are by-products generated by cell respiration and metabolism that mostly happen in the mitochondria (291, 292).

Oxidative stress simply refers to the accumulation of ROS due to the imbalance between the generation and elimination of ROS (291). ROS include singlet oxygen ( $^1\text{O}_2$ ), hydroxyl radical (-OH), hydrogen peroxide ( $\text{H}_2\text{O}_2$ ), superoxide anion ( $\text{O}_2^-$ ) and ozone ( $\text{O}_3$ ) (293). The intracellular ROS level is stringently regulated in normal cells, as different levels of ROS induces different cellular responses (294). Specifically, low to medium level of ROS activates a number of stress-related signaling pathways (e.g. PI3K/AKT and MAPK/ERK) to promote cell survival, proliferation, and differentiation (295), while high level or excessive ROS are toxic to normal cells by damaging DNA, proteins, and other molecules (291).

However, cancer cells generally harbor a relatively high level of ROS mainly as a result of the aberrant oncogenic signals that modulate the cellular metabolism (291). For example, the oncogenic pathways induced by MYC and RAS are the most well-known signaling pathways that regulate the cell metabolism (296, 297). Some other factors have also been involved in the contribution to the high level of ROS in cancer, such as hypoxia stress, metabolic defects, and endoplasmic reticulum (ER) stress (**Figure 1.12**) (292). Correlating well with the high level of ROS, cancer cells also constitute a relatively high level of ROS scavengers, such as nuclear factor erythroid 2-related factor 2 (Nrf2), NADPH, glutathione (GSH) and tumor suppressors (including *FOXO* and *TP53*) (**Figure 1.12**) (291). Interestingly, the ROS level has been shown to be relatively low in CSCs, as compared to the whole population of tumor cells, with the detailed mechanisms being unknown (298). A recent literature has indicated that the low ROS level in breast CSCs is associated with the elevated expression of ROS-scavenging systems in CSCs, such as GSH (299).

ROS of low to medium level in cancer cells has been reported to promote tumor cells growth, proliferation and metastasis (292). Mahalingaiah *et al* reported that ER+ breast cancer cell line MCF-7 cultured with chronic low doses of H<sub>2</sub>O<sub>2</sub> has exhibited enhanced tumorigenicity and chemoresistance, with upregulated gene expressions that are related with pro-metastasis, such as vascular endothelia growth factor (VEGF) and CD44 (300). It has been reported that low to medium level of ROS promotes tumorigenesis by interacting and activating a number of oncogenic proteins or signaling pathways in cancer cells, including MAPK/ERK, Wnt/ $\beta$ -catenin, PI3K/AKT, STAT3 (294), all of which are related to tumor cell growth and proliferation (152, 291, 292, 294, 301, 302). One study revealed that ROS maintains the phosphorylation and oncogenic activity of NPM-ALK kinase in ALK+ALCL cells, and pharmacological inhibition of ROS generation downregulates the expression level of phosphorylated NPM-ALK, as well as pSTAT3<sup>Y705</sup>, pERK1/2<sup>T202/Y204</sup> and pAKT<sup>S473</sup>, all of which are downstream targets of NPM-ALK (303).

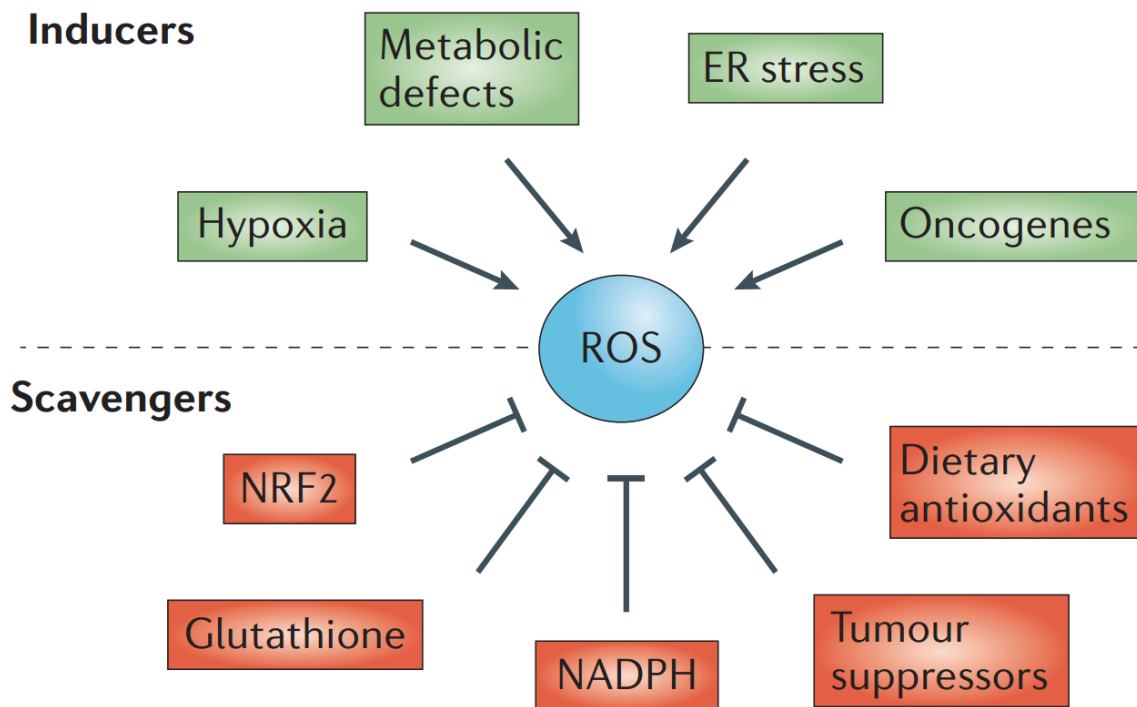


**Figure 1.12 Determination of cellular redox status by a balance between levels of ROS inducers and ROS scavengers.** The production of reactive oxygen species (ROS) can be induced by hypoxia, metabolic defects, endoplasmic reticulum (ER) stress and oncogenes. Conversely, ROS are eliminated by the activation of the transcription factor nuclear factor erythroid 2-related factor 2 (NRF2), the production of glutathione and nicotinamide adenine dinucleotide phosphate (NADPH), the activity of tumour suppressors (such as breast cancer susceptibility 1 (BRCA1), p53, phosphatase and tensin homolog (PTEN) and ataxia telangiectasia mutated (ATM) and the action of dietary antioxidants.

Reprinted with permission from “Gorrini C, *et al.* Modulation of oxidative stress as an anticancer strategy. *Nat Rev Drug Discov.* 2013. 12(12):931-947.” Copyright©2013 Nature Publishing Group. License number: 3976920022852

## **1.7 Thesis overview**

### **1.7.1 Rationale**

ALK+ALCL is an aggressive null/T-cell lymphoma most of which carries the oncogenic fusion tyrosine kinase NPM-ALK (8). It is well-known that NPM-ALK is the key oncogenic driver of this malignance by interacting and activating a number of molecular adaptors involved in multiple oncogenic signaling pathways, such as JAK/STATs and PI3K/AKT(55). Of these signaling pathways, NPM-ALK/STAT3 pathway is the one of the most important pathways (91). It is reported that NPM-ALK/STAT3 not only promotes the genes expression related with anti-apoptosis and cell proliferation but also suppresses the expression of tumor suppressors or negative regulators of NPM-ALK or STAT3 activity, such as Shp1 and STAT5A (45). In general, despite the fact that ALK+ALCL is a favourable and curable disease and the pathobiology of ALK+ALCL has been widely studied in the past 20 years (1), there is still a large portion (up to ~40%) of patients that develop either chemoresistance or tumor relapses after first-line chemotherapy and these relapsed tumors always present in a more aggressive form (55). Therefore, further understandings of the pathobiology of ALK+ALCL are still warranted for designing novel therapeutic strategies. The scope of this thesis is to further understand the oncogenic tyrosine kinase NPM-ALK and the pathobiology of ALK+ALCL, and to focus on the tumor suppressor STAT1 and a highly tumorigenic cell subpopulation derived from ALK+ALCL cells. In general, I will test the hypothesize that the pathobiology of ALK+ALCL, such as tumorigenecity, chemoresistance and cancer stemness, can be attributed to novel NPM-ALK–regulated biochemical defects as well as signaling pathways that are not directly linked to NPM-ALK.

STAT1, a member of STATs family, is generally considered as a tumor suppressor in various types of cancer (90). The decreased STAT1 expression has been observed in a wide range of cancer (304). STAT1 is reported to suppress STAT3 transcriptional activity in some cell models, and *vice versa* (90). Based on the facts that STAT3 is constitutively active in ALK+ALCL and the reciprocal repression between STAT1 and STAT3 activity in some cancer models(90, 91), I hypothesize that STAT1 signaling is deficient in ALK+ALC; if this is the case, STAT1 functions as a tumor suppressor and suppresses STAT3 activity in ALK+ALCL if it is overexpressed to a relatively high level.

Sox2 is one of the four iPS factors, and its biological significance in cancer cells has been documented in a recent review (252). The Lai lab previous revealed two phenotypically distinct cell population in ALK+ALCL cell lines based on their differential response to a Sox2 reporter—SRR2 (239). Cells responsive to SRR2 (RR) are more tumorigenic and chemoresistant than cells unresponsive to the reporter (RU) (239). Nevertheless, the expression level of Sox2 in RU and RR cells is almost identical, indicating other factors being involved in this context (239). MYC is another iPS factor, which is also aberrantly expressed in ALK+ALCL (305). The reciprocal regulation of MYC and Sox2 expression has been identified in breast cancer model (243). More importantly, the preliminary unpublished data indicated that MYC is a putative factor binding SRR2 reporter. In brief, here I hypothesize that MYC is one of the key factors regulating the RU/RR dichotomy, and potentially regulates Sox2 transcriptional activity.

Oxidative stress has been shown to induce the conversion of RU cells to RR cells derived from ER+ breast cancer cells and esophagus squamous cancer cells, presenting a biological process of tumor plasticity (221, 306). However, tumor plasticity



is poorly understood and studied in haematological malignancies, including ALK+ALCL. Using RU/RR cells model derived from ALK+ALCL, I hypothesize that RU cells can be induced to convert to RR cells by oxidative stress.

### **1.7.2 Objectives**

In Chapter 2, my objective is to evaluate the expression level of STAT1 in ALK+ALCL cell lines and patient samples. If STAT1 is indeed downregulated in this type of malignancy, then mechanisms behind this will be investigated. Next, two questions will be explored, including whether STAT1 signaling pathway is functionally intact and whether STAT1 is a potent tumor suppressor if its expression is restored in ALK+ALCL cells. Lastly, my objective involves the study of whether STAT1 indeed suppresses STAT3 transcriptional activity in ALK+ALCL.

In Chapter 3, my main objective is to delineate the key regulator(s) involved in RU/RR dichotomy and the biochemical features of RR cells. In addition, the regulation between this key regulator(s) and Sox2 will be investigated; furthermore, how this regulator(s) is differentially expressed or regulated between RU and RR cells will be explored as well. Lastly, whether the RR cells, according to the distinctive biochemical features of RR cells, are existed in ALK+ALCL patient samples will be evaluated.

In Chapter 4, my objective is study “tumor plasticity” using RU/RR model derived from ALK+ALCL. The question for me is whether RU can be induced to convert to RR cells upon oxidative stress. If oxidative challenge can convert RU cells to RR cells, whether these converted RR cells share similar biological and biochemical features with native

RR cells will be also determined. Furthermore, the molecular mechanisms underlining this phenomenon will be investigated.

## 1.8 References

1. Hapgood G, Savage KJ. The biology and management of systemic anaplastic large cell lymphoma. *Blood*. 2015;126(1):17-25.
2. Mora J, Filippa DA, Thaler HT, Polyak T, Cranor ML, Wollner N. Large cell non-Hodgkin lymphoma of childhood: Analysis of 78 consecutive patients enrolled in 2 consecutive protocols at the Memorial Sloan-Kettering Cancer Center. *Cancer*. 2000;88(1):186-97.
3. Kinney MC, Higgins RA, Medina EA. Anaplastic large cell lymphoma: twenty-five years of discovery. *Archives of pathology & laboratory medicine*. 2011;135(1):19-43.
4. Rizzardi GP, Tambussi G, Barcellini W, Capiluppi B, Clerici E, Maestra LL, et al. Soluble CD30, tumour necrosis factor (TNF)-alpha, and TNF receptors in primary HIV-1 infection: relationship with HIV-1, RNA, clinical outcome and early antiviral therapy. *Journal of biological regulators and homeostatic agents*. 1997;11(1-2):43-9.
5. Morris SW, Kirstein MN, Valentine MB, Dittmer KG, Shapiro DN, Saltman DL, et al. Fusion of a kinase gene, ALK, to a nucleolar protein gene, NPM, in non-Hodgkin's lymphoma. *Science*. 1994;263(5151):1281-4.
6. Xing X, Feldman AL. Anaplastic large cell lymphomas: ALK positive, ALK negative, and primary cutaneous. *Advances in anatomic pathology*. 2015;22(1):29-49.
7. Piccaluga PP, Gazzola A, Mannu C, Agostinelli C, Bacci F, Sabattini E, et al. Pathobiology of anaplastic large cell lymphoma. *Adv Hematol*. 2010:345053.

8. Ferreri AJ, Govi S, Pileri SA, Savage KJ. Anaplastic large cell lymphoma, ALK-positive. *Crit Rev Oncol Hematol*. 2012;83(2):293-302.
9. Pileri S, Falini B, Delsol G, Stein H, Baglioni P, Poggi S, et al. Lymphohistiocytic T-cell lymphoma (anaplastic large cell lymphoma CD30+/Ki-1 + with a high content of reactive histiocytes). *Histopathology*. 1990;16(4):383-91.
10. Kinney MC, Collins RD, Greer JP, Whitlock JA, Sioutos N, Kadin ME. A small-cell-predominant variant of primary Ki-1 (CD30)+ T-cell lymphoma. *The American journal of surgical pathology*. 1993;17(9):859-68.
11. Nakamura S, Shiota M, Nakagawa A, Yatabe Y, Kojima M, Motoori T, et al. Anaplastic large cell lymphoma: a distinct molecular pathologic entity: a reappraisal with special reference to p80(NPM/ALK) expression. *The American journal of surgical pathology*. 1997;21(12):1420-32.
12. Vassallo J, Lamant L, Brugieres L, Gaillard F, Campo E, Brousset P, et al. ALK-positive anaplastic large cell lymphoma mimicking nodular sclerosis Hodgkin's lymphoma: report of 10 cases. *The American journal of surgical pathology*. 2006;30(2):223-9.
13. Medeiros LJ, Elenitoba-Johnson KS. Anaplastic Large Cell Lymphoma. *American journal of clinical pathology*. 2007;127(5):707-22.
14. Benharroch D, Meguerian-Bedoyan Z, Lamant L, Amin C, Brugieres L, Terrier-Lacombe MJ, et al. ALK-positive lymphoma: a single disease with a broad spectrum of morphology. *Blood*. 1998;91(6):2076-84.
15. Alzona M, Jack HM, Fisher RI, Ellis TM. CD30 defines a subset of activated human T cells that produce IFN-gamma and IL-5 and exhibit enhanced B cell helper activity. *J Immunol*. 1994;153(7):2861-7.

16. ten Berge RL, Snijdwint FG, von Mensdorff-Pouilly S, Poort-Keesom RJ, Oudejans JJ, Meijer JW, et al. MUC1 (EMA) is preferentially expressed by ALK positive anaplastic large cell lymphoma, in the normally glycosylated or only partly hypoglycosylated form. *Journal of clinical pathology*. 2001;54(12):933-9.
17. Nath S, Mukherjee P. MUC1: a multifaceted oncoprotein with a key role in cancer progression. *Trends Mol Med*. 2014;20(6):332-42.
18. Felgar RE, Salhany KE, Macon WR, Pietra GG, Kinney MC. The expression of TIA-1+ cytolytic-type granules and other cytolytic lymphocyte-associated markers in CD30+ anaplastic large cell lymphomas (ALCL): correlation with morphology, immunophenotype, ultrastructure, and clinical features. *Human pathology*. 1999;30(2):228-36.
19. Krenacs L, Wellmann A, Sorbara L, Himmelmann AW, Bagdi E, Jaffe ES, et al. Cytotoxic cell antigen expression in anaplastic large cell lymphomas of T- and null-cell type and Hodgkin's disease: evidence for distinct cellular origin. *Blood*. 1997;89(3):980-9.
20. Foss HD, Anagnostopoulos I, Araujo I, Assaf C, Demel G, Kummer JA, et al. Anaplastic large-cell lymphomas of T-cell and null-cell phenotype express cytotoxic molecules. *Blood*. 1996;88(10):4005-11.
21. Foss HD, Demel G, Anagnostopoulos I, Araujo I, Hummel M, Stein H. Uniform expression of cytotoxic molecules in anaplastic large cell lymphoma of null/T cell phenotype and in cell lines derived from anaplastic large cell lymphoma. *Pathobiology*. 1997;65(2):83-90.

22. Bonzheim I, Geissinger E, Roth S, Zettl A, Marx A, Rosenwald A, et al. Anaplastic large cell lymphomas lack the expression of T-cell receptor molecules or molecules of proximal T-cell receptor signaling. *Blood*. 2004;104(10):3358-60.
23. Kesler MV, Paranjape GS, Asplund SL, McKenna RW, Jamal S, Kroft SH. Anaplastic large cell lymphoma: a flow cytometric analysis of 29 cases. *American journal of clinical pathology*. 2007;128(2):314-22.
24. ten Berge RL, Oudejans JJ, Ossenkoppele GJ, Pulford K, Willemze R, Falini B, et al. ALK expression in extranodal anaplastic large cell lymphoma favours systemic disease with (primary) nodal involvement and a good prognosis and occurs before dissemination. *Journal of clinical pathology*. 2000;53(6):445-50.
25. Vose J, Armitage J, Weisenburger D, International TCLP. International peripheral T-cell and natural killer/T-cell lymphoma study: pathology findings and clinical outcomes. *Journal of clinical oncology : official journal of the American Society of Clinical Oncology*. 2008;26(25):4124-30.
26. Chiarle R, Voena C, Ambrogio C, Piva R, Inghirami G. The anaplastic lymphoma kinase in the pathogenesis of cancer. *Nature reviews Cancer*. 2008;8(1):11-23.
27. Wellstein A. ALK receptor activation, ligands and therapeutic targeting in glioblastoma and in other cancers. *Frontiers in oncology*. 2012;2:192.
28. Lee HH, Norris A, Weiss JB, Frasch M. Jelly belly protein activates the receptor tyrosine kinase Alk to specify visceral muscle pioneers. *Nature*. 2003;425(6957):507-12.
29. Stoica GE, Kuo A, Powers C, Bowden ET, Sale EB, Riegel AT, et al. Midkine binds to anaplastic lymphoma kinase (ALK) and acts as a growth factor for different cell types. *The Journal of biological chemistry*. 2002;277(39):35990-8.

30. Bowden ET, Stoica GE, Wellstein A. Anti-apoptotic signaling of pleiotrophin through its receptor, anaplastic lymphoma kinase. *The Journal of biological chemistry*. 2002;277(39):35862-8.
31. Moog-Lutz C, Degoutin J, Gouzi JY, Frobert Y, Brunet-de Carvalho N, Bureau J, et al. Activation and inhibition of anaplastic lymphoma kinase receptor tyrosine kinase by monoclonal antibodies and absence of agonist activity of pleiotrophin. *The Journal of biological chemistry*. 2005;280(28):26039-48.
32. Mathivet T, Mazot P, Vigny M. In contrast to agonist monoclonal antibodies, both C-terminal truncated form and full length form of Pleiotrophin failed to activate vertebrate ALK (anaplastic lymphoma kinase)? *Cellular signalling*. 2007;19(12):2434-43.
33. Murray PB, Lax I, Reshetnyak A, Ligon GF, Lillquist JS, Natoli EJ, Jr., et al. Heparin is an activating ligand of the orphan receptor tyrosine kinase ALK. *Sci Signal*. 2015;8(360):ra6.
34. Guan J, Umapathy G, Yamazaki Y, Wolfstetter G, Mendoza P, Pfeifer K, et al. FAM150A and FAM150B are activating ligands for anaplastic lymphoma kinase. *eLife*. 2015;4:e09811.
35. Reshetnyak AV, Murray PB, Shi X, Mo ES, Mohanty J, Tome F, et al. Augmentor alpha and beta (FAM150) are ligands of the receptor tyrosine kinases ALK and LTK: Hierarchy and specificity of ligand-receptor interactions. *Proceedings of the National Academy of Sciences of the United States of America*. 2015;112(52):15862-7.
36. Iwahara T, Fujimoto J, Wen D, Cupples R, Bucay N, Arakawa T, et al. Molecular characterization of ALK, a receptor tyrosine kinase expressed specifically in the nervous system. *Oncogene*. 1997;14(4):439-49.

37. Bilsland JG, Wheeldon A, Mead A, Znamenskiy P, Almond S, Waters KA, et al. Behavioral and neurochemical alterations in mice deficient in anaplastic lymphoma kinase suggest therapeutic potential for psychiatric indications. *Neuropsychopharmacology*. 2008;33(3):685-700.
38. Lamant L, Pulford K, Bischof D, Morris SW, Mason DY, Delsol G, et al. Expression of the ALK tyrosine kinase gene in neuroblastoma. *Am J Pathol*. 2000;156(5):1711-21.
39. Koyama-Nasu R, Haruta R, Nasu-Nishimura Y, Taniue K, Katou Y, Shirahige K, et al. The pleiotrophin-ALK axis is required for tumorigenicity of glioblastoma stem cells. *Oncogene*. 2014;33(17):2236-44.
40. Chen Y, Takita J, Choi YL, Kato M, Ohira M, Sanada M, et al. Oncogenic mutations of ALK kinase in neuroblastoma. *Nature*. 2008;455(7215):971-4.
41. Wallace GC, Dixon-Mah YN, Vandergrift WA, 3rd, Ray SK, Haar CP, Mittendorf AM, et al. Targeting oncogenic ALK and MET: a promising therapeutic strategy for glioblastoma. *Metab Brain Dis*. 2013;28(3):355-66.
42. Grisendi S, Mecucci C, Falini B, Pandolfi PP. Nucleophosmin and cancer. *Nature reviews Cancer*. 2006;6(7):493-505.
43. Box JK, Paquet N, Adams MN, Boucher D, Bolderson E, O'Byrne KJ, et al. Nucleophosmin: from structure and function to disease development. *BMC molecular biology*. 2016;17(1):19.
44. Colombo E, Bonetti P, Lazzerini Denchi E, Martinelli P, Zamponi R, Marine JC, et al. Nucleophosmin is required for DNA integrity and p19Arf protein stability. *Molecular and cellular biology*. 2005;25(20):8874-86.

45. Lin CY, Tan BC, Liu H, Shih CJ, Chien KY, Lin CL, et al. Dephosphorylation of nucleophosmin by PP1beta facilitates pRB binding and consequent E2F1-dependent DNA repair. *Molecular biology of the cell*. 2010;21(24):4409-17.
46. Greenland C, Dastugue N, Touriol C, Lamant L, Delsol G, Brousset P. Anaplastic large cell lymphoma with the t(2;5)(p23;q35) NPM/ALK chromosomal translocation and duplication of the short arm of the non-translocated chromosome 2 involving the full length of the ALK gene. *Journal of clinical pathology*. 2001;54(2):152-4.
47. Falini B, Mecucci C, Tiacci E, Alcalay M, Rosati R, Pasqualucci L, et al. Cytoplasmic nucleophosmin in acute myelogenous leukemia with a normal karyotype. *The New England journal of medicine*. 2005;352(3):254-66.
48. Gogineni SK, Shah HO, Chester M, Lin JH, Garrison M, Alidina A, et al. Variant complex translocations involving chromosomes 1, 9, 9, 15 and 17 in acute promyelocytic leukemia without RAR alpha/PML gene fusion rearrangement. *Leukemia*. 1997;11(4):514-8.
49. Drexler HG, Gignac SM, von Wasielewski R, Werner M, Dirks WG. Pathobiology of NPM-ALK and variant fusion genes in anaplastic large cell lymphoma and other lymphomas. *Leukemia*. 2000;14(9):1533-59.
50. Giuriato S, Turner SD. Twenty years of modelling NPM-ALK-induced lymphomagenesis. *Frontiers in bioscience*. 2015;7:236-47.
51. Lai R, Ingham RJ. The pathobiology of the oncogenic tyrosine kinase NPM-ALK: a brief update. *Therapeutic advances in hematology*. 2013;4(2):119-31.
52. Hallberg B, Palmer RH. Mechanistic insight into ALK receptor tyrosine kinase in human cancer biology. *Nature reviews Cancer*. 2013;13(10):685-700.



53. Zhang Q, Raghunath PN, Xue L, Majewski M, Carpentieri DF, Odum N, et al. Multilevel dysregulation of STAT3 activation in anaplastic lymphoma kinase-positive T/null-cell lymphoma. *J Immunol.* 2002;168(1):466-74.
54. Slupianek A, Nieborowska-Skorska M, Hoser G, Morrione A, Majewski M, Xue L, et al. Role of phosphatidylinositol 3-kinase-Akt pathway in nucleophosmin/anaplastic lymphoma kinase-mediated lymphomagenesis. *Cancer research.* 2001;61(5):2194-9.
55. Amin HM, Lai R. Pathobiology of ALK+ anaplastic large-cell lymphoma. *Blood.* 2007;110(7):2259-67.
56. Pearson JD, Lee JK, Bacani JT, Lai R, Ingham RJ. NPM-ALK: The Prototypic Member of a Family of Oncogenic Fusion Tyrosine Kinases. *J Signal Transduct.* 2012;2012:123253.
57. Tabbo F, Barreca A, Piva R, Inghirami G. ALK Signaling and Target Therapy in Anaplastic Large Cell Lymphoma. *Frontiers in oncology.* 2012;2:41.
58. Klemperer SJ, Cohen DW, Costa DB. ALK translocation in non-small cell lung cancer with adenocarcinoma and squamous cell carcinoma markers. *Journal of thoracic oncology : official publication of the International Association for the Study of Lung Cancer.* 2011;6(8):1439-40.
59. Aisner DL, Nguyen TT, Paskulin DD, Le AT, Haney J, Schulte N, et al. ROS1 and ALK fusions in colorectal cancer, with evidence of intratumoral heterogeneity for molecular drivers. *Molecular cancer research : MCR.* 2014;12(1):111-8.
60. Lange K, Uckert W, Blankenstein T, Nadrowitz R, Bittner C, Renauld JC, et al. Overexpression of NPM-ALK induces different types of malignant lymphomas in IL-9 transgenic mice. *Oncogene.* 2003;22(4):517-27.

61. Zhang Q, Wei F, Wang HY, Liu X, Roy D, Xiong QB, et al. The potent oncogene NPM-ALK mediates malignant transformation of normal human CD4(+) T lymphocytes. *The American journal of pathology*. 2013;183(6):1971-80.
62. Jager R, Hahne J, Jacob A, Egert A, Schenkel J, Wernert N, et al. Mice transgenic for NPM-ALK develop non-Hodgkin lymphomas. *Anticancer research*. 2005;25(5):3191-6.
63. Chiarle R, Gong JZ, Guasparri I, Pesci A, Cai J, Liu J, et al. NPM-ALK transgenic mice spontaneously develop T-cell lymphomas and plasma cell tumors. *Blood*. 2003;101(5):1919-27.
64. Turner SD, Tooze R, MacLennan K, Alexander DR. Vav-promoter regulated oncogenic fusion protein NPM-ALK in transgenic mice causes B-cell lymphomas with hyperactive Jun kinase. *Oncogene*. 2003;22(49):7750-61.
65. Turner SD, Merz H, Yeung D, Alexander DR. CD2 promoter regulated nucleophosmin-anaplastic lymphoma kinase in transgenic mice causes B lymphoid malignancy. *Anticancer research*. 2006;26(5A):3275-9.
66. Giuriato S, Foisseau M, Dejean E, Felsher DW, Al Saati T, Demur C, et al. Conditional TPM3-ALK and NPM-ALK transgenic mice develop reversible ALK-positive early B-cell lymphoma/leukemia. *Blood*. 2010;115(20):4061-70.
67. Malcolm TI, Villarese P, Fairbairn CJ, Lamant L, Trinquand A, Hook CE, et al. Anaplastic large cell lymphoma arises in thymocytes and requires transient TCR expression for thymic egress. *Nature communications*. 2016;7:10087.
68. Maes B, Vanhentenrijk V, Wlodarska I, Cools J, Peeters B, Marynen P, et al. The NPM-ALK and the ATIC-ALK fusion genes can be detected in non-neoplastic cells. *The American journal of pathology*. 2001;158(6):2185-93.

69. Crockett DK, Lin Z, Elenitoba-Johnson KS, Lim MS. Identification of NPM-ALK interacting proteins by tandem mass spectrometry. *Oncogene*. 2004;23(15):2617-29.
70. Voena C, Conte C, Ambrogio C, Boeri Erba E, Boccalatte F, Mohammed S, et al. The tyrosine phosphatase Shp2 interacts with NPM-ALK and regulates anaplastic lymphoma cell growth and migration. *Cancer research*. 2007;67(9):4278-86.
71. Galletta A, Gunby RH, Redaelli S, Stano P, Carniti C, Bachi A, et al. NPM/ALK binds and phosphorylates the RNA/DNA-binding protein PSF in anaplastic large-cell lymphoma. *Blood*. 2007;110(7):2600-9.
72. Wu F, Wang P, Young LC, Lai R, Li L. Proteome-wide identification of novel binding partners to the oncogenic fusion gene protein, NPM-ALK, using tandem affinity purification and mass spectrometry. *The American journal of pathology*. 2009;174(2):361-70.
73. Murga-Zamalloa CA, Mendoza-Reinoso V, Sahasrabudde AA, Rolland D, Hwang SR, McDonnell SR, et al. NPM-ALK phosphorylates WASp Y102 and contributes to oncogenesis of anaplastic large cell lymphoma. *Oncogene*. 2016.
74. Marzec M, Kasprzycka M, Liu X, El-Salem M, Halasa K, Raghunath PN, et al. Oncogenic tyrosine kinase NPM/ALK induces activation of the rapamycin-sensitive mTOR signaling pathway. *Oncogene*. 2007;26(38):5606-14.
75. Bai RY, Dieter P, Peschel C, Morris SW, Duyster J. Nucleophosmin-anaplastic lymphoma kinase of large-cell anaplastic lymphoma is a constitutively active tyrosine kinase that utilizes phospholipase C-gamma to mediate its mitogenicity. *Molecular and cellular biology*. 1998;18(12):6951-61.

76. Zamo A, Chiarle R, Piva R, Howes J, Fan Y, Chilosi M, et al. Anaplastic lymphoma kinase (ALK) activates Stat3 and protects hematopoietic cells from cell death. *Oncogene*. 2002;21(7):1038-47.
77. Yu H, Lee H, Herrmann A, Buettner R, Jove R. Revisiting STAT3 signalling in cancer: new and unexpected biological functions. *Nature reviews Cancer*. 2014;14(11):736-46.
78. Johnston PA, Grandis JR. STAT3 signaling: anticancer strategies and challenges. *Molecular interventions*. 2011;11(1):18-26.
79. Khoury JD, Medeiros LJ, Rassidakis GZ, Yared MA, Tsioli P, Leventaki V, et al. Differential expression and clinical significance of tyrosine-phosphorylated STAT3 in ALK+ and ALK- anaplastic large cell lymphoma. *Clinical cancer research : an official journal of the American Association for Cancer Research*. 2003;9(10 Pt 1):3692-9.
80. Kirken RA, Rui H, Malabarba MG, Howard OM, Kawamura M, O'Shea JJ, et al. Activation of JAK3, but not JAK1, is critical for IL-2-induced proliferation and STAT5 recruitment by a COOH-terminal region of the IL-2 receptor beta-chain. *Cytokine*. 1995;7(7):689-700.
81. Fenghao X, Saxon A, Nguyen A, Ke Z, Diaz-Sanchez D, Nel A. Interleukin 4 activates a signal transducer and activator of transcription (Stat) protein which interacts with an interferon-gamma activation site-like sequence upstream of the I epsilon exon in a human B cell line. Evidence for the involvement of Janus kinase 3 and interleukin-4 Stat. *The Journal of clinical investigation*. 1995;96(2):907-14.
82. Malabarba MG, Rui H, Deutsch HH, Chung J, Kalthoff FS, Farrar WL, et al. Interleukin-13 is a potent activator of JAK3 and STAT6 in cells expressing interleukin-2

receptor-gamma and interleukin-4 receptor-alpha. *The Biochemical journal*. 1996;319 ( Pt 3):865-72.

83. Ortmann RA, Cheng T, Visconti R, Frucht DM, O'Shea JJ. Janus kinases and signal transducers and activators of transcription: their roles in cytokine signaling, development and immunoregulation. *Arthritis research*. 2000;2(1):16-32.

84. Dien Bard J, Gelebart P, Anand M, Zak Z, Hegazy SA, Amin HM, et al. IL-21 contributes to JAK3/STAT3 activation and promotes cell growth in ALK-positive anaplastic large cell lymphoma. *The American journal of pathology*. 2009;175(2):825-34.

85. Demoulin JB, Uyttenhove C, Van Roost E, DeLestre B, Donckers D, Van Snick J, et al. A single tyrosine of the interleukin-9 (IL-9) receptor is required for STAT activation, antiapoptotic activity, and growth regulation by IL-9. *Molecular and cellular biology*. 1996;16(9):4710-6.

86. Amin HM, Medeiros LJ, Ma Y, Feretzaki M, Das P, Leventaki V, et al. Inhibition of JAK3 induces apoptosis and decreases anaplastic lymphoma kinase activity in anaplastic large cell lymphoma. *Oncogene*. 2003;22(35):5399-407.

87. Qiu L, Lai R, Lin Q, Lau E, Thomazy DM, Calame D, et al. Autocrine release of interleukin-9 promotes Jak3-dependent survival of ALK+ anaplastic large-cell lymphoma cells. *Blood*. 2006;108(7):2407-15.

88. Amin HM, Lin Q, Lai R. Jak3 contributes to the activation of ALK and Stat3 in ALK(+) anaplastic large cell lymphoma. *Laboratory investigation; a journal of technical methods and pathology*. 2006;86(4):417-9; author reply 20-1.

89. Bard JD, Gelebart P, Anand M, Amin HM, Lai R. Aberrant expression of IL-22 receptor 1 and autocrine IL-22 stimulation contribute to tumorigenicity in ALK+ anaplastic large cell lymphoma. *Leukemia*. 2008;22(8):1595-603.
90. Avalle L, Pensa S, Regis G, Novelli F, Poli V. STAT1 and STAT3 in tumorigenesis: A matter of balance. *Jak-Stat*. 2012;1(2):65-72.
91. Chiarle R, Simmons WJ, Cai H, Dhall G, Zamo A, Raz R, et al. Stat3 is required for ALK-mediated lymphomagenesis and provides a possible therapeutic target. *Nature medicine*. 2005;11(6):623-9.
92. Carpenter RL, Lo HW. STAT3 Target Genes Relevant to Human Cancers. *Cancers*. 2014;6(2):897-925.
93. Bowman T, Garcia R, Turkson J, Jove R. STATs in oncogenesis. *Oncogene*. 2000;19(21):2474-88.
94. Buettner R, Mora LB, Jove R. Activated STAT signaling in human tumors provides novel molecular targets for therapeutic intervention. *Clinical cancer research : an official journal of the American Association for Cancer Research*. 2002;8(4):945-54.
95. Thomas SJ, Snowden JA, Zeidler MP, Danson SJ. The role of JAK/STAT signalling in the pathogenesis, prognosis and treatment of solid tumours. *British journal of cancer*. 2015;113(3):365-71.
96. Amin HM, McDonnell TJ, Ma Y, Lin Q, Fujio Y, Kunisada K, et al. Selective inhibition of STAT3 induces apoptosis and G(1) cell cycle arrest in ALK-positive anaplastic large cell lymphoma. *Oncogene*. 2004;23(32):5426-34.
97. Wu C, Molavi O, Zhang H, Gupta N, Alshareef A, Bone KM, et al. STAT1 is phosphorylated and downregulated by the oncogenic tyrosine kinase NPM-ALK in ALK-positive anaplastic large-cell lymphoma. *Blood*. 2015;126(3):336-45.

98. Piva R, Agnelli L, Pellegrino E, Todoerti K, Grosso V, Tamagno I, et al. Gene expression profiling uncovers molecular classifiers for the recognition of anaplastic large-cell lymphoma within peripheral T-cell neoplasms. *Journal of clinical oncology : official journal of the American Society of Clinical Oncology*. 2010;28(9):1583-90.
99. Zhang Q, Wang HY, Marzec M, Raghunath PN, Nagasawa T, Wasik MA. STAT3- and DNA methyltransferase 1-mediated epigenetic silencing of SHP-1 tyrosine phosphatase tumor suppressor gene in malignant T lymphocytes. *Proceedings of the National Academy of Sciences of the United States of America*. 2005;102(19):6948-53.
100. Zhang Q, Wang HY, Woetmann A, Raghunath PN, Odum N, Wasik MA. STAT3 induces transcription of the DNA methyltransferase 1 gene (DNMT1) in malignant T lymphocytes. *Blood*. 2006;108(3):1058-64.
101. Honorat JF, Ragab A, Lamant L, Delsol G, Ragab-Thomas J. SHP1 tyrosine phosphatase negatively regulates NPM-ALK tyrosine kinase signaling. *Blood*. 2006;107(10):4130-8.
102. Han Y, Amin HM, Franko B, Frantz C, Shi X, Lai R. Loss of SHP1 enhances JAK3/STAT3 signaling and decreases proteasome degradation of JAK3 and NPM-ALK in ALK+ anaplastic large-cell lymphoma. *Blood*. 2006;108(8):2796-803.
103. Zhang Q, Wang HY, Liu X, Wasik MA. STAT5A is epigenetically silenced by the tyrosine kinase NPM1-ALK and acts as a tumor suppressor by reciprocally inhibiting NPM1-ALK expression. *Nature medicine*. 2007;13(11):1341-8.
104. Nieborowska-Skorska M, Slupianek A, Xue L, Zhang Q, Raghunath PN, Hoser G, et al. Role of signal transducer and activator of transcription 5 in nucleophosmin/ anaplastic lymphoma kinase-mediated malignant transformation of lymphoid cells. *Cancer research*. 2001;61(17):6517-23.

105. Kim HS, Lee MS. STAT1 as a key modulator of cell death. *Cellular signalling*. 2007;19(3):454-65.
106. Decker T, Muller M, Stockinger S. The yin and yang of type I interferon activity in bacterial infection. *Nature reviews Immunology*. 2005;5(9):675-87.
107. Ramana CV, Chatterjee-Kishore M, Nguyen H, Stark GR. Complex roles of Stat1 in regulating gene expression. *Oncogene*. 2000;19(21):2619-27.
108. Zetter BR, Mangold U. Ubiquitin-independent degradation and its implication in cancer. *Future oncology*. 2005;1(5):567-70.
109. Chen D, Dou QP. The ubiquitin-proteasome system as a prospective molecular target for cancer treatment and prevention. *Current protein & peptide science*. 2010;11(6):459-70.
110. Lawrence DW, Kornbluth J. E3 ubiquitin ligase NKLAM ubiquitinates STAT1 and positively regulates STAT1-mediated transcriptional activity. *Cellular signalling*. 2016;28(12):1833-41.
111. Ren Y, Zhao P, Liu J, Yuan Y, Cheng Q, Zuo Y, et al. Deubiquitinase USP2a Sustains Interferons Antiviral Activity by Restricting Ubiquitination of Activated STAT1 in the Nucleus. *PLoS pathogens*. 2016;12(7):e1005764.
112. Soond SM, Townsend PA, Barry SP, Knight RA, Latchman DS, Stephanou A. ERK and the F-box protein betaTRCP target STAT1 for degradation. *The Journal of biological chemistry*. 2008;283(23):16077-83.
113. Yuan C, Qi J, Zhao X, Gao C. Smurf1 protein negatively regulates interferon-gamma signaling through promoting STAT1 protein ubiquitination and degradation. *The Journal of biological chemistry*. 2012;287(21):17006-15.



114. Gao C, Mi Z, Guo H, Kuo PC. Osteopontin regulates ubiquitin-dependent degradation of Stat1 in murine mammary epithelial tumor cells. *Neoplasia*. 2007;9(9):699-706.
115. Kim TK, Maniatis T. Regulation of interferon-gamma-activated STAT1 by the ubiquitin-proteasome pathway. *Science*. 1996;273(5282):1717-9.
116. Wang Y, Ren Z, Tao D, Tilwalli S, Goswami R, Balabanov R. STAT1/IRF-1 signaling pathway mediates the injurious effect of interferon-gamma on oligodendrocyte progenitor cells. *Glia*. 2010;58(2):195-208.
117. Sironi JJ, Ouchi T. STAT1-induced apoptosis is mediated by caspases 2, 3, and 7. *The Journal of biological chemistry*. 2004;279(6):4066-74.
118. Choi EA, Lei H, Maron DJ, Wilson JM, Barsoum J, Fraker DL, et al. Stat1-dependent induction of tumor necrosis factor-related apoptosis-inducing ligand and the cell-surface death signaling pathway by interferon beta in human cancer cells. *Cancer research*. 2003;63(17):5299-307.
119. Ning Y, Riggins RB, Mulla JE, Chung H, Zwart A, Clarke R. IFNgamma restores breast cancer sensitivity to fulvestrant by regulating STAT1, IFN regulatory factor 1, NF-kappaB, BCL2 family members, and signaling to caspase-dependent apoptosis. *Molecular cancer therapeutics*. 2010;9(5):1274-85.
120. Stephanou A, Brar BK, Knight RA, Latchman DS. Opposing actions of STAT-1 and STAT-3 on the Bcl-2 and Bcl-x promoters. *Cell death and differentiation*. 2000;7(3):329-30.
121. Hong F, Jaruga B, Kim WH, Radaeva S, El-Assal ON, Tian Z, et al. Opposing roles of STAT1 and STAT3 in T cell-mediated hepatitis: regulation by SOCS. *Journal of Clinical Investigation*. 2002;110(10):1503-13.

122. Dimberg LY, Dimberg A, Ivarsson K, Fryknas M, Rickardson L, Tobin G, et al. Stat1 activation attenuates IL-6 induced Stat3 activity but does not alter apoptosis sensitivity in multiple myeloma. *BMC cancer*. 2012;12:318.
123. Meraz MA, White JM, Sheehan KC, Bach EA, Rodig SJ, Dighe AS, et al. Targeted disruption of the Stat1 gene in mice reveals unexpected physiologic specificity in the JAK-STAT signaling pathway. *Cell*. 1996;84(3):431-42.
124. Kaplan DH, Shankaran V, Dighe AS, Stockert E, Aguet M, Old LJ, et al. Demonstration of an interferon gamma-dependent tumor surveillance system in immunocompetent mice. *Proceedings of the National Academy of Sciences of the United States of America*. 1998;95(13):7556-61.
125. Chan SR, Vermi W, Luo J, Lucini L, Rickert C, Fowler AM, et al. STAT1-deficient mice spontaneously develop estrogen receptor alpha-positive luminal mammary carcinomas. *Breast cancer research : BCR*. 2012;14(1):R16.
126. Laimer K, Spizzo G, Obrist P, Gastl G, Brunhuber T, Schafer G, et al. STAT1 activation in squamous cell cancer of the oral cavity: a potential predictive marker of response to adjuvant chemotherapy. *Cancer*. 2007;110(2):326-33.
127. Wong LH, Krauer KG, Hatzinisiriou I, Estcourt MJ, Hersey P, Tam ND, et al. Interferon-resistant human melanoma cells are deficient in ISGF3 components, STAT1, STAT2, and p48-ISGF3gamma. *The Journal of biological chemistry*. 1997;272(45):28779-85.
128. Kovarik J, Boudny V, Kocak I, Lauerova L, Fait V, Vagundova M. Malignant melanoma associates with deficient IFN-induced STAT 1 phosphorylation. *International journal of molecular medicine*. 2003;12(3):335-40.

129. Sun WH, Pabon C, Alsayed Y, Huang PP, Jandeska S, Uddin S, et al. Interferon-alpha resistance in a cutaneous T-cell lymphoma cell line is associated with lack of STAT1 expression. *Blood*. 1998;91(2):570-6.
130. Widschwendter A, Tonko-Geymayer S, Welte T, Daxenbichler G, Marth C, Doppler W. Prognostic significance of signal transducer and activator of transcription 1 activation in breast cancer. *Clinical cancer research : an official journal of the American Association for Cancer Research*. 2002;8(10):3065-74.
131. Zhang Y, Molavi O, Su M, Lai R. The clinical and biological significance of STAT1 in esophageal squamous cell carcinoma. *BMC cancer*. 2014;14:791.
132. Zhang Y, Zhang Y, Yun H, Lai R, Su M. Correlation of STAT1 with apoptosis and cell-cycle markers in esophageal squamous cell carcinoma. *PloS one*. 2014;9(12):e113928.
133. Xi S, Dyer KF, Kimak M, Zhang Q, Gooding WE, Chaillet JR, et al. Decreased STAT1 expression by promoter methylation in squamous cell carcinogenesis. *Journal of the National Cancer Institute*. 2006;98(3):181-9.
134. Khodarev N, Ahmad R, Rajabi H, Pitroda S, Kufe T, McClary C, et al. Cooperativity of the MUC1 oncoprotein and STAT1 pathway in poor prognosis human breast cancer. *Oncogene*. 2010;29(6):920-9.
135. Sanda T, Tyner JW, Gutierrez A, Ngo VN, Glover J, Chang BH, et al. TYK2-STAT1-BCL2 pathway dependence in T-cell acute lymphoblastic leukemia. *Cancer discovery*. 2013;3(5):564-77.
136. Schultz J, Koczan D, Schmitz U, Ibrahim SM, Pilch D, Landsberg J, et al. Tumor-promoting role of signal transducer and activator of transcription (Stat)1 in late-stage melanoma growth. *Clinical & experimental metastasis*. 2010;27(3):133-40.

137. Schlessinger J. Phospholipase Cgamma activation and phosphoinositide hydrolysis are essential for embryonal development. *Proceedings of the National Academy of Sciences of the United States of America*. 1997;94(7):2798-9.
138. Park JB, Lee CS, Jang JH, Ghim J, Kim YJ, You S, et al. Phospholipase signalling networks in cancer. *Nature reviews Cancer*. 2012;12(11):782-92.
139. Vega F, Medeiros LJ, Leventaki V, Atwell C, Cho-Vega JH, Tian L, et al. Activation of mammalian target of rapamycin signaling pathway contributes to tumor cell survival in anaplastic lymphoma kinase-positive anaplastic large cell lymphoma. *Cancer research*. 2006;66(13):6589-97.
140. Vanhaesebroeck B, Stephens L, Hawkins P. PI3K signalling: the path to discovery and understanding. *Nature reviews Molecular cell biology*. 2012;13(3):195-203.
141. Hemmings BA, Restuccia DF. PI3K-PKB/Akt pathway. *Cold Spring Harbor perspectives in biology*. 2012;4(9):a011189.
142. Song G, Ouyang G, Bao S. The activation of Akt/PKB signaling pathway and cell survival. *Journal of cellular and molecular medicine*. 2005;9(1):59-71.
143. Datta SR, Dudek H, Tao X, Masters S, Fu H, Gotoh Y, et al. Akt phosphorylation of BAD couples survival signals to the cell-intrinsic death machinery. *Cell*. 1997;91(2):231-41.
144. Romashkova JA, Makarov SS. NF-kappaB is a target of AKT in anti-apoptotic PDGF signalling. *Nature*. 1999;401(6748):86-90.
145. Riobo NA, Lu K, Ai X, Haines GM, Emerson CP, Jr. Phosphoinositide 3-kinase and Akt are essential for Sonic Hedgehog signaling. *Proceedings of the National Academy of Sciences of the United States of America*. 2006;103(12):4505-10.

146. Singh RR, Cho-Vega JH, Davuluri Y, Ma S, Kasbidi F, Milito C, et al. Sonic hedgehog signaling pathway is activated in ALK-positive anaplastic large cell lymphoma. *Cancer research*. 2009;69(6):2550-8.
147. Wang SJ, Omori N, Li F, Jin G, Zhang WR, Hamakawa Y, et al. Potentiation of Akt and suppression of caspase-9 activations by electroacupuncture after transient middle cerebral artery occlusion in rats. *Neuroscience letters*. 2002;331(2):115-8.
148. Suhara T, Kim HS, Kirshenbaum LA, Walsh K. Suppression of Akt signaling induces Fas ligand expression: involvement of caspase and Jun kinase activation in Akt-mediated Fas ligand regulation. *Molecular and cellular biology*. 2002;22(2):680-91.
149. Kawano T, Morioka M, Yano S, Hamada J, Ushio Y, Miyamoto E, et al. Decreased akt activity is associated with activation of forkhead transcription factor after transient forebrain ischemia in gerbil hippocampus. *Journal of cerebral blood flow and metabolism : official journal of the International Society of Cerebral Blood Flow and Metabolism*. 2002;22(8):926-34.
150. Santo EE, Stroeken P, Sluis PV, Koster J, Versteeg R, Westerhout EM. FOXO3a is a major target of inactivation by PI3K/AKT signaling in aggressive neuroblastoma. *Cancer research*. 2013;73(7):2189-98.
151. Das TP, Suman S, Alatassi H, Ankem MK, Damodaran C. Inhibition of AKT promotes FOXO3a-dependent apoptosis in prostate cancer. *Cell death & disease*. 2016;7:e2111.
152. McCubrey JA, Steelman LS, Chappell WH, Abrams SL, Wong EW, Chang F, et al. Roles of the Raf/MEK/ERK pathway in cell growth, malignant transformation and drug resistance. *Biochimica et biophysica acta*. 2007;1773(8):1263-84.

153. Chang F, Steelman LS, Lee JT, Shelton JG, Navolanic PM, Blalock WL, et al. Signal transduction mediated by the Ras/Raf/MEK/ERK pathway from cytokine receptors to transcription factors: potential targeting for therapeutic intervention. *Leukemia*. 2003;17(7):1263-93.
154. Marzec M, Kasprzycka M, Liu X, Raghunath PN, Wlodarski P, Wasik MA. Oncogenic tyrosine kinase NPM/ALK induces activation of the MEK/ERK signaling pathway independently of c-Raf. *Oncogene*. 2007;26(6):813-21.
155. Watanabe M, Itoh K, Togano T, Kadin ME, Watanabe T, Higashihara M, et al. Ets-1 activates overexpression of JunB and CD30 in Hodgkin's lymphoma and anaplastic large-cell lymphoma. *The American journal of pathology*. 2012;180(2):831-8.
156. Watanabe M, Sasaki M, Itoh K, Higashihara M, Umezawa K, Kadin ME, et al. JunB induced by constitutive CD30-extracellular signal-regulated kinase 1/2 mitogen-activated protein kinase signaling activates the CD30 promoter in anaplastic large cell lymphoma and reed-sternberg cells of Hodgkin lymphoma. *Cancer research*. 2005;65(17):7628-34.
157. Staber PB, Vesely P, Haq N, Ott RG, Funato K, Bambach I, et al. The oncoprotein NPM-ALK of anaplastic large-cell lymphoma induces JUNB transcription via ERK1/2 and JunB translation via mTOR signaling. *Blood*. 2007;110(9):3374-83.
158. Gao J, Yin M, Zhu Y, Gu L, Zhang Y, Li Q, et al. Prognostic significance and therapeutic potential of the activation of anaplastic lymphoma kinase/protein kinase B/mammalian target of rapamycin signaling pathway in anaplastic large cell lymphoma. *BMC cancer*. 2013;13:471.

159. Hansel DE, Platt E, Orloff M, Harwalker J, Sethu S, Hicks JL, et al. Mammalian target of rapamycin (mTOR) regulates cellular proliferation and tumor growth in urothelial carcinoma. *The American journal of pathology*. 2010;176(6):3062-72.
160. Laplante M, Sabatini DM. mTOR signaling in growth control and disease. *Cell*. 2012;149(2):274-93.
161. Babchia N, Calipel A, Mouriaux F, Faussat AM, Mascarelli F. The PI3K/Akt and mTOR/P70S6K signaling pathways in human uveal melanoma cells: interaction with B-Raf/ERK. *Investigative ophthalmology & visual science*. 2010;51(1):421-9.
162. Fanale MA, Horwitz SM, Forero-Torres A, Bartlett NL, Advani RH, Pro B, et al. Brentuximab vedotin in the front-line treatment of patients with CD30+ peripheral T-cell lymphomas: results of a phase I study. *Journal of clinical oncology : official journal of the American Society of Clinical Oncology*. 2014;32(28):3137-43.
163. George SK, Vishwamitra D, Manshouri R, Shi P, Amin HM. The ALK inhibitor ASP3026 eradicates NPM-ALK(+) T-cell anaplastic large-cell lymphoma in vitro and in a systemic xenograft lymphoma model. *Oncotarget*. 2014;5(14):5750-63.
164. Galkin AV, Melnick JS, Kim S, Hood TL, Li N, Li L, et al. Identification of NVP-TAE684, a potent, selective, and efficacious inhibitor of NPM-ALK. *Proceedings of the National Academy of Sciences of the United States of America*. 2007;104(1):270-5.
165. Kothari S, Ud-Din N, Lisi M, Coyle T. Crizotinib in anaplastic lymphoma kinase-positive anaplastic large cell lymphoma in the setting of renal insufficiency: a case report. *Journal of medical case reports*. 2016;10:176.
166. Wu J, Savooji J, Liu D. Second- and third-generation ALK inhibitors for non-small cell lung cancer. *Journal of hematology & oncology*. 2016;9:19.

167. Sullivan I, Planchard D. ALK inhibitors in non-small cell lung cancer: the latest evidence and developments. *Therapeutic advances in medical oncology*. 2016;8(1):32-47.
168. Farina F, Gambacorti-Passerini C. ALK inhibitors for clinical use in cancer therapy. *Front Biosci (Elite Ed)*. 2016;8:46-60.
169. Kazandjian D, Blumenthal GM, Chen HY, He K, Patel M, Justice R, et al. FDA approval summary: crizotinib for the treatment of metastatic non-small cell lung cancer with anaplastic lymphoma kinase rearrangements. *The oncologist*. 2014;19(10):e5-11.
170. Mosse YP, Lim MS, Voss SD, Wilner K, Ruffner K, Laliberte J, et al. Safety and activity of crizotinib for paediatric patients with refractory solid tumours or anaplastic large-cell lymphoma: a Children's Oncology Group phase 1 consortium study. *The Lancet Oncology*. 2013;14(6):472-80.
171. Ou SH, Bartlett CH, Mino-Kenudson M, Cui J, Iafrate AJ. Crizotinib for the treatment of ALK-rearranged non-small cell lung cancer: a success story to usher in the second decade of molecular targeted therapy in oncology. *The oncologist*. 2012;17(11):1351-75.
172. Zdzalik D, Dymek B, Grygielewicz P, Gunerka P, Bujak A, Lamparska-Przybysz M, et al. Activating mutations in ALK kinase domain confer resistance to structurally unrelated ALK inhibitors in NPM-ALK-positive anaplastic large-cell lymphoma. *Journal of cancer research and clinical oncology*. 2014;140(4):589-98.
173. Ceccon M, Mologni L, Bisson W, Scapozza L, Gambacorti-Passerini C. Crizotinib-resistant NPM-ALK mutants confer differential sensitivity to unrelated Alk inhibitors. *Molecular cancer research : MCR*. 2013;11(2):122-32.



174. Merkel O, Hamacher F, Sifft E, Kenner L, Greil R. Novel therapeutic options in anaplastic large cell lymphoma: molecular targets and immunological tools. *Molecular cancer therapeutics*. 2011;10(7):1127-36.
175. MacDonald BT, Tamai K, He X. Wnt/beta-catenin signaling: components, mechanisms, and diseases. *Developmental cell*. 2009;17(1):9-26.
176. Anastas JN, Moon RT. WNT signalling pathways as therapeutic targets in cancer. *Nature reviews Cancer*. 2013;13(1):11-26.
177. Duchartre Y, Kim YM, Kahn M. The Wnt signaling pathway in cancer. *Critical reviews in oncology/hematology*. 2016;99:141-9.
178. Moon RT, Kohn AD, De Ferrari GV, Kaykas A. WNT and beta-catenin signalling: diseases and therapies. *Nature reviews Genetics*. 2004;5(9):691-701.
179. Bellei B, Pacchiarotti A, Perez M, Faraggiana T. Frequent beta-catenin overexpression without exon 3 mutation in cutaneous lymphomas. *Modern pathology : an official journal of the United States and Canadian Academy of Pathology, Inc*. 2004;17(10):1275-81.
180. Gelebart P, Anand M, Armanious H, Peters AC, Dien Bard J, Amin HM, et al. Constitutive activation of the Wnt canonical pathway in mantle cell lymphoma. *Blood*. 2008;112(13):5171-9.
181. Hegazy SA, Alshareef A, Gelebart P, Anand M, Armanious H, Ingham RJ, et al. Disheveled proteins promote cell growth and tumorigenicity in ALK-positive anaplastic large cell lymphoma. *Cellular signalling*. 2013;25(1):295-307.
182. Anand M, Lai R, Gelebart P. beta-catenin is constitutively active and increases STAT3 expression/activation in anaplastic lymphoma kinase-positive anaplastic large cell lymphoma. *Haematologica*. 2011;96(2):253-61.

183. Coluccia AM, Vacca A, Dunach M, Mologni L, Redaelli S, Bustos VH, et al. Bcr-Abl stabilizes beta-catenin in chronic myeloid leukemia through its tyrosine phosphorylation. *The EMBO journal*. 2007;26(5):1456-66.
184. McDonnell SR, Hwang SR, Basrur V, Conlon KP, Fermin D, Wey E, et al. NPM-ALK signals through glycogen synthase kinase 3beta to promote oncogenesis. *Oncogene*. 2012;31(32):3733-40.
185. O'Brien CA, Kreso A, Dick JE. Cancer stem cells in solid tumors: an overview. *Seminars in radiation oncology*. 2009;19(2):71-7.
186. O'Brien CA, Kreso A, Jamieson CH. Cancer stem cells and self-renewal. *Clinical cancer research : an official journal of the American Association for Cancer Research*. 2010;16(12):3113-20.
187. Hadjimichael C, Chanoumidou K, Papadopoulou N, Arampatzi P, Papamatheakis J, Kretsovali A. Common stemness regulators of embryonic and cancer stem cells. *World journal of stem cells*. 2015;7(9):1150-84.
188. Han L, Shi S, Gong T, Zhang Z, Sun X. Cancer stem cells: therapeutic implications and perspectives in cancer therapy. *Acta Pharmaceutica Sinica B*. 2013;3(2):65-75.
189. Bonnet D, Dick JE. Human acute myeloid leukemia is organized as a hierarchy that originates from a primitive hematopoietic cell. *Nature medicine*. 1997;3(7):730-7.
190. Golebiewska A, Brons NH, Bjerkvig R, Niclou SP. Critical appraisal of the side population assay in stem cell and cancer stem cell research. *Cell stem cell*. 2011;8(2):136-47.

191. Boesch M, Zeimet AG, Reimer D, Schmidt S, Gastl G, Parson W, et al. The side population of ovarian cancer cells defines a heterogeneous compartment exhibiting stem cell characteristics. *Oncotarget*. 2014;5(16):7027-39.
192. Yasuda K, Torigoe T, Morita R, Kuroda T, Takahashi A, Matsuzaki J, et al. Ovarian cancer stem cells are enriched in side population and aldehyde dehydrogenase bright overlapping population. *PloS one*. 2013;8(8):e68187.
193. Christgen M, Ballmaier M, Lehmann U, Kreipe H. Detection of putative cancer stem cells of the side population phenotype in human tumor cell cultures. *Methods in molecular biology*. 2012;878:201-15.
194. Britton KM, Kirby JA, Lennard TW, Meeson AP. Cancer stem cells and side population cells in breast cancer and metastasis. *Cancers*. 2011;3(2):2106-30.
195. Tabor MH, Clay MR, Owen JH, Bradford CR, Carey TE, Wolf GT, et al. Head and neck cancer stem cells: the side population. *The Laryngoscope*. 2011;121(3):527-33.
196. Huang B, Huang YJ, Yao ZJ, Chen X, Guo SJ, Mao XP, et al. Cancer stem cell-like side population cells in clear cell renal cell carcinoma cell line 769P. *PloS one*. 2013;8(7):e68293.
197. Moti N, Malcolm T, Hamoudi R, Mian S, Garland G, Hook CE, et al. Anaplastic large cell lymphoma-propagating cells are detectable by side population analysis and possess an expression profile reflective of a primitive origin. *Oncogene*. 2015;34(14):1843-52.
198. Ding XW, Wu JH, Jiang CP. ABCG2: a potential marker of stem cells and novel target in stem cell and cancer therapy. *Life sciences*. 2010;86(17-18):631-7.

199. Fujiwara D, Kato K, Nohara S, Iwanuma Y, Kajiyama Y. The usefulness of three-dimensional cell culture in induction of cancer stem cells from esophageal squamous cell carcinoma cell lines. *Biochemical and biophysical research communications*. 2013;434(4):773-8.
200. Yang L, Ren Y, Yu X, Qian F, Bian BS, Xiao HL, et al. ALDH1A1 defines invasive cancer stem-like cells and predicts poor prognosis in patients with esophageal squamous cell carcinoma. *Modern pathology : an official journal of the United States and Canadian Academy of Pathology, Inc.* 2014;27(5):775-83.
201. Zhao JS, Li WJ, Ge D, Zhang PJ, Li JJ, Lu CL, et al. Tumor initiating cells in esophageal squamous cell carcinomas express high levels of CD44. *PloS one*. 2011;6(6):e21419.
202. de Beca FF, Caetano P, Gerhard R, Alvarenga CA, Gomes M, Paredes J, et al. Cancer stem cells markers CD44, CD24 and ALDH1 in breast cancer special histological types. *Journal of clinical pathology*. 2013;66(3):187-91.
203. Ricardo S, Vieira AF, Gerhard R, Leitao D, Pinto R, Cameselle-Teijeiro JF, et al. Breast cancer stem cell markers CD44, CD24 and ALDH1: expression distribution within intrinsic molecular subtype. *Journal of clinical pathology*. 2011;64(11):937-46.
204. Wang C, Xie J, Guo J, Manning HC, Gore JC, Guo N. Evaluation of CD44 and CD133 as cancer stem cell markers for colorectal cancer. *Oncology reports*. 2012;28(4):1301-8.
205. Singh SK, Hawkins C, Clarke ID, Squire JA, Bayani J, Hide T, et al. Identification of human brain tumour initiating cells. *Nature*. 2004;432(7015):396-401.
206. McCauley HA, Guasch G. Serial orthotopic transplantation of epithelial tumors in single-cell suspension. *Methods in molecular biology*. 2013;1035:231-45.

207. Piva M, Domenici G, Iriando O, Rabano M, Simoes BM, Comaills V, et al. Sox2 promotes tamoxifen resistance in breast cancer cells. *EMBO molecular medicine*. 2014;6(1):66-79.
208. Arif K, Hussain I, Rea C, El-Sheemy M. The role of Nanog expression in tamoxifen-resistant breast cancer cells. *OncoTargets and therapy*. 2015;8:1327-34.
209. Wang J, Wang H, Li Z, Wu Q, Lathia JD, McLendon RE, et al. c-Myc is required for maintenance of glioma cancer stem cells. *PloS one*. 2008;3(11):e3769.
210. Zhang Y, Chen HX, Zhou SY, Wang SX, Zheng K, Xu DD, et al. Sp1 and c-Myc modulate drug resistance of leukemia stem cells by regulating survivin expression through the ERK-MSK MAPK signaling pathway. *Molecular cancer*. 2015;14:56.
211. Ho MM, Ng AV, Lam S, Hung JY. Side population in human lung cancer cell lines and tumors is enriched with stem-like cancer cells. *Cancer research*. 2007;67(10):4827-33.
212. Shi GM, Xu Y, Fan J, Zhou J, Yang XR, Qiu SJ, et al. Identification of side population cells in human hepatocellular carcinoma cell lines with stepwise metastatic potentials. *Journal of cancer research and clinical oncology*. 2008;134(11):1155-63.
213. Seigel GM, Campbell LM, Narayan M, Gonzalez-Fernandez F. Cancer stem cell characteristics in retinoblastoma. *Molecular vision*. 2005;11:729-37.
214. Blank U, Karlsson G, Karlsson S. Signaling pathways governing stem-cell fate. *Blood*. 2008;111(2):492-503.
215. Cabrera MC, Hollingsworth RE, Hurt EM. Cancer stem cell plasticity and tumor hierarchy. *World journal of stem cells*. 2015;7(1):27-36.

216. Jang GB, Kim JY, Cho SD, Park KS, Jung JY, Lee HY, et al. Blockade of Wnt/beta-catenin signaling suppresses breast cancer metastasis by inhibiting CSC-like phenotype. *Scientific reports*. 2015;5:12465.
217. Yeung J, Esposito MT, Gandillet A, Zeisig BB, Griessinger E, Bonnet D, et al. beta-Catenin mediates the establishment and drug resistance of MLL leukemic stem cells. *Cancer cell*. 2010;18(6):606-18.
218. Luis TC, Naber BA, Roozen PP, Brugman MH, de Haas EF, Ghazvini M, et al. Canonical wnt signaling regulates hematopoiesis in a dosage-dependent fashion. *Cell stem cell*. 2011;9(4):345-56.
219. Zhao C, Blum J, Chen A, Kwon HY, Jung SH, Cook JM, et al. Loss of beta-catenin impairs the renewal of normal and CML stem cells in vivo. *Cancer cell*. 2007;12(6):528-41.
220. Hu Y, Chen Y, Douglas L, Li S. beta-Catenin is essential for survival of leukemic stem cells insensitive to kinase inhibition in mice with BCR-ABL-induced chronic myeloid leukemia. *Leukemia*. 2009;23(1):109-16.
221. Zhang HF, Wu C, Alshareef A, Gupta N, Zhao Q, Xu XE, et al. The PI3K/AKT/c-MYC axis promotes the acquisition of cancer stem-like features in esophageal squamous cell carcinoma. *Stem Cells*. 2016.
222. Justilien V, Walsh MP, Ali SA, Thompson EA, Murray NR, Fields AP. The PRKCI and SOX2 oncogenes are coamplified and cooperate to activate Hedgehog signaling in lung squamous cell carcinoma. *Cancer cell*. 2014;25(2):139-51.
223. Merkel O, Kenner L, Turner SD. Stem cell hunt in NHL. *Oncoscience*. 2015;2(10):809-10.

224. Basso K, Dalla-Favera R. Germinal centres and B cell lymphomagenesis. *Nature reviews Immunology*. 2015;15(3):172-84.
225. Hassler MR, Pulverer W, Lakshminarasimhan R, Redl E, Hacker J, Garland GD, et al. Insights into the Pathogenesis of Anaplastic Large-Cell Lymphoma through Genome-wide DNA Methylation Profiling. *Cell reports*. 2016;17(2):596-608.
226. Nishikawa S, Goldstein RA, Nierras CR. The promise of human induced pluripotent stem cells for research and therapy. *Nature reviews Molecular cell biology*. 2008;9(9):725-9.
227. Karagiannis P, Eto K. Ten years of induced pluripotency: from basic mechanisms to therapeutic applications. *Development*. 2016;143(12):2039-43.
228. Zhao R, Daley GQ. From fibroblasts to iPS cells: induced pluripotency by defined factors. *Journal of cellular biochemistry*. 2008;105(4):949-55.
229. Kim J, Orkin SH. Embryonic stem cell-specific signatures in cancer: insights into genomic regulatory networks and implications for medicine. *Genome Med*. 2011;3(11):75.
230. Amaya CN, Bryan BA. Enrichment of the embryonic stem cell reprogramming factors Oct4, Nanog, Myc, and Sox2 in benign and malignant vascular tumors. *BMC Clin Pathol*. 2015;15:18.
231. Wei D, Kanai M, Jia Z, Le X, Xie K. Kruppel-like factor 4 induces p27Kip1 expression in and suppresses the growth and metastasis of human pancreatic cancer cells. *Cancer research*. 2008;68(12):4631-9.
232. Leis O, Eguiara A, Lopez-Arribillaga E, Alberdi MJ, Hernandez-Garcia S, Elorriaga K, et al. Sox2 expression in breast tumours and activation in breast cancer stem cells. *Oncogene*. 2012;31(11):1354-65.

233. Singhi AD, Cimino-Mathews A, Jenkins RB, Lan F, Fink SR, Nassar H, et al. MYC gene amplification is often acquired in lethal distant breast cancer metastases of unamplified primary tumors. *Modern pathology : an official journal of the United States and Canadian Academy of Pathology, Inc.* 2012;25(3):378-87.
234. Sarkar A, Hochedlinger K. The sox family of transcription factors: versatile regulators of stem and progenitor cell fate. *Cell stem cell.* 2013;12(1):15-30.
235. Kamachi Y, Kondoh H. Sox proteins: regulators of cell fate specification and differentiation. *Development.* 2013;140(20):4129-44.
236. Rizzino A. Concise review: The Sox2-Oct4 connection: critical players in a much larger interdependent network integrated at multiple levels. *Stem cells.* 2013;31(6):1033-9.
237. Neumann J, Bahr F, Horst D, Kriegl L, Engel J, Luque RM, et al. SOX2 expression correlates with lymph-node metastases and distant spread in right-sided colon cancer. *BMC cancer.* 2011;11:518.
238. Gordon A, Conlon C, Collin J, Peto T, Gray D, Hands L, et al. An eight year experience of conservative management for aortic graft sepsis. *European journal of vascular surgery.* 1994;8(5):611-6.
239. Gelebart P, Hegazy SA, Wang P, Bone KM, Anand M, Sharon D, et al. Aberrant expression and biological significance of Sox2, an embryonic stem cell transcriptional factor, in ALK-positive anaplastic large cell lymphoma. *Blood Cancer J.* 2012;2:e82.
240. Lu YX, Yuan L, Xue XL, Zhou M, Liu Y, Zhang C, et al. Regulation of colorectal carcinoma stemness, growth, and metastasis by an miR-200c-Sox2-negative feedback loop mechanism. *Clinical cancer research : an official journal of the American Association for Cancer Research.* 2014;20(10):2631-42.



241. Han X, Fang X, Lou X, Hua D, Ding W, Foltz G, et al. Silencing SOX2 induced mesenchymal-epithelial transition and its expression predicts liver and lymph node metastasis of CRC patients. *PloS one*. 2012;7(8):e41335.
242. Santini R, Pietrobono S, Pandolfi S, Montagnani V, D'Amico M, Penachioni JY, et al. SOX2 regulates self-renewal and tumorigenicity of human melanoma-initiating cells. *Oncogene*. 2014;33(38):4697-708.
243. Zhao D, Pan C, Sun J, Gilbert C, Drews-Elger K, Azzam DJ, et al. VEGF drives cancer-initiating stem cells through VEGFR-2/Stat3 signaling to upregulate Myc and Sox2. *Oncogene*. 2015;34(24):3107-19.
244. Basu-Roy U, Bayin NS, Rattanakorn K, Han E, Placantonakis DG, Mansukhani A, et al. Sox2 antagonizes the Hippo pathway to maintain stemness in cancer cells. *Nature communications*. 2015;6:6411.
245. Chen Y, Shi L, Zhang L, Li R, Liang J, Yu W, et al. The molecular mechanism governing the oncogenic potential of SOX2 in breast cancer. *The Journal of biological chemistry*. 2008;283(26):17969-78.
246. Chen S, Xu Y, Chen Y, Li X, Mou W, Wang L, et al. SOX2 gene regulates the transcriptional network of oncogenes and affects tumorigenesis of human lung cancer cells. *PloS one*. 2012;7(5):e36326.
247. Gen Y, Yasui K, Nishikawa T, Yoshikawa T. SOX2 promotes tumor growth of esophageal squamous cell carcinoma through the AKT/mammalian target of rapamycin complex 1 signaling pathway. *Cancer science*. 2013;104(7):810-6.
248. Tian Y, Jia X, Wang S, Li Y, Zhao P, Cai D, et al. SOX2 oncogenes amplified and operate to activate AKT signaling in gastric cancer and predict immunotherapy responsiveness. *Journal of cancer research and clinical oncology*. 2014;140(7):1117-24.

249. Herreros-Villanueva M, Zhang JS, Koenig A, Abel EV, Smyrk TC, Bamlet WR, et al. SOX2 promotes dedifferentiation and imparts stem cell-like features to pancreatic cancer cells. *Oncogenesis*. 2013;2:e61.
250. Yang N, Hui L, Wang Y, Yang H, Jiang X. Overexpression of SOX2 promotes migration, invasion, and epithelial-mesenchymal transition through the Wnt/beta-catenin pathway in laryngeal cancer Hep-2 cells. *Tumour biology : the journal of the International Society for Oncodevelopmental Biology and Medicine*. 2014;35(8):7965-73.
251. Gao H, Teng C, Huang W, Peng J, Wang C. SOX2 Promotes the Epithelial to Mesenchymal Transition of Esophageal Squamous Cells by Modulating Slug Expression through the Activation of STAT3/HIF-alpha Signaling. *International journal of molecular sciences*. 2015;16(9):21643-57.
252. Weina K, Utikal J. SOX2 and cancer: current research and its implications in the clinic. *Clinical and translational medicine*. 2014;3:19.
253. Wu F, Zhang J, Wang P, Ye X, Jung K, Bone KM, et al. Identification of two novel phenotypically distinct breast cancer cell subsets based on Sox2 transcription activity. *Cellular signalling*. 2012;24(11):1989-98.
254. Zhang S, Cui W. Sox2, a key factor in the regulation of pluripotency and neural differentiation. *World journal of stem cells*. 2014;6(3):305-11.
255. Jeong CH, Cho YY, Kim MO, Kim SH, Cho EJ, Lee SY, et al. Phosphorylation of Sox2 cooperates in reprogramming to pluripotent stem cells. *Stem cells*. 2010;28(12):2141-50.

256. Fang L, Zhang L, Wei W, Jin X, Wang P, Tong Y, et al. A methylation-phosphorylation switch determines Sox2 stability and function in ESC maintenance or differentiation. *Molecular cell*. 2014;55(4):537-51.
257. Myers SA, Peddada S, Chatterjee N, Friedrich T, Tomoda K, Krings G, et al. SOX2 O-GlcNAcylation alters its protein-protein interactions and genomic occupancy to modulate gene expression in pluripotent cells. *eLife*. 2016;5:e10647.
258. Qi D, Wang Q, Yu M, Lan R, Li S, Lu F. Mitotic phosphorylation of SOX2 mediated by Aurora kinase A is critical for the stem-cell like cell maintenance in PA-1 cells. *Cell cycle*. 2016;15(15):2009-18.
259. Dang CV. c-Myc target genes involved in cell growth, apoptosis, and metabolism. *Molecular and cellular biology*. 1999;19(1):1-11.
260. DePinho RA, Hatton KS, Tesfaye A, Yancopoulos GD, Alt FW. The human myc gene family: structure and activity of L-myc and an L-myc pseudogene. *Genes & development*. 1987;1(10):1311-26.
261. Hurlin PJ. N-Myc functions in transcription and development. *Birth defects research Part C, Embryo today : reviews*. 2005;75(4):340-52.
262. Funa K, Steinholtz L, Nou E, Bergh J. Increased expression of N-myc in human small cell lung cancer biopsies predicts lack of response to chemotherapy and poor prognosis. *American journal of clinical pathology*. 1987;88(2):216-20.
263. Rubie H, Hartmann O, Michon J, Frappaz D, Coze C, Chastagner P, et al. N-Myc gene amplification is a major prognostic factor in localized neuroblastoma: results of the French NBL 90 study. Neuroblastoma Study Group of the Societe Francaise d'Oncologie Pediatrique. *Journal of clinical oncology : official journal of the American Society of Clinical Oncology*. 1997;15(3):1171-82.

264. Beltran H. The N-myc Oncogene: Maximizing its Targets, Regulation, and Therapeutic Potential. *Molecular cancer research : MCR*. 2014;12(6):815-22.
265. Patel JH, Loboda AP, Showe MK, Showe LC, McMahon SB. Analysis of genomic targets reveals complex functions of MYC. *Nature reviews Cancer*. 2004;4(7):562-8.
266. Dang CV. MYC, metabolism, cell growth, and tumorigenesis. *Cold Spring Harbor perspectives in medicine*. 2013;3(8).
267. Gregory MA, Hann SR. c-Myc proteolysis by the ubiquitin-proteasome pathway: stabilization of c-Myc in Burkitt's lymphoma cells. *Molecular and cellular biology*. 2000;20(7):2423-35.
268. Dang CV. MYC on the path to cancer. *Cell*. 2012;149(1):22-35.
269. Stine ZE, Walton ZE, Altman BJ, Hsieh AL, Dang CV. MYC, Metabolism, and Cancer. *Cancer discovery*. 2015;5(10):1024-39.
270. Kress TR, Sabo A, Amati B. MYC: connecting selective transcriptional control to global RNA production. *Nature reviews Cancer*. 2015;15(10):593-607.
271. Perna D, Faga G, Verrecchia A, Gorski MM, Barozzi I, Narang V, et al. Genome-wide mapping of Myc binding and gene regulation in serum-stimulated fibroblasts. *Oncogene*. 2012;31(13):1695-709.
272. Casey SC, Tong L, Li Y, Do R, Walz S, Fitzgerald KN, et al. MYC regulates the antitumor immune response through CD47 and PD-L1. *Science*. 2016;352(6282):227-31.
273. Felsher DW. MYC Inactivation Elicits Oncogene Addiction through Both Tumor Cell-Intrinsic and Host-Dependent Mechanisms. *Genes & cancer*. 2010;1(6):597-604.

274. Li S, Lin P, Young KH, Kanagal-Shamanna R, Yin CC, Medeiros LJ. MYC/BCL2 double-hit high-grade B-cell lymphoma. *Advances in anatomic pathology*. 2013;20(5):315-26.
275. Kramer MH, Hermans J, Wijburg E, Philippo K, Geelen E, van Krieken JH, et al. Clinical relevance of BCL2, BCL6, and MYC rearrangements in diffuse large B-cell lymphoma. *Blood*. 1998;92(9):3152-62.
276. Hecht JL, Aster JC. Molecular biology of Burkitt's lymphoma. *Journal of clinical oncology : official journal of the American Society of Clinical Oncology*. 2000;18(21):3707-21.
277. Chen YQ. [Frequency on N-ras as a transforming gene, DNA rearrangement and amplification, and over-expression of C-myc in human primary hepatic cancer]. *Zhonghua yi xue za zhi*. 1987;67(4):197-9, 14.
278. Little CD, Nau MM, Carney DN, Gazdar AF, Minna JD. Amplification and expression of the c-myc oncogene in human lung cancer cell lines. *Nature*. 1983;306(5939):194-6.
279. Baker VV, Borst MP, Dixon D, Hatch KD, Shingleton HM, Miller D. c-myc amplification in ovarian cancer. *Gynecologic oncology*. 1990;38(3):340-2.
280. Rodrigues AB, Zoranovic T, Ayala-Camargo A, Grewal S, Reyes-Robles T, Krasny M, et al. Activated STAT regulates growth and induces competitive interactions independently of Myc, Yorkie, Wingless and ribosome biogenesis. *Development*. 2012;139(21):4051-61.
281. Zhang S, Li Y, Wu Y, Shi K, Bing L, Hao J. Wnt/beta-catenin signaling pathway upregulates c-Myc expression to promote cell proliferation of P19 teratocarcinoma cells. *Anatomical record*. 2012;295(12):2104-13.

282. Weng AP, Millholland JM, Yashiro-Ohtani Y, Arcangeli ML, Lau A, Wai C, et al. c-Myc is an important direct target of Notch1 in T-cell acute lymphoblastic leukemia/lymphoma. *Genes & development*. 2006;20(15):2096-109.
283. Sears R, Nuckolls F, Haura E, Taya Y, Tamai K, Nevins JR. Multiple Ras-dependent phosphorylation pathways regulate Myc protein stability. *Genes & development*. 2000;14(19):2501-14.
284. Zhu J, Blenis J, Yuan J. Activation of PI3K/Akt and MAPK pathways regulates Myc-mediated transcription by phosphorylating and promoting the degradation of Mad1. *Proceedings of the National Academy of Sciences of the United States of America*. 2008;105(18):6584-9.
285. Roberts PJ, Der CJ. Targeting the Raf-MEK-ERK mitogen-activated protein kinase cascade for the treatment of cancer. *Oncogene*. 2007;26(22):3291-310.
286. Dhillon AS, Hagan S, Rath O, Kolch W. MAP kinase signalling pathways in cancer. *Oncogene*. 2007;26(22):3279-90.
287. Wang J, Kim J, Roh M, Franco OE, Hayward SW, Wills ML, et al. Pim1 kinase synergizes with c-MYC to induce advanced prostate carcinoma. *Oncogene*. 2010;29(17):2477-87.
288. Wang X, Cunningham M, Zhang X, Tokarz S, Laraway B, Troxell M, et al. Phosphorylation regulates c-Myc's oncogenic activity in the mammary gland. *Cancer research*. 2011;71(3):925-36.
289. Yada M, Hatakeyama S, Kamura T, Nishiyama M, Tsunematsu R, Imaki H, et al. Phosphorylation-dependent degradation of c-Myc is mediated by the F-box protein Fbw7. *The EMBO journal*. 2004;23(10):2116-25.

290. Farrell AS, Sears RC. MYC degradation. Cold Spring Harbor perspectives in medicine. 2014;4(3).
291. Gorrini C, Harris IS, Mak TW. Modulation of oxidative stress as an anticancer strategy. Nature reviews Drug discovery. 2013;12(12):931-47.
292. Sosa V, Moline T, Somoza R, Paciucci R, Kondoh H, ME LL. Oxidative stress and cancer: an overview. Ageing research reviews. 2013;12(1):376-90.
293. Simic MG, Bergtold DS, Karam LR. Generation of oxy radicals in biosystems. Mutation research. 1989;214(1):3-12.
294. Klaunig JE, Kamendulis LM, Hocevar BA. Oxidative stress and oxidative damage in carcinogenesis. Toxicologic pathology. 2010;38(1):96-109.
295. Janssen-Heininger YM, Mossman BT, Heintz NH, Forman HJ, Kalyanaraman B, Finkel T, et al. Redox-based regulation of signal transduction: principles, pitfalls, and promises. Free radical biology & medicine. 2008;45(1):1-17.
296. Miller DM, Thomas SD, Islam A, Muench D, Sedoris K. c-Myc and cancer metabolism. Clinical cancer research : an official journal of the American Association for Cancer Research. 2012;18(20):5546-53.
297. Kim MH, Kim H. Oncogenes and tumor suppressors regulate glutamine metabolism in cancer cells. Journal of cancer prevention. 2013;18(3):221-6.
298. Dayem AA, Choi HY, Kim JH, Cho SG. Role of oxidative stress in stem, cancer, and cancer stem cells. Cancers. 2010;2(2):859-84.
299. Diehn M, Cho RW, Lobo NA, Kalisky T, Dorie MJ, Kulp AN, et al. Association of reactive oxygen species levels and radioresistance in cancer stem cells. Nature. 2009;458(7239):780-3.

300. Mahalingaiah PK, Singh KP. Chronic oxidative stress increases growth and tumorigenic potential of MCF-7 breast cancer cells. *PLoS one*. 2014;9(1):e87371.
301. Reuter S, Gupta SC, Chaturvedi MM, Aggarwal BB. Oxidative stress, inflammation, and cancer: how are they linked? *Free radical biology & medicine*. 2010;49(11):1603-16.
302. Waris G, Ahsan H. Reactive oxygen species: role in the development of cancer and various chronic conditions. *Journal of carcinogenesis*. 2006;5:14.
303. Thornber K, Colomba A, Ceccato L, Delsol G, Payrastre B, Gaits-Iacovoni F. Reactive oxygen species and lipoxygenases regulate the oncogenicity of NPM-ALK-positive anaplastic large cell lymphomas. *Oncogene*. 2009;28(29):2690-6.
304. Meissl K, Macho-Maschler S, Muller M, Strobl B. The good and the bad faces of STAT1 in solid tumours. *Cytokine*. 2015.
305. Weilemann A, Grau M, Erdmann T, Merkel O, Sobhiafshar U, Anagnostopoulos I, et al. Essential role of IRF4 and MYC signaling for survival of anaplastic large cell lymphoma. *Blood*. 2015;125(1):124-32.
306. Gopal K, Gupta N, Zhang H, Alshareef A, Alqahtani H, Bigras G, et al. Oxidative stress induces the acquisition of cancer stem-like phenotype in breast cancer detectable by using a Sox2 regulatory region-2 (SRR2) reporter. *Oncotarget*. 2016;7(3):3111-27.



## CHAPTER 2

### **STAT1 is phosphorylated and downregulated by the oncogenic tyrosine kinase NPM-ALK in ALK-positive anaplastic large-cell lymphoma<sup>1</sup>**

---

<sup>1</sup>This chapter has been modified from a previous publication: Wu C, Molavi O, Zhang H, Gupta N, Alshareef A, Bone K.M, Gopal K, Wu F, Lewis J.T, Douglas D.N, Kneteman N.M, and Lai R. STAT1 is phosphorylated and downregulated by the oncogenic tyrosine kinase NPM-ALK in ALK-positive anaplastic large-cell lymphoma. *Blood*. 2015; 126(3):336-345. The content of this publication has been included in this thesis with permission from the publisher (License number: 3981420253343).

I prepared the first draft and revisions based on the suggestions and comments of the co-authors. I designed and performed most of the experiments described herein, except for the following: O.M. performed some studies, data shown in Figure 2.1A and Figure 2.4F-G; H.Z., N.G., A.A., and F.W. performed portions of the experiments and provided technical support and intellectual input. K.B. provided the SupM2 and Karpas 299 cell lines stably transfected with Tet on system. N.G., K.G., J.L., D. D., and N.K. were responsible for the animal study design, conducting euthanization of the SCID mouse and data analysis. R.L. provided numerous comments and final review of the manuscript before it was submitted for publication.

## 2.1 Introduction

Signal transducer and activator of transcription 1 (STAT1), a member of the STAT family of transcription factors, is a major mediator of  $\gamma$ -interferon (IFN $\gamma$ ) signaling (1). Subjection of IFN $\gamma$  leads to phosphorylation of STAT1 at tyrosine 701, which is known as an active form of STAT1, and phosphorylated STAT1 at tyrosine 701 subsequently form STAT1 homo/heterodimers with other STAT family members, followed by migration into nucleus to execute their transcriptional functions (2). STAT1 is also reported to carry tumor suppressor functions (1-3). In comparison, STAT3, another STAT family member, is oncogenic when inappropriately activated (4, 5). Correlating with their opposing roles, STAT1 and STAT3 are known to have functional interactions. For instance, STAT1 and STAT3 can form heterodimers (4, 6-8), and the expression of gene targets regulated by STAT1 and STAT3 is dependent on the relative proportions of STAT1 homodimers, STAT3 homodimers and the STAT1/STAT3 heterodimers (9, 10). This concept is well exemplified by the observation that treatment of multiple myeloma cell lines with  $\alpha$ -interferon triggers a shift from STAT3 homodimers to STAT1 homodimers and STAT3/STAT1 heterodimers, and this biochemical change correlates with a switch from cell proliferation to apoptosis (10). Several other studies also have shown that STAT1 and STAT3 can directly antagonize each other functionally (11-15). It has been reported that activated STAT3 suppresses the DNA-binding of STAT1 homodimers in myeloid cells although it does not affect STAT1 tyrosine phosphorylation or its nuclear translocation (11). In contrast, IFN $\gamma$  is reported to selectively inhibit STAT3-dependent IL-6 signaling in human endothelial cells by increasing the expression of SOCS3, which inhibits STAT3 signaling (14).

STAT1 expression is reported to be downregulated in various types of cancer, including oral squamous cell carcinoma (16), melanoma (17, 18), cutaneous T-cell lymphoma (19), breast cancer (20) and esophagus squamous cancer (21, 22). How STAT1 is downregulated in cancer remains poorly studied. However, a number of studies have indicated that STAT1 is degraded in ubiquitin-dependent proteasome pathway in some other cell models (23-28). For instance, Soond *et al* reported that ERK1/2 phosphorylates STAT1 at serine 727 (p-STAT1<sup>S727</sup>, an active form of STAT1) and promotes its degradation in proteasome pathway in E3 ligase  $\beta$ TRCP dependent manner in mouse fibroblast cells (25). A more recent study revealed that IFNs induces phosphorylation and ubiquitination of activated STAT1 (p-STAT1<sup>Y705</sup>, or pSTAT1), thus promoting its degradation in proteasome pathway in human embryonic kidney 293T cells (24). Intriguingly, a recent study showed that NKLAM, as an E3 ubiquitin ligase, ubiquitinates STAT1 but positively regulates STAT1 transcriptional activity and its DNA binding ability in mice macrophage cells (23).

ALK-positive anaplastic large-cell lymphoma (ALK+ALCL) is a specific type of non-Hodgkin lymphoma of mature T-cell lineage (29). The characteristic chromosomal translocation,  $t(2;5)(p23;q35)$ , is observed in 80% of ALK+ALCL tumors, and this aberrancy results in the generation of the oncogenic fusion protein, NPM-ALK (29, 30). NPM-ALK interacts and activates a host of cellular signaling proteins, such as JAK, STAT3 and PI3K, thereby deregulating these pathways and leading to increased cell proliferation and survival (29, 30). The pivotal role of STAT3 signaling in mediating the oncogenic effects of NPM-ALK has been particularly highlighted (29). As STAT1 can

inhibit STAT3, as discussed above, we hypothesize that the STAT1 expression and/or signaling is defective in ALK+ALCL, leaving the STAT3 activation unchecked. The expression and functional status of STAT1 in ALK+ALCL have never been examined.

In this study, the expression and the functional status of STAT1 in ALK+ALCL cells were evaluated. The results indicated that NPM-ALK directly contributes to the relatively low expression of STAT1 in ALK+ALCL tumors and this process is proteasomal- and STAT3-dependent. The data from this study also demonstrated that STAT1, if it is overexpressed to a higher expression level, exerts tumor suppressor functions.

## **2.2 Methods and materials**

### **2.2.1 Primary tumors and cell lines**

All primary tumors were diagnosed at the Cross Cancer Institute (Edmonton, Alberta, Canada) and the diagnostic criteria were based on those described in the WHO Classification Scheme. The use of these patient samples for research has received research ethics approval at Feb 17<sup>th</sup> of 2016, by the Human Research Ethics Board at the University of Alberta, with approval number: Pro00062737. Karpas 299, established from blast cells in the peripheral blood of a 25-year-old white man diagnosed with ALK+ALCL, was a gift from Dr. Marshal Kadin (Boston, MA). SupM2 cell line, established from the cerebrospinal fluid of a 5-year-old-girl with refractory ALK+ALCL, and SU-DHL1 cell line, established from peritoneal effusion of a 10-year-old boy diagnosed with ALK+ALCL, were both purchased from Deutsche Sammlung von Mikroorganismen und Zellkulturen GmbH, DSMZ, Germany. All three ALK+ALCL cell

lines express CD30 and carry chromosome translocation t(2;5)(p23;q35), resulting in the generation of NPM-ALK fusion gene. All three cell lines were grown and expanded in RPMI 1640 (Invitrogen, Life Technologies, Grand Island, NY) supplemented with 10% fetal bovine serum (FBS, Invitrogen) in 5% CO<sub>2</sub> atmosphere at 37°C. GP293 cell line, an advanced version of human embryonic kidney cells 293, was grown in the DMEM medium supplemented with 10% FBS (Invitrogen) in 5% CO<sub>2</sub> atmosphere at 37°C.

### **2.2.2 Chemical treatments**

MG132, cycloheximide, IFN $\gamma$ , crizotinib, Stattic, U0126, and 5-aza-2'-deoxycytidine were all purchased from Sigma Aldrich (St Louis, MO). All above reagents were dissolved in Dimethyl Sulfoxide (DMSO) (Sigma Aldrich). 0.1 $\mu$ M and 0.5  $\mu$ M 5 aza-2'-deoxycytidine were used in this study to evaluate whether STAT1 gene is methylated in SupM2 cells. 0.5 mM, 1 mM and 2 mM U0126 were used to treat SupM2 cells for 5 hours to assess the relationship between STAT1 and MEK/ERK pathway. 5 $\mu$ M MG132 and 100  $\mu$ g/mL cycloheximide were subjected to SupM2 and Karpas 299 cells for 2 hours and 6 hours, respectively, to assess the half-life of STAT1. Various doses of crizotinib ranging from 0 to 50 nM were applied to study the relationship between NPM-ALK and STAT1 in ALK+ALCL cells. Various doses (ranging from 0 to 50 ng/mL) of IFN $\gamma$  were utilized to activate STAT1 signaling in ALK+ALCL cells in a time-course experiment. Stattic (ranging from 0 to 5 nM) was used to inhibit STAT3 activity in this study.

### **2.2.3 Immunohistochemistry**

Immunohistochemistry was performed using standard technique as previously described (31). In brief, formalin-fixed, paraffin-embedded tissue sections (4  $\mu\text{M}$  thickness) were deparaffinized and hydrated. Heat-induced epitope retrieval was executed by using citrate buffer (pH=6) in a pressure cooker, followed by incubation of tissue sections with 3%  $\text{H}_2\text{O}_2$  for 10 minutes to block endogenous peroxidase activity at room temperature. The tissue sections were incubated with anti-STAT1 antibody (1:500) (42H3, Cell Signaling Technology Inc; Danvers, MA) overnight in a humidified chamber in 4°C cold room. The next day, tissue sections, after 3 X PBS washes, were subsequently incubated with anti-Rabbit IgG (EnVison; Dako, Santa Clara, CA) for 40 minutes at room temperature. Next, tissue sections were incubated with 3,3'-diaminobenzidine/ $\text{H}_2\text{O}_2$  (Dako) for color development and counterstained with hematoxylin for 1 minute. Pictures were taken on a Zeiss Axioscope 2 microscope (Carl Zeiss, Heidelberg, Germany).

### **2.2.4 Short interfering RNA and transfections**

siRNA (SMART pool) for STAT1, STAT3 and scrambled siRNA (SMART pool) were purchased from Dharmacon (Lafayette, CO). Individual STAT1 siRNA 1 and 2 were also purchased from Dharmacon. All siRNAs were diluted with dd $\text{H}_2\text{O}$  and stocked with the concentration of 20  $\mu\text{M}$ . Transfection of GP293 cells with siRNAs (final concentration: 200 nM) were performed using lipofectamine 2000 reagents (Invitrogen). In brief, 1 million GP293 cells seeded in 10 cm-diameter cell culture plate (Corning<sup>TM</sup>, ThermoFisher Scientific Canada) were transfected with 200 nM siRNA using lipofectamine 2000 reagent (Invitrogen). Transient transfections of 5 million of

ALK+ALCL cells with siRNAs (final concentration: 600 nM) were performed using BTX Electro Square Porator ECM830 (225 V, 8.5 milliseconds, 3 pulses) (Harvard Apparatus; Holliston MA). The efficiency of target gene inhibition was assessed using Western blotting.

### **2.2.5 Plasmid constructs and transfections**

pRK5-HA-Ubiquitin-WT was a gift from Ted Dawson (Addgene plasmid #17608) (Cambridge, MA). *STAT1C-flag* in pcDNA3.1 was a gift from Dr. OUCHI (19). Transient transfections of Karpas 299 and SupM2 cells (5 million cells) with 10 µg plasmid were performed using the BTX Electro Square Porator ECM830 (225 V, 8.5 milliseconds, 3 pulses). *NPM-ALK* in pcDNA3.1 was generated by the Lai lab (32). Transient transfections of GP293 cells (1 million cells) with 2 µg of either *NPM-ALK* or pcDNA3.1, or GP293 cells co-transfected with both *NPM-ALK* and pcDNA3.1-STAT1-flag (Addgene) or STAT1<sup>Y701F</sup>-flag (Addgene) were performed using lipofectamine 2000 reagents (Invitrogen). In brief, 1 million cells seeded in 10 cm-diameter cell culture plate (Corning™, ThermoFisher Scientific Canada) were transfected with 2 µg plasmid using lipofectamine 2000 reagents (Invitrogen).

### **2.2.6 Generation of Tet on inducible stable cell lines**

To generate the *STAT1C*-inducible stable cell lines, two ALK+ALCL cell lines, SupM2 and Karpas 299, were infected with retroviral supernatant generated by transfecting Phoenix packaging cells with the pRetro-X Tet on Advanced plasmid (Clontech, Mountain View, CA) using lipofectamine 2000 (Invitrogen) following the manufacturer's suggested protocol. These cells were maintained in 200 µg/mL G418 (Invitrogen), 100

units/mL penicillin and 100 µg/mL streptomycin (Invitrogen) for two weeks to select for stable cells. *STAT1C* cDNA was cloned by GenScript (Piscataway, NJ) into a retroviral vector pRetro-Tight-Pur (Clontech) under the control of a doxycycline-inducible promoter, and viral supernatant was, used to transduce Tet on SupM2 and Karpas 299 cells and selected by puromycin up to 2 µg/mL (Invitrogen) for 1 month. Empty vector was also transduced in these cells as controls. The expression of phosphorylated STAT1<sup>Y701</sup> and STAT1 were confirmed by treating the cells in culture with doxycycline (Sigma Aldrich) at different concentrations for 48 hours in RPMI 1640 supplemented with 10% Tet system-approved FBS (Clontech).

### **2.2.7 Cell-cycle assay**

To evaluate cell-cycle and apoptosis in the ALK+ALCL cell lines, the cells were stained with propidium iodide, a late marker of cell apoptosis, and the cell-cycle analysis was performed by flow cytometry (BD FACS Calibur, Flow Cytometry Lab, Department of Experimental Oncology, Cross Cancer Institute, University of Alberta, Canada). In brief, following treatment, cells were fixed with ice-cold 70% ethanol for 24 hours. Cells were then washed gently with cold 1 X PBS three times, following by suspension with 50 µl of (100 µg/mL stock) RNase and 200 µl of (50 µg/mL stock) propidium iodide in dark at 37 °C for 15 minutes. Then cells were processed for flow cytometry (BD FACS Calibur) to measure the forward scatter and side scatter to identify single cells. Data acquisition was gated using pulse width versus pulse area to exclude apoptotic cells and cell doublets, and the cell-cycle phase distribution was determined using the CellQuest program (20,000 events were counted). The experiments were performed in triplicate.



### **2.2.8 Western blotting and co-immunoprecipitation**

Western blotting was performed using standard techniques. Briefly, the cells were washed with cold 1 x PBS (pH7.0) and lysed in 1 x RIPA lysis and extraction buffer (ThermoFisher Scientific Canada) containing protease inhibitor cocktail (Sigma Aldrich) and phosphatase inhibitor cocktail (Sigma Aldrich). After incubation on ice for 30 minutes, the cell lysates were subjected to centrifuge at 14,000 g for 15 minutes at 4°C, and the supernatants were collected. The protein concentration was assessed using BCA protein assay kit (Bio-Rad, Hercules, CA, USA). The protein lysates were then heated with 4 X loading buffer (240 mM Tris-HCL pH 6.8, 40% glycerol, 8% SDS, 0.04% bromophenol blue, 5%  $\beta$ -mercaptoethanol) at 100°C for 5 minutes. 12% or 10% SDS-polyacrylamide gel (SDS-PAGE) was used. After electrophoresis and transfer to nitrocellulose membranes (Bio-Rad) by electroblotting, the membranes were probed with primary antibodies (1:1000) (overnight, 4°C) and secondary antibodies (1:1000) (1 hour, room temperature), followed by the enhanced chemiluminescence (ECL) Western blotting detection system (Bio-Rad).

Co-immunoprecipitation was performed and described briefly as below. Cells were harvested and washed with cold 1X PBS for 2 times, then were lysated with CellLytic M buffer (Sigma Aldrich) containing protease inhibitor cocktails (P8340, Sigma Aldrich) and phosphatase inhibitor cocktails (P5726, Sigma Aldrich). After incubation on ice for 30 minutes, the cell lysates were proceeded to centrifuge at 14,000 X g for 15 minutes at 4°C. The supernatants (protein lysates) were collected and quantitated by using Pierce™ BCA protein Assay Kit (ThermoFisher Scientific Canada). In principle, in this protein quantification assay, protein lysates can reduce  $\text{Cu}^{2+}$  to  $\text{Cu}^{1+}$  in an alkaline

medium, and bicinchoninic acid (BCA) subsequently reacts with  $\text{Cu}^{1+}$ , forming a water soluble complex that exhibits strong absorbance at 562 nm. Then 500  $\mu\text{g}$  protein lysates were incubated with 3  $\mu\text{g}$  primary antibody and rotated at 4 °C for overnight. Next day, the 1 X PBS-washed protein A Plus/Protein G agarose (ThermoFisher Scientific Canada) were added to the protein lysates and rotated at 4°C for additional 3 hours. Last, the protein lysates were centrifuged at 8000 X g for 3 minutes and the agaroses were kept and washed gently with cold 1 X PBS for three times. Subsequently, the agaroses were diluted in 50  $\mu\text{l}$  4 X loading buffer (40% glycerol, 240 mM Tris-HCl pH 6.0, 8% SDS, 0.04% bromophenol blue, and 5%  $\beta$ -mercaptoethanol) and heated for 5 minutes at 100 °C, followed by centrifuge at 14000 X g for 15 minutes. The supernatant were collected and thereafter were proceed to SDS-PAGE.

Antibodies against for phosphorylated STAT1<sup>Y701</sup> (58D6), STAT1 (D1K9Y), phosphorylated ALK<sup>Y1604</sup> (#3341), ALK (C26G7), phosphorylated STAT3<sup>Y705</sup> (D3A7), IRF-1 (D5E4), Cleaved PARP (D64E10), T-bet (D6N8N), Bcl-2 (D55G8), Caspas 3 (8G10), PARP (46D11), IRF-7 (D2A1J), Survivin (71G4B7) were purchased from Cell Signaling Technology (Danvers, MA). Antibodies against  $\beta$ -actin (C4),  $\gamma$ -tubulin (C20), HA (Y11), Ub (FL-76), STAT3 (H-190), SOCS-1 (H-93) were purchased from Santa Cruz Biotechnology (Santa Cruz, CA). Anti-flag (clone M2) antibody was purchased from Sigma Aldrich. The above antibodies were diluted by 1000 folds with TBS buffer, 0.5% Tween 20 (Sigma Aldrich) and 5% BSA (Sigma Aldrich) for use. Secondary antibodies anti-Rabbit IgG (1:2000) and anti-Mouse IgG (1:2000) were purchased from Cell Signaling Technology.

The densitometry value of Western blotting bands was analyzed with Image J software (Bethesda, WA).

### **2.2.9 Methylcellulose colony formation assay**

Methylcellulose-based media was purchased from R&D systems Inc (Minneapolis, MN), and the methylcellulose colony formation assay was performed as below. Briefly, 1000 cells were seeded in each well of 6-well plate with 4 mL methylcellulose-based media containing 1.2% methylcellulose agarose, 30% FBS, 1% bovine serum albumin, 0.1% penicillin/streptomycin (Thermo Fisher Scientific), and 0.1%  $\beta$ -mercaptoethanol. The colonies with more than 40  $\mu$ m in diameter were counted after 10-14 days of culture.

### **2.2.10 Dual luciferase assay**

To assess the transcriptional activity of STAT3 affected by STAT1C in ALK+ALCL, the dual luciferase assay kit (Dual-Glo<sup>TM</sup> Luciferase Assay System, Promega, Madison, WI) was used. Tet on SupM2-STAT1C cells were transiently transfected with 1  $\mu$ g of pRL Renilla Luciferase Reporter Vector (Promega) and 10  $\mu$ g of pLUCTSK3 (Promega), using the BTX Electro Square Porator ECM830 (225 V, 8.5 million seconds, 3 pulses). Cells exposed with different doses of doxycycline were harvested at 24 hours post transfection, and the firefly and *Renilla* luciferases were measured sequentially from a single sample according to the manufacturer's instructions. In brief, firstly, the firefly luciferase reporter was measured by adding luciferase assay reagent II (provided in the kit) in the cell pellets after 3 X cold 1 X PBS wash to generate a luminescent signaling (last for ~1 minute), after the reaction is quenched, the *Renilla* luciferase reaction was initiated by adding Stop & Glo<sup>®</sup> Reagent (provided in the kit), which produced stabilized

signal from the *Renilla* luciferase. The luciferase values were read by FLUOstar Omega microplate reader (BMG LabTech, ThermoFisher Scientific Canada). This experiment was performed in triplicate.

### 2.2.11 STAT3 DNA probe binding assay

Tet on SupM2-STAT1C cells were induced with 0, 20, 200 ng/mL doxycycline for 48 hours, then the cells were harvested and washed with cold PBS twice, following by cytoplasmic and nuclear fractionation using the Pierce NE-PER kit (ThermoFisher Scientific Canada). This kit can efficiently solubilize and separate cytoplasmic and nuclear proteins into fractions. In brief, CER I and CER II buffer provided in the kit were used to lysate the cells to extract cytoplasmic fraction, and NER buffer in the kit was utilized to extract nuclear fraction. 300 ng nuclear protein was incubated with 3 pmol of either mutant or wild-type biotin-labeled STAT3 probe (constructed by IDT, Edmonton, Alberta, Canada) for 0.5 hour by rotating at room temperature. Streptavidin agarose beads (75  $\mu$ l, ThermoFisher Scientific Canada) were added to each sample, and the samples were rotated on UltraRocker<sup>TM</sup> Rocking Platform (Bio-Rad) by overnight at 4°C. The next day, the samples were washed with cold 1 X PBS three times, and protein was eluted at 100°C in 4 X protein loading buffer and loaded on SDS-PAGE gels.

Wild-type STAT3 probe: 5'-GATCTAGGAAT**TTCCCAGAA**GG-3';

Mutant STAT3 probe: 5'-GATCTAGGAACCTTTGACGGG-3'.

The underlined bolded sequence is STAT3 consensus DNA binding sequence.

### **2.2.12 Trypan blue exclusion assay and MTS assay**

Cell viability was assessed by trypan blue exclusion assay. Trypan blue was purchased from ThermoFisher Scientific Canada. The viable cells were calculated as the total number of cells within the grids on the hemacytometer. Viable cells do not take up trypan blue but non-viable cells do. The CellTiter 96® AQueous One Solution Cell Proliferation Assay kit was purchased from Promega (Madison, WI) for MTS assay to assess the cell growth. This assay was performed by adding 20 µl of 3-(4,5-dimethylthiazol-2-yl)-5-(3-carboxymethoxyphenyl)-2-(4-sulfophenyl)-2H-tetrazolium (MTS) reagent provided in the kit directly to the wells containing live cells in 96-well plate (Corning), with incubating time ranging from 1 to 5 hours. Then the absorption values were read by FLUOstar Omega microplate reader (BMG LabTech, ThermoFisher Scientific Canada).

### **2.2.13 RNA extraction, cDNA synthesis, and quantitative reverse transcriptase**

#### **PCR (quantitative RT-PCR)**

Total RNA extraction was performed with the Qiagen RNeasy Kit (Qiagen, Toronto, Ontario, Canada) according to the manufacturer's protocol. In brief, cells after 1 X cold PBS three times wash and centrifuge (300 X g) were lysed and then homogenized. Ethanol was added to the cell lysate, which subsequently were loaded onto the RNeasy silica membrane (provided in the kit). RNA can bind to the membrane, but all other contaminants were washed away. 1 µg of RNA was reverse-transcribed using Superscript II (Invitrogen) to generate cDNA. 1 µL of the resulting cDNA mixture was added to the Power SYBR Green PCR Master Mix (Invitrogen) and amplified with gene

specific primers on the Applied Biosystems 7900HT (Carlsbad, CA; The Applied Genomics Centre, Edmonton, Alberta, Canada).

Primer sequences were as below:

IFN  $\gamma$ : Forward – TCGGTAAGTACTGACTTGAATGTCCA

Reverse – TCGCTTCCCTGTTTTAGCTGC

IRF-1: Forward – ATGCCCATCACTCGGATGC

Reverse – CCCTGCTTTGTATCGGCCTG

GAPDH: Forward – ACAACTTTGGTATCGTGGAAGG

Reverse – GCCATCACGCCACAGTTTC

All genes of interest were normalized to GAPDH transcript expression levels.

#### **2.2.14 SCID mouse xenograft studies**

Eight of CB-17 strain severe combined immunodeficiency (SCID) mice, purchased from Taconic (Hudson, NY, USA), were housed in a virus- and antigen-free facility supported by the Health Sciences Laboratory Animal Services at the University of Alberta. The animal studies had received ethical approval by the Animal Care and Use Committee (ACUC) at Dec 10th of 2015, with approval number: AUP00000782. Briefly,  $5 \times 10^6$  Tet on-SupM2-STAT1C or Tet on-SupM2-empty vector cells growing exponentially were injected into the left or right flank of 4-week-old male mice. Two days later, the 8 mice were split into two groups (4 each), and fed with water containing 1 mg/mL sucrose and either 2 or 5 mg/mL doxycycline. These animals were euthanized when a tumor of >10 mm in the greatest dimension became palpable. Tumor cells from the harvested mouse xenografts were isolated using the Macs tumor dissociation kit (Miltenyi Biotec Inc, CA) as per manufacturer's protocol. Briefly, the mouse tumor tissues were enzymatically

digested using the Enzyme mix provided in the kit, and the gentleMACS™ Dissociators (provided in the kit) were applied for the mechanical dissociation steps. After tumor dissociation, the tumor samples were filtered to single-cell suspension, following by Western blotting analysis.

### **2.2.15 Statistical analysis**

Data were expressed as mean  $\pm$  standard deviation. Half maximal inhibitory concentration (IC50) was calculated by Graphpad Prism (La Jolla, CA). Significance was determined by using Student's *t*-test and *Fisher exact* test. Statistical significance is denoted by \* ( $P<0.05$ ) and \*\*( $P<0.01$ ).

## **2.3 Results**

### **2.3.1 STAT1 is expressed at a low level in ALK+ALCL tumors and cell lines**

Western blotting was employed to evaluate the expression level of STAT1 in ALK+ALCL cells. As compared to peripheral blood T-cells from healthy donors, the total STAT1 levels in all 3 frozen tumors were low (**Figure 2.1A**). When the same Western blot was probed with an antibody reactive with pSTAT1, 2 of 3 cases showed a relatively low level of pSTAT1. On the right panel, all three ALK+ALCL cell lines expressed a relatively low level of total STAT1. Again, 2 of 3 cell lines showed a low pSTAT1 expression level.

Then immunohistochemistry was employed to evaluate the expression of STAT1 in formalin-fixed/paraffin-embedded tissues. As shown in **Figure 2.1B**, STAT1 was

strongly expressed by the tonsillar interfollicular T-cells (left panel, white arrow) but only weakly by germinal center B-cells (left panel, black arrow). All ALK+ALCL tumors examined (n=7) consistently showed no/weak STAT1 expression relative to the surrounding benign lymphocytes and macrophages (middle panel). In contrast, all 5 ALK-negative ALCL (ALK-ALCL) tumors showed a relatively high level of STAT1 expression (right panel). This difference in STAT1 expression between ALK+ALCL and ALK-ALCL tumors is statistically significant ( $P=0.0013$ , Fisher exact test).

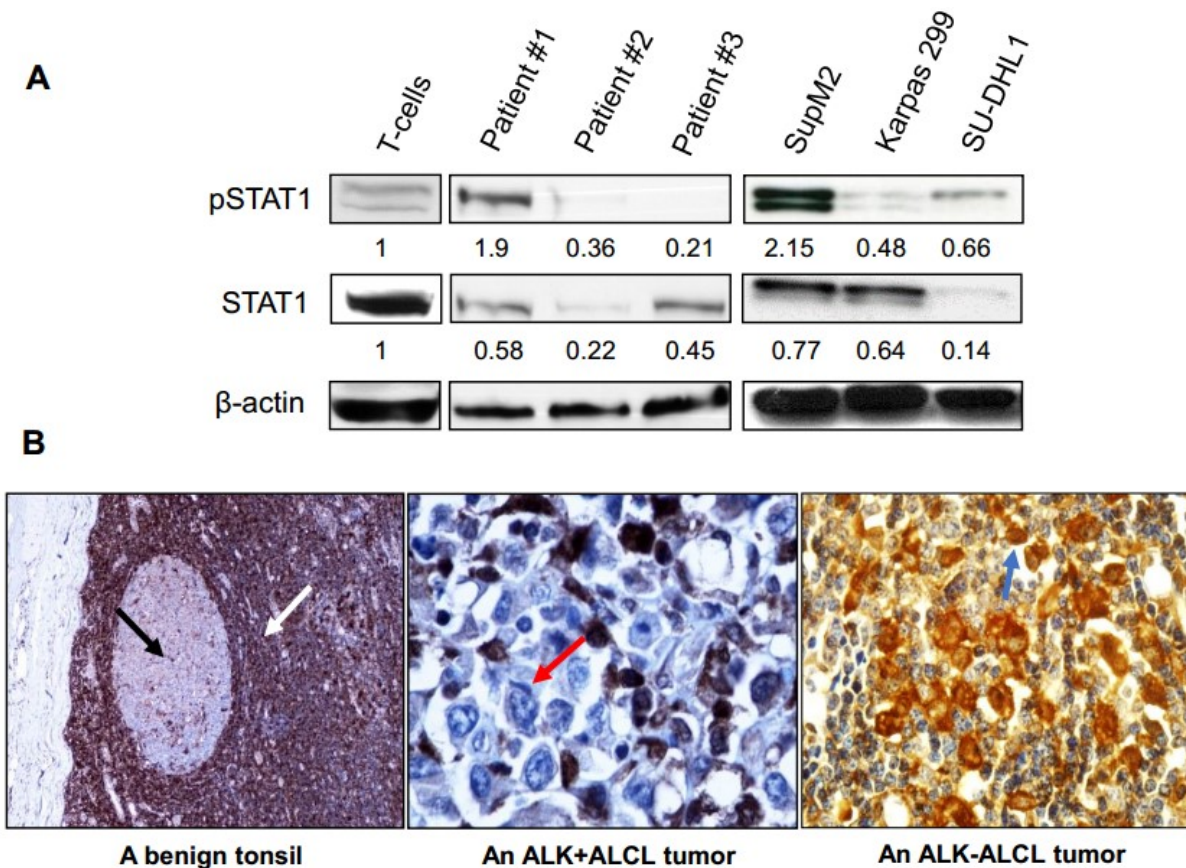


**Figure 2.1 Expression of STAT1 in ALK+ALCL cell lines and patient samples.**

A) Western blotting studies revealed a relatively low expression level of STAT1 in 3 ALK+ALCL tumors and 3 cell lines, compared to that of normal peripheral blood T-cells. Densitometry values shown were normalized to the  $\beta$ -actin bands. Most cases also had a low expression level of pSTAT1. B) Immunohistochemical study results showed the expression of STAT1 in paraffin-embedded tissues derived from a representative



benign tonsil (left, 100X magnification) a representative ALK+ALCL tumor (middle, 400X magnification) and a representative ALK-ALCL tumor (right, 200X magnification). In benign tonsils, the interfollicular T-cells (white arrow) were strongly STAT1-positive, whereas the germinal center B-cells (black arrow) were STAT1-weak. In the ALK+ALCL tumor, the infiltrating T-cells were strongly positive for STAT1 whereas the large lymphoma cells (red arrow) were virtually negative for STAT1. In the ALK-ALCL tumor, the large lymphoma cells (blue arrow) were strongly positive for STAT1.

### **2.3.2 The ubiquitin-proteasome pathway is involved in the downregulation of STAT1 in ALK+ALCL cells**

Some literature suggested that several possible mechanisms of STAT1 downregulation. First, the *STAT1* gene promoter has been reported to be methylated and silenced in head and neck squamous carcinoma (33). Thus, SupM2 cells were subjected with 5-aza-2'-deoxycytidine up to 7 days; however, no restoration of STAT1 was found (**Figure 2.2A**). Second, another literature suggested that the MEK signaling pathway can downregulate STAT1 in mouse embryonic fibroblasts (25); however, the addition of a MEK inhibitor (U0126) to SupM2 cells also did not appreciably change the STAT1 level detected by Western blotting (**Figure 2.2B**). Lastly, in the same study, the authors revealed that both STAT1 and pSTAT1 are degraded via the ubiquitin-proteasome pathway after oxidative stress in mouse embryonic fibroblasts (25). Thus, we subjected SupM2 and Karpas 299 cells to MG132, a proteasome inhibitor. As shown in **Figure 2.2C-D**, both STAT1 and pSTAT1 levels increased in a dose/time-dependent manner. Furthermore, the amount of ubiquitinated STAT1 increased with MG132 treatment in the same time frame (**Figure 2.2E-F**). As shown in **Figure 2.2G-H**, in the presence of

cycloheximide(CHX), MG132 treatment was found to dramatically prolong the half-life of STAT1 in SupM2 and Karpas 299 cells.

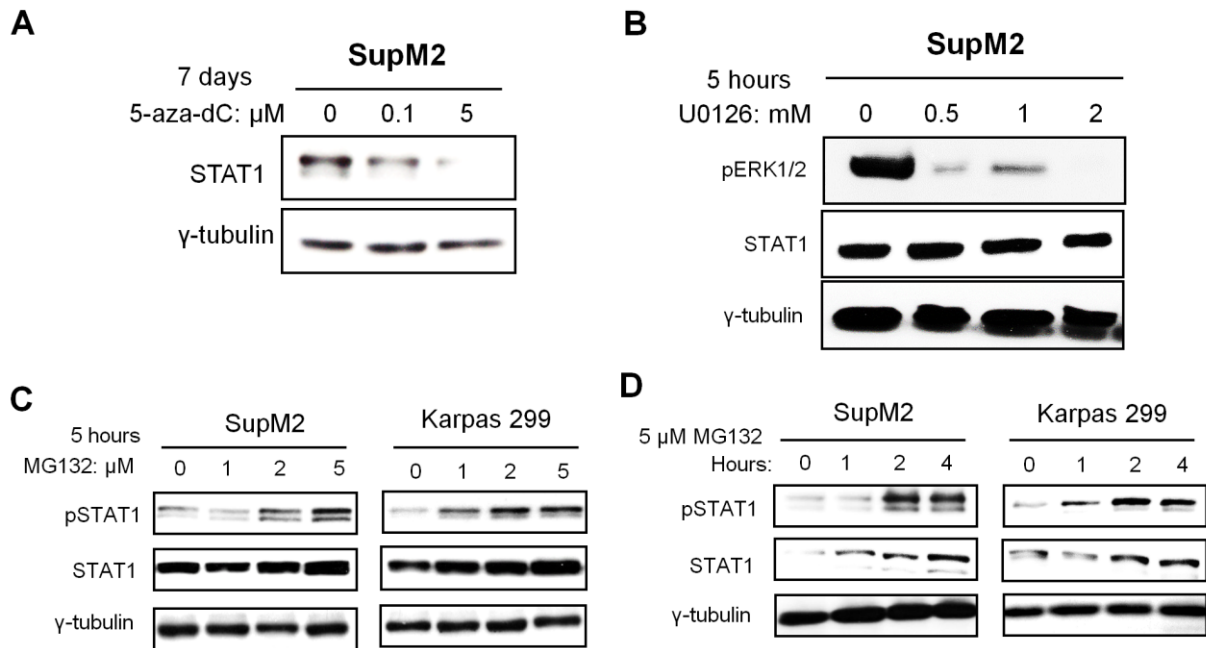


**Figure 2.2 The ubiquitin-proteasome pathway is involved in the downregulation of STAT1 in ALK+ALCL cells.** A) SupM2 cells were subjected with 0.1  $\mu$ M, 5  $\mu$ M 5-aza-2'-deoxycytidine (5-aza-dC) up to 7 days, and the expression of STAT1 was not restored. B) SupM2 cells were subjected with various doses of MEK inhibitor U0126 for 5 hours, STAT1 expression was not altered in this experiment. C) SupM2 and Karpas 299 cells were treated with varying doses of MG132 for 5 hours. pSTAT1 and STAT1 were upregulated in response to MG132 in a dose dependent manner. D) A time course experiment in which SupM2 and Karpas 299 cells were treated with 5  $\mu$ M of MG132 was performed; pSTAT1 and STAT1 were upregulated in a time-dependent manner.

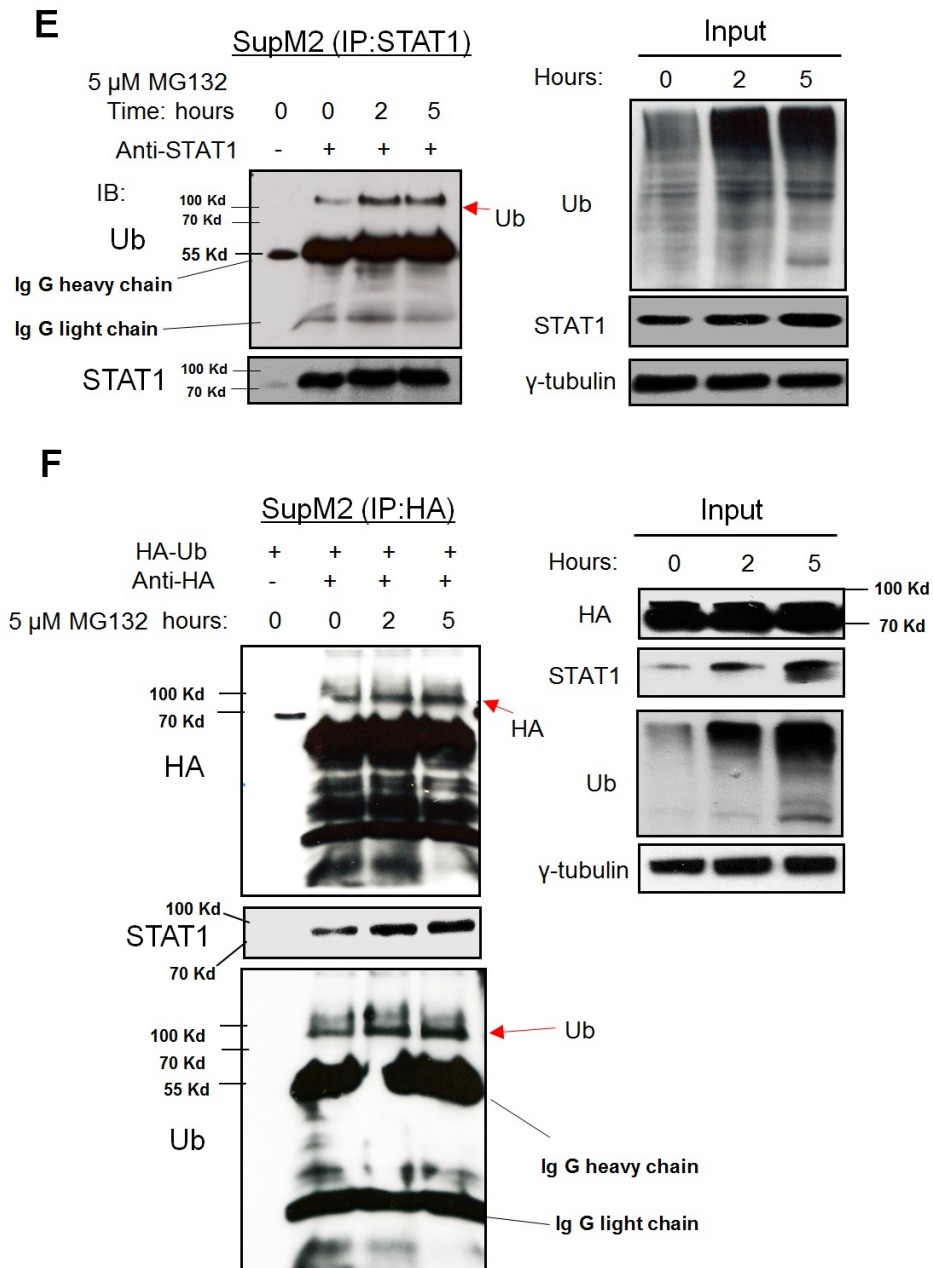


**Figure 2.2E-F** E) Co-immunoprecipitation experiment using anti-STAT1 for the pull down showed that ubiquitinated STAT1 in SupM2 cells treated with MG132 increased in a time-dependent manner (left panel). The input for this experiment is shown in the right panel. F) SupM2 cells were transfected with the pRK5-HA-Ubiquitin-WT plasmid. Reciprocal pull down experiment using anti-HA was done and the results also suggested that the amount of ubiquitinated STAT1 increased with MG132 treatment in a time dependent manner.

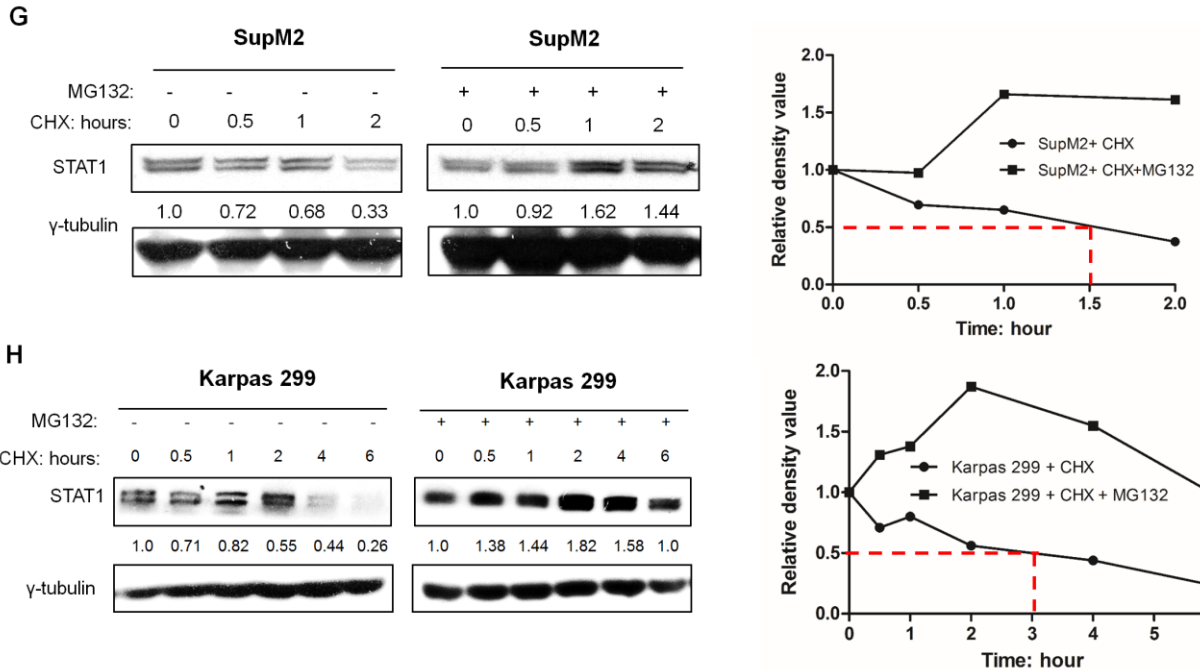


**Figure 2.2G-H** G, H) SupM2 and Karpas 299 cells were treated with or without 5 $\mu$ M MG132 in the presence of 100  $\mu$ g/mL cycloheximide (CHX) up to 2 or 6 hours. The results from both cell lines are graphically illustrated at the right panel. The half-life of STAT1 in SupM2 and Karpas 299 are 1.5 hours and 3 hours, respectively. MG132 potently extended the half-life of STAT1 in the two cell lines. Image J software was used to analyze the densitometry value of Western blots bands. Results shown were representative of three independent experiments.

### 2.3.3 NPM-ALK promotes STAT1 phosphorylation at Y701 and downregulates STAT1

The NPM-ALK/STAT3 axis is a critical oncogenic driver in ALK+ALCL (29). Thus, we asked if this axis contributes to the low expression of STAT1. As shown in **Figure 2.3A**, with crizotinib-induced ALK inhibition, pSTAT1 decreased while total STAT1 increased in a dose-dependent manner in both cell lines. As shown in **Figure 2.3B**, crizotinib also induced time-dependent changes in pSTAT1 and total STAT1; importantly, the levels of

pSTAT1 decreased at the same time as phosphorylated ALK<sup>Y1604</sup> (pALK) decreased, and before the total STAT1 levels increased. The observations suggest that NPM-ALK may promote tyrosine phosphorylation of STAT1 and decrease the protein level of STAT1. In support of this hypothesis, NPM-ALK is found to bind to STAT1, and this interaction dramatically decreased after crizotinib treatment (**Figure 2.3C**).

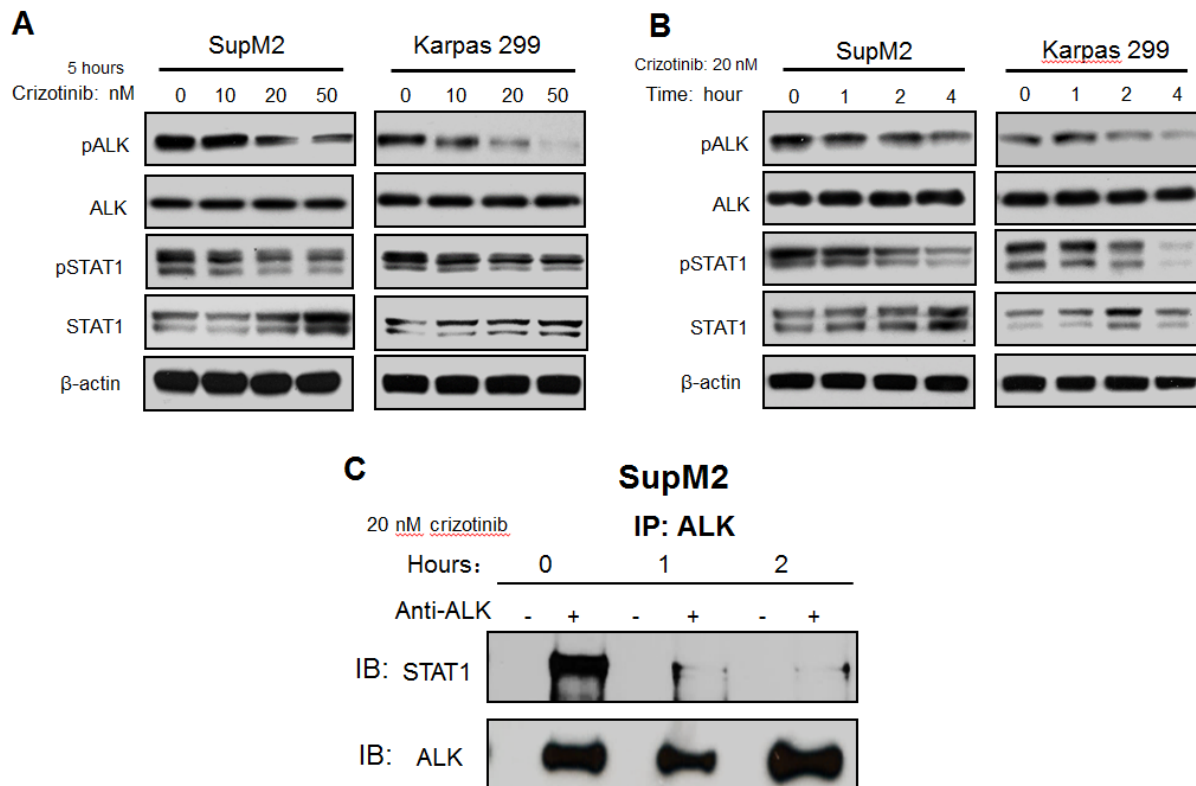


**Figure 2.3 NPM-ALK promotes STAT1 phosphorylation at Y701 and downregulates STAT1.** A) SupM2 cells were treated with different doses of the ALK inhibitor, crizotinib, for 5 hours. The decrease in pALK supported that the inhibitor was effective. In the same experiment, pSTAT1 decreased whereas the total STAT1 level gradually increased in a dose-dependent manner. B) Time course experiment showed that pSTAT1 decreased along with pALK almost simultaneously. Furthermore, total STAT1 increased after the downregulation of pALK. C) The treatment of crizotinib in SupM2 cells resulted in the dramatic decrease of the binding of NPM-ALK and STAT1

(i.e. at the time point of 1 hour and 2 hour), assessed by co-immunoprecipitation assay. Results shown were representative of 3 independent experiments. Results shown were representative of three independent experiments.

Furthermore, transient transfection of *NPM-ALK* into GP293 cells resulted in a dramatic increase in pSTAT1, and this change was accompanied by a reciprocal decrease in total STAT1 (**Figure 2.3D**). As shown in **Figure 2.3E**, the effect on total STAT1 due to enforced NPM-ALK expression in GP293 cells was dependent on the proteasomal degradation pathway, since MG132 almost completely abrogated this effect.

Then we questioned if the phosphorylation of STAT1 at its tyrosine residue 701 is necessary for its downregulation. Thus, GP293 cells were co-transfected *NPM-ALK* with wild-type *STAT1* or mutant *STAT1*<sup>Y701F</sup>. As shown in **Figure 2.3F**, NPM-ALK effectively phosphorylated STAT1 when cells were co-transfected with wild-type *STAT1*. There was only a relatively small increase in pSTAT1 in cells co-transfected with *STAT1*<sup>Y701F</sup>, suggesting the tyrosine residue 701 is the predominant tyrosine phosphorylation site of STAT1 for NPM-ALK. After 24 hours of gene transfection, cells transfected with wild-type *STAT1* expressed only a small amount of total STAT1 as compared to that in cells transfected with *STAT1*<sup>Y701F</sup>. Taken together, the data suggested that NPM-ALK promotes STAT1 phosphorylation at predominantly the Y701 residue, and by doing so, promotes its degradation.

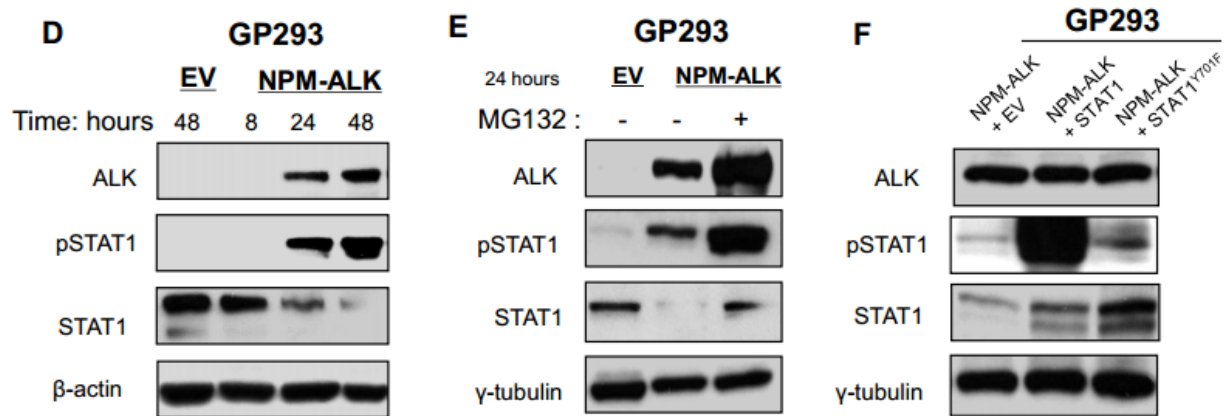


**Figure 2.3D-F** D, E) Transfection of *NPM-ALK* in GP293 cells led to a marked increase in STAT1 phosphorylation, which correlated with a dramatic decrease in the total STAT1 level. Importantly, the treatment of 5  $\mu$ M of MG132 for 6 hours largely abrogated the downregulation of STAT1 by *NPM-ALK*, even though the pSTAT1 level increased dramatically. F) Compared to the co-transfection of *NPM-ALK* and wild-type *STAT1*, co-transfection of *NPM-ALK* and mutant *STAT1*<sup>Y701F</sup> resulted in a higher total STAT1 level, indicating that the phosphorylation of Y701 is crucial for the downregulation of STAT1 by *NPM-ALK*. Results shown were representative of three independent experiments.

### 2.3.4 STAT3 is necessary for the downregulation of STAT1 mediated by *NPM-ALK*

Since STAT3 is a crucial mediator of the oncogenic effects of *NPM-ALK*, we questioned that if STAT3 is also involved in the *NPM-ALK*–mediated downregulation of STAT1. In GP293 cells transfected with both *NPM-ALK* and *STAT1*, siRNA knockdown of STAT3 in these cells resulted in a dramatic inhibition of the *NPM-ALK*–mediated downregulation of STAT1 (**Figure 2.3G**). Accordingly, Interferon-response factor 1 (IRF-1), one of the known STAT1 downstream targets (34), was substantially upregulated in response to STAT3 knockdown. To confirm the notion that *NPM-ALK* downregulates STAT1 expression in a STAT3-dependent manner in ALK+ALCL, STAT3 was knocked down by using siRNA in SupM2 and Karpas 299 cells, and the

results suggested that a readily detectable upregulation of STAT1 in both cell lines was observed after STAT3 knockdown (**Figure 2.3H**).

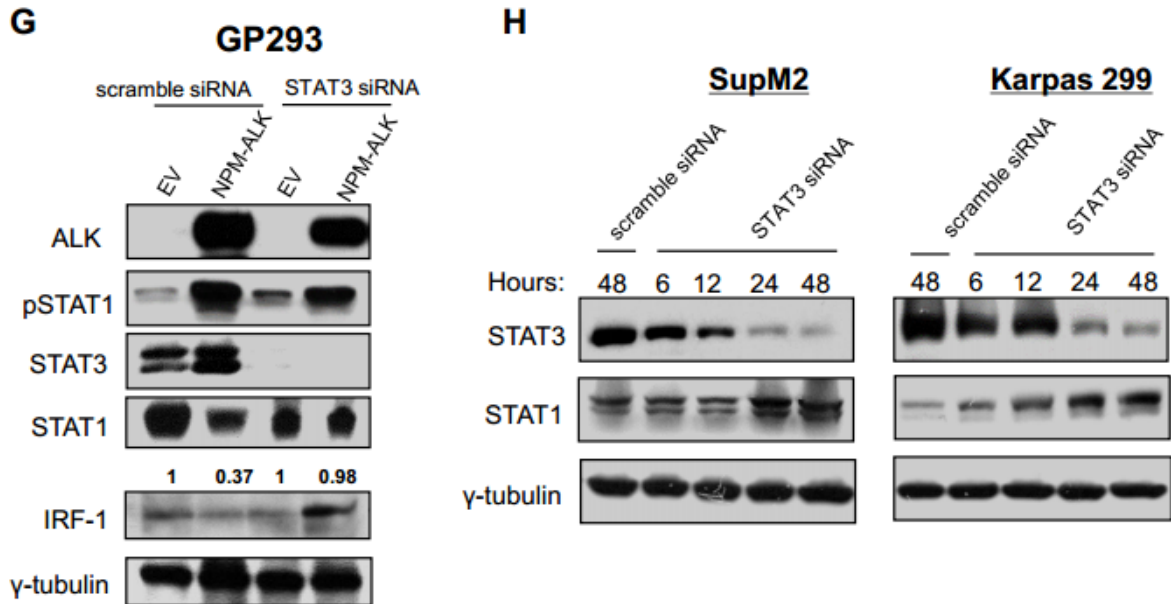


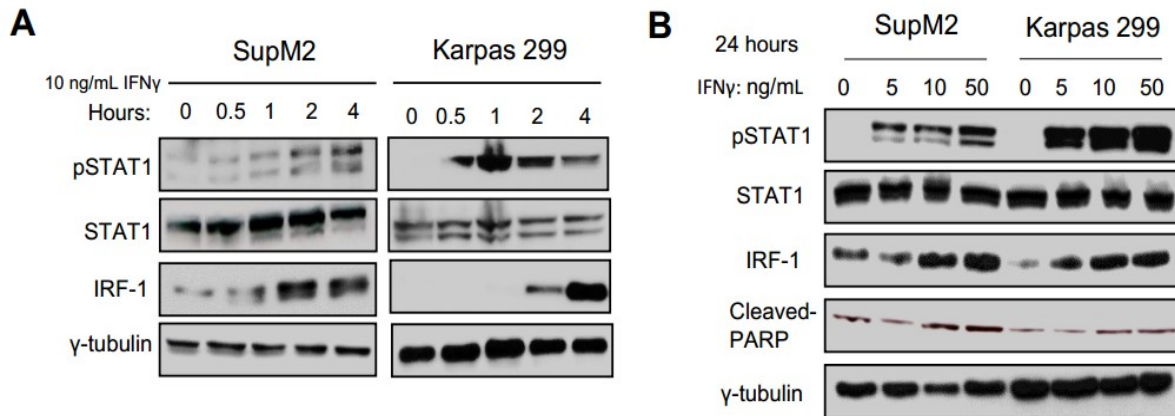
**Figure 2.3G-H** G) With the siRNA knockdown of STAT3, the NPM-ALK–mediated downregulation of STAT1 was largely abrogated. Correlating with this finding, IRF-1 (a STAT1 downstream target) was higher when STAT3 was silenced in presence of NPM-ALK. H) Time course experiment of siRNA knockdown of STAT3 in the two ALK+ALCL cell lines correlated with the reciprocal increase in the total STAT1 level. Results shown were representative of three independent experiments.

### 2.3.5 STAT1 signaling is functionally intact in ALK+ALCL

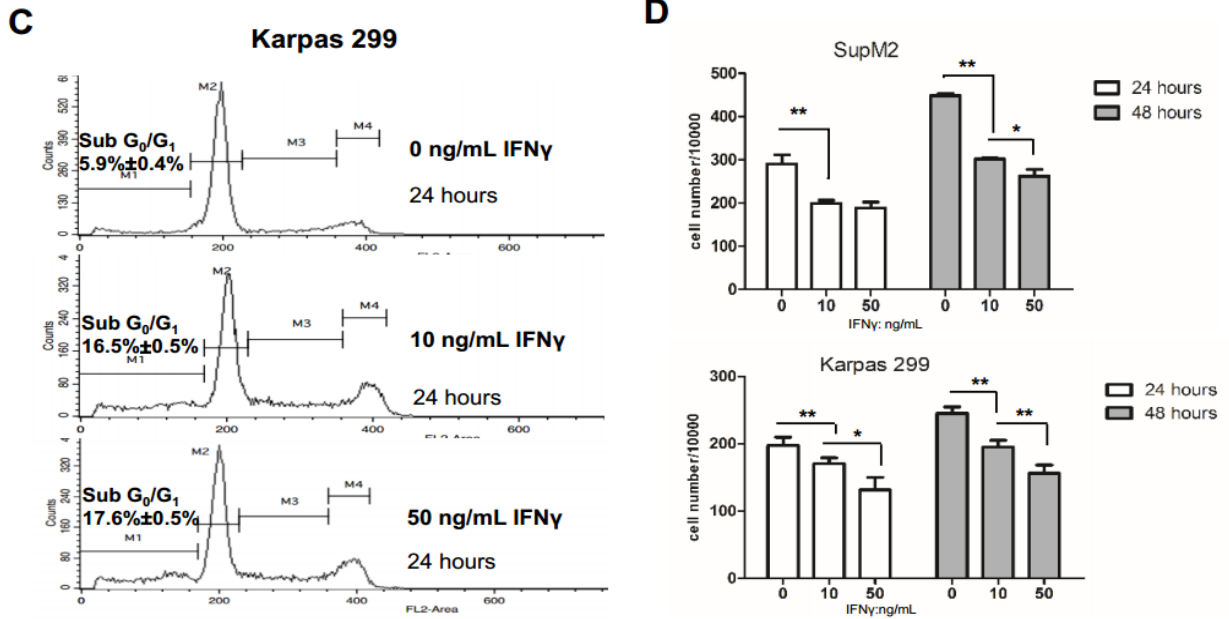
We then asked if the STAT1 signaling pathway in ALK+ALCL is functionally intact. As shown in **Figure 2.4A**, STAT1 was rapidly phosphorylated in ALK+ALCL cells in response to IFN $\gamma$ . The protein level of IRF-1 was expectedly upregulated. Furthermore, at 24 hours, both cell lines showed evidence of apoptosis, as evidenced by the expression of cleaved PARP detectable by Western blotting and the significant increase in the sub G<sub>0</sub>/G<sub>1</sub> phase detectable by flow cytometry (**Figure 2.4B and 2.4C**).



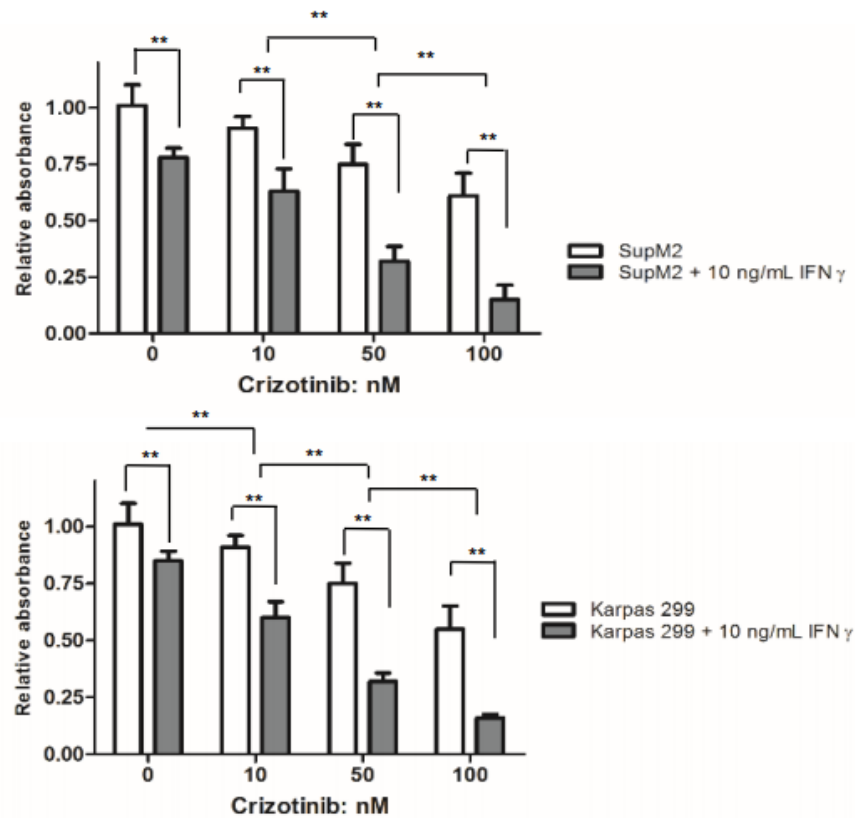
As shown in **Figure 2.4D and 2.4E**, we found that IFN $\gamma$  significantly suppressed cell growth and synergized with crizotinib in inhibiting the growth of both cell lines.



**Figure 2.4 STAT1 signaling is functionally intact in ALK+ALCL.** A) IFN $\gamma$  triggered STAT1 phosphorylation and increased the expression of IRF-1 (a STAT1 downstream target) in SupM2 and Karpas 299 cells. STAT1 was not changed in this time frame. B) Western blots showed that STAT1 was activated and phosphorylated in response to IFN $\gamma$  stimulation in a dose-dependent manner for 24 hours. The downstream target IRF-1 also increased with IFN $\gamma$  stimulation. The cleaved-PARP was blotted and it increased in a dose-dependent manner in response to IFN $\gamma$  at 24 hours. Results shown were representative of three independent experiments.



**Figure 2.4C-D** C) Cell-cycle analysis suggested that the percent of cells in Sub G<sub>0</sub>/G<sub>1</sub> significantly increased upon the treatment of various doses of IFN $\gamma$  for 24 hours in Karpas 299 cells. D) The trypan blue exclusion assay suggested that IFN $\gamma$  significantly decreased cell growth in both ALK+ALCL cell lines in a dose-dependent manner. Statistical significance is denoted by \* ( $P < 0.05$ ) and \*\* ( $P < 0.01$ ). Results shown were representative of triplicate experiments.

**E**

**Figure 2.4E** E) The MTS assay suggested that IFN $\gamma$  synergized with crizotinib in suppressing cell growth in both ALK+ALCL cell lines. Statistical significance is denoted by \* ( $P < 0.05$ ) and \*\* ( $P < 0.01$ ). Experiments were performed in triplicate.

To further evaluate the functionality of STAT1, we transfected Karpas 299 cells with the constitutively active STAT1 construct (i.e. *STAT1C*). Western blot studies showed the efficiency of *STAT1C* transfection (**Figure 2.4F**). As shown in **Figure 2.4G**, cell-cycle analysis showed that STAT1C induced a significant increase in the sub  $G_0/G_1$  phase and a significant decrease in the S phase in Karpas 299 cells.

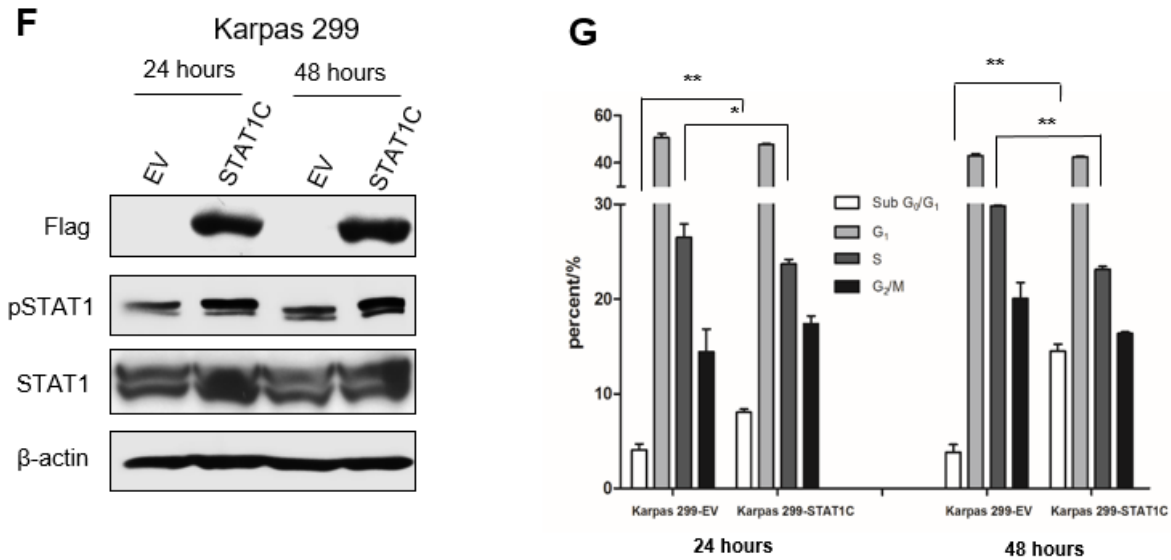


**Figure 2.4F-G** F, G) Karpas 299 cells transfected with *STAT1C-flag* showed a significant accumulation of the sub G<sub>0</sub>/G<sub>1</sub> fraction. Statistical significance was calculated by Student's *t*-test where \**P*<0.05, \*\**P*<0.01.

To further examine the biological significance of STAT1 in ALK+ALCL, we established two conditional *STAT1C*-stably transfected ALK+ALCL cell lines where the expression of STAT1C can be induced in a dose-dependent manner with the addition of doxycycline (*i.e.* Dox), labeled Tet on-SupM2-STAT1C and Tet on-Karpas 299-STAT1C. The Dox-dose dependent expression of STAT1C in these two cell lines was confirmed by Western blotting (**Figure 2.5A**). Using Tet on-SupM2-STAT1C cells, we found a positive correlation between STAT1 and that of IRF-7 and T-bet, two STAT1 downstream targets (35, 36). SOCS-1, a negative regulator of the STAT1 signaling pathway (37), was also upregulated. In contrast, the protein levels of STAT3 and phosphorylated STAT3<sup>Y705</sup> (pSTAT3) did not change appreciably. Interestingly, two STAT3 target genes, Bcl-2 and Survivin (38, 39), were downregulated in a dose dependent manner (**Figure 2.5A**). As shown in **Figure 2.5B-C**, the induced expression

of STAT1C induced cell growth inhibition in Tet on-SupM2-STAT1C cells. Again, the expression of cleaved-PARP and cleaved-caspase 3, detectable by Western blotting, suggested the cell apoptosis induced by STAT1C in Tet on-SupM2-STAT1C cells (Figure 2.5A).

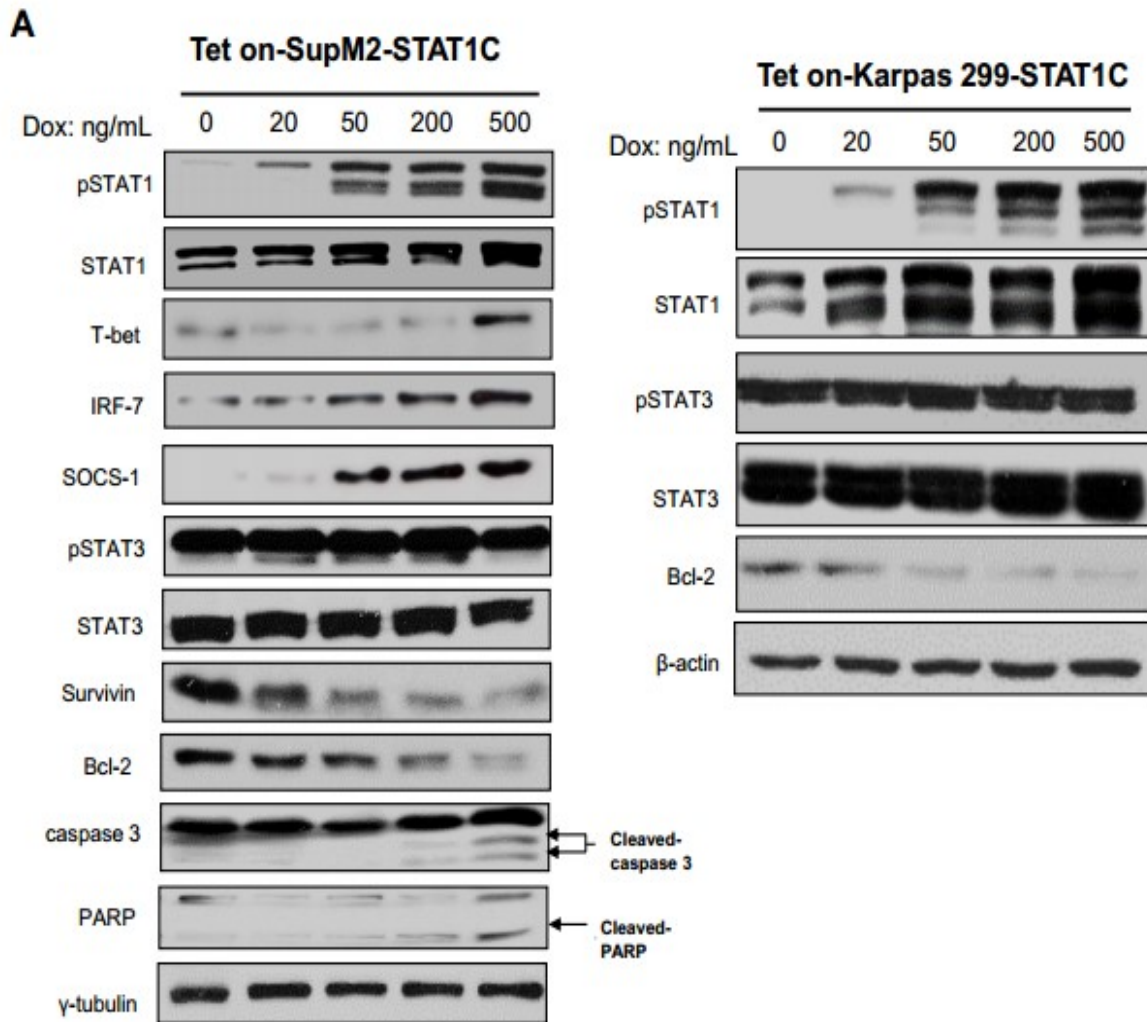


**Figure 2.5 STAT1 provides tumor suppressor function in ALK+ALCL *in vitro*.**

A) Tet on-SupM2-STAT1C expressed an increased level of pSTAT1 and STAT1 in a Dox dose-dependent manner. STAT1 target genes IRF-7, T-bet, SOCS-1 were all upregulated. In contrast, Survivin and Bcl-2, two known STAT3 target genes, were downregulated in a dose-dependent method. Cleaved caspase 3 and cleaved PARP

were expressed, indicating the occurrence of apoptosis. The right panel showed similar results in Tet on-Karpas 299-STAT1C cells upon doxycycline induction for 48 hours.

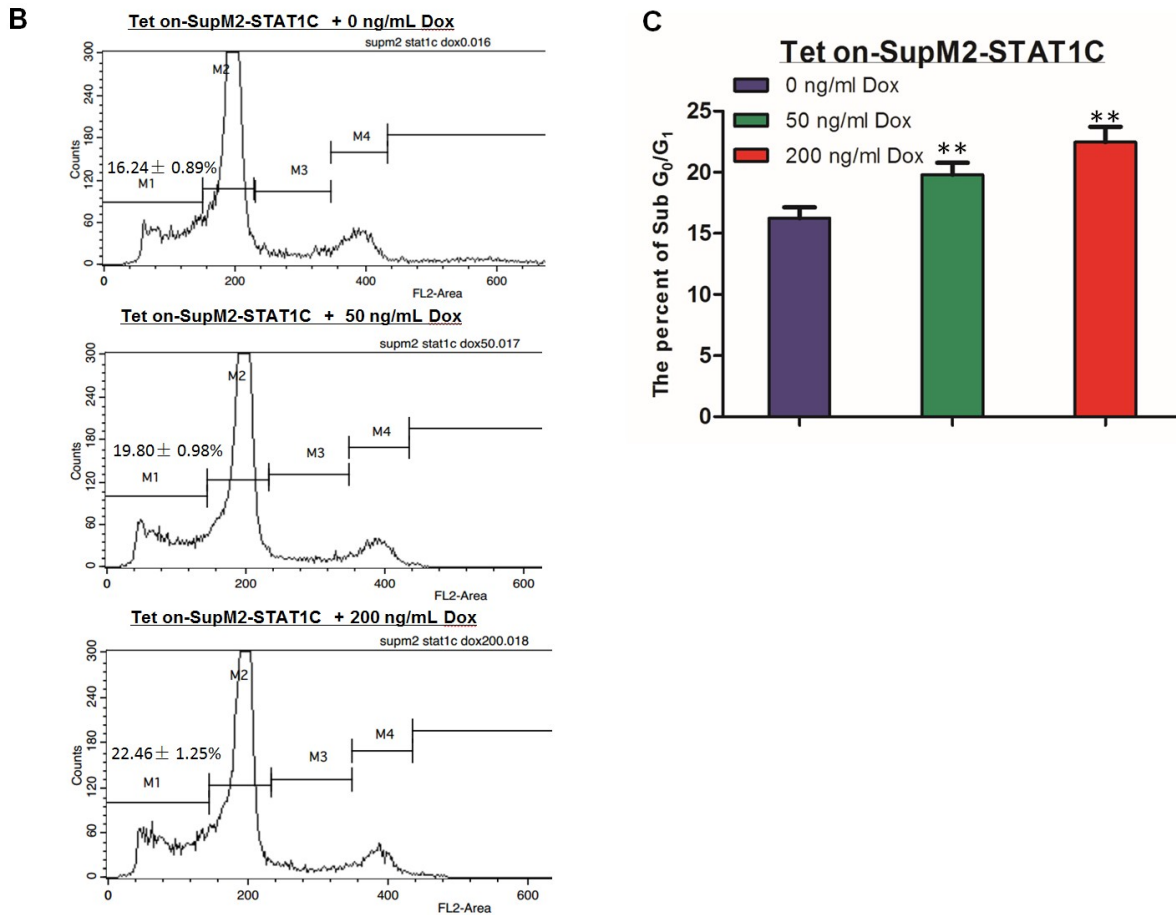


**Figure 2.5B-C** B, C) Cell-cycle analysis suggested that more cells are in Sub G<sub>0</sub>/G<sub>1</sub> phase upon 50 ng/mL and 200 ng/mL doxorubicin induction for 48 hours in Tet on-SupM2-STAT1C cells, as compared to cells without doxycycline induction. M1 shown in B represents Sub G<sub>0</sub>/G<sub>1</sub> phase in the cell-cycle analysis. B showed one representative data from triplicate experiments and C showed the analyzed percentages of cells in Sub G<sub>0</sub>/G<sub>1</sub> phase after doxycycline induction from triplicate experiments. Statistical significance is denoted by \* ( $P < 0.05$ ) and \*\* ( $P < 0.01$ ). Experiments were performed in triplicate.

### 2.3.6 The STAT1-IFN $\gamma$ positive feedback loop

IFN $\gamma$ , a major stimulator of STAT1, can be induced by T-bet, which is one of the STAT1 downstream targets in CD4-positive T-cells (36, 40, 41). Thus, STAT1 and IFN $\gamma$  form a positive feedback loop in normal T-cells. We hypothesized that this loop may exist in ALK+ALCL cells. To test this hypothesis, we employed the Tet on-SupM2-STAT1C cells. As shown in **Figure 2.5A**, the expression of STAT1C increased the expression of T-bet in a dose-dependent manner. Correlating with these observations, the expression of STAT1C increased the production of IFN $\gamma$  in a dose-dependent manner, detectable by quantitative RT-PCR; IRF-1 was used as a positive control (**Figure 2.6A**). Consistent results were obtained with both ALK+ALCL cell lines transiently transfected with *STAT1C* for 24 hours (**Figure 2.6B**). To further support the existence of the STAT1-IFN $\gamma$  positive feedback loop in ALK+ALCL, we found that the cell culture media harvested from Karpas 299 cells transiently transfected with *STAT1C* effectively induced STAT1 activation in parental Karpas 299 cells (**Figure 2.6C**). In contrast, the culture media of Karpas 299 cells transfected with an empty vector (EV) did not have this effect.

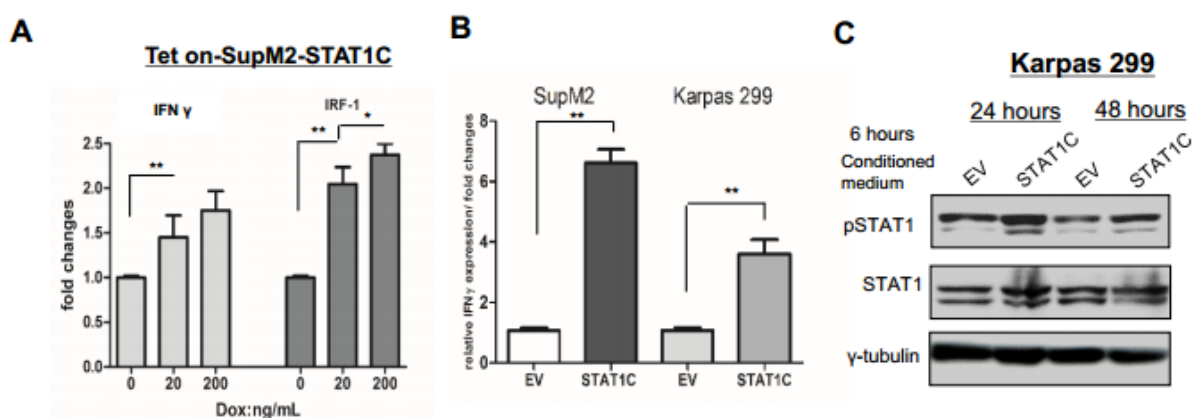


**Figure 2.6 Overexpression of STAT1 induces the expression of IFN $\gamma$  in ALK+ALCL and suppresses the tumor cell growth *in vivo*.** A) Quantitative RT-PCR

studies using Tet on-SupM2-STAT1C cells showed increased mRNA expression of IFN $\gamma$  and IRF-1 in a STAT1C dose-dependent manner. B) When SupM2 and Karpas 299 cells were transiently transfected with *STAT1C-flag* for 24 hours, the increase of IFN $\gamma$  mRNA was also detected using quantitative RT-PCR. C) Karpas 299 cells cultured in the medium harvested from Karpas 299 cells transfected with STAT1C showed the upregulated pSTAT1 in 6 hours, as compared to cells cultured in the medium harvest from Karpas 299 cells transfected with empty vector (EV). Statistical significance is denoted by \* ( $P<0.05$ ) and \*\* ( $P<0.01$ ). Results shown were representative of three independent experiments.

### **2.3.7 STAT1C is a tumor suppressor in ALK+ALCL *in vitro* and *in vivo***

We then determined if STAT1C inhibits the growth in ALK+ALCL cells. We found that STAT1C significantly suppressed cell growth in a Dox dose-dependent manner ( $P<0.01$  and  $P<0.01$ , respectively) (**Figure 2.6D**). We also found that STAT1C sensitized ALK+ALCL cells to doxorubicin (**Figure 2.6E**). Specifically, at the dose of 0.5  $\mu$ M and 1  $\mu$ M of doxorubicin, the expression of STAT1C (at Dox 20 ng/mL and 200 ng/mL) resulted in a significant decrease in the number of viable cells. Of note, at the high dose of doxorubicin ( $\geq 0.5$   $\mu$ M), the use of 200 ng/mL of Dox (i.e. a relatively high level of STAT1C) did not result in any substantial further decrease in the number of viable cells, as compared to the use of 20 ng/mL of Dox. These observations suggested that a relatively small increase in STAT1C is sufficient to facilitate doxorubicin-induced apoptosis. Using methylcellulose colony formation assay, we also found that the expression of STAT1C resulted in a significant decrease in the tumorigenic potential of ALK+ALCL cells (**Figure 2.6F**). Lastly, to assess the tumor suppressor functions of STAT1C *in vivo*, we transplanted Tet on-SupM2-empty vector (EV) and Tet on-SupM2-STAT1C cells in the right or left flank of mice. We added 2 or 5 mg/mL of Dox to the



drinking water to induce STAT1C expression (**Figure 2.6G**). Tet on-SupM2-STAT1C cells showed significantly smaller tumor sizes than the empty vector group (**Figure 2.6H**) ( $P < 0.01$  for both). The tumors of the two groups were illustrated in **Figure 2.6I**, and the STAT1 protein levels in four representative tumors from mice #1 and mice #6 were analysed using Western blotting, as shown in **Figure 2.6J**.

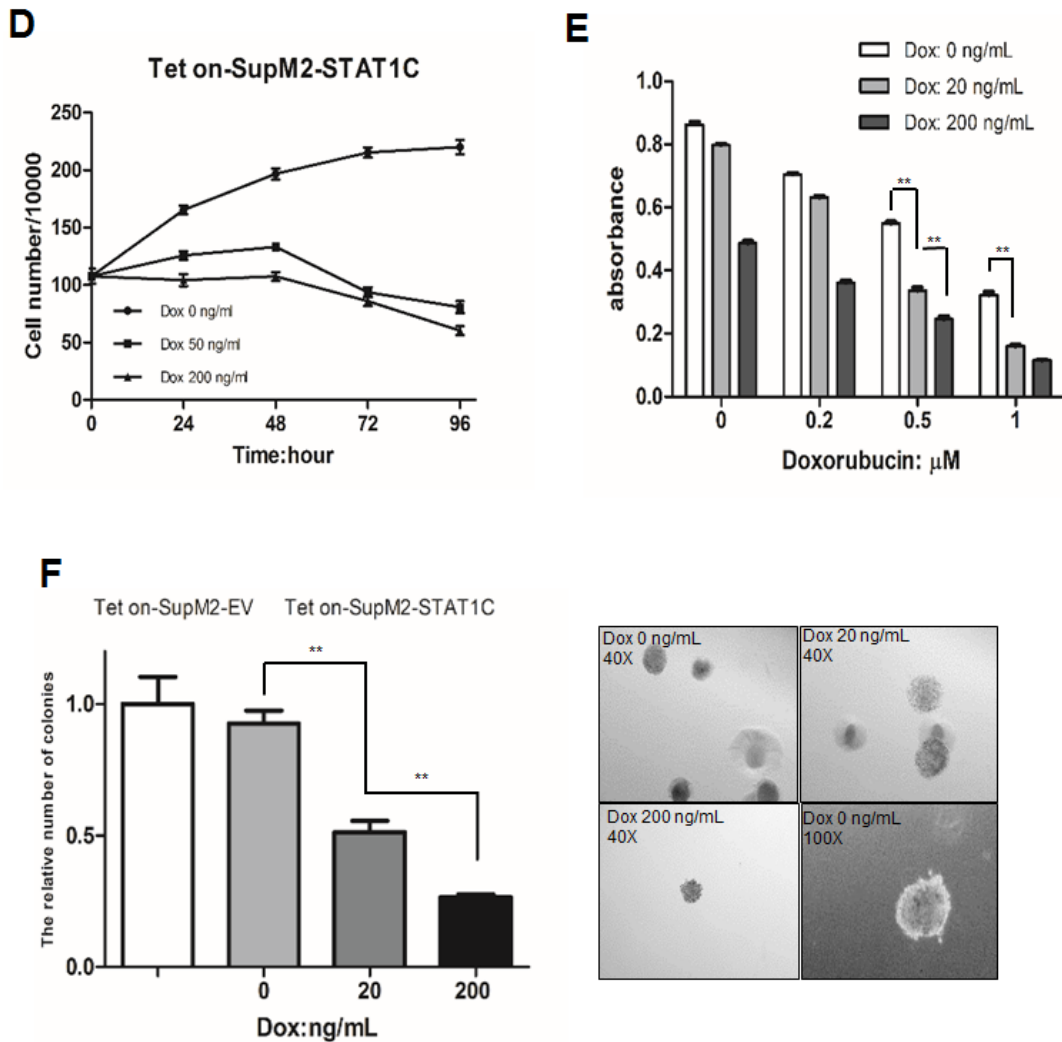


**Figure 2.6D-E** D) Using Tet on-SupM2-STAT1C cells, we found a significant decrease in the number of viable cells with increasing Dox. E) Using Tet on-SupM2-STAT1C cells, we found that STAT1C sensitizes cells to doxorubicin-induced cell growth inhibition at 0.5 and 1.0  $\mu$ M of doxorubicin. F) Colony formation significantly decreased with

increasing doses of Dox and STAT1C expression. The right panel illustrates the morphology of the colonies (40X, 100X magnification, respectively). Statistical significance is denoted by \* ( $P<0.05$ ) and \*\* ( $P<0.01$ ). Results shown were representative of three independent experiments.

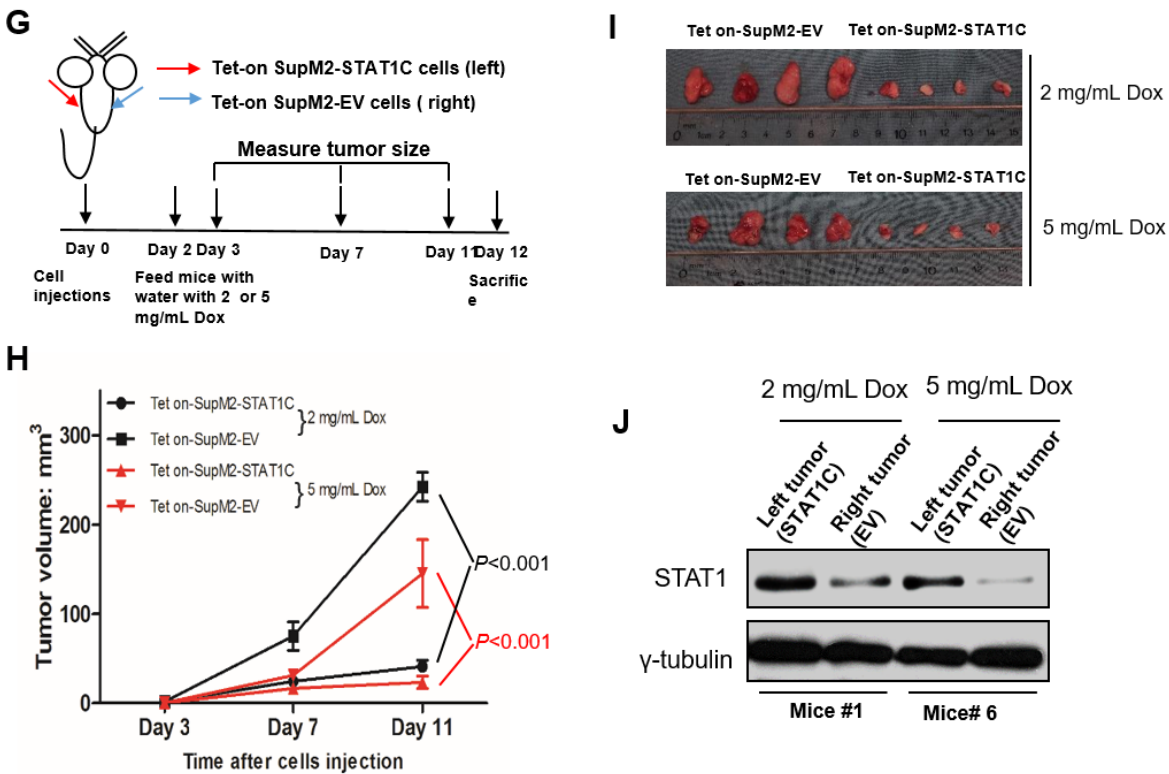


**Figure 2.6G-J** G-J) SCID mouse xenograft studies showed that the expression of STAT1C significantly decreased the tumorigenicity of Tet on-SupM2 STAT1C cells. Tet on-SupM2-EV cells were used as the negative controls. The xenografts and STAT1 expression levels in the harvested xenografts are also illustrated. Statistical significance is denoted by \* ( $P<0.05$ ) and \*\* ( $P<0.01$ ).

### 2.3.8 STAT1C significantly decreases STAT3 transcriptional activity

As shown in **Figure 2.5A**, STAT1C downregulated several STAT3 target genes (e.g. Bcl-2) without appreciably affecting the expression of STAT3/pSTAT3. These findings raise the possibility that STAT1C may interfere with the STAT3 transcriptional activity in

ALK+ALCL cells. As shown in **Figure 2.7A**, increasing levels of STAT1C in the Tet on-SupM2-STAT1C cells resulted in a dose-dependent decrease in the STAT3 transcriptional activity, as measured by dual luciferase assay. Using the same cell line, we found that STAT1C inhibited STAT3 binding to its consensus DNA sequence in a dose-dependent manner (**Figure 2.7B**). In addition, using co-immunoprecipitation assay and the Tet on-SupM2-STAT1C cells, we found that expression of STAT1C increased the formation of STAT1/STAT3 heterodimers, presumably at the expense of STAT3 homodimers, as the total STAT3 protein level did not change appreciably in this experiment (**Figure 2.7C**).

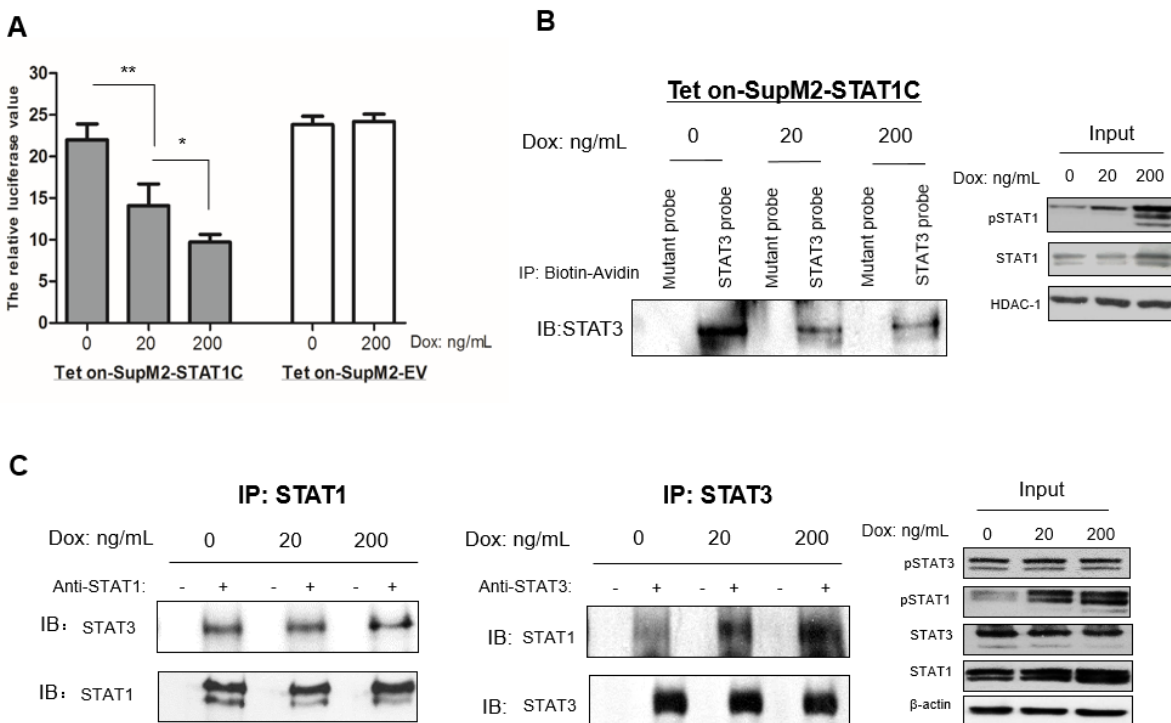


**Figure 2.7 STAT1C significantly decreases STAT3 transcriptional activity.**

A) STAT3 luciferase reporter assay showed STAT1C significantly decreased STAT3 transcriptional activity in a Dox-dose dependent manner. Treatment of 200 ng/mL of Dox in Tet on-SupM2- EV cells showed low-dose Dox has unappreciable effects on STAT3 transcriptional activity. B) STAT3 consensus DNA probe binding assay showed

STAT1C sequestered STAT3 DNA binding ability in a Dox-dose dependent manner, and the Western blotting in the right panel showed the input of cell nuclear lysates. Histone Deacetylase 1(HDAC-1) was used as loading control for nuclear lysates. C) Co-immunoprecipitation assay showed induction of STAT1C expression leads to more STAT1/STAT3 heterodimers formations, at the expense of STAT3 homodimers. The right panel showed the input. Statistical significance is denoted by \* ( $P<0.05$ ) and \*\* ( $P<0.01$ ). Results shown were representative of three independent experiments.

### **2.3.9 siRNA knockdown of STAT1 confers resistance to STAT3 inhibition-induced cell death**

We investigated if STAT1 plays a role in STAT3 inhibition-induced apoptosis in ALK+ALCL, a well-published phenomenon (42). As shown in **Figure 2.8A**, treatment of SupM2 with Stattic, a widely used STAT3 inhibitor (43), dramatically decreased pSTAT3 level. Transfection of STAT1 siRNA significantly decreased the inhibitory effect of Stattic, and the IC50 increased significantly compared to SupM2 cells transfected with scramble siRNA (**Figure 2.8B**). These findings suggest that STAT3 inhibition-induced apoptosis is partly STAT1-dependent. In parallel with these findings, co-transfection of STAT1 siRNA and STAT3 siRNA in SupM2 cells led to decreased cell killing, as compared to transfection of STAT3 siRNA alone (**Figure 2.8C**). Western blots shown in **Figure 2.8C** also showed the efficiency of siRNAs knockdown in SupM2 cells. Of note, transfection of STAT3 siRNA substantially increased the STAT1 total protein level, and this result was consistent to that shown in **Figure 2.3H**.

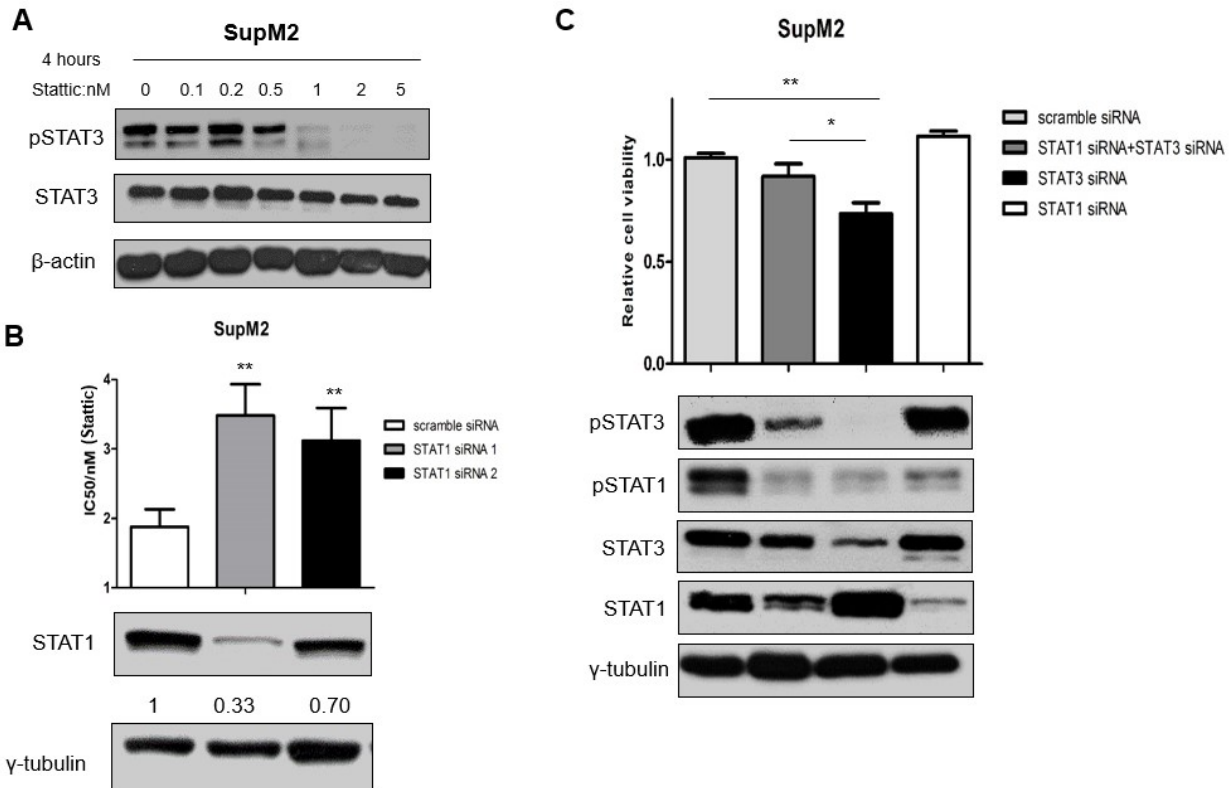


**Figure 2.8 siRNA knockdown of STAT1 confers resistance to STAT3 inhibition-induced cell death.** A) SupM2 were exposed to varying doses of Stattic for 4 hours, Western blotting showed the decrease of pSTAT3 in a dose-dependent method. B) SupM2 cells transfected with two species of STAT1 siRNA showed significantly higher IC<sub>50</sub> to Stattic compared to cells transfected with scramble siRNA transfection. Western blotting studies showed the siRNA knockdown efficiency, which was higher with STAT1 siRNA 1 compared to STAT1 siRNA 2. The densitometry values shown were normalized to the band of γ-tubulin. C) Transfection of STAT1 siRNA significantly reduced the suppression of cell growth induced by STAT3 siRNA in SupM2 cells. The Western blotting results showed the efficiency of siRNA knockdowns. Image J software was used to analyze the densitometry value of Western blots bands. Statistical significance is denoted by \* ( $P < 0.05$ ) and \*\* ( $P < 0.01$ ). Results shown were representative of 3 independent experiments.

## 2.4 Discussion

A key finding of this study is that STAT1 is consistently downregulated in ALK+ALCL cell lines and tumors. Regarding the Western blots results (**Figure 2.1A**), we speculate that the STAT1 signals detected in the ALK+ALCL tumors were likely an over-estimation of STAT1 expression in the neoplastic cells, since some of the STAT1 signal detected was likely derived from the benign intra-tumoral T-cells and macrophages. In support of this concept, by immunohistochemistry, intra-tumoral T-cells and macrophages were STAT1-strong whereas the ALK+ALCL cells were consistently weak or negative. Downregulation of STAT1 is not unique to ALK+ALCL cells, as this abnormality has been reported in breast cancer (20, 44), oral squamous cell carcinoma (16), melanoma (17, 18, 45, 46), gastric adenocarcinoma and cutaneous T-cell lymphoma (19, 47). In contrast with the total STAT1 levels, the pSTAT1 levels found in ALK+ALCL cell lines and tumors were more variable, being relatively high in 1/3 patient samples and 1/3 cell lines. We do not have the exact explanation but we have considered the following possibilities. First, NPM-ALK is more efficient in promoting STAT1 phosphorylation in these cases, possibly due to better subcellular colocalization of the two proteins and/or a difference in the activation status of NPM-ALK. Second, the lack of the expression and/or activity of specific tyrosine phosphatase(s) may have contributed to this difference. Lastly, the proteasomal degradation machinery in these cells may be relatively inefficient; in support of this concept, ALK+ALCL cells (patient #1 and SupM2) that showed high pSTAT1 also expressed a high level of total STAT1.

The mechanisms underlying the downregulation of STAT1 in cancer cells have not been extensively studied. Our data indicates that the ubiquitin-proteasome pathway

contributes to the low transcriptional level of STAT1 in ALK+ALCL. This study also has revealed a novel phenomenon in which NPM-ALK plays a key role in promoting the proteasomal degradation of STAT1. Specifically, we found that NPM-ALK binds to, induces the phosphorylation of STAT1 at Y701 and promotes its degradation. It is possible that NPM-ALK (ALK kinase domain) directly interact with STAT1 at Src homology domain 2 (SH2) where tyrosine 701 is located, while further studies are required to answer whether NPM-ALK directly interacts with STAT1 and whether mutated STAT1<sup>Y701F</sup> is able to interact with NPM-ALK directly. To highlight the importance of NPM-ALK in this process, co-transfection of the mutant STAT1<sup>Y701F</sup> and NPM-ALK in GP293 cells dramatically increased the total STAT1 expression. To our knowledge, this is the first report describing the phosphorylation of STAT1 by an oncogenic tyrosine kinase being important in its degradation, and it will be of interest if other oncogenic tyrosine kinases exert the same effect on STAT1. Another important observation we have made is that STAT3 is critical to the NPM-ALK-mediated downregulation of STAT1, as siRNA knockdown of STAT3 largely abrogated this effect. While the underlying mechanism requires further studies, we are aware of a very recent publication in which STAT3 was found to promote proteasomal degradation of p53 by upregulating MDM2, an E3 ubiquitin ligase (48). In addition, another recent study revealed that pSTAT1 is the primary form of ubiquitinated STAT1 induced by IFNs (24). Thus, it is possible that NPM-ALK-mediated downregulation of STAT1 is dependent on specific E3 ubiquitin ligase(s) that promotes pSTAT1 ubiquitination, which are regulated by STAT3.

The tumor suppressor function of STAT1 has been demonstrated in many cancer cell types including breast cancer, oral squamous cell carcinoma and melanoma (16-18, 20, 44-46). It is proposed that STAT1 exerts its tumor suppressor effects by modulating the transcription of a host of pro-apoptotic and anti-proliferative genes (1, 49), such as IRF-1 (34), caspases (49), members of the death receptor family, iNOS, the Fas/FasL, and TNF related apoptosis ligand (TRAIL), Bcl-X<sub>L</sub> and Bcl-2 (50-54). Nonetheless, there is evidence suggesting that STAT1 may be oncogenic in specific experimental models and/or cell types, as highlighted in a recent review article (4). For instance, it was found that STAT1-deficient mice are protected from leukemia development (55). STAT1 was found to be important for the expansion of leukemia initiating cells (56). STAT1 was also shown to be critical for cell survival in T-cell acute lymphoblastic leukemia (57). Thus, the biological function of STAT1 is dependent on the cellular context (58). With this background, we examined whether STAT1 function as a tumor suppressor in ALK+ALCL if its expression is restored. We found that gene transfection of *STAT1C* into ALK+ALCL cells triggered effective apoptosis and cell-cycle arrest, and sensitized cells to doxorubicin-induced apoptosis. The functionality of STAT1 is further supported by the observation that enforced expression of *STAT1C* led to an increase in T-bet and IRF-7, two known STAT1 downstream targets (35, 36). Since STAT1 typically works closely with IFN $\gamma$ , we asked if the IFN-STAT1 signaling pathway is functional in ALK+ALCL. Our findings strongly suggest that this signaling pathway is intact, since IFN $\gamma$  can effectively induce STAT1 phosphorylation. This is in contrast to some cancer cells that are known to have defects in the IFN-STAT1 signaling pathway (17-19, 45-47, 59). Based on our data, IFN $\gamma$  is an effective activator of STAT1 signaling in ALK+ALCL, and effectively synergize with crizotinib *in vitro*, providing insights into the therapeutic



strategy in clinic. Importantly, we also found that STAT1C can effectively induce IFN $\gamma$  expression, which in turn induces further STAT1 activation, thus creating a positive feedback loop in ALK+ALCL. Taken together, our findings support the concept that suppression of STAT1, which can function as an effective tumor suppressor in conjunction with IFN $\gamma$ , is important to the pathogenesis of ALK+ALCL, and this biochemical defect represents an important mediator of the oncogenic effect of NPM-ALK.

Our study has shed some insights into the functional interaction between STAT1 and STAT3, a process that has been largely studied in cell lines. Although we did not find appreciable changes of the STAT3 protein level after *STAT1C* transfection into ALK+ALCL cells, we found that STAT1C can significantly downregulate the STAT3 transcriptional activity. Our results have led us to believe that enforced expression of STAT1C changes the ratios among STAT1 homodimers, STAT3 homodimers and STAT1/STAT3 heterodimers. Thus, STAT1C expression increased the STAT1/STAT3 heterodimers at the expense of STAT3 homodimers. Since it is generally accepted that the STAT1/STAT3 heterodimers have less ability to bind DNA and regulate gene expression than STAT3 homodimers do (11), our results correlate well with the observation that gene transfection of *STAT1C* resulted in decreased DNA binding of STAT3. The functional interference of STAT3 by STAT1 may have contributed to the tumor suppressor function of STAT1, particularly in tumors with a high level of STAT3 activation, as in ALK+ALCL.

It has been well documented that inhibition of STAT3 is an effective way to kill cancer

cells that express constitutively activated STAT3 (60), including ALK+ALCL cells (42). Based on our results presented here, one may speculate that apoptosis induced by STAT3 inhibition in ALK+ALCL may be dependent on STAT1. Specifically, a relatively high level of STAT1 expression in ALK+ALCL will lower the threshold of apoptosis due to STAT3 inhibition, whereas siRNA knockdown of STAT1 will provide resistance of apoptosis induced by STAT3 inhibition. In keeping with this concept, we found that siRNA knockdown of STAT1 in ALK+ALCL indeed led to increased resistance to Stattic, a well-studied STAT3 inhibitor (43). These findings also further highlight the biological importance of the functional interactions between STAT1 and STAT3 in dictating the cell fate of cancer cells. In brief, the schematic working model of STAT1 in ALK+ALCL has been demonstrated in **Figure 2.9**.

To conclude, we report that STAT1 is consistently downregulated in ALK+ALCL. In view of the observations that the STAT1 signaling is intact and STAT1 (if sufficiently expressed) exerts potent tumor suppressor effect, we conclude that the downregulation of STAT1 by NPM-ALK represents a novel mechanism by which this oncogenic tyrosine kinase promotes tumorigenesis. Our results have also shed important insight into the functional interaction between STAT1 and STAT3 in cancer cells, and the biological significance of this interaction in dictating the cell fate. We believe that enhancing the STAT1 signaling might be an attractive therapeutic strategy in treating cancer, especially when STAT3 is constitutively active.

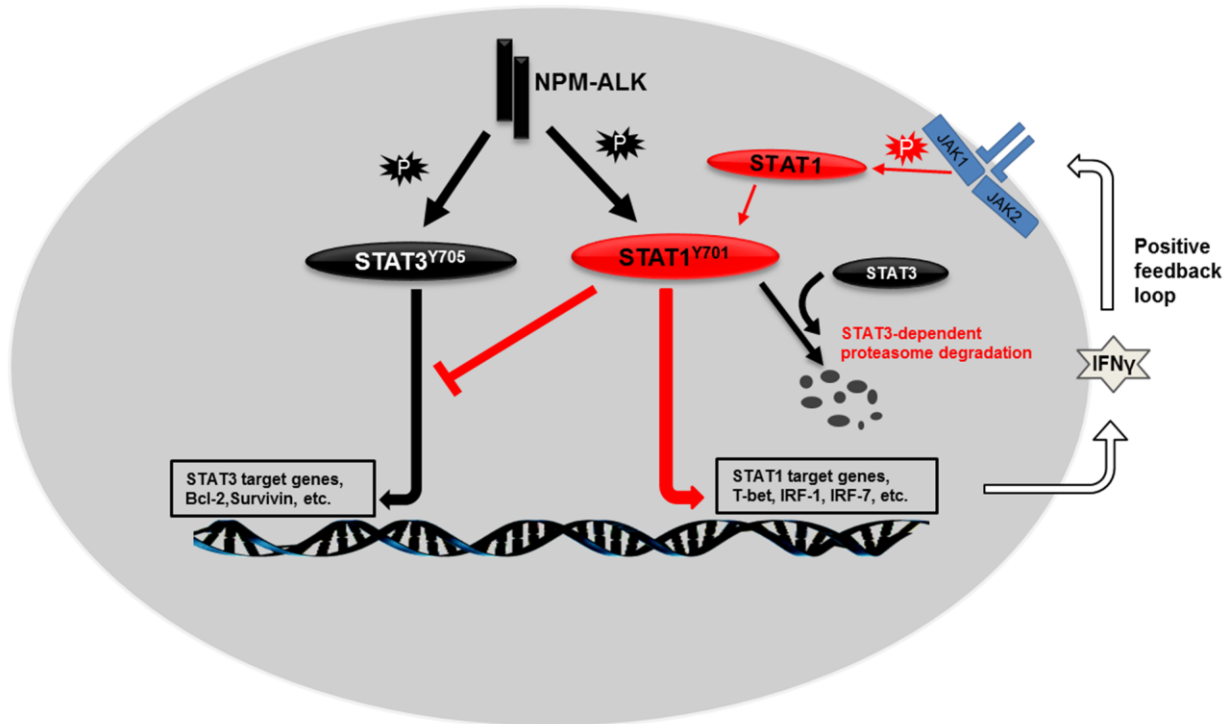


**Figure 2.9 Schematic model of STAT1 in ALK+ ALCL.**

NPM-ALK promotes STAT1 phosphorylation at Y701, and thereby, downregulates STAT1 in a STAT3-dependent proteasome pathway. If STAT1 expression is restored to a certain high level in ALK+ALCL, it is sufficient to induce cell growth inhibition and cell apoptosis by suppressing STAT3 transcriptional activity and inducing T-bet expression which stimulates the transcription of IFN $\gamma$ , thus resulting in a positive forward loop for STAT1 activation.

STAT: Signal transducer and activator of transcription; IRF: interferon response factor; Bcl-2: B-cell lymphoma 2; IFN $\gamma$ : interferon gamma; JAK: Janus kinase; T-bet: T-box transcription factor TBX21.

## 2.5 References

1. Kim HS, Lee MS. STAT1 as a key modulator of cell death. Cellular signalling. 2007;19(3):454-65.

2. Schroder K, Hertzog PJ, Ravasi T, Hume DA. Interferon-gamma: an overview of signals, mechanisms and functions. *Journal of leukocyte biology*. 2004;75(2):163-89.
3. Koromilas AE, Sexl V. The tumor suppressor function of STAT1 in breast cancer. *Jak-Stat*. 2013;2(2):e23353.
4. Avalle L, Pensa S, Regis G, Novelli F, Poli V. STAT1 and STAT3 in tumorigenesis: A matter of balance. *Jak-Stat*. 2012;1(2):65-72.
5. Bowman T, Garcia R, Turkson J, Jove R. STATs in oncogenesis. *Oncogene*. 2000;19(21):2474-88.
6. Guzzo C, Che Mat NF, Gee K. Interleukin-27 induces a STAT1/3- and NF-kappaB-dependent proinflammatory cytokine profile in human monocytes. *The Journal of biological chemistry*. 2010;285(32):24404-11.
7. Sato T, Selleri C, Young NS, Maciejewski JP. Inhibition of interferon regulatory factor-1 expression results in predominance of cell growth stimulatory effects of interferon-gamma due to phosphorylation of Stat1 and Stat3. *Blood*. 1997;90(12):4749-58.
8. Stancato LF, David M, Carter-Su C, Larner AC, Pratt WB. Preassociation of STAT1 with STAT2 and STAT3 in separate signalling complexes prior to cytokine stimulation. *The Journal of biological chemistry*. 1996;271(8):4134-7.
9. Regis G, Pensa S, Boselli D, Novelli F, Poli V. Ups and downs: the STAT1:STAT3 seesaw of Interferon and gp130 receptor signalling. *Semin Cell Dev Biol*. 2008;19(4):351-9.
10. Thyrell L, Arulampalam V, Hjortsberg L, Farnebo M, Grandér D, Pokrovskaja Tamm K. Interferon alpha induces cell death through interference with interleukin 6

signaling and inhibition of STAT3 activity. *Experimental cell research*. 2007;313(19):4015-24.

11. Ho HH, Ivashkiv LB. Role of STAT3 in type I interferon responses. Negative regulation of STAT1-dependent inflammatory gene activation. *The Journal of biological chemistry*. 2006;281(20):14111-8.

12. Shen Y, Devgan G, Darnell JE, Jr., Bromberg JF. Constitutively activated Stat3 protects fibroblasts from serum withdrawal and UV-induced apoptosis and antagonizes the proapoptotic effects of activated Stat1. *Proceedings of the National Academy of Sciences of the United States of America*. 2001;98(4):1543-8.

13. Kortylewski M, Kujawski M, Wang T, Wei S, Zhang S, Pilon-Thomas S, et al. Inhibiting Stat3 signaling in the hematopoietic system elicits multicomponent antitumor immunity. *Nature medicine*. 2005;11(12):1314-21.

14. Bluysen HA, Rastmanesh MM, Tilburgs C, Jie K, Wesseling S, Goumans MJ, et al. IFN gamma-dependent SOCS3 expression inhibits IL-6-induced STAT3 phosphorylation and differentially affects IL-6 mediated transcriptional responses in endothelial cells. *American journal of physiology Cell physiology*. 2010;299(2):C354-62.

15. Dimberg LY, Dimberg A, Ivarsson K, Fryknas M, Rickardson L, Tobin G, et al. Stat1 activation attenuates IL-6 induced Stat3 activity but does not alter apoptosis sensitivity in multiple myeloma. *BMC cancer*. 2012;12:318.

16. Laimer K, Spizzo G, Obrist P, Gastl G, Brunhuber T, Schafer G, et al. STAT1 activation in squamous cell cancer of the oral cavity: a potential predictive marker of response to adjuvant chemotherapy. *Cancer*. 2007;110(2):326-33.

17. Wong LH, Krauer KG, Hatzinisiriou I, Estcourt MJ, Hersey P, Tam ND, et al. Interferon-resistant human melanoma cells are deficient in ISGF3 components, STAT1,

STAT2, and p48-ISGF3gamma. The Journal of biological chemistry. 1997;272(45):28779-85.

18. Kovarik J, Boudny V, Kocak I, Lauerova L, Fait V, Vagundova M. Malignant melanoma associates with deficient IFN-induced STAT 1 phosphorylation. International journal of molecular medicine. 2003;12(3):335-40.

19. Sun WH, Pabon C, Alsayed Y, Huang PP, Jandeska S, Uddin S, et al. Interferon-alpha resistance in a cutaneous T-cell lymphoma cell line is associated with lack of STAT1 expression. Blood. 1998;91(2):570-6.

20. Widschwendter A, Tonko-Geymayer S, Welte T, Daxenbichler G, Marth C, Doppler W. Prognostic significance of signal transducer and activator of transcription 1 activation in breast cancer. Clinical cancer research : an official journal of the American Association for Cancer Research. 2002;8(10):3065-74.

21. Zhang Y, Molavi O, Su M, Lai R. The clinical and biological significance of STAT1 in esophageal squamous cell carcinoma. BMC cancer. 2014;14:791.

22. Zhang Y, Zhang Y, Yun H, Lai R, Su M. Correlation of STAT1 with apoptosis and cell-cycle markers in esophageal squamous cell carcinoma. PloS one. 2014;9(12):e113928.

23. Lawrence DW, Kornbluth J. E3 ubiquitin ligase NKLAM ubiquitinates STAT1 and positively regulates STAT1-mediated transcriptional activity. Cellular signalling. 2016;28(12):1833-41.

24. Ren Y, Zhao P, Liu J, Yuan Y, Cheng Q, Zuo Y, et al. Deubiquitinase USP2a Sustains Interferons Antiviral Activity by Restricting Ubiquitination of Activated STAT1 in the Nucleus. PLoS pathogens. 2016;12(7):e1005764.

25. Soond SM, Townsend PA, Barry SP, Knight RA, Latchman DS, Stephanou A. ERK and the F-box protein betaTRCP target STAT1 for degradation. *The Journal of biological chemistry*. 2008;283(23):16077-83.
26. Yuan C, Qi J, Zhao X, Gao C. Smurf1 protein negatively regulates interferon-gamma signaling through promoting STAT1 protein ubiquitination and degradation. *The Journal of biological chemistry*. 2012;287(21):17006-15.
27. Gao C, Mi Z, Guo H, Kuo PC. Osteopontin regulates ubiquitin-dependent degradation of Stat1 in murine mammary epithelial tumor cells. *Neoplasia*. 2007;9(9):699-706.
28. Kim TK, Maniatis T. Regulation of interferon-gamma-activated STAT1 by the ubiquitin-proteasome pathway. *Science*. 1996;273(5282):1717-9.
29. Amin HM, Lai R. Pathobiology of ALK+ anaplastic large-cell lymphoma. *Blood*. 2007;110(7):2259-67.
30. Chiarle R, Voena C, Ambrogio C, Piva R, Inghirami G. The anaplastic lymphoma kinase in the pathogenesis of cancer. *Nature reviews Cancer*. 2008;8(1):11-23.
31. Gelebart P, Anand M, Armanious H, Peters AC, Dien Bard J, Amin HM, et al. Constitutive activation of the Wnt canonical pathway in mantle cell lymphoma. *Blood*. 2008;112(13):5171-9.
32. Wu F, Wang P, Young LC, Lai R, Li L. Proteome-wide identification of novel binding partners to the oncogenic fusion gene protein, NPM-ALK, using tandem affinity purification and mass spectrometry. *The American journal of pathology*. 2009;174(2):361-70.

33. Xi S, Dyer KF, Kimak M, Zhang Q, Gooding WE, Chaillet JR, et al. Decreased STAT1 expression by promoter methylation in squamous cell carcinogenesis. *Journal of the National Cancer Institute*. 2006;98(3):181-9.
34. Fulda S, Debatin KM. IFN $\gamma$  sensitizes for apoptosis by upregulating caspase-8 expression through the Stat1 pathway. *Oncogene*. 2002;21(15):2295-308.
35. Wang F, Gao X, Barrett JW, Shao Q, Barteel E, Mohamed MR, et al. RIG-I mediates the co-induction of tumor necrosis factor and type I interferon elicited by myxoma virus in primary human macrophages. *PLoS pathogens*. 2008;4(7):e1000099.
36. Afkarian M, Sedy JR, Yang J, Jacobson NG, Cereb N, Yang SY, et al. T-bet is a STAT1-induced regulator of IL-12R expression in naive CD4<sup>+</sup> T cells. *Nat Immunol*. 2002;3(6):549-57.
37. Dai X, Sayama K, Yamasaki K, Tohyama M, Shirakata Y, Hanakawa Y, et al. SOCS1-negative feedback of STAT1 activation is a key pathway in the dsRNA-induced innate immune response of human keratinocytes. *The Journal of investigative dermatology*. 2006;126(7):1574-81.
38. Bhattacharya S, Ray RM, Johnson LR. STAT3-mediated transcription of Bcl-2, Mcl-1 and c-IAP2 prevents apoptosis in polyamine-depleted cells. *The Biochemical journal*. 2005;392(Pt 2):335-44.
39. Gritsko T, Williams A, Turkson J, Kaneko S, Bowman T, Huang M, et al. Persistent activation of stat3 signaling induces survivin gene expression and confers resistance to apoptosis in human breast cancer cells. *Clinical cancer research : an official journal of the American Association for Cancer Research*. 2006;12(1):11-9.
40. Lighvani AA, Frucht DM, Jankovic D, Yamane H, Aliberti J, Hissong BD, et al. T-bet is rapidly induced by interferon-gamma in lymphoid and myeloid cells. *Proceedings*



of the National Academy of Sciences of the United States of America. 2001;98(26):15137-42.

41. Szabo SJ, Kim ST, Costa GL, Zhang X, Fathman CG, Glimcher LH. A novel transcription factor, T-bet, directs Th1 lineage commitment. *Cell*. 2000;100(6):655-69.

42. Amin HM, McDonnell TJ, Ma Y, Lin Q, Fujio Y, Kunisada K, et al. Selective inhibition of STAT3 induces apoptosis and G(1) cell cycle arrest in ALK-positive anaplastic large cell lymphoma. *Oncogene*. 2004;23(32):5426-34.

43. Schust J, Sperl B, Hollis A, Mayer TU, Berg T. Stattic: a small-molecule inhibitor of STAT3 activation and dimerization. *Chemistry & biology*. 2006;13(11):1235-42.

44. Chan SR, Vermi W, Luo J, Lucini L, Rickert C, Fowler AM, et al. STAT1-deficient mice spontaneously develop estrogen receptor alpha-positive luminal mammary carcinomas. *Breast cancer research : BCR*. 2012;14(1):R16.

45. Pansky A, Hildebrand P, Fasler-Kan E, Baselgia L, Ketterer S, Beglinger C, et al. Defective Jak-STAT signal transduction pathway in melanoma cells resistant to growth inhibition by interferon-alpha. *International journal of cancer*. 2000;85(5):720-5.

46. Boudny V, Dusek L, Adamkova L, Chumchalova J, Kocak I, Fait V, et al. Lack of STAT 1 phosphorylation at TYR 701 by IFNgamma correlates with disease outcome in melanoma patients. *Neoplasma*. 2005;52(4):330-7.

47. Abril E, Real LM, Serrano A, Jimenez P, Garcia A, Canton J, et al. Unresponsiveness to interferon associated with STAT1 protein deficiency in a gastric adenocarcinoma cell line. *Cancer immunology, immunotherapy : CII*. 1998;47(2):113-20.

48. Yu H, Yue X, Zhao Y, Li X, Wu L, Zhang C, et al. LIF negatively regulates tumour-suppressor p53 through Stat3/ID1/MDM2 in colorectal cancers. *Nature communications*. 2014;5:5218.
49. Sironi JJ, Ouchi T. STAT1-induced apoptosis is mediated by caspases 2, 3, and 7. *The Journal of biological chemistry*. 2004;279(6):4066-74.
50. Miura Y, Tsujioka T, Nishimura Y, Sakaguchi H, Maeda M, Hayashi H, et al. TRAIL expression up-regulated by interferon-gamma via phosphorylation of STAT1 induces myeloma cell death. *Anticancer research*. 2006;26(6B):4115-24.
51. Choi EA, Lei H, Maron DJ, Wilson JM, Barsoum J, Fraker DL, et al. Stat1-dependent induction of tumor necrosis factor-related apoptosis-inducing ligand and the cell-surface death signaling pathway by interferon beta in human cancer cells. *Cancer research*. 2003;63(17):5299-307.
52. Ning Y, Riggins RB, Mulla JE, Chung H, Zwart A, Clarke R. IFNgamma restores breast cancer sensitivity to fulvestrant by regulating STAT1, IFN regulatory factor 1, NF-kappaB, BCL2 family members, and signaling to caspase-dependent apoptosis. *Molecular cancer therapeutics*. 2010;9(5):1274-85.
53. Bernabei P, Coccia EM, Rigamonti L, Bosticardo M, Forni G, Pestka S, et al. Interferon-gamma receptor 2 expression as the deciding factor in human T, B, and myeloid cell proliferation or death. *Journal of leukocyte biology*. 2001;70(6):950-60.
54. Stephanou A, Brar BK, Knight RA, Latchman DS. Opposing actions of STAT-1 and STAT-3 on the Bcl-2 and Bcl-x promoters. *Cell death and differentiation*. 2000;7(3):329-30.
55. Kovacic B, Stoiber D, Moriggl R, Weisz E, Ott RG, Kreibich R, et al. STAT1 acts as a tumor promoter for leukemia development. *Cancer cell*. 2006;10(1):77-87.

56. Heuser M, Sly LM, Argiropoulos B, Kuchenbauer F, Lai C, Weng A, et al. Modeling the functional heterogeneity of leukemia stem cells: role of STAT5 in leukemia stem cell self-renewal. *Blood*. 2009;114(19):3983-93.
57. Sanda T, Tyner JW, Gutierrez A, Ngo VN, Glover J, Chang BH, et al. TYK2-STAT1-BCL2 pathway dependence in T-cell acute lymphoblastic leukemia. *Cancer discovery*. 2013;3(5):564-77.
58. Wang H, Yang Y, Sharma N, Tarasova NI, Timofeeva OA, Winkler-Pickett RT, et al. STAT1 activation regulates proliferation and differentiation of renal progenitors. *Cellular signalling*. 2010;22(11):1717-26.
59. Dunn GP, Sheehan KC, Old LJ, Schreiber RD. IFN unresponsiveness in LNCaP cells due to the lack of JAK1 gene expression. *Cancer research*. 2005;65(8):3447-53.
60. Sellier H, Rebillard A, Guette C, Barre B, Coqueret O. How should we define STAT3 as an oncogene and as a potential target for therapy? *Jak-Stat*. 2013;2(3):e24716.

## CHAPTER 3

### **A positive feedback involving the Wnt/ $\beta$ -catenin/MYC/Sox2 axis defines a highly tumorigenic cell subpopulation in ALK-positive anaplastic large-cell lymphoma<sup>1</sup>**

---

<sup>1</sup>A version of this chapter has been published:

Wu C, Zhang H, Gupta N, Alshareef A, Wang Q, Huang Y-H, Lewis T.J, Douglas D.N, Kneteman N.M, and Lai R. A positive feedback involving the Wnt/ $\beta$ -catenin/MYC/Sox2 axis defines a highly tumorigenic cell subpopulation in ALK-positive anaplastic large-cell lymphoma. *Journal of Hematology and Oncology*. 2016 9(1):120. *Journal of Hematology and Oncology* is an open-access journal, and copyright of the any paper published in this journal is retained by the author(s).

As first author, I prepared the first draft and revisions based on the suggestions and comments of the co-authors. I designed and performed most of the experiments described herein, except for the following: N.G. performed the ChIP-qPCR experiment and data analysis, shown in Figure 3.4E; A.A. performed the Wnt signaling pathway PCR array and data analysis, shown in Figure 3.6; H.Z., Q.W., and Y.H. have contribution to the Figure 3.3C and Figure 3.11A. H.Z., N.G. and A.A. also provided significant intellectual input. J.L., D.D., and N.K. were responsible for the animal study design, conducting euthanization of the SCID mouse and data analysis. R.L. provided numerous comments and final review of the manuscript before it was submitted for publication.

### 3.1 Introduction

ALK-positive anaplastic large-cell lymphoma (ALK+ALCL) is a specific type of non-Hodgkin lymphoma of null/T-cell lineage, and these tumors occur most frequently in young adults and children (1, 2). Approximately 80% of ALK+ALCL patients carry the chromosomal translocation,  $t(2;5)(p23;q35)$ , which results in the generation of the abnormal fusion protein NPM-ALK (1, 2). NPM-ALK has been extensively studied and shown to be the major oncogenic driver in these tumors. By virtue of its constitutively active tyrosine kinase activity, NPM-ALK drives oncogenesis primarily by binding to and phosphorylating a host of signaling proteins, such as STAT3 and PI3K, thereby deregulating these signaling pathways (2). As a result of these biochemical aberrancies, NPM-ALK promotes unregulated cell growth and survival, silences the expression of tumor suppressors and deregulates cellular metabolism (2). From the clinical perspective, ALK+ALCL tumors are clinically aggressive (1). Although complete remission can be induced in most pediatric ALK+ALCL patients after conventional combination chemotherapy, chemoresistance and disease relapses occur in a substantial proportion of adult patients (2). The biological basis of chemoresistance in ALK+ALCL patients is incompletely understood, but a recent report (3) describing the existence of cancer stem-like cells (CSCs) in ALK+ALCL raises the possibility that these cells may be implicated, similar to how CSCs might contribute to chemoresistance and cancer relapses in other cancer models (4, 5).

Sox2, one of the four master transcription factors involved in re-programming fibroblasts to inducible pluripotent stem cells, is normally expressed only in embryonic

stem cells (6). In recent years, aberrant expression of Sox2 has been found in a relatively large number of cancer types, including breast cancer (7), melanoma (8), as well as ALK+ALCL (9). Sox2 expression in these cancers has been shown to correlate with properties commonly associated with cancer stemness, such as chemoresistance (10), tumor-initiation (8, 10) and self-renewal (10). Using a Sox2 reporter containing the SRR2 (Sox2 Regulatory Region-2) sequence, the Lai lab has previously identified the existence of two phenotypically distinct cell subpopulations in ALK+ALCL cell lines, with a small subset of cells being Sox2<sup>active</sup> (currently denoted as Reporter Responsive, RR) and the majority of the cells being Sox2<sup>inactive</sup> (denoted as Reporter Unresponsive, RU) (9). Importantly, RR cells were found to be significantly more tumorigenic and stem-like than RU cells (9). Sox2 is directly involved in conferring these stem-like features, since siRNA knockdown of Sox2 resulted in a dramatic abrogation of these features (9). As the expression level and subcellular localization of Sox2 were similar between RU and RR cells, it is proposed that the RU/RR dichotomy is not simply a result of a differential Sox2 expression and localization between these two cell subsets(9). It is of paramount importance to understand the biochemical basis of how the RU/RR dichotomy is regulated, as the RR phenotype links with CSC features in ALK+ALCL. It is likely that the identification of the key regulators for this dichotomy may facilitate the design of new therapeutics targeting CSCs in ALK+ALCL.

The aim of this study was to identify the key regulator(s) of the RU/RR dichotomy. The hypothesis is that Sox2 is more transcriptionally active in RR cells because Sox2 can bind to DNA more efficiently in this cell subset. The experimental strategy involved an

analysis of the SRR2 sequence, in an attempt to identify potential transcription factor(s) that regulate the DNA binding of Sox2. A positive feedback loop involving the Wnt/ $\beta$ -catenin/MYC/Sox2 axis was identified to define a highly tumorigenic and chemoresistant cell subset in ALK+ALCL.

## **3.2 Methods and materials**

### **3.2.1 Primary tumors, cell lines and treatments**

All primary tumors were diagnosed at the Cross Cancer Institute (Edmonton, Alberta, Canada) and the diagnostic criteria were based on those described in the WHO Classification Scheme. The use of these patient samples for research had received research ethics approval at Feb 17<sup>th</sup> of 2016, by the Human Research Ethics Board at the University of Alberta, with approval number: Pro00062737. The details of the cell lines used in this study were described in section 2.2.1 of Chapter 2. SupM2 and Karpas 299 cell lines were grown and expanded in RPMI 1640 medium (Invitrogen, Life Technologies, Grand Island, NY), supplemented with 10% fetal bovine serum (FBS, Invitrogen) and 1% penicillin streptomycin (Thermo Fisher Scientific) in 5% CO<sub>2</sub> atmosphere at 37°C. All cell lines that were stably transfected with Sox2 reporter were grown and expanded in RPMI 1640 (Invitrogen) supplemented with 10% FBS (Invitrogen), 1% penicillin streptomycin (ThermoFisher Scientific Canada) and 200  $\mu$ g/mL puromycin dihydrochloride (Sigma Aldrich, St Louis, MO) in 5% CO<sub>2</sub> atmosphere at 37°C. 10074-G5, quercetin, doxorubicin, crizotinib, Stattic, iodonitrotetrazolium chloride and G418 were all purchased from Sigma Aldrich. All of the treatments were

performed following the manufacturer's instructions. In brief, 10074-G5, quercetin, doxorubicin, crizotinib and Stattic were also dissolved in DMSO (Sigma Aldrich). RU or RR cells were subjected with 10  $\mu$ M 10074-G5, 50  $\mu$ M quercetin, 100 nM crizotinib, or 10 nM Stattic for 24 hours, cells with DMSO treatment were included as control. The MYC protein level and Sox2 reporter luciferase activity were analyzed after these treatments. RU and RR cells were subjected with various doses of 10074-G5 or doxorubicin for 48 or 72 hours to assess the cell viability after treatments. 5  $\mu$ M 10074-G5 and 20 ng/mL doxorubicin were combined for the drug combination treatment (48 hours treatment).

### **3.2.2 Short interfering RNA and transfections**

SMARTpool short interfering RNAs (siRNAs) for MYC,  $\beta$ -catenin, Sox2 and scrambled siRNA were purchased from Dharmacon (Lafayette, CO). All siRNAs were diluted to a stock concentration of 20  $\mu$ M. Transient transfections of ALK+ALCL cells with siRNAs (final concentration: 600 nM) were performed as previously described in section 2.2.4 of Chapter 2.

### **3.2.3 RNA extraction, cDNA synthesis, quantitative reverse transcriptase PCR (quantitative RT-PCR) and chromatin-immunoprecipitation PCR**

Total RNA extraction was performed with the Qiagen RNeasy Kit (Qiagen, Toronto, Ontario, Canada) according to the manufacturer's protocol. This assay was performed as previously described in section 2.2.13 of Chapter 2. Regular quantitative RT-PCR



assay was described in section 2.2.13 of Chapter 2. MAGnify™ ChIP kit was purchased from ThermoFisher Scientific Canada for Chromatin-immunoprecipitation PCR experiment. The procedures were following the manufacture's protocol. In brief, cells were firstly treated with formaldehyde to generate protein-protein and protein-DNA crosslinks within chromatin complex, and then the cells were lysed. The cell chromatin were released from the nuclei and sheared by sonication to reduce the DNA fragment size to 200-500 bp for analysis. The DNA fragments of interest were immunoprecipitate with Sox2 antibody (D6D9, Cell Signaling Technology), and the DNA fragments were utilized for quantitative RT-PCR.

Primers for SRR2 probe for ChIP-PCR experiment are shown as below:

Forward primer: 5'- ACATTGTA CTGGGAAGGGACA-3',

Reverse primer: 5'- AGCAAGAACTGGCGAATGTG-3'.

All genes of interest were normalized to GAPDH transcript expression levels.

All other primer sequences were listed as below:

**Table 3.1 Primers used for quantitative RT-PCR**

<b>Gene</b>	<b>Forward Primers</b>	<b>Reverse Primers</b>
ARNT	5'-CTGCCAACCCCGAAATGACAT-3'	5'-CGCCGCTTAATAGCCCTCTG-3'
USF1	5'-CTGCTGTTGTTACTACCCAGG-3'	5'- TCTGACTTCGGGGAATAAGGG-3'
FEV	5'- CACGGCGAGTTCAAGCTCA-3'	5'- CTGGAAGTCGAAGCGGTAGG-3'
HOXA5	5'- AACTCATTTTGCGGTCGCTAT-3'	5'- TCCCTGAATTGCTCGCTCAC-3'
E2F1	5'- ACGCTATGAGACCTCACTGAA-3'	5'- TCCTGGGTCAACCCCTCAAG-3'
SOX10	5'- CCTCACAGATCGCCTACACC-3'	5'- CATATAGGAGAAGGCCGAGTAGA-3'
SOX9	5'- AGCGAACGCACATCAAGAC-3'	5'- CTGTAGGCGATCTGTTGGGG-3'
POU5F1	5'- CTGGGTTGATCCTCGGACCT-3'	5'- CCATCGGAGTTGCTCTCCA-3'
BCL9	5'- GGCCATACCCCTAAAGCACTC-3'	5'- CGGAAATACTTCGCTCCCTTTT-3'
AXIN2	5'- CAACACCAGGCGGAACGAA-3'	5'- GCCCAATAAGGAGTGTAAGGACT-3'
CTNNB1	5'- AAAGCGGCTGTTAGTCACTGG-3'	5'- CGAGTCATTGCATACTGTCCAT-3'
LEF1	5'- AGAACACCCCGATGACGGA-3'	5'- GGCATCATTATGTACCCGGAAT-3'
SOX2	5'- GCCGAGTGAAACTTTTGTGCG-3'	5'- GGCAGCGTGTACTTATCCTTCT-3'
SOX17	5'- GTGGACCGCACGGAATTTG-3'	5'- GGAGATTCACACCGGAGTCA-3'
MYC	5'-TACCCTCTCAACGACAGC AG-3'	5'-TCTTGACATTCTCCTCGGTG-3'
WNT2B	5'-GATCAAGATGGTGCCAACTTC-3'	5'-CCAAGACACAGTAATCTGGAGAG -3'
ABCC1	5'-CTCTATCTCTCCCGACATGACC-3'	5'-AGCAGACGATCCACAGCAAAA-3'
ABCC2	5'-CCCTGCTGTTGATATACCAATC-3'	5'-TCGAGAGAATCCAGAATAGGGAC-3'
ABCC3	5'-TGGGGTGAAGTTTCGTA CTGG-3'	5'-CACGTTTGACTGAGTTGGTGATA-3'
ABCC4	5'-AGCTGAGAATGACGCACAGAA-3'	5'-ATATGGGCTGGATTACTTTGGC-3'
ABCC5	5'-AGTCCTGGGTATAGAAGTGTGAG-3'	5'-ATTCCAACGGTCGAGTTCTCC-3'
ABCG2	5'-CAGGTGGAGGCAAATCTTCGT-3'	5'-ACCCTGTTAATCCGTTCTGTTTT-3'
GAPDH	5'- GGAGCGAGATCCCTCCAAAAT-3'	5'- GGCTGTTGTCATACTTCTCATGG-3'

The Wnt/ $\beta$ -catenin pathway PCR-array was purchased from Qiagen. The PCR array (96-well plate) was utilized to analyze the expression of Wnt/  $\beta$ -catenin pathway-related genes. This 96-well PCR array plate contains SYBR<sup>®</sup> Green-optimized primers for simultaneously detecting 87 genes related with Wnt/  $\beta$ -catenin pathway. The similar

experimental process was followed as regular quantitative RT-PCR (see section 2.2.13 of Chapter 2).

### **3.2.4 Immunohistochemistry and immunofluorescence studies**

The MYC antibody (Y69) and active  $\beta$ -catenin antibody (8E7) were purchased from Abcam (Cambridge, MA) and Millipore (Billerica, MA), respectively. 1:100 dilution of MYC antibody was used in the immunohistochemistry assay. 1:200 dilution of MYC antibody and 1:200 dilution of active  $\beta$ -catenin antibody were used in immunofluorescence double staining. The procedures of Immunohistochemistry were described in the previous publication and section 2.2.3 of Chapter 2 (11). For the immunofluorescence assay, the procedures were described as below. Briefly, formalin-fixed, paraffin-embedded tissue sections were deparaffinized and hydrated. Heat-induced epitope retrieval was performed using citrate buffer (pH=6.0) and a pressure cooker using microwave. Tissue sections were then permeabilized for 10 min with 0.2% Triton X-100 in 1x PBS containing 10mM HEPES (ThermoFisher Scientific Canada) and 3% BSA (Sigma Aldrich), followed by the block with 1x PBS containing 10mM HEPES (ThermoFisher Scientific Canada) and 3% BSA (Sigma Aldrich) for 1 hour. The tissue sections were incubated with the primary antibodies, anti-active  $\beta$ -catenin and MYC diluted in 1 X PBS with 10 mM HEPES and 1% BSA overnight in 4 °C. In the second day, after three times of washes with 1 x PBS (30 minutes in total), tissue sections were incubated with secondary antibodies (Alexa Fluor 594 goat anti-rabbit antibody and Alexa Fluor 488 goat anti-mouse antibody, Invitrogen, Burlington, CA), diluted in 1x PBS, 1:300 for 1 hour. After wash in 1 X PBS, tissues were incubated in 1

µg/mL Hoechst 33342 (Sigma Aldrich, B2261) for 10 minutes, followed by washes in 1 X PBS and mounted with Mounting Medium (Dako, Mississauga, ON, Canada). Cells were visualized with a Zeiss LSM510 confocal microscope (Carl Zeiss, Heidelberg, Germany) at the Core Cell Imaging Facility, Cross Cancer Institute, University of Alberta, Edmonton, Canada.

### **3.2.5 Plasmid constructs and transfection**

pcDNA3.3-MYC was a gift from Derrick Rossi (Addgene plasmid # 26818) and pcDNA-delta N89 Beta-catenin was a gift from Eric Fearon (Addgene plasmid # 19288), Myc-Mad-HA plasmid was a gift from Bert Vogelstein (Addgene plasmid #16557). pcDNA empty vector was purchased from Addgene (Cambridge, MA). pcDNA-Flag-Sox2 plasmid was generated by the Lai lab. The procedures for transfection were described in section 2.2.5 of Chapter 2. The stable cell lines were established by the following steps. 10 million of RU cells originated from SupM2 were transfected with 20 µg pcDNA3.3-MYC or pcDNA, and then cultured for 3 weeks in selection medium with increasing concentration of G418 up to 200 µg/mL. RR cells derived from SupM2 that was stably transfected with pcDNA were also established following the same procedure.

### **3.2.6 Western blotting**

Western blotting studies were performed as described in section 2.2.8 of Chapter 2.

Antibodies reactive to phosphorylated MYC<sup>S62</sup> (E1J4K), MYC (D84C12), Sox2 (D6D9), β-catenin (D10A8), phosphorylated GSK3β<sup>S9</sup> (D85E12), LEF1(C18A7), γ-tubulin

antibody (#5886) and Histone deacetylase 1 (HDAC-1) antibody (#2062) were purchased from Cell Signaling Technology (Danvers, MA),  $\alpha$ -tubulin antibody (TU-02) and  $\beta$ -actin antibody (sc-130300) were purchased from Santa Cruz (Dallas, Texas), antibody reactive to active  $\beta$ -catenin (8E7) was purchased from Merck Millipore (Toronto, ON, Canada). Secondary antibodies anti-Rabbit IgG (1:2000) and anti-Mouse IgG (1:2000) were purchased from Cell Signaling Technology.

### **3.2.7 Luciferase assay**

The luciferase assay kit was purchased from Promega (Madison, WI), the procedure for luciferase assay was performed following the manufacture's protocol. Briefly, cell pellets after cold 1 X PBS wash for three times were lysed by 100  $\mu$ l 1 X lysis buffer (5 X lysis buffer provided in kit were diluted by double distilled water), then the cell lysates were processed for assess protein concentrations and luciferase values. The luciferase values were read by FLUOstar Omega microplate reader (BMG LabTech, ThermoFisher Scientific Canada), and normalized to their protein concentrations. The luciferase activity of RU cells was normalized to 1 when compared to it in RR cells in this study. Each experiment was performed in triplicate.

### **3.2.8 Transwell assay**

The 6-well plates of polyester transwell permeable supports with 0.4 $\mu$ m pore size were purchased from Corning Inc (Toronto, ON, Canada). Briefly, 0.5 million of RU cells and the same number of RR cells, diluted RR cells (diluted with RU cells ) or parental

SupM2 cells were seeded in the upper chamber and lower chamber, respectively, and cultured for 72 hours. The same number of RU cells co-cultured with RU cells in the lower chamber was included as control group. Then the luciferase assay and Western blotting studies were performed.

### **3.2.9 Cell-cycle and MTS assay**

The experimental procedures were described in section 2.2.7 and section 2.2.12 of Chapter 2.

### **3.2.10 SRR2 probe binding assay**

Cells were harvested and washed with cold 1x PBS twice, following by cytoplasmic and nuclear fractionation using the Pierce NE-PER kit (ThermoFisher Scientific Canada). 300 µg nuclear proteins were incubated with or without 3 pmol of biotin-labeled SRR2 probe (constructed by IDT, Edmonton, Alberta, Canada) for 0.5 hour by rotating at room temperature. Streptavidin agarose beads (75 µl, ThermoFisher Scientific Canada) were added to each sample, and the samples were rotated by overnight at 4°C. The next day, the samples were washed with cold 1 X PBS three times, and protein was eluted at 100°C in 4 X protein loading buffer (40% glycerol, 240 mM Tris-HCl pH 6.0, 8% SDS, 0.04% bromophenol blue, and 5% β-mercaptoethanol) for 5 minutes, and Western blotting studies were performed. The sequence of the SRR2 probe: '5-AAGAATTTCCCGGGCTCGGGCAGCCCATTGTGATGCATATAGGATTATTCACGTGGTAATG-3'

The underlined sequence is SRR2 consensus sequence.

### **3.2.11 Nuclear cytoplasm fractionation assay**

The nuclear-cytoplasmic fractionation kit was purchased from ThermoFisher Scientific.

The experiment was performed as described in section 2.2.11 of Chapter 2.

### **3.2.12 Methylcellulose colony formation assay**

Methylcellulose-based media was purchased from R&D systems Inc, and the methylcellulose colony formation assay was performed as previously described in section 2.2.14 of Chapter 2. After 10 days of culture, the colonies were stained with iodinitrotetrazolium chloride overnight and images were acquired using Alphamager HP (ThermoFisher Scientific Canada).

### **3.2.13 SCID mouse xenograft studies**

Twelve CB-17 strain SCID male mice, purchased from Taconic (Hudson, NY), were housed in a virus- and antigen-free facility supported by the Health Sciences Laboratory Animal Services at the University of Alberta and were cared for in accordance with the Canadian Council on Animal Care guidelines. The animal studies had received ethical approval by the Animal Care and Use Committee (ACUC) at Dec 10th of 2015, with approval number: AUP00000782. Briefly, 2 million cells of SupM2-RU-EV, SupM2-RU-MYC and SupM2-RR-EV growing exponentially were injected into

both flanks of 4-week-old mice, four mice each group. The tumor sizes were measured twice every week. These animals were euthanized when a tumor reached 10 mm in the greatest dimension.

### **3.2.14 Side population assay**

The side population assay was performed as previously described by Moti *et al* (3). In brief,  $1 \times 10^6$  cells/mL were washed and resuspended in prewarmed 1 X PBS containing 2% FBS and 10 mM HEPES (Life Technology). Samples were incubated with 5  $\mu$ g/mL Hoechst 33342 (Sigma Aldrich) with or without 100  $\mu$ M Verapamil (Sigma Aldrich) for 90 minutes at 37°C in a water bath in the dark. After incubation, the samples were incubated on ice for 10 minutes and washed with cold 1X PBS, following by counterstaining with 2  $\mu$ g/mL of propidium iodide (Sigma Aldrich) before flow cytometric analysis.

### **3.2.15 Statistical analysis**

Data were expressed as mean  $\pm$  standard deviation. The statistical analysis was performed using Graphpad Prism 5 (La Jolla, CA), and the significance of two independent groups of samples was determined using Student's *t*-test or *Chi-square* test. Statistical significance is denoted by \* ( $P < 0.05$ ) and \*\* ( $P < 0.01$ ).



### 3.3 Results

#### 3.3.1 The identification of MYC as a key regulator of the RU/RR dichotomy

The Lai lab has previously shown that Sox2 is a major contributing factor to the SRR2 reporter activity and the associated phenotype in ALK+ALCL cells(9). In further support of this concept, we found that siRNA knockdown of Sox2 significantly attenuated the SRR2 luciferase activity in RR cells (**Figure 3.1**). As shown in the previous publication, the Lai lab has already demonstrated that the RU/RR dichotomy cannot be attributed to a substantial difference in the Sox2 protein expression level or its nuclear localization between these two cell subsets (9).

To decipher the factor(s) that regulate the RU/RR dichotomy, we examined SRR2 using the JASPAR motif matches analysis. As summarized in **Table 3.2**, we identified a number of transcription factors that show a high probability of binding to SRR2. Among these candidates, MYC was found to be the highest expressed factor in RU/RR cell subsets derived from SupM2 and Karpas 299 cells (**Figure 3.2A**). Accordingly, RR cells derived from both cell lines expressed a significantly higher level of MYC mRNA compared to their RU counterparts (**Figure 3.2A**). This finding correlates well with that of Western blotting study (**Figure 3.2B**). We also found that RR cells harbor a higher level of phosphorylated MYC<sup>S62</sup> (*i.e.* p-MYC<sup>S62</sup>), the active form of MYC (12), than RU cells (**Figure 3.2B**). By nuclear cytoplasmic fractionation, we found that most of the MYC protein expressed in both RU and RR cells was predominantly localized in the nuclei (**Figure 3.2C**).

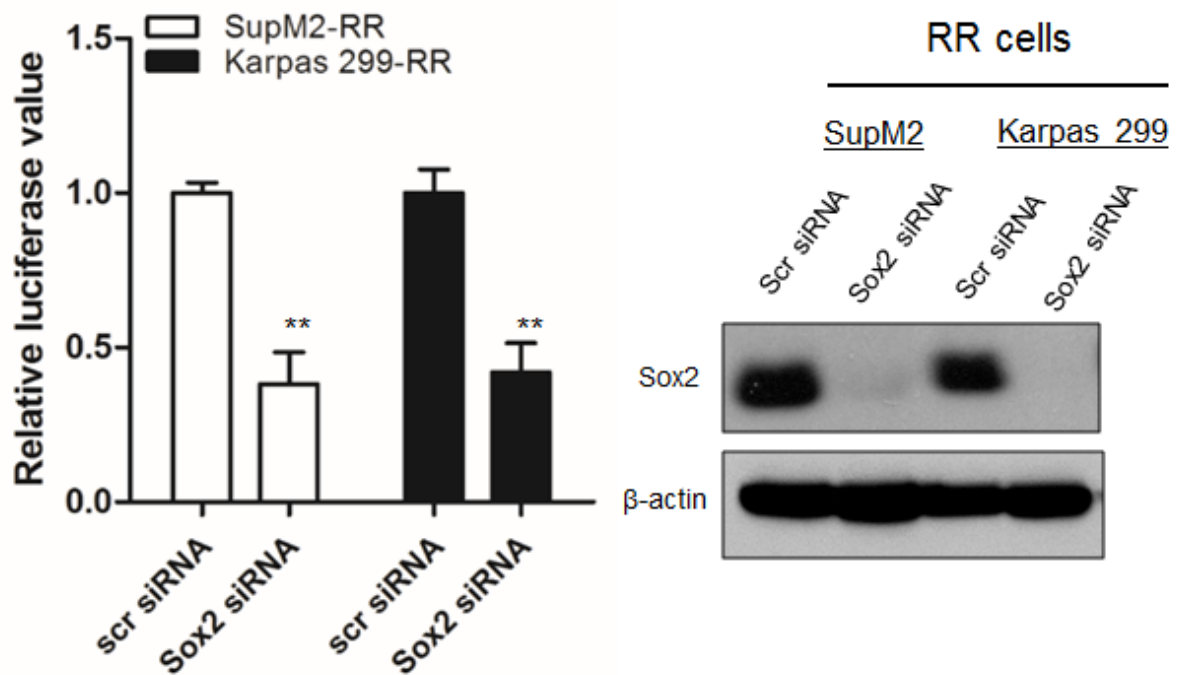


**Figure 3.1 Knockdown of Sox2 by siRNA significantly downregulates the SRR2 luciferase activity in RR cells.** A) The SRR2 luciferase activity in RR cells derived from SupM2 and Karpas 299 with scrambled siRNA (scr siRNA) or Sox2 siRNA transfection. The Western blots on the right panel showed the knockdown efficiency of Sox2 protein expression. Statistical significance is denoted by \* ( $P<0.05$ ) and \*\* ( $P<0.01$ ). Results shown were representative of three independent experiments.

**Table 3.2 The top putative factors that are predicated to bind to SRR2 sequence by JASPAR motif matches analysis at  $P < 0.001$ .**

Name	Motif	Score	Seq	P-Val
SOX2	MA0143.1	17.1451	CCATTGTGATGCATA	4.08e-07
POU5F1	MA0142.1	17.1234	CATTGTGATGCATAT	7.35e-07
USF1	MA0093.1	13.0387	CACGTGG	4.39e-05
ARNT	MA0004.1	11.8782	CACGTG	0.000195
SOX17	MA0078.1	11.1474	GCCATTGTG	0.000114
FEV	MA0156.1	10.7683	CGGGAAAT	0.000126
MYC:MAX	MA0059.1	10.2128	ATTCACGTGGT	7.22e-05
HOXA5	MA0158.1	9.62563	CATTAATT	0.000305
E2F1	MA0024.1	9.41838	TTTCCCGG	9.64e-05
SOX10	MA0442.1	9.35232	CATTGT	0.000578
SOX9	MA0077.1	9.29627	TCACAATGG	0.00024

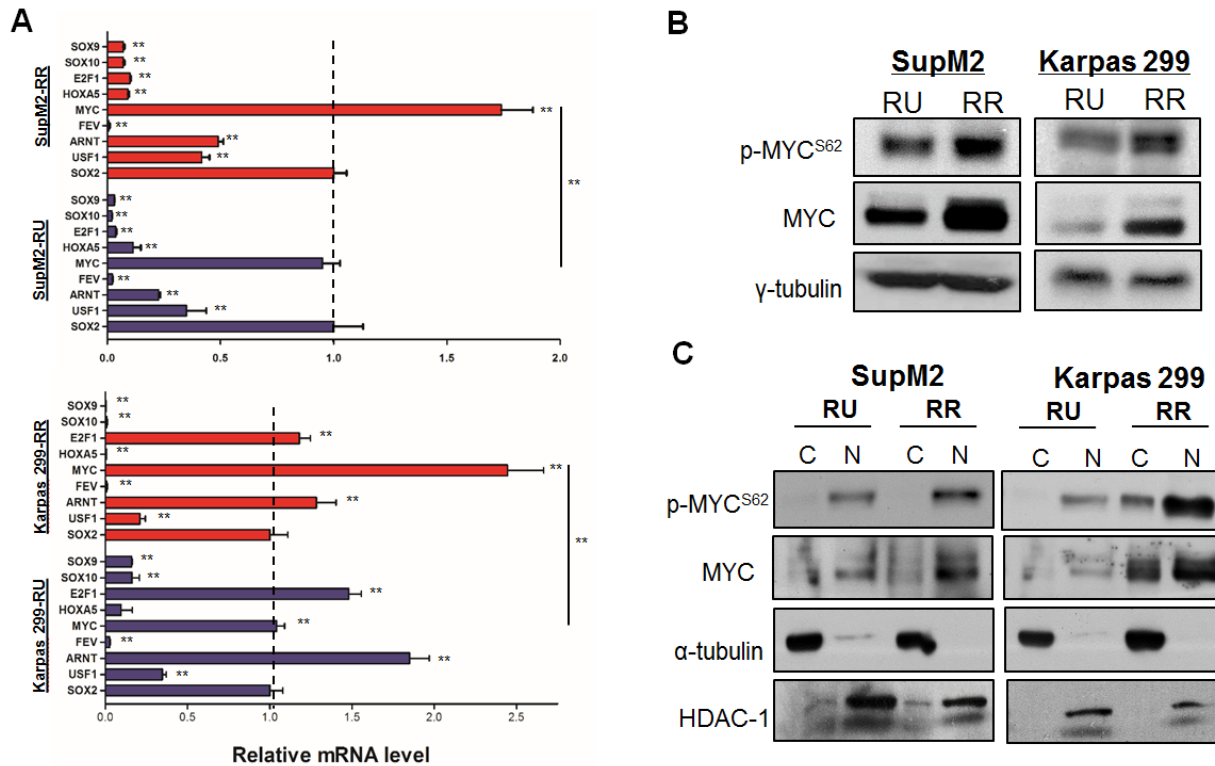


**Figure 3.2 RR cells express a substantially higher level of MYC than RU cells.**

A) The relative mRNA expression levels of putative SRR2 binding factors assessed by quantitative RT-PCR (qRT-PCR). GAPDH was used as internal control, and all the mRNA expression levels were normalized to that of Sox2 in RU cells. B) The levels of p-MYC<sup>S62</sup> and MYC in RU and RR cells derived from SupM2 and Karpas 299. C) The subcellular localization of p-MYC<sup>S62</sup> and MYC in RU and RR cells derived from SupM2 and Karpas 299, assessed by the nuclear cytoplasmic fractionation assay. Statistical significance is denoted by \* ( $P < 0.05$ ) and \*\* ( $P < 0.01$ ).

To evaluate the relevance of MYC in the context of SRR2 reporter responsiveness, we knocked down MYC expression using siRNA and found that SRR2 luciferase activity was significantly reduced by ~40-60% in RR cells derived from SupM2 and Karpas 299 cells (**Figure 3.3A**). Similar results were obtained when MYC was inhibited by using 10074-G5, a pharmacological agent known to inhibit Myc-Max heterodimerization and their DNA binding (13), (**Figure 3.3B**). As a comparison, siRNA knockdown of Sox2

resulted in a similar reduction in SRR2 luciferase activity (**Figure 3.1**). Correlating with these findings, transfection of *MYC* into RU derived from the two cell lines resulted in a significant increase in SRR2 luciferase activity, even though the level remained to be substantially lower than that of RR cells (**Figure 3.3C-D**). As expected, transfection of *MYC* into RR cells from both cell lines also led to a significantly increased SRR2 reporter activity (**Figure 3.3C-D**). Taken together, these findings suggest that *MYC* is a key regulator of the SRR2 reporter activity.

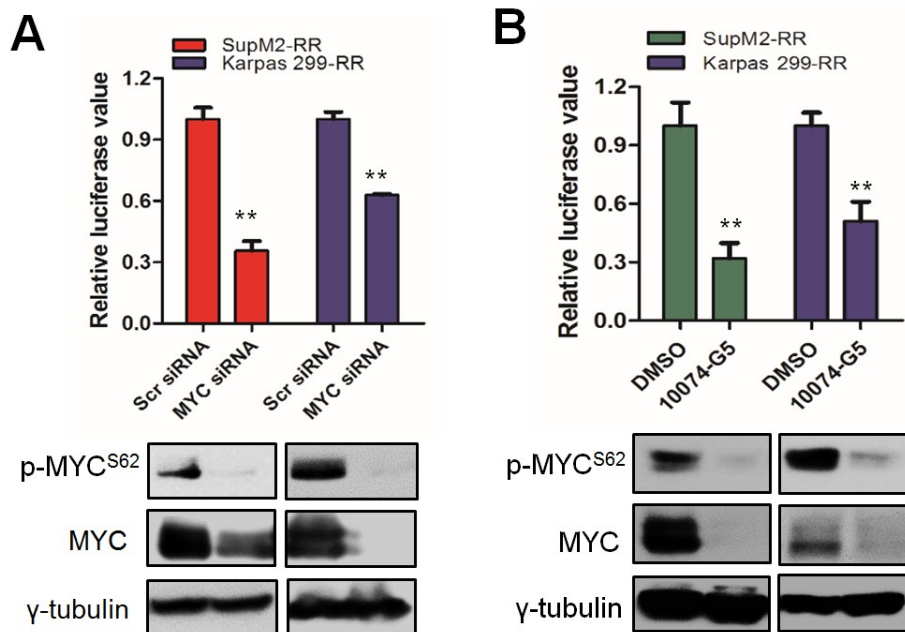


**Figure 3.3 The high MYC expression contributes to the RR phenotype.** A) The SRR2 luciferase activity in RR cells derived from SupM2 and Karpas 299 cells with scr siRNA or MYC siRNA transfection. The Western blots below showed the knockdown efficiency of MYC. B) The SRR2 luciferase activity in RR cells with the treatment of 10  $\mu$ M 10074-G5 for 24 hours. Cells with DMSO treatment were used as a negative control. Statistical significance is denoted by \* ( $P < 0.05$ ) and \*\* ( $P < 0.01$ ). Results shown were representative of three independent experiments.

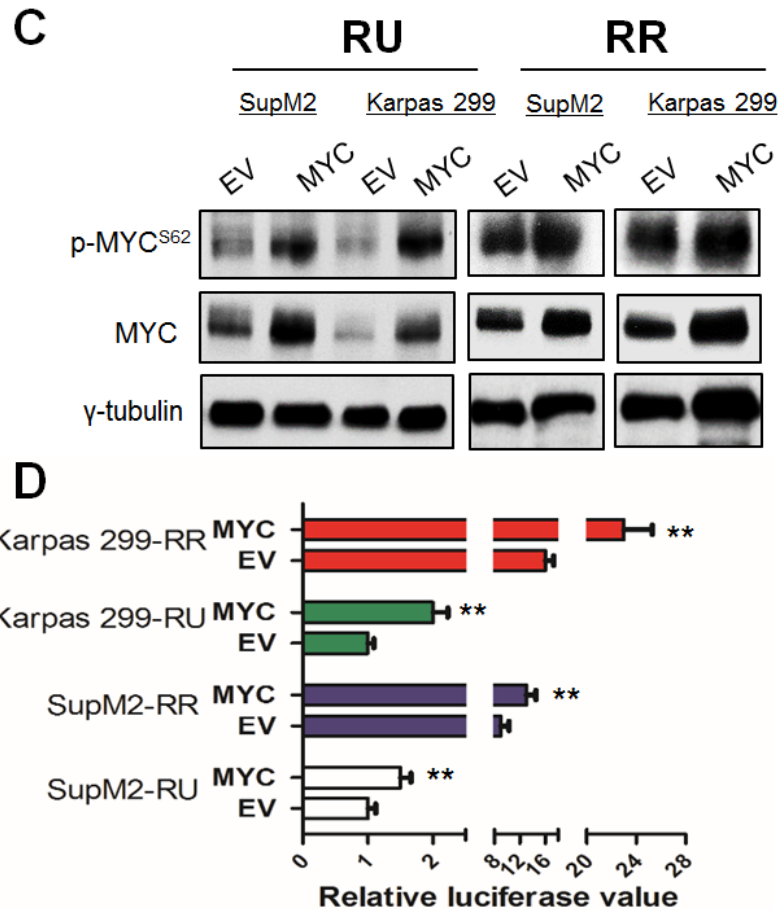


**Figure 3.3C-D** C) RU and RR cells derived from both cell lines were transiently transfected with pcDNA3.3-MYC (*i.e.* MYC). pcDNA empty vector (EV) was included as a negative control. The Western blots showed the MYC transfection efficiency. D) The SRR2 luciferase activity in RU and RR cells with either EV or MYC transient transfection. Statistical significance is denoted by \* ( $P<0.05$ ) and \*\* ( $P<0.01$ ). Results shown were representative of three independent experiments.

We then asked if inhibition of MYC in RR cells also decrease the clonogenicity and chemoresistance that are associated with the RR phenotype. As shown in **Figure 3.3E-G**, pharmacologic inhibition of MYC using 10074-G5 in RR cells resulted in a significant decrease in methylcellulose colony formation and sensitization of these cells

to doxorubicin-induced cell growth inhibition. In addition, that treatment of RR cells with 10074-G5 also led to a significant increase number of apoptotic cells induced by doxorubicin (**Figure 3.3G, lower panel**). Accordingly, compared to RR cells, RU cells were significantly less sensitive to cell growth inhibition induced by 10074-G5 (**Figure 3.3H**). Furthermore, compared to cells transfected with empty vector, RU cells originated from SupM2 with *MYC* transfection exhibited significantly increased doxorubicin-resistance and clonogenicity in methylcellulose soft agar (**Figure 3.3I-J**). Again, a significantly increased clonogenicity was also observed in RR cells with *MYC* transfection, as compared to negative control (**Figure 3.3J**).

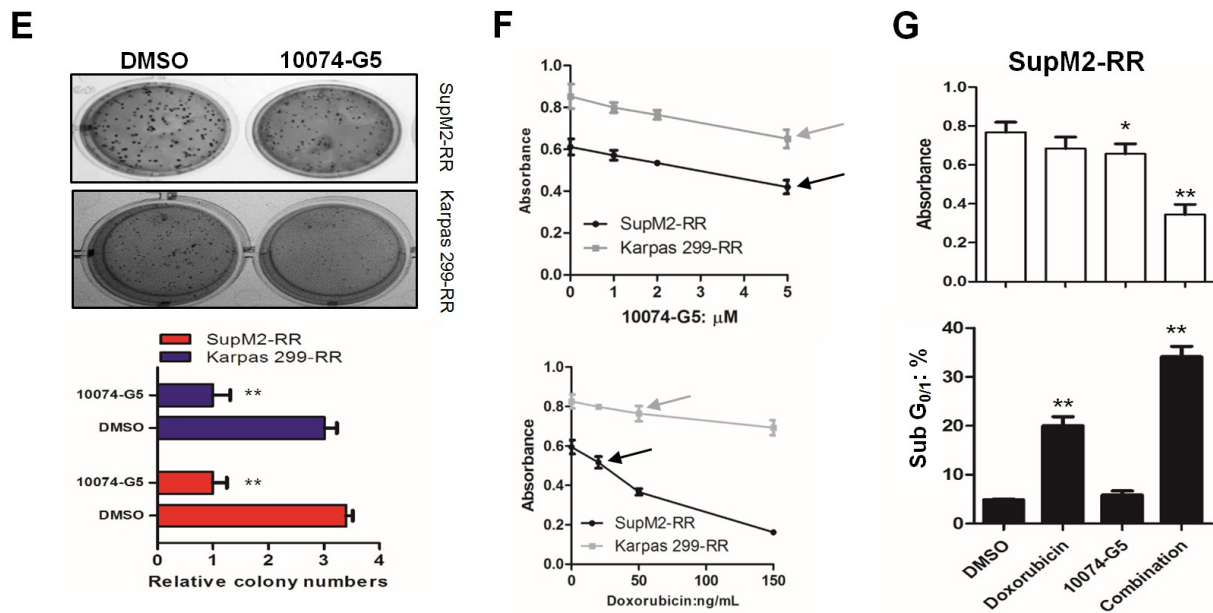


**Figure 3.3E-G.** E) The clonogenicity of RR cells in the presence of 5  $\mu$ M 10074-G5 by using the methylcellulose colony formation assay. Cells with DMSO treatment were included as a control. The relative colony numbers analyzed in triplicate were shown in the lower panel. The colony with more than 50 cells (for RR cells from SupM2) and 20 cells (for RR cells from Karpas 299) was counted. One representative result was shown here. F) RR cells originated from SupM2 and Karpas 299 were treated with varying

dosages of MYC inhibitor 10074-G5 for 48 hours, and then the cell growth was assessed by MTS assay. The dosage of 5  $\mu\text{M}$  10074-G5 was chosen for the following drug combination study. Also, RR cells were treated with varying dosages of doxorubicin for 48 hours, and then the cell growth was assessed by the MTS assay. 50 ng/mL and 20 ng/mL doxorubicin were chosen in RR derived from Karpas 299 and SupM2, respectively, for the following drug combination study. G) The cell growth inhibition in RR cells originated from SupM2 induced by the treatment of doxorubicin (20 ng/mL), or 10074-G5 (5  $\mu\text{M}$ ), or combination of the doxorubicin and 10074-G5 for 48 hours (upper panel), assessed by MTS assay. The cell-cycle analysis (lower panel) showed the percentages of cells with different treatments in Sub  $G_{0/1}$  phase. Statistical significance is denoted by \* ( $P<0.05$ ) and \*\* ( $P<0.01$ ). Representative results from triplicate experiments were shown.

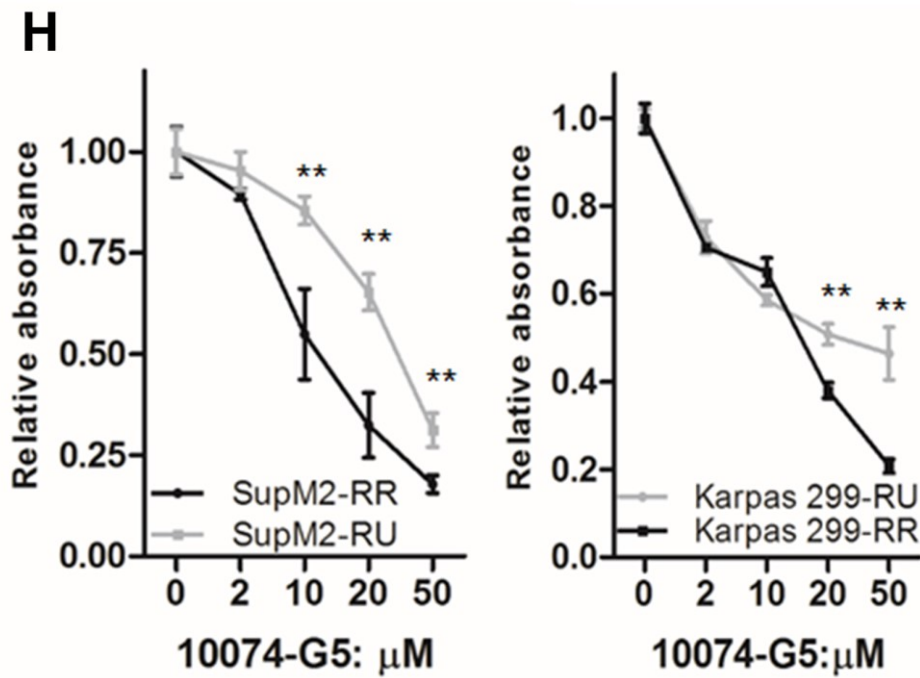


**Figure 3.3H.** H) RU and RR cells were treated with varying doses of 10074-G5 for 72 hours, then followed by the MTS assay to assess the cell growth. Statistical significance is denoted by \* ( $P<0.05$ ) and \*\* ( $P<0.01$ ). Results shown were representative of three independent experiments.



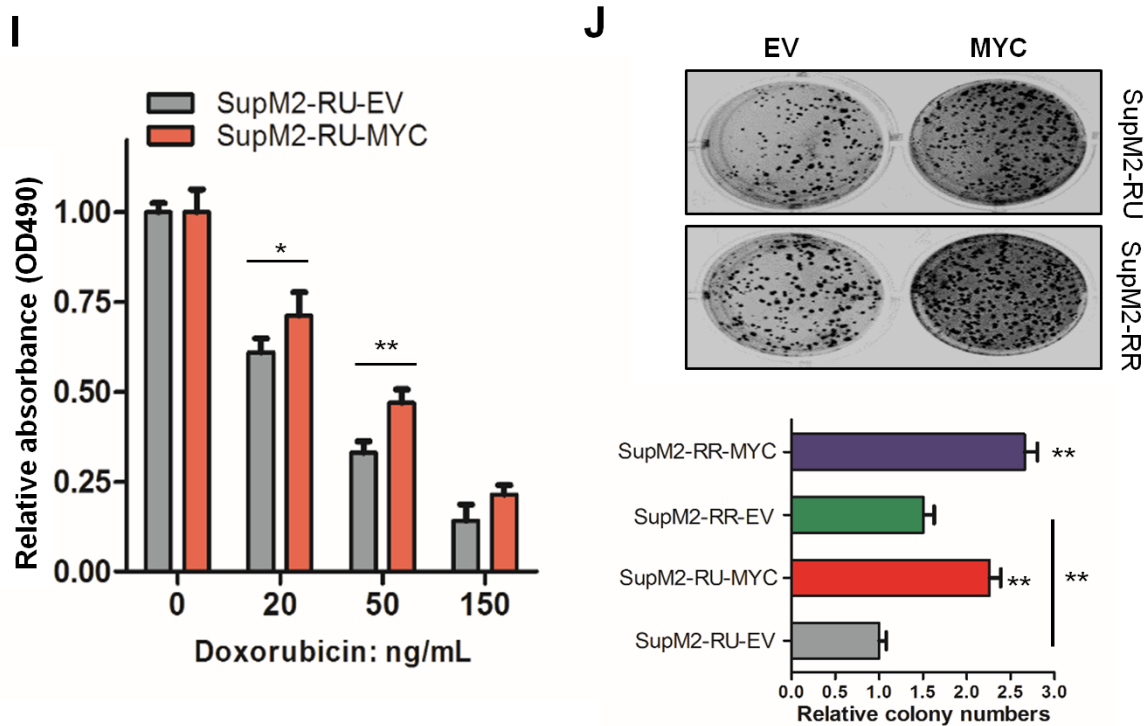
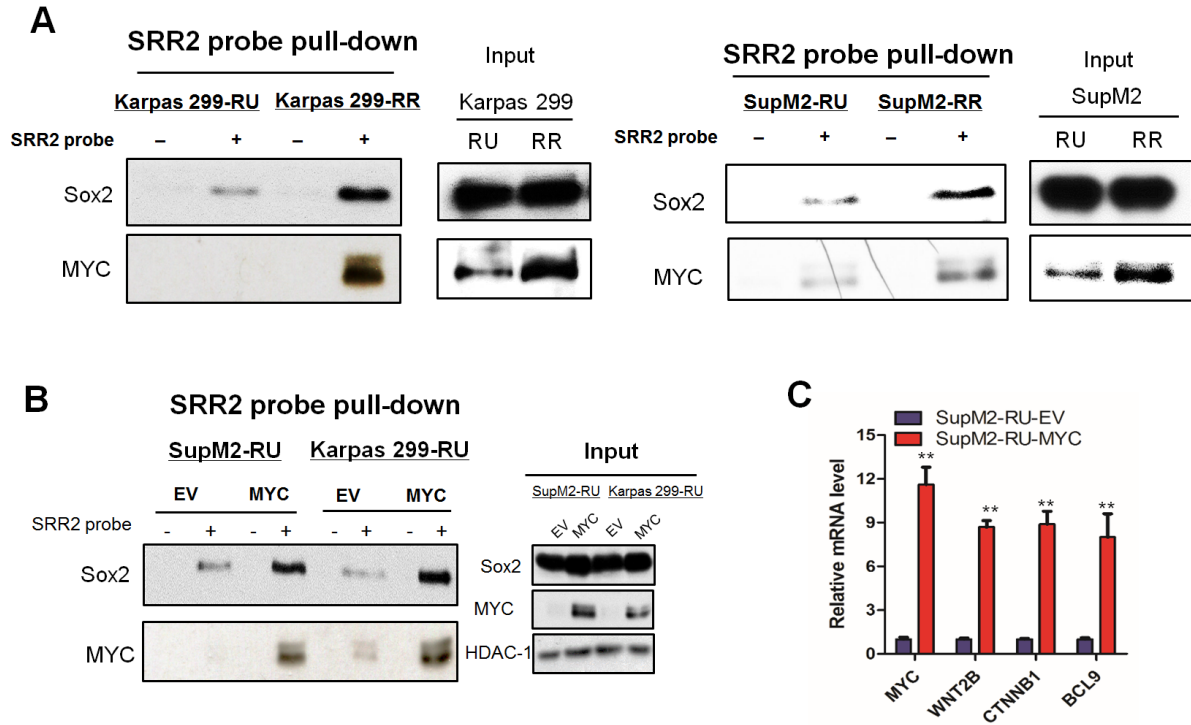


**Figure 3.3I-J** I) The cell growth inhibition induced by varying doses of doxorubicin for 48 hours in RU cells from SupM2 cells that were transiently transfected with either EV or *MYC*, assessed by the MTS assay. J) The clonogenicity of RU and RR cells from SupM2 with either EV or *MYC* transient transfection, assessed by the methylcellulose colony formation assay. The relative colony numbers analyzed in triplicate were shown in the lower panel. The colony with more than 50 cells was counted. Statistical significance is denoted by \* ( $P < 0.05$ ) and \*\* ( $P < 0.01$ ). Representative results from triplicate experiments were shown.

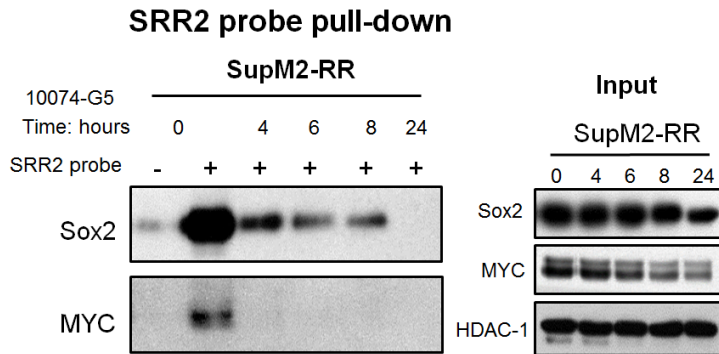
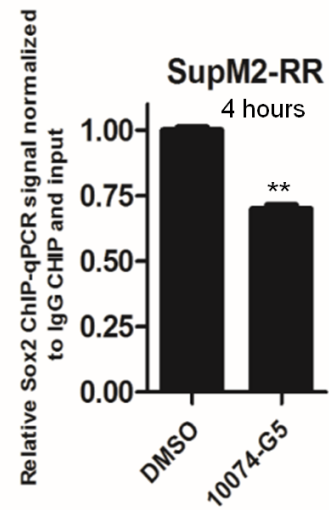
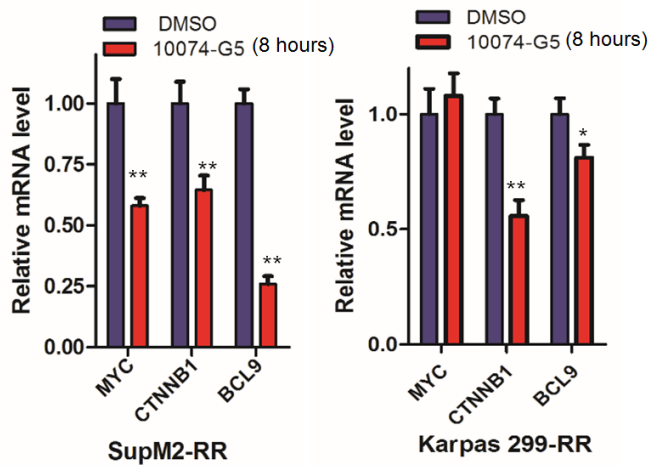
### 3.3.2 MYC promotes Sox2-SRR2 binding and the transcriptional activity of Sox2

The observation that both RU and RR cell subsets express a similar level of Sox2 protein raised the possibility that MYC upregulates SRR2 activity by increasing Sox2-SRR2 binding and Sox2 transcriptional activity. In support of this concept, when we performed pull-down assay using a biotin-labeled SRR2 probe, we found abundant

MYC-SRR2 binding in RR cells but not RU cells (**Figure 3.4A**); a similar pattern of the Sox2-SRR2 interaction was also found in RU and RR cells (**Figure 3.4A**). Furthermore, enforced expression of MYC in RU cells led to substantially more Sox2 pulled down by the SRR2 probe, while the total Sox2 protein level only faintly increased in this experiment (**Figure 3.4B**). Correlating with this increased Sox2-SRR2 binding, the mRNA levels of several genes including *WNT2B*, *CTNNB1* and *BCL9* were significantly increased (**Figure 3.4C**), all of which were shown to be Sox2 downstream targets in RR cells (see section 4). Additionally, 10074-G5 treatment of RR cells from SupM2 cells resulted in a rapid and dramatic decrease in Sox2-SRR2 binding (**Figure 3.4D**), with the total protein levels of MYC and Sox2 being unaffected in this timeframe (*i.e.*, 4 hours). Sox2-SRR2 binding also significantly decreased at 4 hours upon 10074-G5 treatment when we employed chromatin immunoprecipitation-qPCR (**Figure 3.4E**). Correlating with this decreased Sox2-SRR2 binding, the mRNA levels of two Sox2 downstream targets including *CTNNB1* and *BCL9* were also significantly downregulated in RR cells upon MYC inhibition by using 10074-G5 at 8 hours, with the Sox2 protein level not appreciably altered in this time point (**Figure 3.4F**).



**Figure 3.4 MYC promotes the SRR2 probe binding and the transcriptional activity of Sox2.** A) SRR2 probe pull-down assay was performed in RU and RR cells originated from Karpas 299 and SupM2 cells to compare the bindings between Sox2, MYC and SRR2 probe. The Western blots in the right panel showed the input of the pull-down assay. B) The SRR2 probe pull-down assay was performed to assess the Sox2, MYC and SRR2 binding in RU cells with *MYC* transient transfection, as compared to cells with EV transfection. The Western blots in the right panel showed the input of the pull-down assay. C) The relative mRNA levels of Sox2 downstream target genes such as *WNT2B*, *CTNNB1* and *BCL9* in RU cells originated from SupM2 with EV or *MYC* transient transfection at 48 hours. Statistical significance is denoted by \* ( $P<0.05$ ) and \*\* ( $P<0.01$ ).

**D****E****F**

**Figure 3.4D-F.** D) RR cells derived from SupM2 were subjected with 10  $\mu$ M MYC inhibitor 10074-G5 for 0, 4, 6, 8, 24 hours, and then the SRR2 probe pull-down assay was performed. The Western blots in the right panel showed the input. E) Chromatin-immunoprecipitation-qPCR assay was employed to analyze the Sox2-SRR2 probe binding in RR cells derived from SupM2 after 10  $\mu$ M 10074-G5 treatment for 4 hours. F) RR cells originated from both cell lines were subjected with 10  $\mu$ M 10074-G5 for 8 hours, then qRT-PCR assay was performed to assess the mRNA levels of *MYC*, *CTNNB1* and *BCL9*. Statistical significance is denoted by \* ( $P < 0.05$ ) and \*\* ( $P < 0.01$ ). Results shown were representative of three independent experiments.

We found evidence that Sox2 alone is not sufficient to regulate Sox2-SRR2 binding and the SRR2 activity in RU cells. As shown in the left panel of **Figure 3.4G**, We transfected *SOX2-FLAG* in these two cell subsets derived from SupM2, and it is evident that Sox2 overexpression did not significantly increase SRR2 luciferase activity in RU cells; in contrast, the same experimental manipulation led to a significant increase in the reporter activity in RR cells. Accordingly, Sox2-flag overexpression did not appreciably increase Sox2-SRR2 binding in RU cells, but a substantial increase of Sox2-SRR2 binding was observed in RR cells (**Figure 3.4H**).

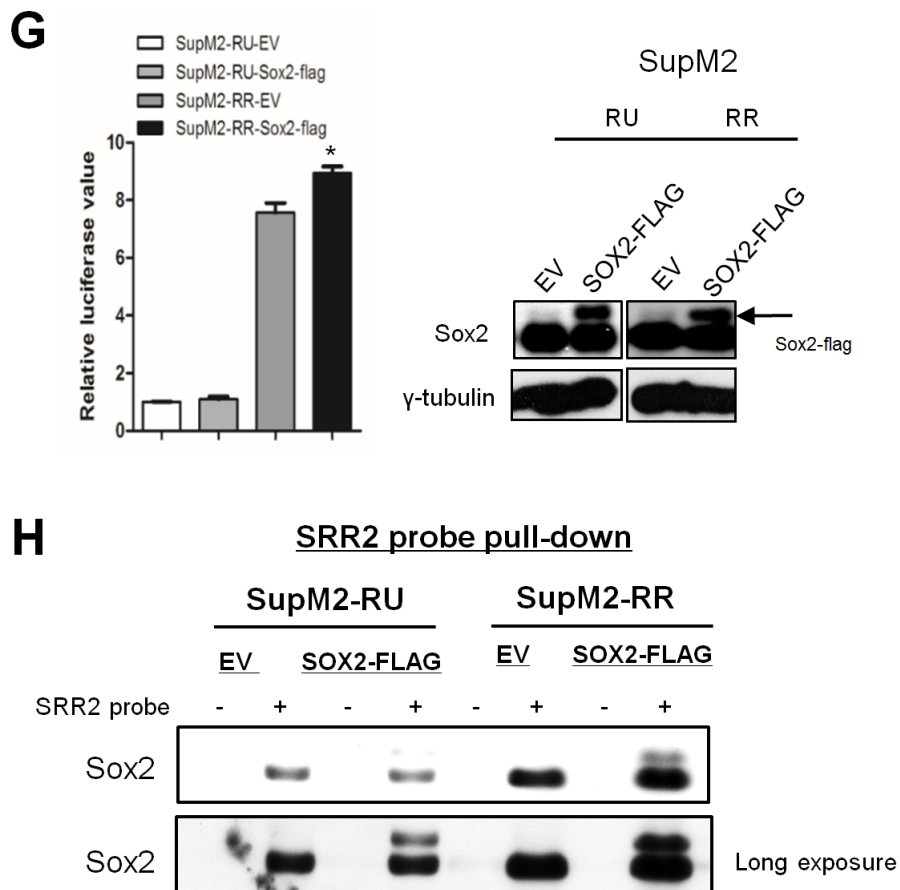


**Figure 3.4G-H** G) The SRR2 luciferase activity in RU and RR cells originated from SupM2 with EV or pcDNA-*SOX2-FLAG* (*i.e.* *SOX2-FLAG*) transfection at 48 hours. The Western blots showed the transfection efficiency of *SOX2-FLAG*. H) The Sox2-SRR2

binding ability in RU and RR cells originated from SupM2 with EV or *SOX2-FLAG* transfection at 48 hours. Statistical significance is denoted by \* ( $P<0.05$ ) and \*\* ( $P<0.01$ ).

### **3.3.3 The high level of MYC in RR cells is attributed to the Wnt/ $\beta$ -catenin pathway**

To explain why MYC is preferentially expressed at a high level in RR cells, We first evaluated the activation status of NPM-ALK/STAT3 axis between these two cell subsets. Consistent with the Lai lab's previous studies (9), the expression and activation levels of NPM-ALK and STAT3 were similar between RU and RR cells (**Figure 3.5A**). Pharmacologic inhibition of NPM-ALK (crizotinib) or STAT3 (stattic) dramatically decreased the expression of both Sox2 and MYC in RU and RR cells equally well, and these findings correlated with a reduction of the SRR2 luciferase activity by ~50-70% in both cell subsets (**Figure 3.5B-C**). Based on these findings, it is evident that, while the NPM-ALK/STAT3 axis contributes to a basal expression level of MYC, it does not explain the differential MYC expression between RU and RR cells.

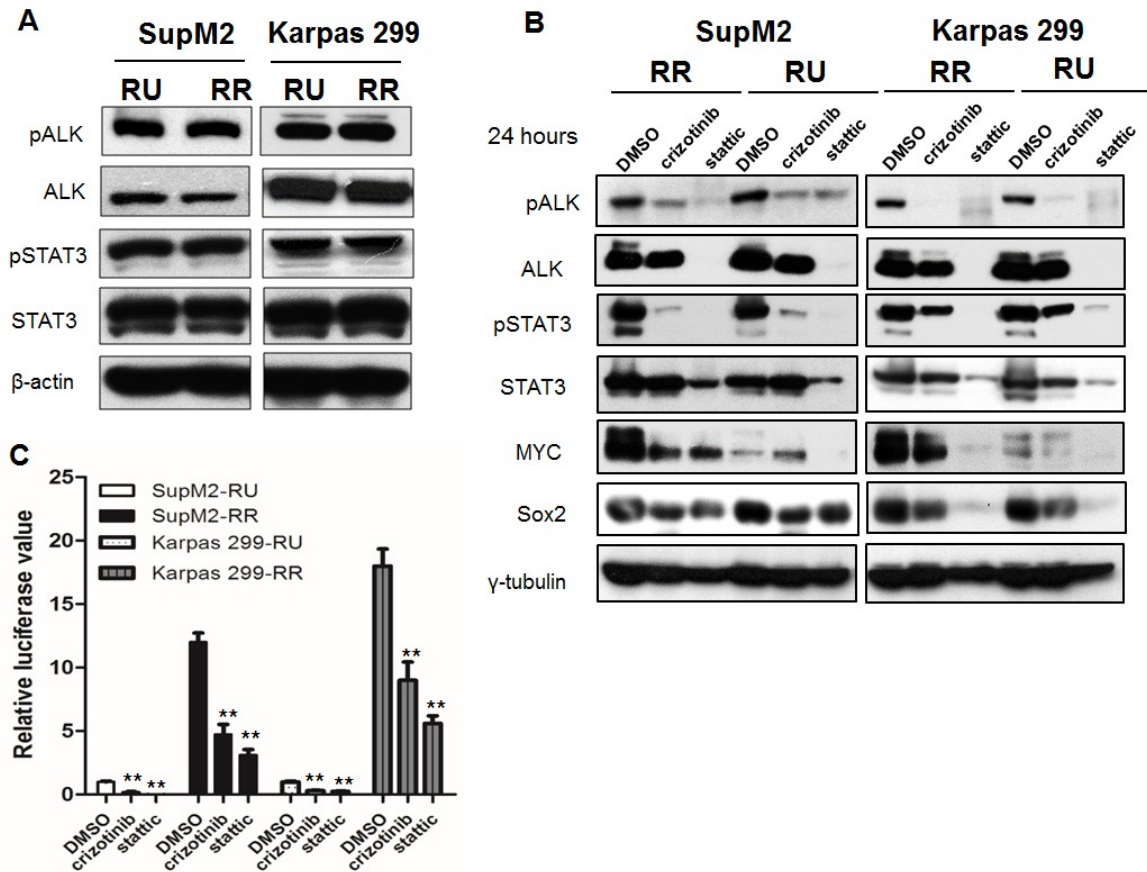


**Figure 3.5 NPM-ALK/STAT3 is not differentially activated or expressed between RU and RR cells.** A) The protein levels of pALK, ALK, pSTAT3, and STAT3 in RU and RR cells derived from SupM2 and Karpas 299. B-C) RR and RU cells were treated with either DMSO, or 100 nM ALK inhibitor crizotinib, or 10 nM STAT3 inhibitor stattic for 24 hours. The Western blots were employed to assess the expression/activation levels of NPM-ALK, STAT3, MYC and Sox2 in both RU and RR cells. The SRR2 luciferase activity in RU and RR cells was also evaluated by the luciferase assay. Statistical significance is denoted by \* ( $P < 0.05$ ) and \*\* ( $P < 0.01$ ). Results shown were representative of three independent experiments.

We then asked if the Wnt/ $\beta$ -catenin pathway is a contributing factor, as this pathway is known to upregulate MYC in other cancer cell types (14-16). Firstly, we performed the Wnt signaling pathway PCR array to compare RU and RR cells derived from SupM2.

Compared to RU cells, RR cells expressed higher levels (>1.4 fold) of gene expression in 24 of the 87 targets included in the array (**Figure 3.6**). We then employed quantitative RT-PCR and confirmed 5 of the 24 targets being significantly different between RU and RR cells. Other than *MYC*, 4 targets (*WNT2B*, *CTNNB1*, *LEF1* and *BCL9*) are known to be directly related to the Wnt/ $\beta$ -catenin pathway (**Figure 3.7A**). Western blot studies showed that RR cells expressed a substantially higher level of the active form of  $\beta$ -catenin (non-phosphorylated  $\beta$ -catenin), total  $\beta$ -catenin, phosphorylated GSK3 $\beta$ <sup>S9</sup> (*i.e.* pGSK3 $\beta$ <sup>S9</sup>) and LEF1 (**Figure 3.7B**), strongly suggesting that the Wnt/ $\beta$ -catenin pathway is indeed highly activated in RR cells but not RU cells.

To provide evidence that the Wnt/ $\beta$ -catenin pathway contributes to the differential *MYC* expression and SRR2 activity between RU and RR cells, we knocked down  $\beta$ -catenin using siRNA, and found that siRNA knockdown of  $\beta$ -catenin in RR cells led to a dramatic decrease in the *MYC* expression level and SRR2 luciferase activity (**Figure 3.7C**). Similar results were obtained when RR cells were subjected with quercetin, a  $\beta$ -catenin pharmacologic inhibitor (**Figure 3.7D**) (17). Importantly, enforced expression of *MYC* in RR cells abrogated the inhibitory effects of quercetin on SRR2 luciferase activity (**Figure 3.7E**).



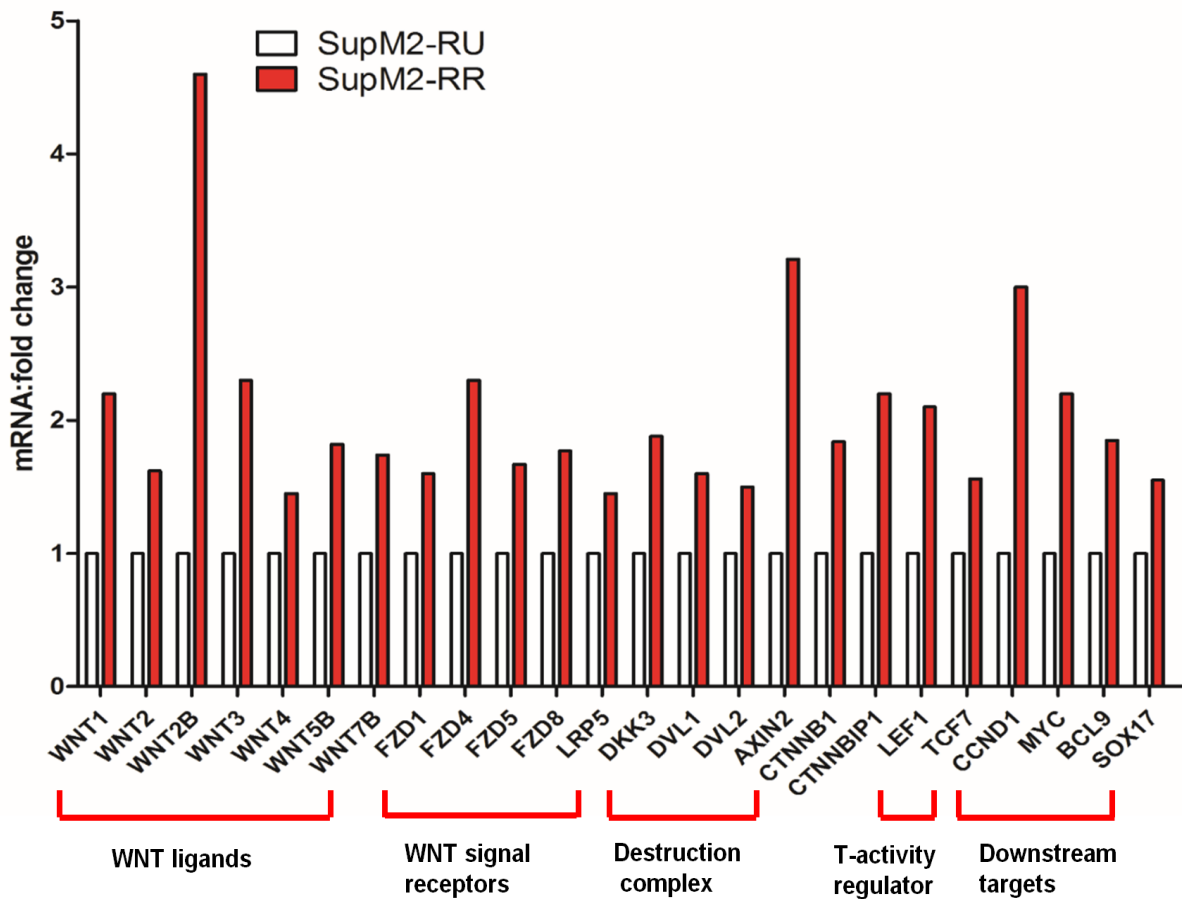


**Figure 3.6** The Wnt signaling is highly expressed in SupM2-RR cells in comparison to SupM2-RU cells. The Wnt pathway-specific oligonucleotide PCR array was performed in RU and RR cells derived from SupM2 cells. The data suggested 24 out of 87 genes related with the Wnt pathway were more highly expressed in mRNA level (>1.4 fold) in RR cells than in RU cells. One time experiment was performed.

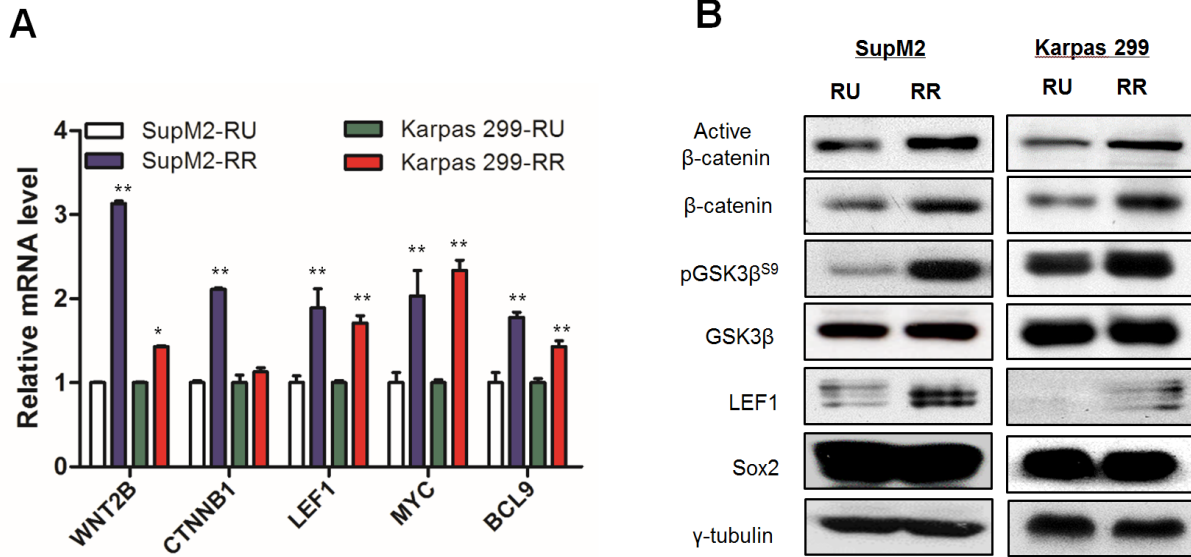


**Figure 3.7 The Wnt/ $\beta$ -catenin pathway contributes to the high MYC expression in RR cells.** A) The relative mRNA levels of *WNT2B*, *CTNNB1*, *LEF1*, *MYC* and *BCL9* in RU and RR cells derived from SupM2 and Karpas 299, assessed by qRT-PCR. B) The protein levels of active  $\beta$ -catenin,  $\beta$ -catenin, pGSK3 $\beta^{\text{S9}}$ , GSK3 $\beta$ , LEF1 and Sox2 in RU and RR cells. Statistical significance is denoted by \* ( $P < 0.05$ ) and \*\* ( $P < 0.01$ ). Results shown were representative of three independent experiments.

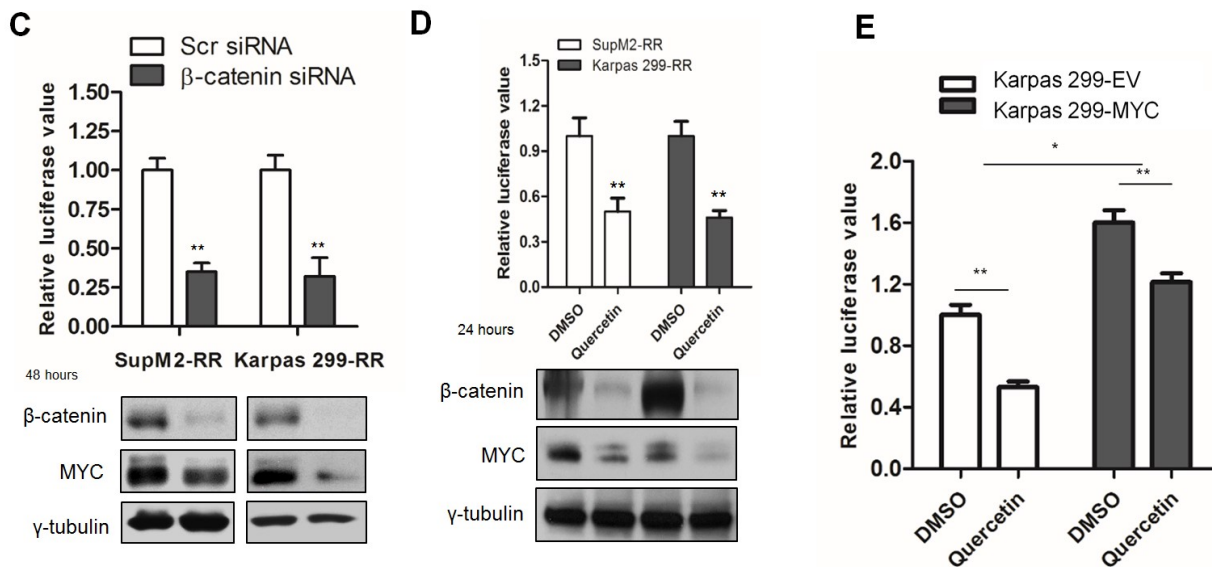


**Figure 3.7C-E** C) The SRR2 luciferase activity in RR cells with scr siRNA or  $\beta$ -catenin siRNA transfection at 48 hours. The Western blots below showed the knockdown efficiency of  $\beta$ -catenin and MYC. D) The SRR2 luciferase activity in RR cells treated with DMSO or 50  $\mu$ M quercetin, a pharmacological  $\beta$ -catenin inhibitor for 24 hours. The Western blots below showed the knockdown efficiency of  $\beta$ -catenin and MYC. E) The SRR2 luciferase activity in RR cells derived from Karpas 299 with EV or *c-MYC* transfection in the presence of 50  $\mu$ M quercetin for 24 hours; cells with DMSO treatment were included as a negative control. The SRR2 luciferase activity decreased by ~50% in RR cells from Karpas 299 with EV transfection upon quercetin treatment, whereas it only decreased by ~25% in cells with *c-MYC* transfection. The *MYC* transfection efficiency was validated in Figure 3.3C. Statistical significance is denoted by \* ( $P < 0.05$ ) and \*\* ( $P < 0.01$ ). Representative results from three independent experiments were shown.

Since RR cells expressed more ligands for the Wnt/ $\beta$ -catenin pathway (such as Wnt2B) than RU cells, we asked if soluble factors produced by RR cells can increase MYC expression and SRR2 activity in RU cells. To test this, we used the transwell co-culture system that is illustrated in **Figure 3.7F**. As shown in **Figure 3.7G**, we found that the SRR2 luciferase activity in RU cells was significantly increased after 72 hours of co-culture with RR cells. By Western blotting studies (**Figure 3.7H**), we confirmed that the Wnt/ $\beta$ -catenin pathway in RU cells was upregulated after 72 hours of co-culture with RR cells, as evidenced by the increased protein expressions of active  $\beta$ -catenin,  $\beta$ -catenin, and LEF1. Accordingly, MYC was also upregulated. However, we did not observe any significant changes of luciferase activity or MYC expression in RU cells when co-cultured with either diluted RR cells or parental SupM2 cells (**Figure 3.7I**).

To further support that the Wnt/ $\beta$ -catenin pathway can upregulate MYC and SRR2 activity in RU cells, we transfected RU cells derived from Karpas 299 with constitutively active *CTNNB1* (i.e. CA-*CTNNB1*), and found that the expression of MYC and SRR2 luciferase activity increased, coupled with the significantly increased clonogenicity (Figure 3.8A-C).

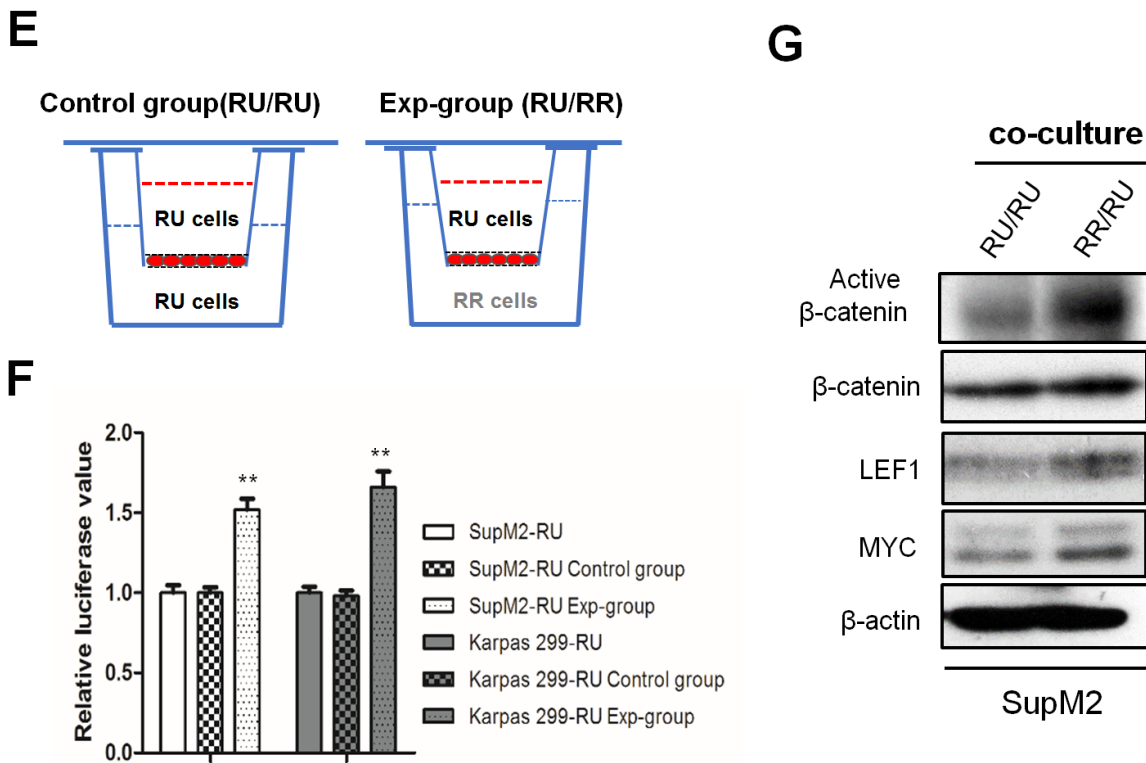


**Figure 3.7F-H** F) The diagram showed the design of transwell co-culture experiment. RU and RR cells were co-cultured for 72 hours in this experiment. G) The SRR2 luciferase activity in RU cells in the control group and the experimental group (Exp-group). H) The Western blots showed the protein levels of active  $\beta$ -catenin,  $\beta$ -catenin, LEF1 and MYC in RU cells derived from SupM2 in the control group and experimental group. Statistical significance is denoted by \* ( $P<0.05$ ) and \*\* ( $P<0.01$ ). Results from three independent experiments were shown.

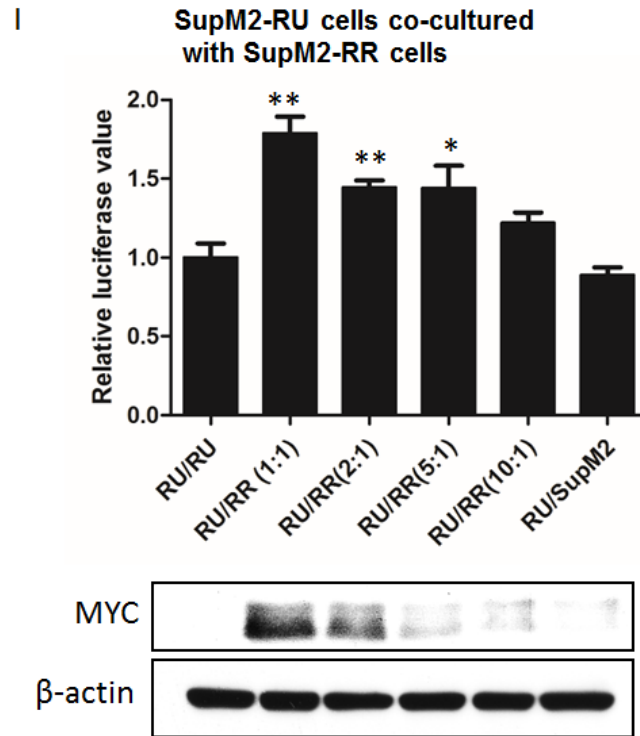


**Figure 3.7 I)** RU cells co-cultured with diluted (10:1) RR cells or parental SupM2 cells for 72 hours did not show significantly increased SRR2 luciferase activity or upregulated MYC expression. Statistical significance is denoted by \* ( $P < 0.05$ ) and \*\* ( $P < 0.01$ ). Results shown were from triplicate experiments.

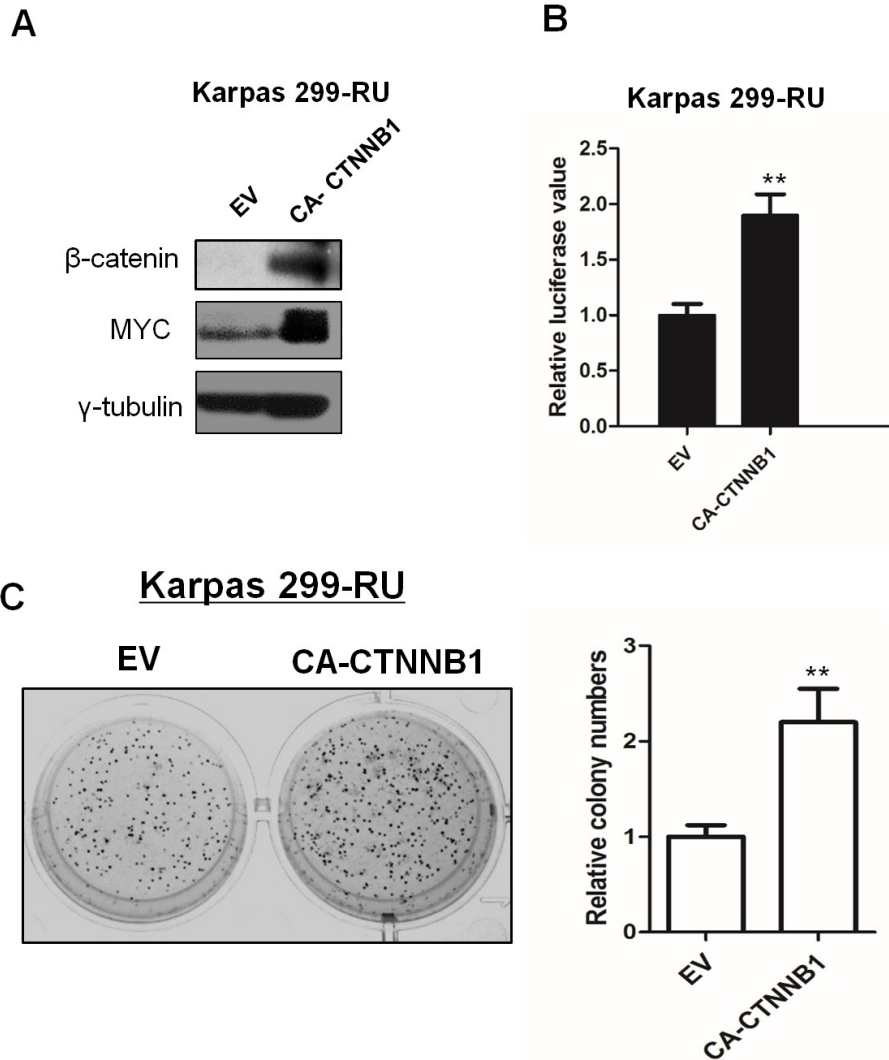


**Figure 3.8** RU cells transfected with the constitutively active *CTNNB1* (*CA-CTNNB1*) acquire the RR phenotype. A) The protein levels of  $\beta$ -catenin and MYC in RU cells derived from Karpas 299 with EV or *CA-CTNNB1* transfection at 48 hours. B). The SRR2 luciferase activity in RU cells derived from Karpas 299 with EV or *CA-CTNNB1* transfection at 48 hours. C) The clonogenicity of RU cells derived from Karpas 299 with EV or *CA-CTNNB1* transfection, assessed by the methylcellulose colony formation assay. The relative colony numbers analyzed in triplicate were shown in the right panel. The colony with more than 40 cells was counted. Statistical significance is denoted by \* ( $P < 0.05$ ) and \*\* ( $P < 0.01$ ). Results shown were representative of triplicate experiments.

### 3.3.4 The positive regulatory loop involving Sox2, Wnt/ $\beta$ -catenin and MYC in RR cells

In view of several recent publications reporting that Sox2 can activate the Wnt/ $\beta$ -catenin pathway in a number of cell types (10, 18, 19), we asked if Sox2 also can exert similar effects in ALK+ALCL. As shown in **Figure 3.9A**, siRNA knockdown of Sox2 in RR cells significantly decreased the transcript levels of *SOX2*, *WNT2B*, *CTNNB1*, *MYC* and *BCL9*. Furthermore, the protein levels of p-MYC<sup>S62</sup> and MYC were dramatically decreased in RR cells upon Sox2 siRNA knockdown (**Figure 3.9B**). Correlating with the fact that Sox2 is relatively transcriptionally quiescent in RU cells, the expressions of p-MYC<sup>S62</sup> and MYC in these cells did not change appreciably in response to Sox2 knockdown (**Figure 3.9B**). Taken together, these findings support the existence of a positive feedback loop involving Wnt/ $\beta$ -catenin, MYC and Sox2 in RR cells. In other words, in RR cells, the high level of MYC promotes the transcriptional activity of Sox2, which in turn activates the Wnt/ $\beta$ -catenin pathway and sustains a high level of MYC expression. By contrast, in RU cells, Sox2 does not effectively activate the Wnt/ $\beta$ -catenin pathway due to the relatively low level of MYC; in the absence of active Wnt/ $\beta$ -catenin pathway, MYC remains to be lowly expressed. A model summarizing this concept is illustrated in **Figure 3.9C**.

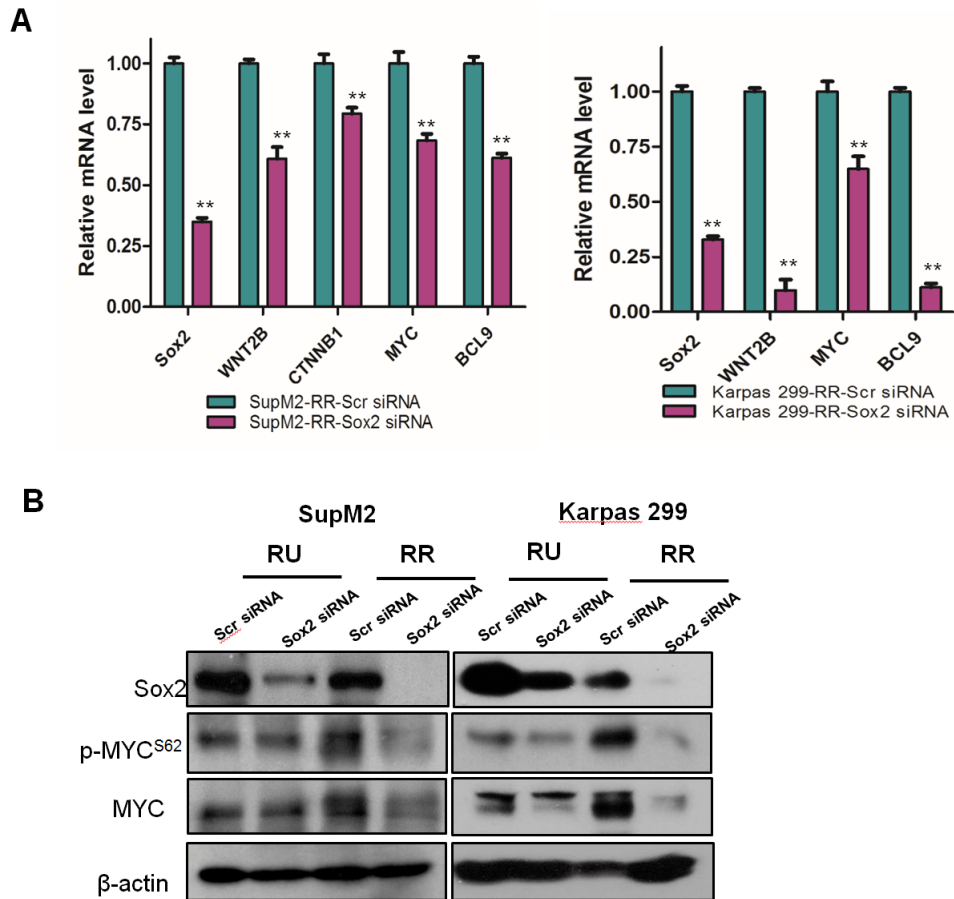


**Figure 3.9 The positive regulatory loop of Sox2–Wnt/β-catenin–MYC in RR cells.**

A) qRT-PCR assay was performed to analyze the relative mRNA levels of *WNT2B*, *CTNNB1*, *MYC* and *BCL9* in RR cells derived from SupM2 and Karpas 299 cells with scr siRNA or Sox2 siRNA transfection at 48 hours. B) The protein levels of Sox2, p-MYC<sup>S62</sup> and MYC in RR cells with scr siRNA or Sox2 siRNA transfection at 48 hours. Results shown are representative of three independent experiments.



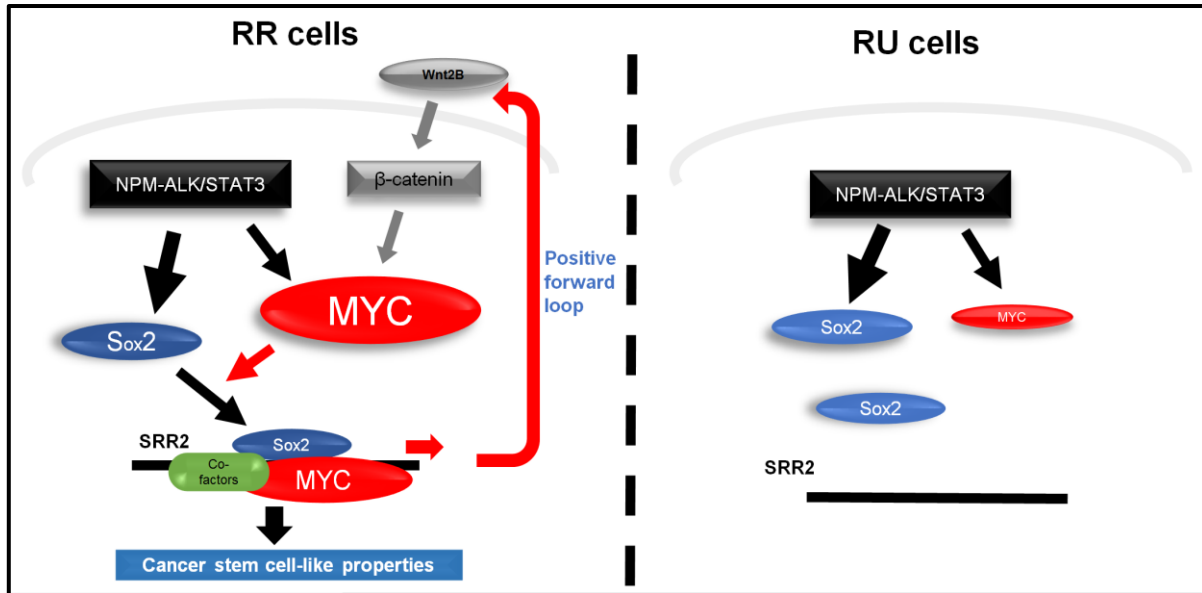


**Figure 3.9C** C) The hypothetical models of RR and RU cells. In RR cells, the highly active Wnt/ $\beta$ -catenin activity induces the high expression of MYC, which promotes the DNA binding and transcriptional activity of Sox2 in the presence of other co-factors. The transcriptionally active Sox2 in turn enhances the expression of Wnt/ $\beta$ -catenin pathway by upregulating the expression of *WNT2B* and *CTNNB1*, thereby forming a positive forward loop involving Wnt/ $\beta$ -catenin/MYC/Sox2. The expression level of NPM-ALK/STAT3 is almost identical between RR and RU cells, but NPM-ALK/STAT3 contributes to the basal expression of MYC and Sox2 in both RU and RR cells. In RU cells, because of the low level of MYC expression, Sox2 can neither efficiently bind to DNA nor transcriptionally regulate the expression of its downstream targets, such as *WNT2B* and *CTNNB1*. As Sox2 is not transcriptionally active, the expression level of Wnt/ $\beta$ -catenin remains low, resulting in the low level of MYC expression in RU cells.

### 3.3.5 MYC is heterogeneously expressed in primary tumor samples, and it co-localizes with active $\beta$ -catenin

Our results suggest that high levels of Wnt/ $\beta$ -catenin activation and MYC expression are the defining features of the RR phenotype. With this model, we examined the

expression of MYC and active  $\beta$ -catenin (as a surrogate marker of Wnt activation) using double immunofluorescence staining analyzed by using confocal microscopy. After evaluating tumor cells (10 random fields) derived from 3 cases, we found a highly significant correlation between the expression of MYC and active  $\beta$ -catenin ( $P < 0.0001$ ) (**Figure 3.10A** and the table below, 400X). We also performed immunohistochemistry to study MYC expression in 7 additional cases of formalin-fixed/paraffin-embedded ALK+ALCL tumors. As illustrated in **Figure 3.10B**, MYC is heterogeneously expressed in tumor cells and two representative fields from a case were shown here (400X). MYC expression was restricted to a small subset (~30%) of neoplastic cells; benign lymphocytes and fibroblasts were negative.

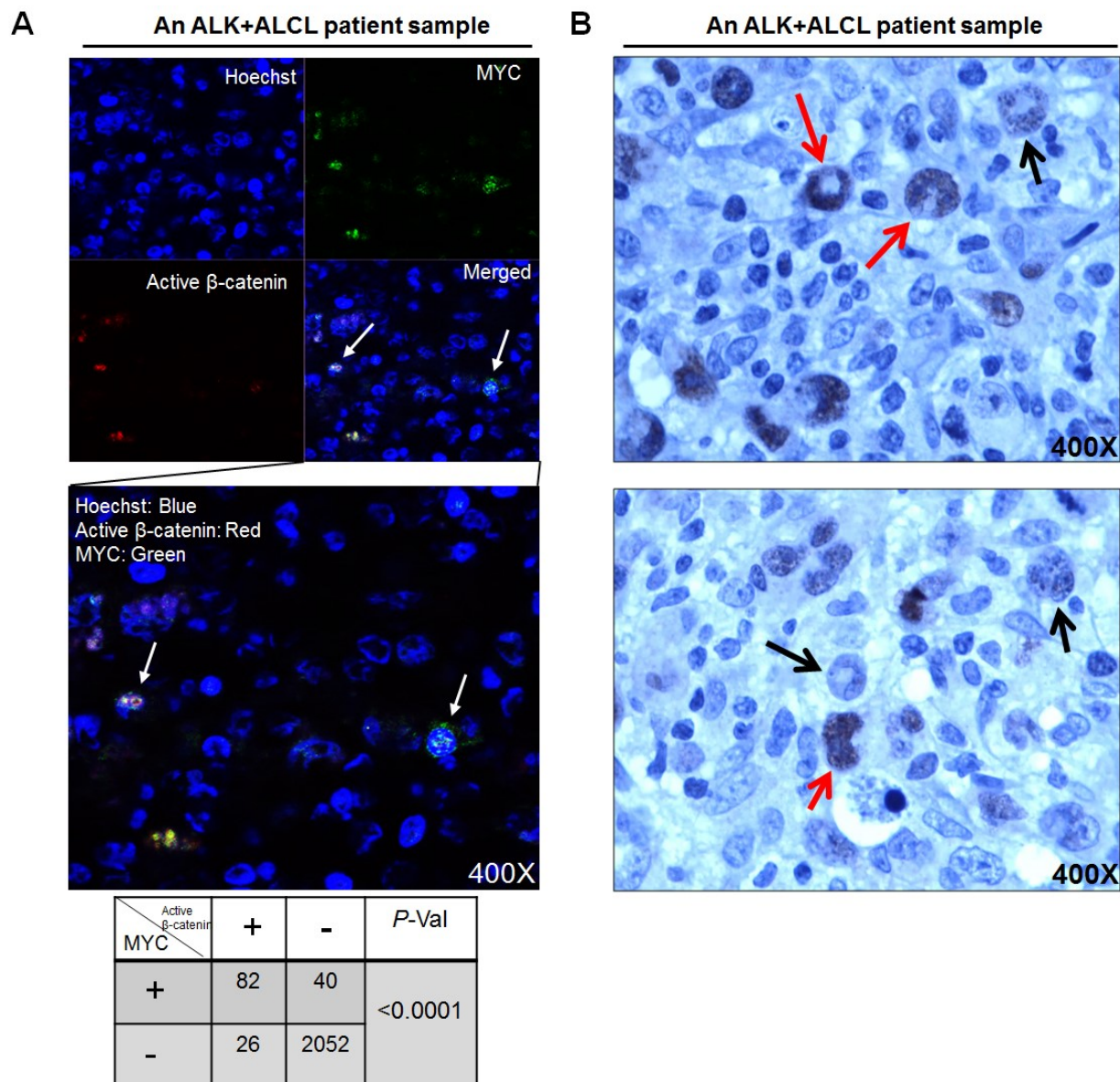


**Figure 3.10 MYC is heterogeneously expressed and its expression is co-localized with active  $\beta$ -catenin in ALK+ALCL tumor cells.** A)

Immunofluorescence assay was performed in 3 cases of primary tumors with MYC and active  $\beta$ -catenin double-staining, and the results showed MYC is significantly ( $p < 0.0001$ ) co-localized with active  $\beta$ -catenin in tumor cells (shown in the table). Ten random fields of the 3 cases were chosen under microscope, and one representative field (X400) was shown here. The correlation analysis was performed by Fisher's exact test. B) Two different fields of a case of ALK+ALCL primary tumor immunostained for MYC were shown. The above showed a focus with many lymphoma cells strongly positive for MYC

(red arrows). A lymphoma cell that was only dimly positive for MYC was also noted (black arrow). Scattered reactive small lymphocytes and benign fibroblasts in the background were negative. The below showed another focus in which lymphoma cells strongly positive for MYC being not as frequent. A good number of lymphoma cells negative or weakly positive for MYC were noted (black arrow, immunohistochemistry, 400X). Statistical significance is denoted by \* ( $P<0.05$ ) and \*\* ( $P<0.01$ ).

### **3.3.6 RU cells stably transfected with MYC are biochemically and phenotypically similar to RR cells**

Finally, to fully assess the biological roles of MYC in ALK+ALCL, we generated RU cell clones derived from SupM2 that were stably transfected with *MYC* (*i.e.* SupM2-RU-MYC). Compared to the negative control cells, SupM2-RU-MYC cells showed activation of the Wnt/ $\beta$ -catenin pathway, as evidenced by their elevated expression levels of active  $\beta$ -catenin, total  $\beta$ -catenin, pGSK3 $\beta$ <sup>S9</sup>, and LEF1 (**Figure 3.11A**). SupM2-RU-MYC cells also expressed higher mRNA levels of *MYC*, *WNT2B*, *CTNNB1* and *BCL9* that were comparable to those of SupM2-RR cells stably transfected with an empty vector (*i.e.* SupM2-RR-EV)(**Figure 3.11B**). We then performed mouse xenograft studies comparing the tumorigenicity of SupM2-RU-MYC cells with SupM2-RU-EV cells or SupM2-RR-EV cells. As shown in **Figure 3.11C-D**, SupM2-RU-MYC cells displayed a significantly higher tumorigenicity compared to SupM2-RU-EV cells, and exhibited comparable tumorigenicity to that of SupM2-RR-EV cells.

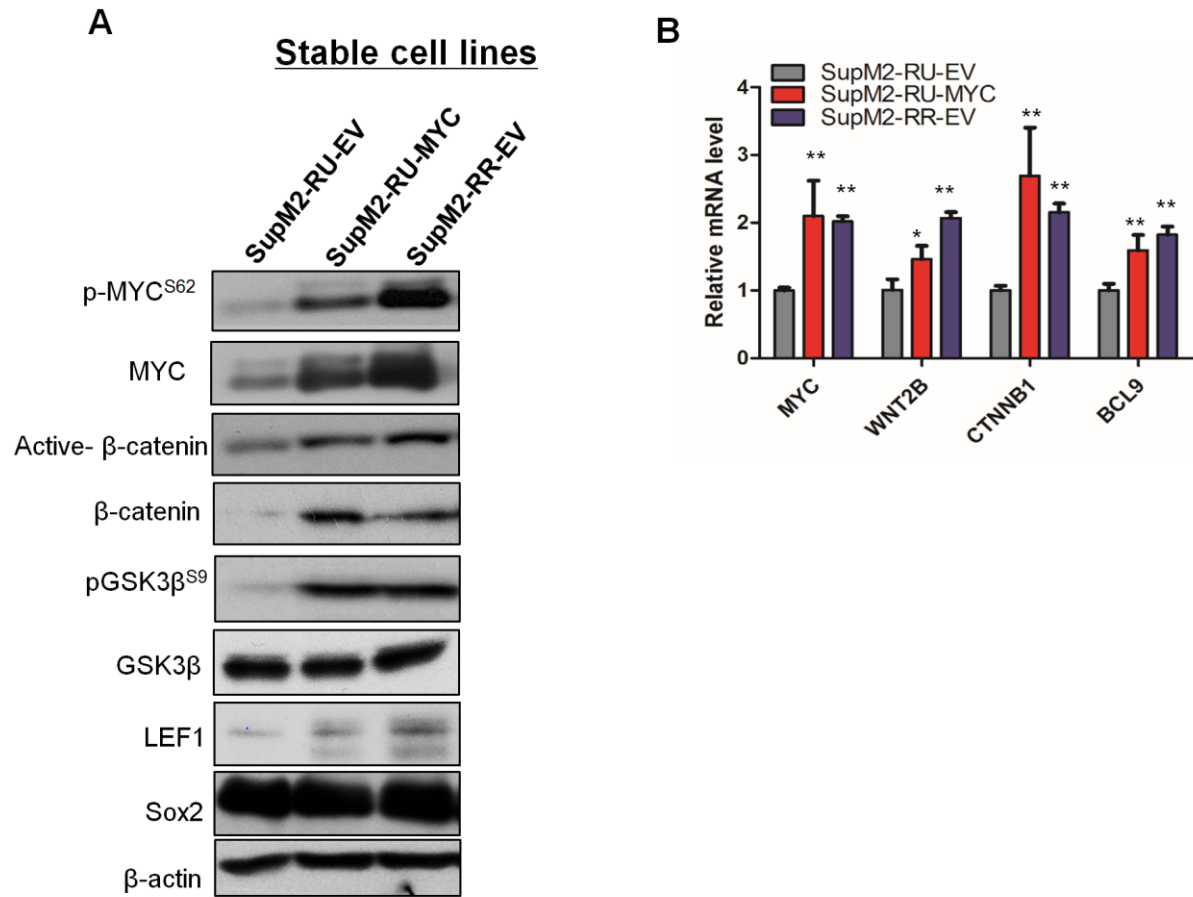


**Figure 3.11 RU cells stably transfected with *MYC* are biochemically and phenotypically similar with RR cells.** A) The protein levels of p-MYC<sup>S62</sup>, MYC, active β-catenin, β-catenin, pGSK3β<sup>S9</sup>, GSK3β, LEF1 and Sox2 in the stably transfected cell lines SupM2-RU-EV, SupM2-RU-MYC and SupM2-RR-EV. B) The relative mRNA levels of *MYC*, *WNT2B*, *CTNNB1* and *BCL9* in the three stable cell lines. Statistical significance is denoted by \* ( $P<0.05$ ) and \*\* ( $P<0.01$ ). One representative result of triplicate experiments was shown here.

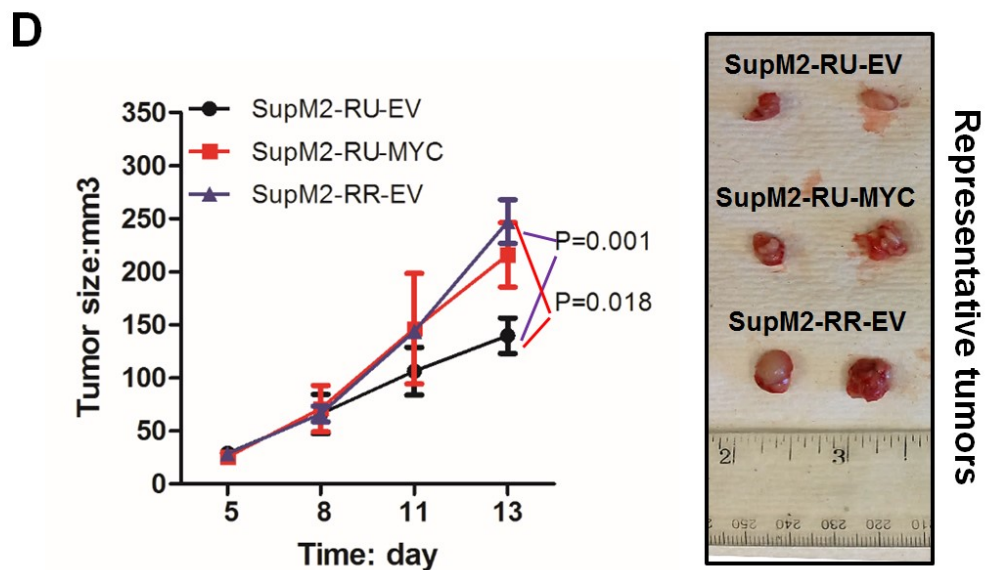
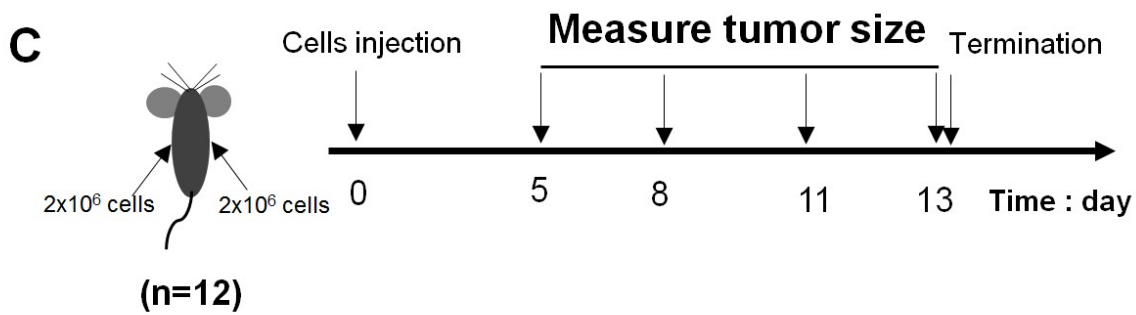


**Figure 3.11C-D** C) The diagram showed the design of mice xenograft study. D) The tumor growth rates of the three stable cell lines in the mouse xenograft study. The right panel showed the representative tumors from the three groups at the termination point. Statistical significance is denoted by \* ( $P < 0.05$ ) and \*\* ( $P < 0.01$ ).

### 3.3.7 Side population cells are not detectable in RU and RR cells and ABCG2 is not significantly differentially expressed in mRNA level between RU and RR cells.

We realized that Moti *et al* recently reported that side population cells are detectable in ALK+ALCL cell lines and patient samples using the Hoechst-efflux assay and the

authors of this study also provided evidence that these side population cells are tumor-propagating cells (3). Therefore, we tested whether side population cells can be also detected in ALK+ALCL cell lines in our hands, and if it is the case, whether RR cells have enriched side population cells in comparison to RU cells. However, we were unable to detect the side population cells in our hands, either in parental SupM2 and Karpas 299 cell lines or RU and RR cells derived from these two cell lines (**Figure 3.12A-B**). In the meanwhile, Moti *et al* declared that the gene expression level of ATP-binding cassette-G2 (ABCG2), a drug cell transporter (20), is higher in the side population cells as compared to the main cell population (3). We then asked whether ABCG2 is also highly expressed in RR cells as compared to RU cells. To this end, we performed quantitative RT-PCR to detect the mRNA level of ABCG2 and also included some other ABC family transporters, including ABCC1, ABCC2, ABCC3, ABCC4, ABCC5, and ABCC6. As shown in **Figure 3.12C**, except ABCC4, all other ABC transporters were not significantly differentially expressed in mRNA level between RU and RR cells derived from SupM2.

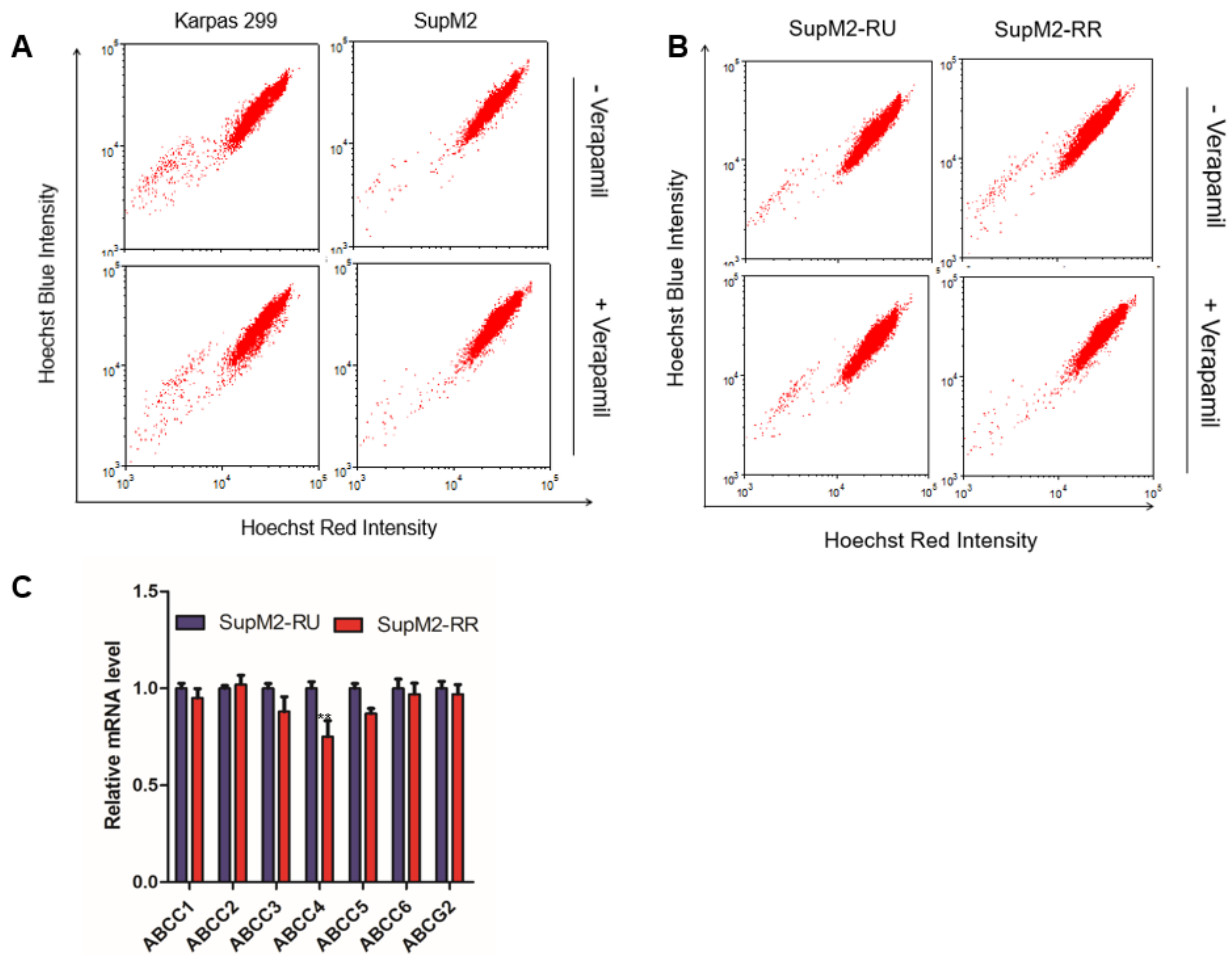


**Figure 3.12 Identification of side population cells by Hoechst-efflux assay and the expression of ABC transporters in RU and RR cells derived from ALK+ALCL.** A-B) Side population cells were not observed in parental Karpas 299 and SupM2 cells in our hands, as well as in RU and RR cells derived from parental SupM2 cells. C) qRT-PCR assay was employed to compare the relative mRNA levels of ABC transporters, including ABCC1, ABCC2, ABCC3, ABCC4, ABCC5, ABCC6 and ABCG2, between RU and RR cells derived from SupM2 cells. Statistical significance is denoted by \* ( $P<0.05$ ) and \*\* ( $P<0.01$ ). Results shown are representative of three independent experiments.



### 3.4 Discussion

The existence of the RU/RR dichotomy in ALK+ALCL is supported by the Lai lab's previously published results (9) as well as data from the current study. Similar RU/RR dichotomy also can be observed in other cancer types, including estrogen receptor-positive breast cancer (21), triple negative breast cancer (22) and esophageal squamous cell carcinoma (23). Importantly, in all of these cancer models, RR cells have been found to be consistently more tumorigenic and stem-like than RU cells. Thus, we believe that the RU/RR dichotomy is a rather universal phenomenon in cancers and an in-depth understanding of the regulation of this phenotypic dichotomy is warranted. It is perceivable that this new knowledge will shed light into the biology and biochemical basis of cancer stemness, and carry significant clinical and therapeutic implications. With this background, we set out to delineate the mechanisms regulating the RU/RR dichotomy using ALK+ALCL as the study model.

One of the key findings of this study is that MYC, a protein which has been strongly implicated in cancer stemness and induced pluripotent stem cells (24-27), appears to be the key regulator of the RU/RR dichotomy in ALK+ALCL. This conclusion is supported by the observation that RR cells express substantially more MYC protein than RU cells, and the finding that experimental manipulation of MYC expression in RU and RR cells can result in significant changes in their SRR2 reporter activity and the associated biological phenotype. Furthermore, we found evidence that the regulatory function of MYC is related to its ability to influence the DNA binding and transcriptional activity of Sox2. This model explains why RU and RR cells have dramatically different

SRR2 activity despite their approximately equal Sox2 protein expression level and nuclear localization. As illustrated in **Figure 3.9C**, a relatively high level of MYC, perhaps exceeding a specific threshold, permits the binding of Sox2 to SRR2 and its execution as a transcription factor. To our knowledge, this is the first report describing this novel relationship between MYC and Sox2 in cancer cells. Exactly how a high level of MYC promotes the DNA binding of Sox2 is unknown. The previously published observation (28) that the target genes of MYC substantially overlap with those of Sox2 suggests that MYC or the MYC protein complex may physically direct Sox2 to the gene promoters, and facilitate its DNA binding. This concept is supported by the previously published data that MYC and Sox2 were found co-localized in a protein complex (29). Furthermore, MYC has been recently reported to regulate gene expression as a general transcriptional amplifier (30, 31). Another possibility is that the some of the proteins present in the MYC protein complex are kinases or methyltransferases, which mediate post-translational modifications of Sox2. The formation of this protein complex is in turn dependent on the MYC protein level. Regarding this possibility, phosphorylation or methylation has been shown positively or negatively regulates the Sox2 transcriptional activity in embryonic stem cells (32, 33).

MYC has been found to be aberrantly expressed in many different types of cancer(34). In cancer cells, MYC is known to contribute to cancer stemness, including the tumor-initiating ability (27, 35, 36), chemoresistance (37, 38) and self-renewal (25). For instance, in a mouse model of T-cell acute lymphoblastic leukemia, inhibition of MYC was found to prevent leukemia initiation (36). Moreover, the expression level of MYC

was found to be relatively high in CSCs derived from several cancer types when compared to bulk cell populations (25, 34, 39-41). A recent study also has highlighted that the CSCs from glioma are more sensitive than the bulk tumor cells to cell death induced by MYC inhibition (25). This observation correlates well with our finding that RR cells derived from ALK+ALCL are more sensitive to cell growth inhibition induced by MYC inhibition, as compared to RU cells. How exactly MYC mediates these biological effects is not completely understood, but it is believed that MYC can regulate as many as ~15% of human genes that are involved in critical cellular processes including chromatin remodeling, cell-cycle control, metabolism and self-renewal (34, 42). Importantly, it has been found that MYC can bind to and regulate SOX2 gene expression in CSCs derived from triple-negative breast cancer, suggesting MYC can regulate cancer stemness by modulating the expression of other critical embryonic stem cell markers such as Sox2 (43). With this context, we believe that findings of this current study has advanced by our understanding of how MYC promotes stemness, namely by enhancing Sox2/DNA binding and Sox2 transcriptional activity.

The role of MYC in ALK+ALCL has not been extensively studied, and we are aware of only two studies that directly examined the biological significance of MYC in these tumors. In a very recent study, shRNA knockdown of MYC was found to reduce the growth of ALK+ALCL cells *in vitro*, although the underlying mechanism was not delineated (44). Consistent with this observation, we also found that pharmacologic inhibition of MYC can significantly inhibit the growth in ALK+ALCL cells. Importantly, we found that RR cells were found to be more sensitive to MYC inhibition than RU cells,

consistent with our model that MYC carries more biological importance in RR cells. The second study published in 2002 described that MYC in ALK+ALCL can be upregulated by NPM-ALK (45), but the biological significance of this observation was not assessed. Correlating with this finding, we also found that NPM-ALK upregulates MYC. However, while the NPM-ALK/STAT3 signaling axis contributes to the expression of MYC in both RU and RR cells, this pathway is not responsible for the differential MYC expression between these two cell subsets. In other words, the NPM-ALK/STAT3 signaling axis is not a key determinant of the RU/RR dichotomy. Overall, we believe that our generated data has further defined the pathogenetic role of MYC in ALK+ALCL.

As we found that the NPM-ALK/STAT3 signaling pathway is not the key contributing factor to the differential expression of MYC, we turned to the Wnt/ $\beta$ -catenin pathway, which has been well documented to upregulate MYC in a variety of human cancers (14, 15, 46). Constitutive activation of the Wnt/ $\beta$ -catenin pathway can be found in CSCs found in various tumor types (47-50). Inhibition of the Wnt/ $\beta$ -catenin pathway has been shown to decrease stemness and tumorigenic potential in cancer cells (46, 49, 51), and there is evidence that MYC is a mediator of the stemness properties conferred by the Wnt/ $\beta$ -catenin pathway (52, 53). A recent study suggested that MYC acts as the ultimate downstream effector of  $\beta$ -catenin to enhance proliferative capacity of basal stem cells, thus results in their amplification and tumorigenesis (52). Our model is in line with these observations, although my model highlights the importance of intra-tumoral heterogeneity and suggests that a high activation level of the Wnt/ $\beta$ -catenin pathway is a characteristic of RR cells (i.e. stem-like cells). While this concept has been

brought up in a previously published paper (48), our data has provided the mechanistic explanation as to how the Wnt/ $\beta$ -catenin pathway promotes stemness for the first time. Specifically, a high level of Wnt/ $\beta$ -catenin activity promotes a relatively high level of MYC expression, which permits Sox2 to exert its transcriptional activity. Furthermore, based on our observations that Sox2 upregulates a number of the Wnt/ $\beta$ -catenin pathway ligands as well as  $\beta$ -catenin, we have demonstrated, for the first time, a positive feedback loop involving Wnt/ $\beta$ -catenin, MYC and Sox2, and my hypothetical model has been illustrated in **Figure 3.9C**. Our data supports a model in which this positive feedback loop is the defining feature of RR cells in ALK+ALCL.

Our results have provided further support for the concept of tumor plasticity, since RU cells can be converted to RR cells by manipulating the Wnt/ $\beta$ -catenin/ MYC axis. Tumor plasticity also has been illustrated by a recent study in which non-stem cells from lung cancer were converted to CSCs when the Wnt/ $\beta$ -catenin pathway is activated by hepatocyte growth factor (48). The Lai lab also recently published that RU cells derived from esophageal squamous cell carcinoma (23) and estrogen receptor-positive breast cancer cell lines, as well as primary breast tumors cells (54), can convert to RR cells upon oxidative stress. Findings from the current study has highlighted the importance of the Wnt/ $\beta$ -catenin/ MYC axis in the context of tumor plasticity.

Results from our immunofluorescence staining/confocal microscopy have provided further evidence to support the existence of the positive feedback loop involving Wnt/ $\beta$ -

catenin in a small cell subset of ALK+ALCL. Thus, MYC significantly co-localizes with active  $\beta$ -catenin in approximately 4% of cells. Interestingly, we found that cells co-expressing these two markers were scattered throughout the tumors, with no good evidence of clustering. This is a rather unexpected observation, since CSCs identified by using immunohistochemistry or immunofluorescence staining published in a very small number of studies have been shown to cluster (*i.e.* approximately 10 cells per cluster) (48, 55-57). Based on these observations, it has been speculated that CSCs thrive in specific microenvironment or 'niche'. In view of the relatively small number of studies of the *in-situ* localization of CSCs, we believe that one cannot come to any specific generalization. Nonetheless, it may be speculated that CSCs in hematologic neoplasms (such as ALK+ALCL) may have different biological behaviors from those in solid tumors, which were the study subjects of most publications reporting the *in-situ* localization of CSCs. Regarding our immunohistochemical studies, we would like to point out that, while we found only ~30% of tumor cells being labeled with MYC, two previous publications showed that MYC immunohistochemical reactivity is detectable in the majority of tumor cells in ALK+ALCL(44, 45). This discrepancy may be due to the use of different MYC antibodies and/or immunostaining protocols. In our experience, a substantially higher number of MYC-positive cells can be obtained if higher concentration of anti-MYC antibody is used. The concentration of anti-MYC antibody we chose was based on the observation that this antibody concentration is optimal in revealing the intra-tumoral heterogeneity of MYC expression.

In light of a recent publication that a tumor-propagating population can be identified and isolated in ALK+ALCL cell lines and tumors using the hoechst-efflux assay (3), we asked if RR cells identified using our study model are enriched in the tumor-propagating population identified using the hoechst-efflux assay. In our hands, we were unable to identify this small cell population in Karpas 299 and SupM2 cells, including RU and RR cells derived from SupM2 (**Figure 3.12A-B**), despite our attempt to follow the experimental protocol described in the publication (3). This discrepancy may be attributed to various technical reasons and/or biological differences between ALK+ALCL cell clones. As the expression level of NPM-ALK and ABCG2 were reported to be expressed at a higher level in the tumor-propagating population (3), we asked if RR cells also carry these characteristics, while we found that RR and RU cells did not differ in the expression of the NPM-ALK or ABCG2 in mRNA level (**Figure 3.5A and Figure 3.12C**). Some other ABC family transporters, such as ABCC1 and ABCC2, were also not significantly different in mRNA level between RU and RR cells (**Figure 3.12C**).

To conclude, we report that MYC is the key regulator of the RU/RR dichotomy in ALK+ALCL. High level of MYC promotes the DNA binding ability and transcriptional activity of Sox2. Our study has highlighted the importance of the Wnt/ $\beta$ -catenin pathway in contributing to the high MYC protein expression in RR cells. The existence of a positive feedback loop involving the Wnt/ $\beta$ -catenin/MYC/Sox2 axis defines a small cell subset in ALK+ALCL that are characterized by high tumorigenicity and chemoresistance.

### 3.5 References

1. Kinney MC, Higgins RA, Medina EA. Anaplastic large cell lymphoma: twenty-five years of discovery. *Archives of pathology & laboratory medicine*. 2011;135(1):19-43.
2. Amin HM, Lai R. Pathobiology of ALK+ anaplastic large-cell lymphoma. *Blood*. 2007;110(7):2259-67.
3. Moti N, Malcolm T, Hamoudi R, Mian S, Garland G, Hook CE, et al. Anaplastic large cell lymphoma-propagating cells are detectable by side population analysis and possess an expression profile reflective of a primitive origin. *Oncogene*. 2015;34(14):1843-52.
4. Marusyk A, Almendro V, Polyak K. Intra-tumour heterogeneity: a looking glass for cancer? *Nature reviews Cancer*. 2012;12(5):323-34.
5. Wernig M, Meissner A, Foreman R, Brambrink T, Ku M, Hochedlinger K, et al. In vitro reprogramming of fibroblasts into a pluripotent ES-cell-like state. *Nature*. 2007;448(7151):318-24.
6. Chen Y, Shi L, Zhang L, Li R, Liang J, Yu W, et al. The molecular mechanism governing the oncogenic potential of SOX2 in breast cancer. *The Journal of biological chemistry*. 2008;283(26):17969-78.
7. Leis O, Eguiara A, Lopez-Arribillaga E, Alberdi MJ, Hernandez-Garcia S, Elorriaga K, et al. Sox2 expression in breast tumours and activation in breast cancer stem cells. *Oncogene*. 2012;31(11):1354-65.
8. Santini R, Pietrobono S, Pandolfi S, Montagnani V, D'Amico M, Penachioni JY, et al. SOX2 regulates self-renewal and tumorigenicity of human melanoma-initiating cells. *Oncogene*. 2014;33(38):4697-708.



9. Gelebart P, Hegazy SA, Wang P, Bone KM, Anand M, Sharon D, et al. Aberrant expression and biological significance of Sox2, an embryonic stem cell transcriptional factor, in ALK-positive anaplastic large cell lymphoma. *Blood Cancer J.* 2012;2:e82.
10. Piva M, Domenici G, Iriando O, Rabano M, Simoes BM, Comaills V, et al. Sox2 promotes tamoxifen resistance in breast cancer cells. *EMBO molecular medicine.* 2014;6(1):66-79.
11. Wu C, Molavi O, Zhang H, Gupta N, Alshareef A, Bone KM, et al. STAT1 is phosphorylated and downregulated by the oncogenic tyrosine kinase NPM-ALK in ALK-positive anaplastic large-cell lymphoma. *Blood.* 2015;126(3):336-45.
12. Marampon F, Ciccarelli C, Zani BM. Down-regulation of c-Myc following MEK/ERK inhibition halts the expression of malignant phenotype in rhabdomyosarcoma and in non muscle-derived human tumors. *Molecular cancer.* 2006;5:31.
13. Wang H, Chauhan J, Hu A, Pendleton K, Yap JL, Sabato PE, et al. Disruption of Myc-Max heterodimerization with improved cell-penetrating analogs of the small molecule 10074-G5. *Oncotarget.* 2013;4(6):936-47.
14. Juan J, Muraguchi T, Iezza G, Sears RC, McMahon M. Diminished WNT -> beta-catenin -> c-MYC signaling is a barrier for malignant progression of BRAFV600E-induced lung tumors. *Genes & development.* 2014;28(6):561-75.
15. Zhang S, Li Y, Wu Y, Shi K, Bing L, Hao J. Wnt/beta-catenin signaling pathway upregulates c-Myc expression to promote cell proliferation of P19 teratocarcinoma cells. *Anatomical record.* 2012;295(12):2104-13.
16. You Z, Saims D, Chen S, Zhang Z, Guttridge DC, Guan KL, et al. Wnt signaling promotes oncogenic transformation by inhibiting c-Myc-induced apoptosis. *The Journal of cell biology.* 2002;157(3):429-40.

17. Gelebart P, Anand M, Armanious H, Peters AC, Dien Bard J, Amin HM, et al. Constitutive activation of the Wnt canonical pathway in mantle cell lymphoma. *Blood*. 2008;112(13):5171-9.
18. Li X, Xu Y, Chen Y, Chen S, Jia X, Sun T, et al. SOX2 promotes tumor metastasis by stimulating epithelial-to-mesenchymal transition via regulation of WNT/beta-catenin signal network. *Cancer letters*. 2013;336(2):379-89.
19. Chen S, Xu Y, Chen Y, Li X, Mou W, Wang L, et al. SOX2 gene regulates the transcriptional network of oncogenes and affects tumorigenesis of human lung cancer cells. *PloS one*. 2012;7(5):e36326.
20. Dean M. ABC transporters, drug resistance, and cancer stem cells. *J Mammary Gland Biol Neoplasia*. 2009;14(1):3-9.
21. Wu F, Zhang J, Wang P, Ye X, Jung K, Bone KM, et al. Identification of two novel phenotypically distinct breast cancer cell subsets based on Sox2 transcription activity. *Cellular signalling*. 2012;24(11):1989-98.
22. Jung K, Gupta N, Wang P, Lewis JT, Gopal K, Wu F, et al. Triple negative breast cancers comprise a highly tumorigenic cell subpopulation detectable by its high responsiveness to a Sox2 regulatory region 2 (SRR2) reporter. *Oncotarget*. 2015;6(12):10366-73.
23. Zhang HF, Wu C, Alshareef A, Gupta N, Zhao Q, Xu XE, et al. The PI3K/AKT/c-MYC axis promotes the acquisition of cancer stem-like features in esophageal squamous cell carcinoma. *Stem cells*. 2016.
24. Wilson A, Murphy MJ, Oskarsson T, Kaloulis K, Bettess MD, Oser GM, et al. c-Myc controls the balance between hematopoietic stem cell self-renewal and differentiation. *Genes & development*. 2004;18(22):2747-63.

25. Morrissey PA, Quinn PB, Sheehy PJ. Newer aspects of micronutrients in chronic disease: vitamin E. *The Proceedings of the Nutrition Society*. 1994;53(3):571-82.
26. Satoh Y, Matsumura I, Tanaka H, Ezoe S, Sugahara H, Mizuki M, et al. Roles for c-Myc in self-renewal of hematopoietic stem cells. *The Journal of biological chemistry*. 2004;279(24):24986-93.
27. Gabay M, Li Y, Felsher DW. MYC activation is a hallmark of cancer initiation and maintenance. *Cold Spring Harbor perspectives in medicine*. 2014;4(6).
28. Kwan KY, Shen J, Corey DP. C-MYC transcriptionally amplifies SOX2 target genes to regulate self-renewal in multipotent otic progenitor cells. *Stem cell reports*. 2015;4(1):47-60.
29. Yang Z, Augustin J, Hu J, Jiang H. Physical Interactions and Functional Coordination between the Core Subunits of Set1/Mll Complexes and the Reprogramming Factors. *PloS one*. 2015;10(12):e0145336.
30. Nie Z, Hu G, Wei G, Cui K, Yamane A, Resch W, et al. c-Myc is a universal amplifier of expressed genes in lymphocytes and embryonic stem cells. *Cell*. 2012;151(1):68-79.
31. Lin CY, Loven J, Rahl PB, Paranal RM, Burge CB, Bradner JE, et al. Transcriptional amplification in tumor cells with elevated c-Myc. *Cell*. 2012;151(1):56-67.
32. Fang L, Zhang L, Wei W, Jin X, Wang P, Tong Y, et al. A methylation-phosphorylation switch determines Sox2 stability and function in ESC maintenance or differentiation. *Molecular cell*. 2014;55(4):537-51.
33. Jeong CH, Cho YY, Kim MO, Kim SH, Cho EJ, Lee SY, et al. Phosphorylation of Sox2 cooperates in reprogramming to pluripotent stem cells. *Stem cells*. 2010;28(12):2141-50.

34. Dang CV. MYC on the path to cancer. *Cell*. 2012;149(1):22-35.
35. Pan XN, Chen JJ, Wang LX, Xiao RZ, Liu LL, Fang ZG, et al. Inhibition of c-Myc overcomes cytotoxic drug resistance in acute myeloid leukemia cells by promoting differentiation. *PloS one*. 2014;9(8):e105381.
36. Roderick JE, Tesell J, Shultz LD, Brehm MA, Greiner DL, Harris MH, et al. c-Myc inhibition prevents leukemia initiation in mice and impairs the growth of relapsed and induction failure pediatric T-ALL cells. *Blood*. 2014;123(7):1040-50.
37. Shen A, Wang L, Huang M, Sun J, Chen Y, Shen YY, et al. c-Myc alterations confer therapeutic response and acquired resistance to c-Met inhibitors in MET-addicted cancers. *Cancer research*. 2015;75(21):4548-59.
38. Zhang Y, Chen HX, Zhou SY, Wang SX, Zheng K, Xu DD, et al. Sp1 and c-Myc modulate drug resistance of leukemia stem cells by regulating survivin expression through the ERK-MSK MAPK signaling pathway. *Molecular cancer*. 2015;14:56.
39. Salcido CD, Larochelle A, Taylor BJ, Dunbar CE, Varticovski L. Molecular characterisation of side population cells with cancer stem cell-like characteristics in small-cell lung cancer. *British journal of cancer*. 2010;102(11):1636-44.
40. Walter D, Satheesha S, Albrecht P, Bornhauser BC, D'Alessandro V, Oesch SM, et al. CD133 positive embryonal rhabdomyosarcoma stem-like cell population is enriched in rhabdospheres. *PloS one*. 2011;6(5):e19506.
41. Akita H, Marquardt JU, Durkin ME, Kitade M, Seo D, Conner EA, et al. MYC activates stem-like cell potential in hepatocarcinoma by a p53-dependent mechanism. *Cancer research*. 2014;74(20):5903-13.
42. Pelengaris S, Khan M, Evan G. c-MYC: more than just a matter of life and death. *Nature reviews Cancer*. 2002;2(10):764-76.

43. Zhao D, Pan C, Sun J, Gilbert C, Drews-Elger K, Azzam DJ, et al. VEGF drives cancer-initiating stem cells through VEGFR-2/Stat3 signaling to upregulate Myc and Sox2. *Oncogene*. 2015;34(24):3107-19.
44. Weilemann A, Grau M, Erdmann T, Merkel O, Sobhiafshar U, Anagnostopoulos I, et al. Essential role of IRF4 and MYC signaling for survival of anaplastic large cell lymphoma. *Blood*. 2015;125(1):124-32.
45. Raetz EA, Perkins SL, Carlson MA, Schooler KP, Carroll WL, Virshup DM. The nucleophosmin-anaplastic lymphoma kinase fusion protein induces c-Myc expression in pediatric anaplastic large cell lymphomas. *The American journal of pathology*. 2002;161(3):875-83.
46. Jang GB, Hong IS, Kim RJ, Lee SY, Park SJ, Lee ES, et al. Wnt/beta-Catenin Small-Molecule Inhibitor CWP232228 Preferentially Inhibits the Growth of Breast Cancer Stem-like Cells. *Cancer research*. 2015;75(8):1691-702.
47. Fodde R, Brabletz T. Wnt/beta-catenin signaling in cancer stemness and malignant behavior. *Current opinion in cell biology*. 2007;19(2):150-8.
48. Vermeulen L, De Sousa EMF, van der Heijden M, Cameron K, de Jong JH, Borovski T, et al. Wnt activity defines colon cancer stem cells and is regulated by the microenvironment. *Nature cell biology*. 2010;12(5):468-76.
49. Giambra V, Jenkins CE, Lam SH, Hoofd C, Belmonte M, Wang X, et al. Leukemia stem cells in T-ALL require active Hif1alpha and Wnt signaling. *Blood*. 2015;125(25):3917-27.
50. Takahashi-Yanaga F, Kahn M. Targeting Wnt signaling: can we safely eradicate cancer stem cells? *Clinical cancer research : an official journal of the American Association for Cancer Research*. 2010;16(12):3153-62.

51. Jang GB, Kim JY, Cho SD, Park KS, Jung JY, Lee HY, et al. Blockade of Wnt/beta-catenin signaling suppresses breast cancer metastasis by inhibiting CSC-like phenotype. *Scientific reports*. 2015;5:12465.
52. Moumen M, Chiche A, Decraene C, Petit V, Gandarillas A, Deugnier MA, et al. Myc is required for beta-catenin-mediated mammary stem cell amplification and tumorigenesis. *Molecular cancer*. 2013;12(1):132.
53. Sansom OJ, Meniel VS, Muncan V, Phesse TJ, Wilkins JA, Reed KR, et al. Myc deletion rescues Apc deficiency in the small intestine. *Nature*. 2007;446(7136):676-9.
54. Gopal K, Gupta N, Zhang H, Alshareef A, Alqahtani H, Bigras G, et al. Oxidative stress induces the acquisition of cancer stem-like phenotype in breast cancer detectable by using a Sox2 regulatory region-2 (SRR2) reporter. *Oncotarget*. 2016;7(3):3111-27.
55. Li L, Neaves WB. Normal stem cells and cancer stem cells: the niche matters. *Cancer research*. 2006;66(9):4553-7.
56. Borovski T, De Sousa EMF, Vermeulen L, Medema JP. Cancer stem cell niche: the place to be. *Cancer research*. 2011;71(3):634-9.
57. Oskarsson T, Batlle E, Massague J. Metastatic stem cells: sources, niches, and vital pathways. *Cell stem cell*. 2014;14(3):306-21.

## CHAPTER 4

### **Oxidative stress promotes the tumorigenicity in ALK-positive anaplastic large-cell lymphoma by activating the Wnt/ $\beta$ -catenin/MYC/Sox2 axis<sup>1</sup>**

---

<sup>1</sup>This chapter has been modified from a manuscript in preparation for submission for publication:

Chengsheng Wu, Nidhi Gupta, Hai-feng Zhang, Yung-Hsing Huang, and Raymond Lai.

Oxidative stress promotes the tumorigenicity in ALK-positive anaplastic large-cell lymphoma by activating the Wnt/ $\beta$ -catenin/MYC/Sox2 axis. In preparation.

I prepared the first draft and revisions based on the suggestions and comments of the co-authors. I designed and performed all the experiments in this study. N.G., H.Z., and Y.H. contributed to Figure 4.3A, provided technical assistance and intellectual input. R.L. provided numerous comments and final review of the manuscript.

## 4.1 Introduction

ALK-positive anaplastic large-cell lymphoma (ALK+ALCL) is a rare subtype of non-Hodgkin lymphoma of null or T-cell lineage, which preferentially occurs in children and young adults (1). Gene translocation involving *ALK* and *NPM* has been detected in approximately 80% of ALK+ALCL cases (2), and the translocation results in the generation of fusion tyrosine kinase NPM-ALK, the key oncogenic driver of this neoplasm (3). The oncogenic potential of NPM-ALK has been well underscored by its interaction and activation of a number of molecular proteins involved in multiple signaling pathways, such as JAK/STATs, MAPK/ERK and PI3K/AKT(3). Among these oncogenic signaling pathways, NPM-ALK/STAT3 is one of the most critical mediators of NPM-ALK-induced transformation, by upregulating the gene expression related with anti-apoptosis and cell growth, including *BCL2*, *Survivin*, and *MYC* (1, 4, 5); and downregulating the negative regulators of NPM-ALK/STAT3 activity, such as Shp1, STAT5A and STAT1 (3, 6-8).

Intra-tumor heterogeneity accounts for the diversity of tumor cells within a tumor and this concept has evolved in the past decade to phenotypical, functional and genetical heterogeneity (9-11). The existence of intra-tumor heterogeneity can be explained by two hypothetical models including the clone evolution and cancer stem cell (CSC) models (11). Briefly, the clone evolution model proposes that tumor progression is an evolutionary process for a single cell clone with acquisition of multiple genetic mutations and also a selection process of more aggressive subclones (9). While the CSC model raises that only a small fraction of tumor cells have the capability to initiate the whole tumor bulks and the ability to self-renewal to maintain this small fraction (9,



11). With these two models, it is well recognized that cancer cells contain a hierarchy of CSCs and non-CSCs (10, 11). More interestingly, recent evidence shows that non-CSCs are able to shift to CSCs under certain circumstances and *vice versa* (9-11). This phenomenon indicates a biological process named CSC plasticity or “acquired cancer stemness” (12). For instance, estrogen receptor-positive (ER+) breast cancer cell line MCF-7 acquires tumorigenic potential and chemoresistance upon the treatment of chronic oxidative stress (13). Hypoxia stress also enriches the CSC population in CD133+ glioma stem cells (14). CSC plasticity has been postulated to be a major mechanism to explain how cancer cells develop chemoresistance, and ultimately, to contribute to cancer treatment failure (15-17). However, to our knowledge, the concept of CSC plasticity remains poorly understood in haematological malignancy, including ALK+ALCL. Thus, we believe an in-depth understanding of CSC plasticity in ALK+ALCL is warranted.

The Lai lab previously identified two distinct cell subpopulations derived from ER+ breast cancer cells (18), esophagus squamous cancer cells (19), and ALK+ALCL cell lines based on their differential responses to a Sox2 reporter – SRR2 carrying GFP and luciferase (20). The reporter responsive (RR) cells are consistently more chemoresistant and tumorigenic than the reporter unresponsive (RU) cells. Our previous study suggested that the positive forward loop involving the Wnt/ $\beta$ -catenin-MYC/Sox2 axis is the defining feature of RR cells derived from ALK+ALCL (21). Although the Lai lab has recently showed that RU cells derived from ER+ breast cancer cells and esophagus squamous cancer cells are able to acquire stemness features upon oxidative stress (19, 22), we do not know whether similar findings can be

observed in ALK+ALCL, since ALK+ALCL is a haematological neoplasm that is very much distinct from solid tumor models, such as cell models of breast cancer and esophagus squamous cancer. In this study, we showed that RU cells can be induced to RR cells (*i.e.* converted RR cells) upon oxidative challenge. These converted RR cells share the similar biological and biochemical characteristics with native RR cells. Furthermore, we found that the activated Wnt/ $\beta$ -catenin/MYC/Sox2 axis upon oxidative challenge is responsible for the conversion of RU cells to RR cells, as pharmacological inhibition of  $\beta$ -catenin or MYC or siRNA knockdown of Sox2 in RU cells significantly abrogates this biological process.

## **4.2 Methods and materials**

### **4.2.1 Cell lines and chemicals**

The cell lines and the condition of cell culture were described in section 2.2.1 of Chapter 2 and section 3.2.1 of Chapter 3. 10074-G5, U0126, doxorubicin, doxycycline, iodonitrotetrazolium chloride, N-acetylcysteine (NAC), and quercetin were all purchased from Sigma Aldrich. Hydrogen peroxide ( $H_2O_2$ ) was purchased from ThermoFisher Scientific Canada. U0126, doxorubicin and doxycycline treatments were described in section 3.2.1 of Chapter 3 and section 2.2.6 of Chapter 2.

### **4.2.2 $H_2O_2$ re-challenge and chemical treatment**

Approximately  $1 \times 10^7$  of cells was started with  $H_2O_2$  re-challenge experiment in this study. Briefly, cells were subjected with various doses of  $H_2O_2$  ranging from 0 to 1 mM

for 3 days, and then cells were changed with fresh culture medium containing various doses of H<sub>2</sub>O<sub>2</sub> and continuously cultured up to day 5, followed by the luciferase reporter assay and flow cytometry assay to assess luciferase activity and GFP expression. Cell viability was also assessed from day 1 to day 3. For the treatment of NAC, cells were subjected with 0.3 mM H<sub>2</sub>O<sub>2</sub> in the presence of various doses of NAC ranging from 0 to 20 mM for 48 hours, and then the luciferase reporter assay and flow cytometry assay were executed to evaluate the SRR2 luciferase activity and GFP expression. For the treatment of 10074-G5 or quercetin, cells were subjected with 5 μM 10074-G5 or 50 μM quercetin from day 4 to day 5 (24 hours) in the H<sub>2</sub>O<sub>2</sub> re-challenge experiment, the luciferase reporter assay was then followed to evaluate the SRR2 reporter activity.

#### **4.2.3 Luciferase assay and flow cytometry**

The luciferase assay kit was purchased from Promega (Madison, WI), and luciferase activity was measured as described previous in section 3.2.7 of Chapter 3. The flow cytometry analyses for assessing GFP expression were performed as below. Cells after treatment were washed with cold 1x PBS three times and were resuspended in 1 X cold PBS before flow cytometry (BD Bioscience). 20,000 live cells were acquired for each run. All the flow cytometry data were analyzed using the FCS Express 5 software from De Novo Software (Glendale, CA).

#### 4.2.4 Trypan blue exclusion assay and MTS assay

Cell viability and cell viability were assessed by trypan blue exclusion assay and MTS assay, and these assays were performed as previously described in section 2.2.12 of Chapter 2.

#### 4.2.5 Short interfering RNA and transfections

SMARTpool short interfering RNAs (siRNAs) for Sox2 and scrambled siRNA were purchased from Dharmacon (Lafayette, CO). See section 2.2.4 of Chapter 2 for more details.

#### 4.2.6 RNA extraction, cDNA synthesis, and quantitative reverse transcriptase PCR (quantitative RT-PCR)

Total RNA extraction was performed with the Qiagen RNeasy Kit (Qiagen, Toronto, Ontario, Canada) according to the manufacturer's protocol. The experimental procedures were described in section 2.2.13 of Chapter 2. All the primer sequences were shown as below:

**Table 4.1 Primers used for quantitative RT-PCR**

<b>Gene</b>	<b>Forward Primers</b>	<b>Reverse Primers</b>
BCL9	5'- GGCCATACCCCTAAAGCACTC-3'	5'- CGGAAATACTTCGCTCCCTTTT-3'
CTNNB1	5'- AAAGCGGCTGTTAGTCACTGG-3'	5'- CGAGTCATTGCATACTGTCCAT-3'
SOX2	5'- GCCGAGTGGAACCTTTTGTCG-3'	5'- GGCAGCGTGTACTTATCCTTCT-3'
WNT2B	5'-GATCAAGATGGTGCCAACTTC-3'	5'-CCAAGACACAGTAATCTGGAGAG -3'
GAPDH	5'- GGAGCGAGATCCCTCCAAAAT-3'	5'- GGCTGTTGTCATACTTCTCATGG-3'

#### **4.2.7 Western blotting**

Western blotting studies were performed as described as previously in section 2.2.8 of Chapter 2.

Antibodies reactive to phosphorylated MYC<sup>S62</sup> (E1J4K), MYC (D84C12), Sox2 (D6D9), and  $\beta$ -catenin (D10A8) were purchased from Cell Signaling Technology (Danvers, MA),  $\beta$ -actin antibody (sc-130300) was purchased from Santa Cruz (Dallas, Texas), and antibody reactive to active  $\beta$ -catenin (8E7) was purchased from Merck Millipore (Toronto, ON, Canada). Secondary antibodies anti-Rabbit IgG (1:2000) and anti-Mouse IgG (1:2000) were purchased from Cell Signaling Technology.

#### **4.2.8 Nuclear cytoplasm fractionation assay**

The nuclear-cytoplasmic fractionation kit was purchased from ThermoFisher Scientific Canada. The experiment was performed as described in section 2.2.11 of Chapter 2.

#### **4.2.9 SRR2 probe binding assay**

SRR2 probe binding assay was performed as previously described in section 3.2.10 of Chapter 3.

#### **4.2.10 Methylcellulose colony formation assay**

The methylcellulose colony formation assay was performed as previously described in section 2.2.9 of Chapter 2 and section 3.2.12 of Chapter 3.

#### **4.2.11 Limiting dilution assay**

Cells with or without H<sub>2</sub>O<sub>2</sub> re-challenge treatment were seeded in RPMI1640 media (Invitrogen) supplemented with 20% fetal bovine serum (Invitrogen), 1% penicillin streptomycin (ThermoFisher Scientific) and 200 µg/mL puromycin dihydrochloride (Sigma Aldrich) in 96-well low adherent plate (Corning) at 10 limiting dilutions ranging from 1 to 1000 cells, and each dilution has triplicate wells. After 7 days, cells in each well were stained with iodinitrotetrazolium chloride (Sigma Aldrich) for 24 hours and images were acquired using Alphascreen HP (ThermoFisher Scientific Canada). The number of visible spheres was counted by eye.

#### **4.2.12 Statistical analysis**

Data were expressed as mean ± standard deviation. The statistical analysis was performed using Graphpad Prism 5 (La Jolla, CA), and the significance of two independent groups of samples was determined using Student's *t*-test. Statistical significance is denoted by \* (*P*<0.05) and \*\* (*P*<0.01).

### **4.3 Results**

#### **4.3.1 Oxidative stress induces a conversion from RU to RR cells**

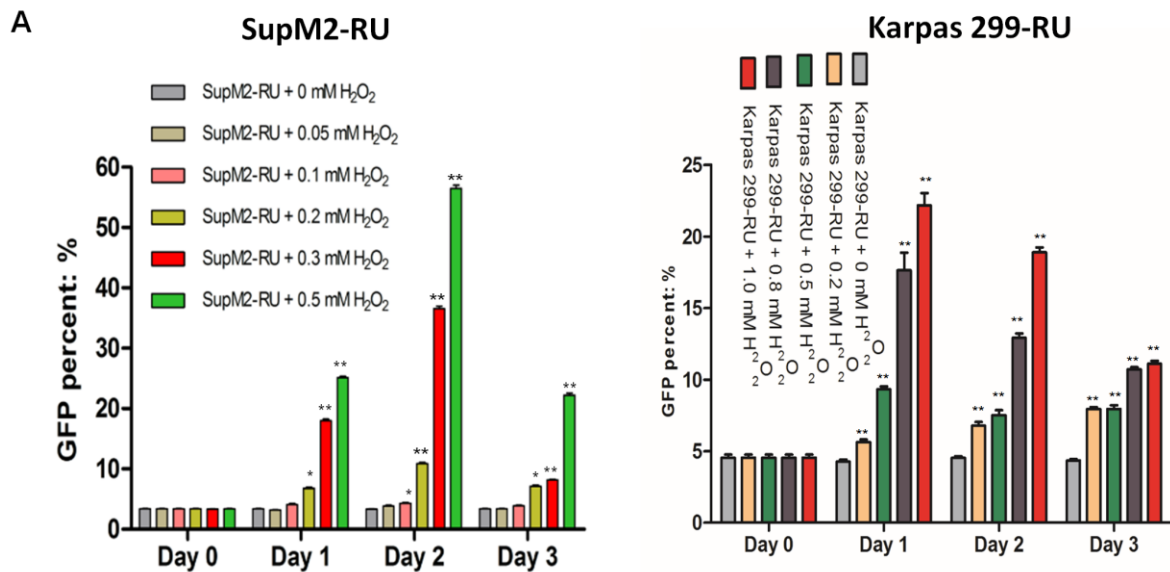
Using relatively low concentrations of H<sub>2</sub>O<sub>2</sub>, an agent known to potently induce oxidative stress and the generation of reactive oxygen species (ROS) (23), we previously successfully converted small subsets of RU cells derived from esophageal

squamous cell carcinoma cells and ER+ breast cancer cells into RR cells (19, 22). We asked if a similar phenomenon can occur in hematopoietic cancers such as ALK+ALCL. Two ALK+ALCL cell lines, namely SupM2 and Karpas 299, were used for this experiment.

As shown in **Figure 4.1A**, upon treatment of various doses of H<sub>2</sub>O<sub>2</sub> for 3 days, RU cells from both cell lines that harbored ~5% GFP-positive cells exhibited significantly increased GFP-positive cells. As high doses of H<sub>2</sub>O<sub>2</sub> are expectedly cytotoxic, we assessed the number of viable cells at different doses of H<sub>2</sub>O<sub>2</sub> from day 1 to day 3. As shown in **Figure 4.1B**, we found that H<sub>2</sub>O<sub>2</sub> retarded the cell growth in a dose-dependent manner. Taking the cell growth inhibition and percentages of GFP-positive cells induced by various doses of H<sub>2</sub>O<sub>2</sub> into consideration, we decided to choose 0.3 mM and 0.5 mM H<sub>2</sub>O<sub>2</sub> for RU cells derived from SupM2 and Karpas 299, respectively, to induce a sufficient percentage of GFP-positive cells, or say converted RR cells. We also found that a re-challenge with H<sub>2</sub>O<sub>2</sub> on day 3 significantly increased the percentages of converted RR cells in both cell lines. As shown in **Figure 4.1C-D**, ~80% of RU cells of SupM2 remaining in the tissue culture were GFP-positive 2 days after the re-challenge. Similarly, ~30% of RU cells derived from Karpas 299 became converted RR cells (**Figure 4.1D**). This H<sub>2</sub>O<sub>2</sub> re-challenge strategy was used to generate converted RR cells for the remainder of the study. Consistent to the results of GFP expression, the luciferase activity in RU cells derived from both cell lines also significantly increased upon H<sub>2</sub>O<sub>2</sub> re-challenge (**Figure 4.1E**). Notably, the RR cells derived from SupM2 also significantly acquired the SRR2 activity based on the

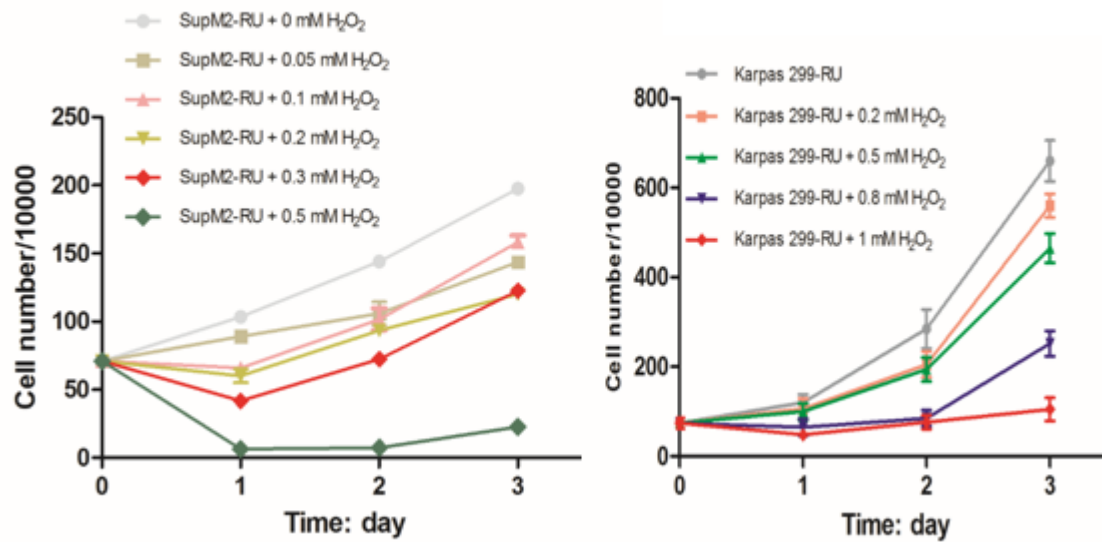
readouts of luciferase activity and GFP expression upon  $H_2O_2$  re-challenge (**Figure 4.1E-F**).

To confirm that the RU to RR cells conversion induced by  $H_2O_2$  was indeed dependent on oxidative stress, we attempted to block this process using N-acetyl-L-cysteine (NAC), a pharmacologic agent known to minimize cellular oxidative stress (24). As shown in **Figure 4.1G-H**, in a dose-dependent manner, NAC significantly lowered the number of  $H_2O_2$ -induced GFP-positive cells as well as luciferase activity upon treatment of 0.3 mM  $H_2O_2$  for 2 days.



**Figure 4.1 Oxidative challenge induces the conversion of RU to RR cells.** A) RU cells derived from SupM2 and Karpas 299 cells were subjected with various doses of  $H_2O_2$  for up to 3 days. The percentages of GFP, one of two surrogate markers of SRR2 activity, were assessed by flow cytometry in both RU cells at day 0, day 1, day 2 and day 3. Statistical significance is denoted by \* ( $P < 0.05$ ) and \*\* ( $P < 0.01$ ). Results shown were representative of three independent experiments.



**B**

**Figure 4.1B B)** The cell numbers of RU cells derived from SupM2 and Karpas 299 upon various doses of H<sub>2</sub>O<sub>2</sub> treatment were counted by trypan blue exclusion assay from day 0 to day 3. Results from triplicate experiments were shown.

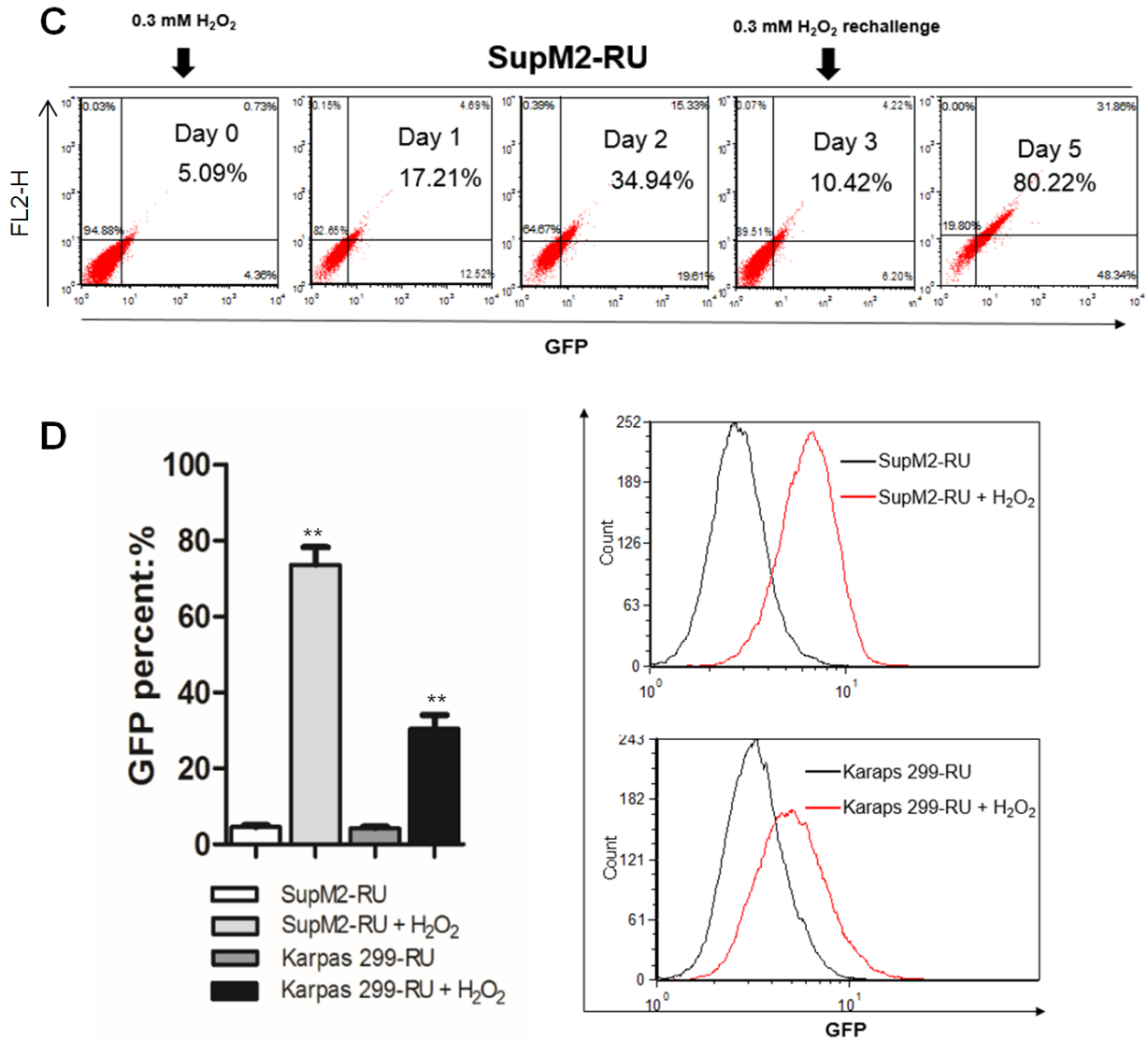


**Figure 4.1C-D** C) the schematic experimental model of 0.3 mM H<sub>2</sub>O<sub>2</sub> re-challenge treatment in RU cells derived from SupM2. D) The percentages of GFP-positive cells and the expression of GFP in RU cells derived from SupM2 and Karpas 299 cells upon 0.3 mM or 0.5 mM H<sub>2</sub>O<sub>2</sub> re-challenge treatment. Statistical significance is denoted by \* ( $P < 0.05$ ) and \*\* ( $P < 0.01$ ). Results shown were representative of three independent experiments.

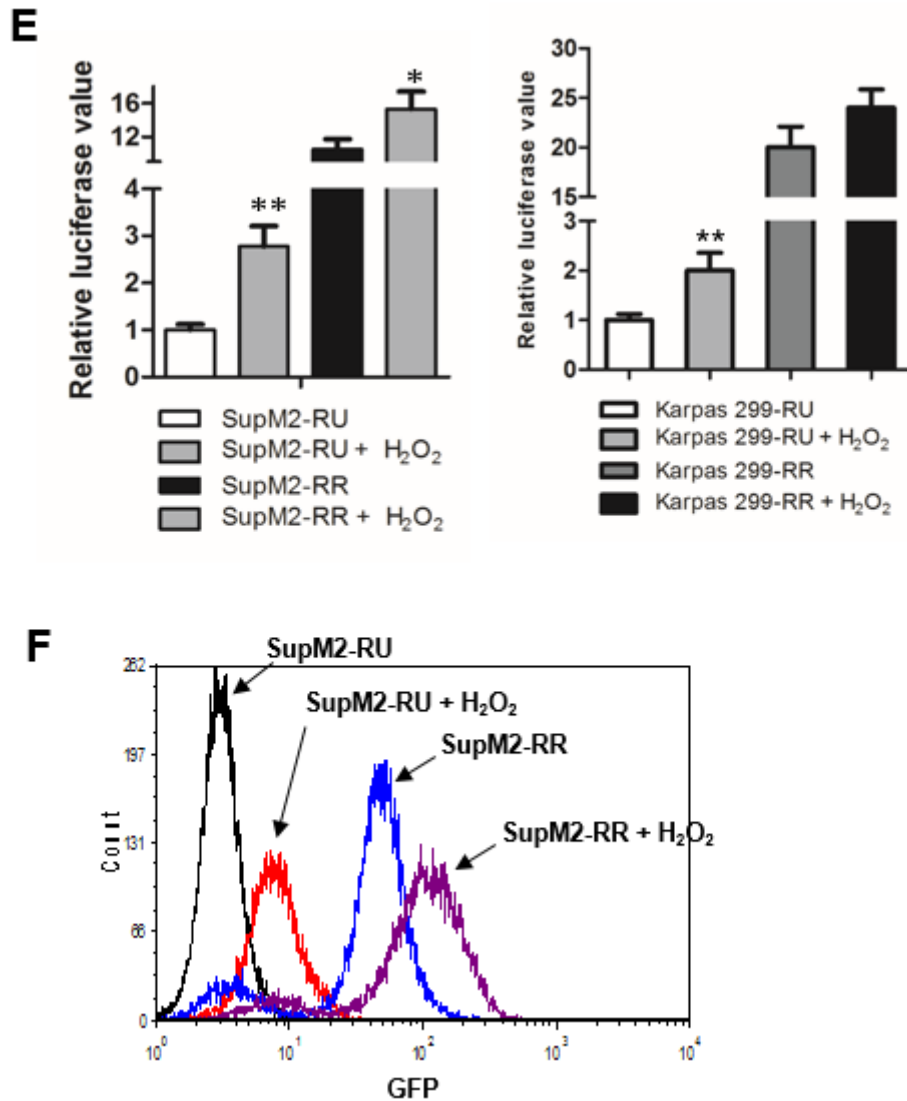


**Figure 4.1E-F** E) the luciferase activity in RU and RR cells derived from SupM2 and Karpas 299 at day 5 upon 0.3 mM and 0.5 mM H<sub>2</sub>O<sub>2</sub> re-challenge treatment. F) the GFP expression in RU and RR cells derived from SupM2 with and without H<sub>2</sub>O<sub>2</sub> re-challenge. Statistical significance is denoted by \* ( $P < 0.05$ ) and \*\* ( $P < 0.01$ ). Results shown were representative of three independent experiments.

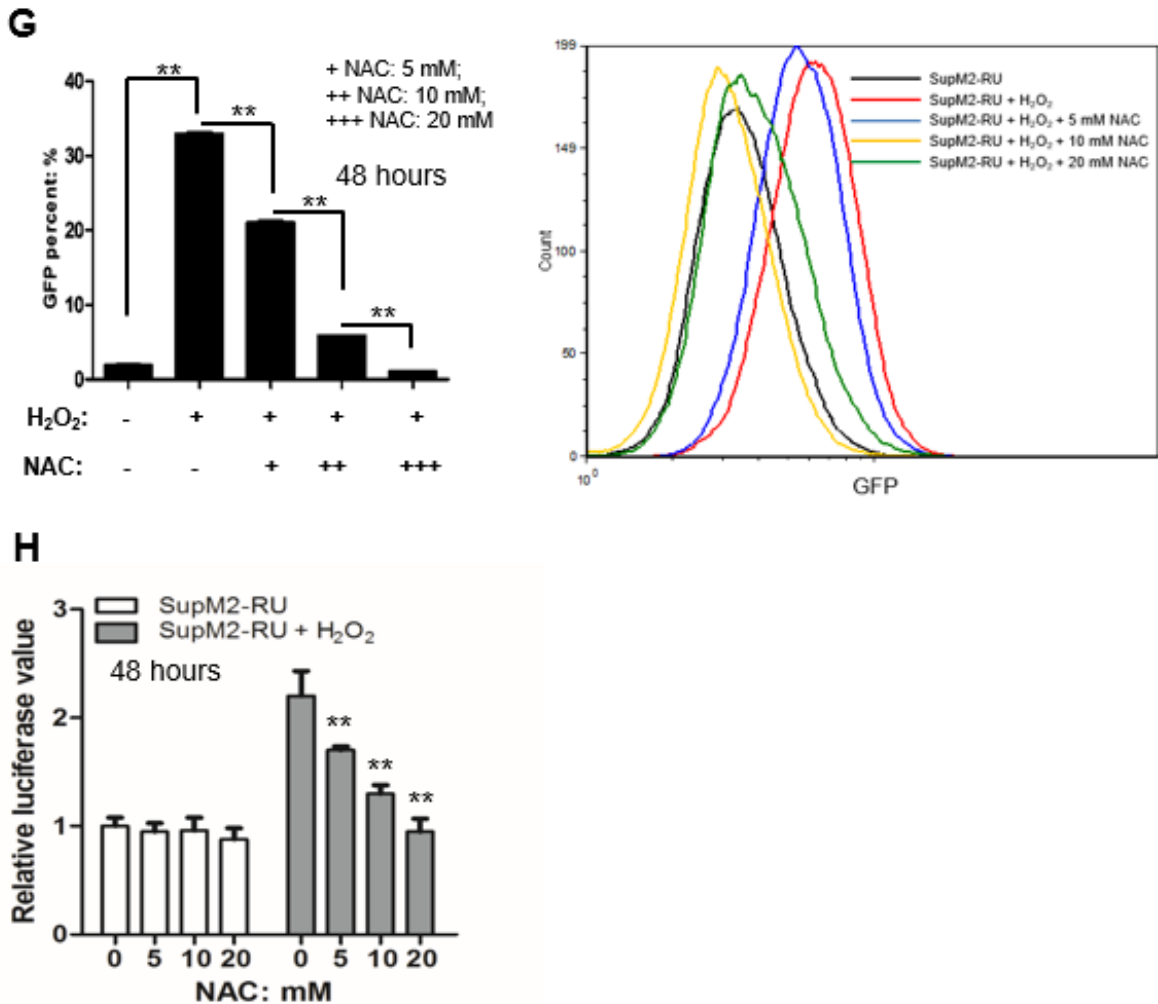


**Figure 4.1G-H** G) Treatment with NAC of 5 mM, 10 mM, 20mM for 48 hours significantly downregulated the number of GFP-positive cells and the expression of GFP in RU cells derived from SupM2 cells upon 0.3 mM H<sub>2</sub>O<sub>2</sub> treatment for 48 hours, as compared to cells treated with DMSO and 0.3 mM H<sub>2</sub>O<sub>2</sub>. H) Treatment with NAC of 5 mM, 10 mM, 20 mM for 48 hours significantly decreased the luciferase activity in RU cells derived from SupM2 cells upon 0.3 mM H<sub>2</sub>O<sub>2</sub> treatment for 48 hours, as compared to that of cells treated with DMSO and 0.3 mM H<sub>2</sub>O<sub>2</sub>. Notably, treatment of various doses of NAC only for 48 hours did not significantly change the luciferase activity in RU cells derived from SupM2 cells. Statistical significance is denoted by \* ( $P<0.05$ ) and \*\* ( $P<0.01$ ). Results from triplicate experiments were shown.

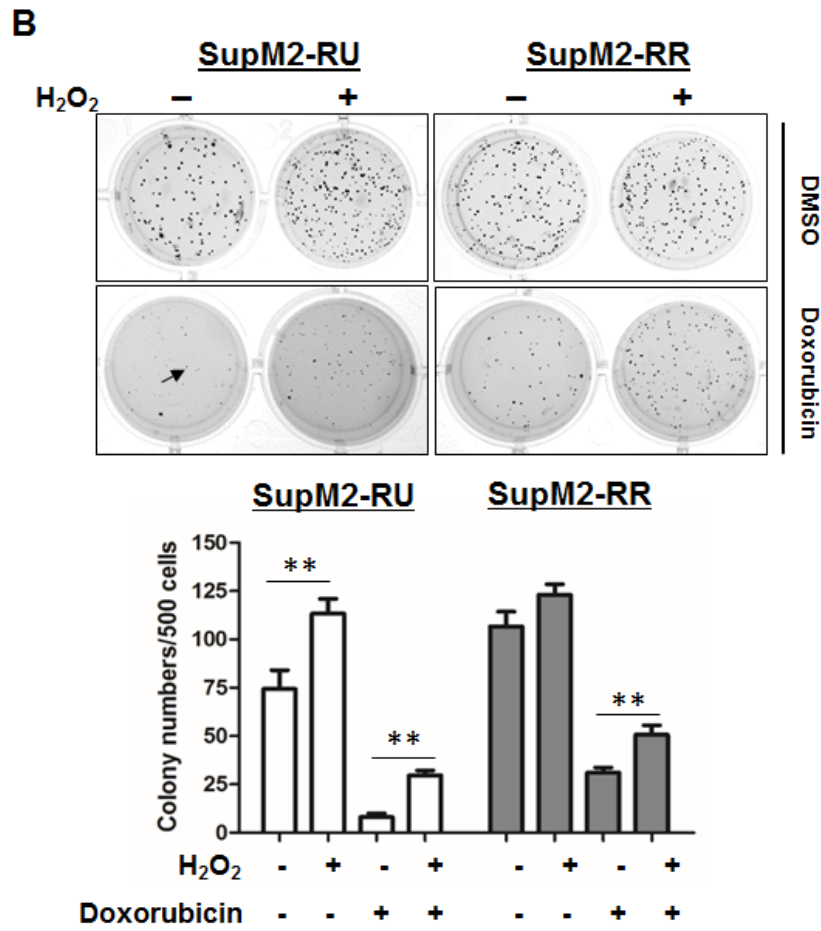
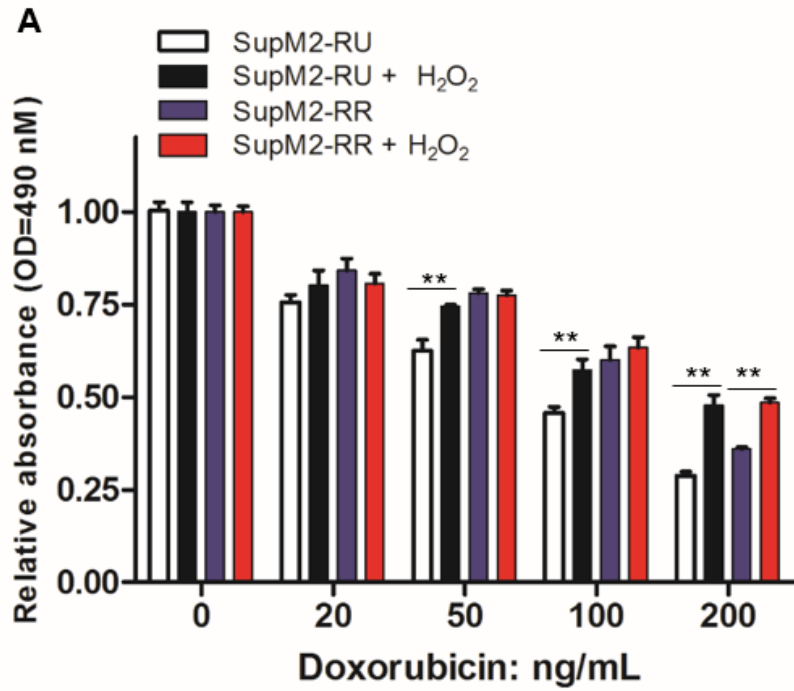
### 4.3.2 The converted RR cells share the similar biological functions with RR cells

Then we asked whether converted RR cells are phenotypically similar with RR cells. Specifically, we were interested in whether converted RR cells showed increased clonogenicity and chemoresistance, as seen in native RR cells. Thus, we subjected native RU and converted RR cells from SupM2 to various doses of doxorubicin, a chemotherapy drug used as front-line chemotherapy for ALK+ALCL patients (1). As shown in **Figure 4.2A**, converted RR cells were found to be significantly more doxorubicin-resistant than native RU cells. Furthermore, the converted RR cells even demonstrated more doxorubicin-resistant than native RR cells at the high dose of doxorubicin (i.e. 200 ng/mL) (**Figure 4.2A**).

Next, we tested the clonogenicity of converted RR cells using methylcellulose colony formation assay. As shown in **Figure 4.2B**, converted RR cells derived from SupM2 formed significantly more colonies than native RU cells in the presence or absence of 50 ng/mL doxorubicin. In addition, when compared to RR cells without H<sub>2</sub>O<sub>2</sub> re-challenge in the presence of 50 ng/mL doxorubicin, RR cells derived from SupM2 after H<sub>2</sub>O<sub>2</sub> re-challenge formed significantly more number of colony in the presence of doxorubicin, despite that no significant changes in the colony numbers was observed between the groups of RR cells with and without H<sub>2</sub>O<sub>2</sub> re-challenge (**Figure 4.2B**).

Then we tested the sphere-forming abilities of RU cells, converted RR cells and native RR cells derived from Karpas 299 using the limiting dilution assay. As shown in **Figure 4.2C**, we seeded a serial diluted cells ranging from 1000 cells to 1 cell in each

well of 96-well plate, and observed that a low number of RU and RR cells upon H<sub>2</sub>O<sub>2</sub> re-challenge (i.e. 125 cells for RU, 63 or 32 cells for RR) indeed formed significantly more spheres, as compared to their native cells (**Figure 4.2C-D**).



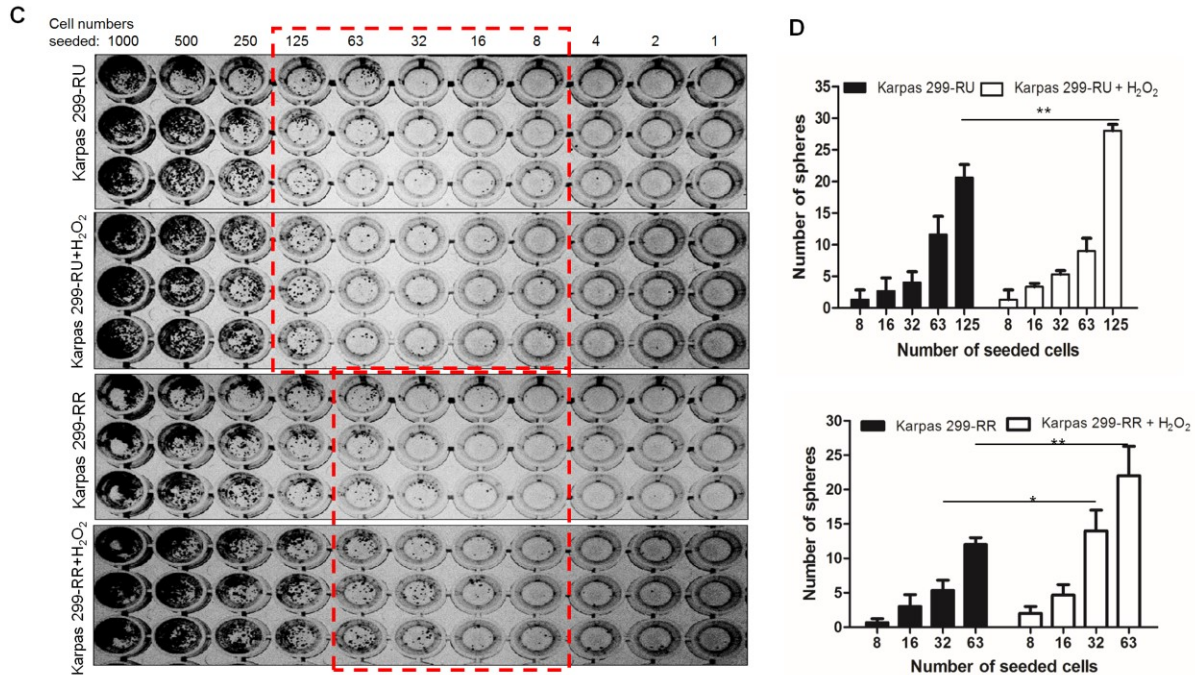


**Figure 4.2 RU and RR cells upon H<sub>2</sub>O<sub>2</sub> re-challenge treatment are more doxorubicin-resistant and clonogenic, and have captured enhanced sphere-forming ability as compared to cells without treatment.** A) RU and RR cells from SupM2 cells were re-challenged with 0.3 mM H<sub>2</sub>O<sub>2</sub> for 5 days. Then the cells were subjected with various doses of doxorubicin for 48 hours. Cells without H<sub>2</sub>O<sub>2</sub> treatment were included as comparison. B) RU and RR cells derived from SupM2 cells were re-challenged with 0.3 mM H<sub>2</sub>O<sub>2</sub> for 5 days. Then the cells were preceded for methylcellulose colony formation assay in the presence/absence of 50 ng/mL doxorubicin, and cells without H<sub>2</sub>O<sub>2</sub> re-challenge were included as comparison. The experiments were repeated in triplicate, and one representative result was shown here. The colonies larger than the one pointed by the bold black arrow were counted only. The graph below demonstrated the number of colonies in the above experimental groups. C-D) The serial diluted RU and RR cells derived from Karpas 299 were seeded in 96-well plate. After 8 days, the number of spheres was counted in the highlighted wells circulated by red broken lines. Results suggested that low number of RU and RR cells (125 cells and 63 cells, respectively) upon H<sub>2</sub>O<sub>2</sub> re-challenge formed significant more spheres than their native cells. This experiment was repeated in triplicate, statistical significance is denoted by \* ( $P < 0.05$ ) and \*\* ( $P < 0.01$ ).



### 4.3.3 The converted RR cells share the similar biochemical characteristics with RR cells

Our previous study suggested that the highly active Wnt/ $\beta$ -catenin/MYC/Sox2 axis defines the RR cells (21). Thus, we asked if converted RR cells showed activation of this signaling axis. As shown in **Figure 4.3A**, converted RR cells derived from SupM2 cells showed upregulated expression of active  $\beta$ -catenin, the total protein level of  $\beta$ -catenin as well as p-MYC<sup>S62</sup>/MYC, as compared to native RU cells. Although the total MYC is not appreciably altered in RR cells upon H<sub>2</sub>O<sub>2</sub> re-challenge, p-MYC<sup>S62</sup>, the active form of MYC (25), markedly increased (**Figure 4.3A**). We also observed that the expression level and activity of NPM-ALK and STAT3 were not appreciably changed in this experiment (**Figure 4.3A**).

Moreover, using quantitative RT-PCR (qRT-PCR), we also were able to demonstrate that Sox2 transcriptional activity was upregulated in converted RR cells; as shown in **Figure 4.3B**, the expression of three known Sox2 downstream targets including *WNT2B*, *CTNNB1* and *BCL9* were significantly higher in converted RR cells in mRNA level, in comparison to their native RU cells (**Figure 4.3B**). Similar results were observed in RR cells after oxidative re-challenge (**Figure 4.3B**).

To substantiate these data, we performed the Sox2-SRR2 probe binding assay to investigate whether the converted RR cells indeed have increased Sox2-DNA binding. As shown **Figure 4.3C**, more Sox2 was pulled down by the biotin-labeled SRR2 probe in the converted RR cells than RU cells; and a visible increase of Sox2-SRR2 binding

also was observed in RR cells upon H<sub>2</sub>O<sub>2</sub> re-challenge (**Figure 4.3C**). Notably, the Sox2 protein level in both RU and RR cells was not appreciably altered in this experiment, as shown in the input of the pull-down assay (**Figure 4.3C**).

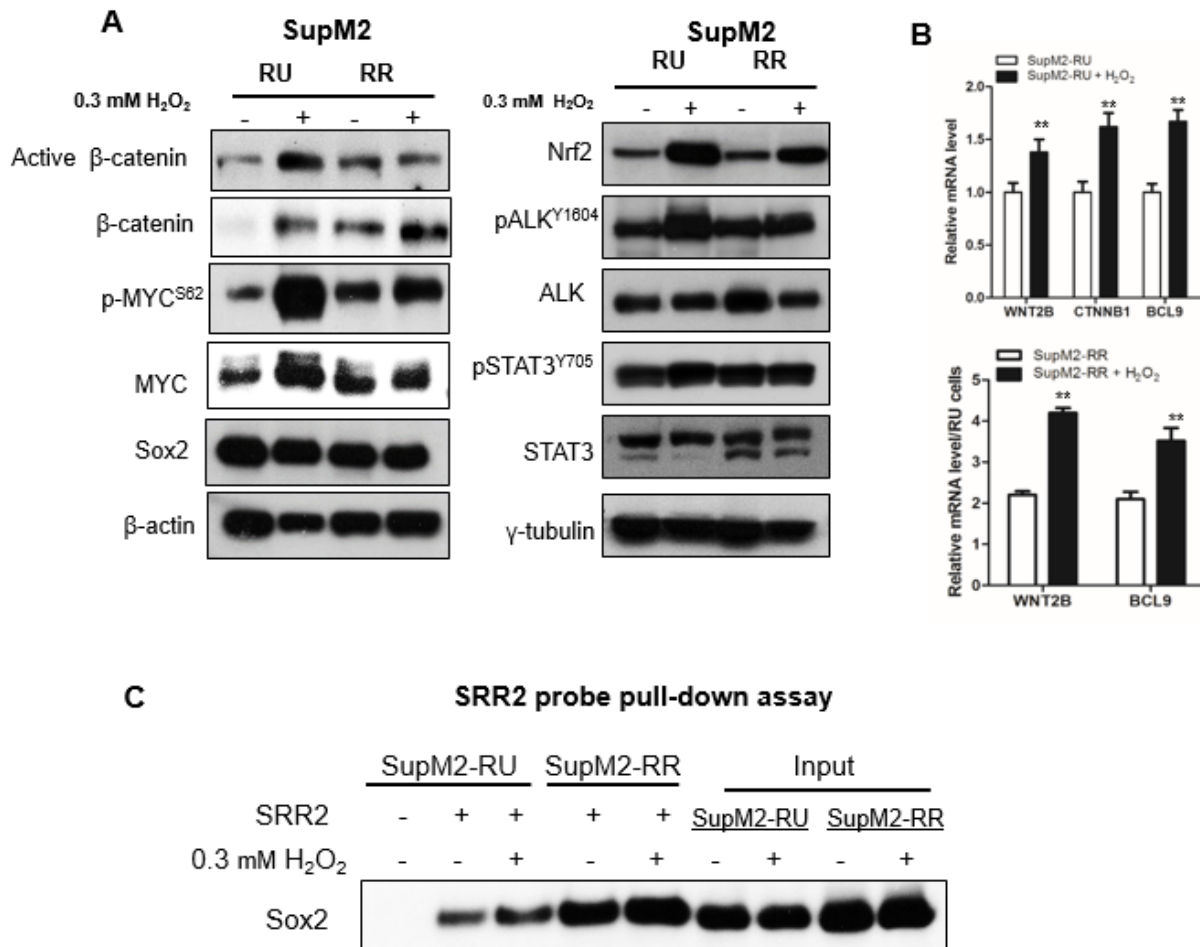


**Figure 4.3 The converted RR cells induced by oxidative stress share the biochemical features with RR cells.** A) The Western blots results suggested that active β-catenin, total β-catenin, p-MYC<sup>S62</sup>, and MYC markedly increased in RU cells derived from SupM2 upon H<sub>2</sub>O<sub>2</sub> re-challenge in comparison to parental RU cells. The β-catenin and p-MYC also dramatically increased in RR cells derived from SupM2 after H<sub>2</sub>O<sub>2</sub> re-challenge. The expression of Sox2 in both RU and RR cells is not appreciably altered in this experimental manipulation. The expression levels of pALK<sup>Y1604</sup>, ALK, pSTAT3<sup>Y705</sup> and STAT3 were not appreciably altered. The nuclear factor erythroid 2-related factor (Nrf 2), as an oxidative stress responder, is included as a control. B) qRT-

PCR assay indicated that the Sox2 downstream targets including WNT2B and BCL9 significantly increased after H<sub>2</sub>O<sub>2</sub> re-challenge in both RU and RR cells derived from SupM2. Results shown were representative of three independent experiments. C) SRR2 probe pull-down assay suggested that more Sox2 is pulled down by biotin-labeled SRR2 probe in RU and RR cells upon H<sub>2</sub>O<sub>2</sub> re-challenge as compared to parental RU and RR cells. The input of the pulldown assay demonstrated that the Sox2 expression is not altered in this experiment. Statistical significance is denoted by \* ( $P<0.05$ ) and \*\* ( $P<0.01$ ).

#### **4.3.4 Inhibition of $\beta$ -catenin/MYC or siRNA knockdown of Sox2 dramatically abrogates the conversion of RU cells to RR cells induced by oxidative stress**

To substantiate the importance of the Wnt/ $\beta$ -catenin/MYC/Sox2 axis being the key regulator of the RU/RR dichotomy in ALK+ALCL, we tested if inhibition of various members of this axis can effectively block RU to RR cells conversion induced by H<sub>2</sub>O<sub>2</sub>. To this end, we subjected RU cells from SupM2 and Karpas 299 cells, that had been re-challenged with H<sub>2</sub>O<sub>2</sub> for 4 days, with quercetin (a  $\beta$ -catenin inhibitor) or 10074-G5 (a MYC inhibitor that blocks the DNA binding of MYC-MAX complex) for 24 hours (26, 27). As shown in **Figure 4.4A**, pharmacological inhibition of MYC or  $\beta$ -catenin significantly decreased the upregulated MYC expression and the luciferase activity in RU cells from both cell lines upon H<sub>2</sub>O<sub>2</sub> re-challenge.

Our previous study indicated that Sox2 is also implicated in RU/RR dichotomy(20). Although Sox2 expression was not altered in this experimental manipulation, siRNA knockdown of Sox2 in RU cells from both cell lines significantly blocks the conversion of RU cells to RR cells upon H<sub>2</sub>O<sub>2</sub> re-challenge, as evidenced by the significantly

downregulated SRR2 luciferase (**Figure 4.4B**). The Western blots in the lower panel suggested the siRNA knockdown efficiency of Sox2 (**Figure 4.4B**).

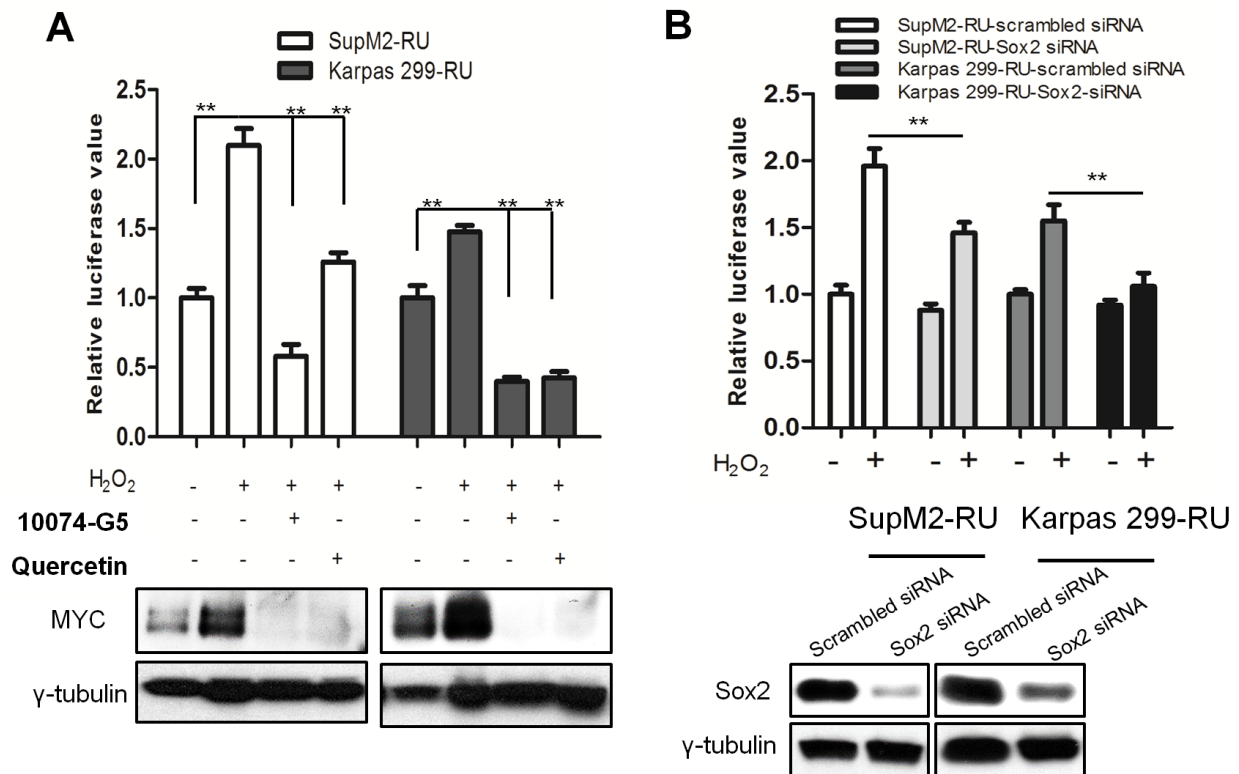


**Figure 4.4 Pharmacological inhibition of MYC or β-catenin, or siRNA knockdown of Sox2 in RU cells significantly abrogates the conversion of RU cells to RR cells.**

A) Pharmacological inhibition of MYC or β-catenin by using 10074-G5 or quercetin for 24 hours decrease the upregulated expression of MYC and the SRR2 luciferase activity induced by H<sub>2</sub>O<sub>2</sub> re-challenge. B) Sox2 knockdown by siRNA in RU cells significantly downregulated the SRR2 luciferase activity in comparison to cells transfected with scrambled siRNA in the presence of H<sub>2</sub>O<sub>2</sub> re-challenge. Statistical significance is denoted by \* ( $P < 0.05$ ) and \*\* ( $P < 0.01$ ). Results shown were representative of triplicate experiments.

#### 4.3.5 ERK1/2 is activated in both RU and RR cells upon H<sub>2</sub>O<sub>2</sub> re-challenge

Our previous publication and our current study both indicated that ERK1/2 is preferentially activated in RR cells, instead of RU cells (**Figure 4.5A**) (20). ERK1/2 is reported to be activated by oxidative stress in multiple cell models, and the activated ERK1/2 is well-known as a positive regulator of MYC protein stability and its transcriptional activity (28-31). Indeed, we observed that ERK1/2 is activated upon H<sub>2</sub>O<sub>2</sub> re-challenge in both RU and RR cells derived from SupM2 (**Figure 4.5B**). Furthermore, we found that blockage of ERK1/2 activity by MEK inhibitor U0126 for 24 hours in RR cells derived from SupM2 and Karpas 299 dramatically reduced the protein level of p-MYC<sup>S62</sup>, MYC and Sox2, along with the significantly decreased SRR2 luciferase activity (**Figure 4.5C-D**), indicating that active ERK1/2 is involved in the RU/RR dichotomy.

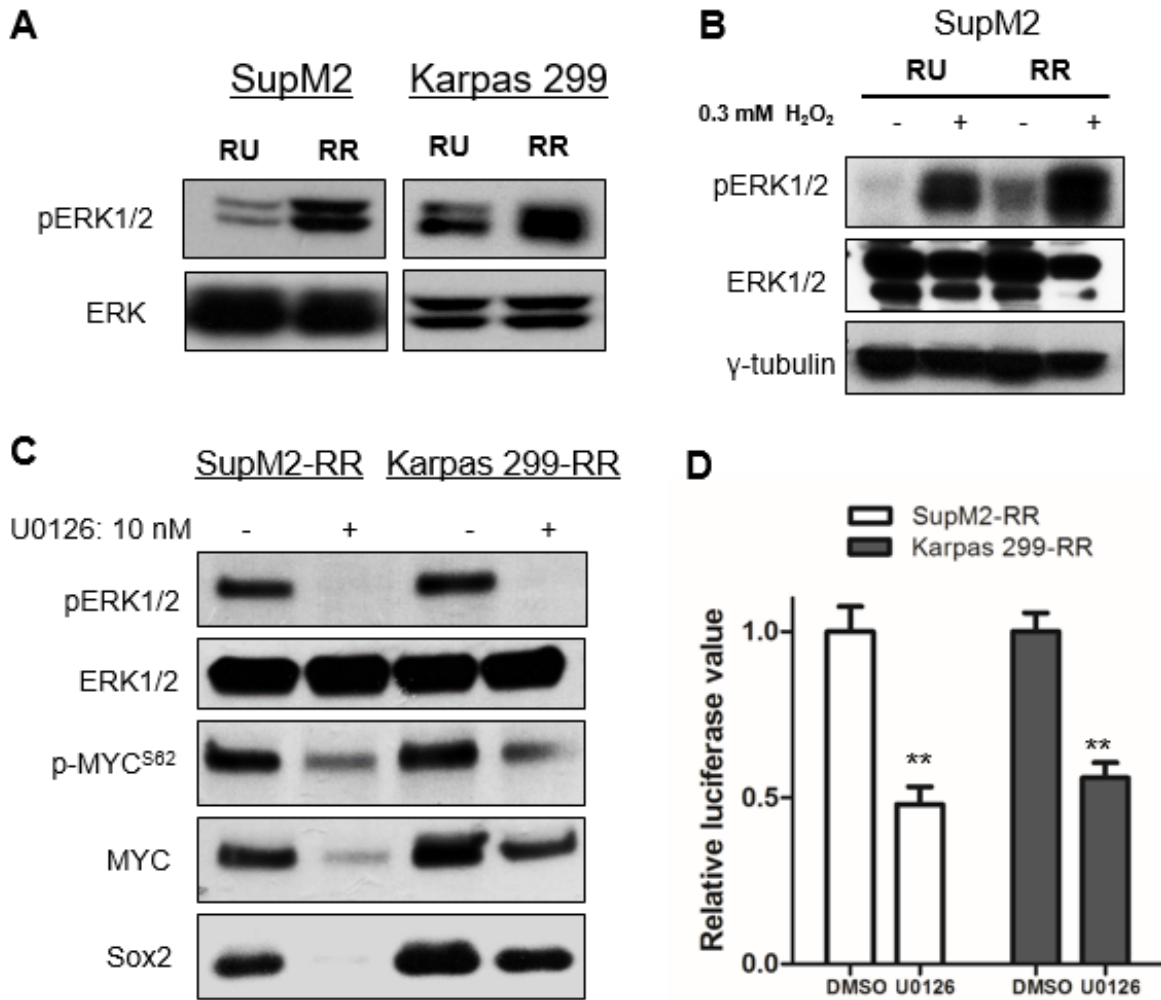


**Figure 4.5 Inhibition of ERK1/2 activity in RR cells dramatically decreases the expression level of MYC and Sox2, as well as the SRR2 luciferase activity.** A) The pERK1/2<sup>T202/Y204</sup> (pERK1/2) is highly expressed in RR cells in comparison to RU cells. B) ERK1/2 is activated in both RU and RR cells upon H<sub>2</sub>O<sub>2</sub> re-challenge. C-D) Inhibition of ERK1/2 activity by MEK inhibitor 10 nM U0126 for 24 hours dramatically decreased the protein levels of p-MYC<sup>S62</sup>, MYC and Sox2 in RR cells, as well as the SRR2 luciferase activity. Results shown were representative of three independent experiments.

#### 4.3.6 STAT1 is activated in both RU and RR cells upon oxidative stress

Our previous study indicated that STAT1 is a potent tumor suppressor in ALK+ALCL (6). Then we asked whether STAT1 is differentially activated or expressed in RU and RR cells, thus partially contributing to the RU/RR dichotomy. However, we did not find any appreciable difference in the protein level of STAT1 between RU and RR cells (**Figure 4.6A-B**), but the level of pSTAT1 presented inconsistent patterns between RU and RR cells derived from SupM2 and Karpas 299 (**Figure 4.6A-B**).

Then we tested if STAT1 is activated in RU and RR cells after oxidative stress. Firstly, we subjected RR and RU cells derived from SupM2 with various doses of H<sub>2</sub>O<sub>2</sub> for 6 hours, and observed that STAT1 was activated in a H<sub>2</sub>O<sub>2</sub> dose-dependent manner, with the total STAT1 protein being not altered in this time frame (**Figure 4.6A**). The protein levels of p-MYC<sup>S62</sup> and MYC decreased in both RU and RR cells in response to the high doses of H<sub>2</sub>O<sub>2</sub> (**Figure 4.6A**). In addition, STAT1 was also found activated in both RU and RR cells derived from SupM2 in H<sub>2</sub>O<sub>2</sub> re-challenge experiment (**Figure 4.6C**). Since STAT1 has been reported to suppress the expression of MYC in some cell models (32, 33), we asked if it is the same case in ALK+ALCL. Using Tet on-SupM2-STAT1C cells where constitutively active STAT1 (STAT1C) can be induced by the addition of doxycycline, we observed that STAT1C indeed downregulates MYC expression (**Figure 4.6D**). Whereas, an in-depth study is required to further understand the biological role of active STAT1 in RU to RR cells conversion induced by oxidative stress.

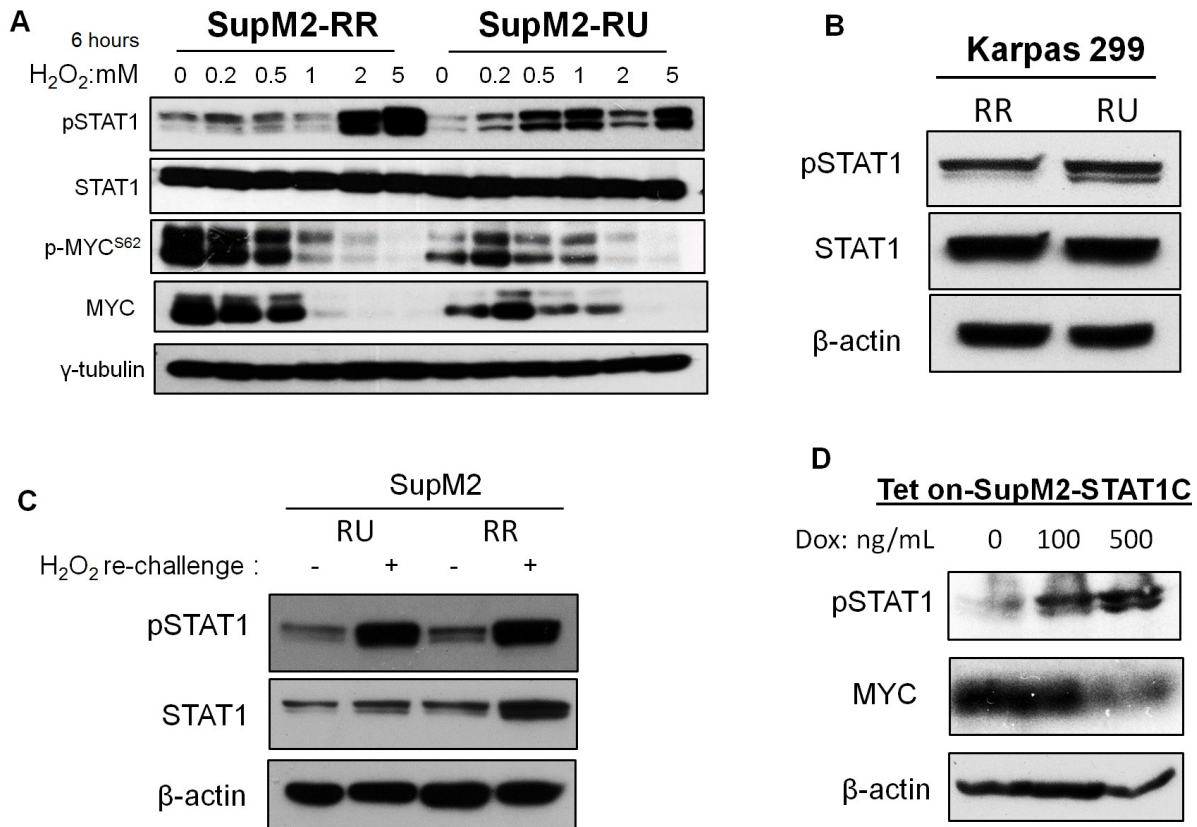


**Figure 4.6 STAT1 is activated in RU and RR cells upon oxidative stress.** A-B) STAT1 is not differentially expressed between RU and RR cells, the expression of activated STAT1 (pSTAT1) is not consistently higher in RU cells derived from SupM2 and Karpas 299 cell lines. In A, STAT1 was also activated in a H<sub>2</sub>O<sub>2</sub>-dose dependent manner at 6 hours in both RU and RR cells. MYC and p-MYC<sup>S62</sup> were downregulated in RU and RR cells treated with higher doses of H<sub>2</sub>O<sub>2</sub>, but were upregulated in RU cells when treated with relatively low doses of H<sub>2</sub>O<sub>2</sub> (such as 0.2 mM and 0.5 mM of H<sub>2</sub>O<sub>2</sub>). C) STAT1 was also activated in both RU and RR cells derived from SupM2 in H<sub>2</sub>O<sub>2</sub> re-challenge experiment. D) In Tet on-SupM2-STAT1C inducible system, induction of STAT1C downregulated the expression of MYC at 72 hours.



#### 4.4 Discussion

Oxidative stress occurs when the generation of various ROS overwhelms the intrinsic cellular anti-oxidant defense (34, 35). ROS includes superoxide anions ( $O_2^-$ ), hydrogen radical ( $OH^-$ ), hydrogen peroxide ( $H_2O_2$ ) and ozone ( $O_3$ ) (35). ROS, normally generated as by-products of cell respiration, can serve as cellular messengers in redox signaling (36). The intracellular ROS level is stringently regulated in normal cells, as different levels of ROS induces different cellular responses (36). Specifically, low to medium level of ROS activates a number of stress-related signalling pathways (e.g. PI3K/AKT and MAPK/ERK) to promote cell survival, proliferation and differentiation (37), and high level or excessive ROS are cytotoxic to normal cells by oxidizing or damaging cellular DNA, proteins, and other macromolecules (38). However, cancer cells usually constitute relatively high level of ROS due to the endoplasmic reticulum (ER) stress and aberrant signaling pathways that are related with cellular metabolism (38). Accompanied with the high level of ROS, cancer cells also contain relatively high level of ROS scavengers, such as nuclear factor erythroid 2-related factor 2 (Nrf2) and glutathione (GSH) (38). Some studies have suggested that ROS in cancer promotes tumorigenesis (36, 39). For instance, chronic oxidative stress has been shown to enhance the tumorigenic potential and chemoresistance of ER+ breast cancer cell line MCF-7 by upregulating a number of pro-metastatic genes including vascular endothelial growth factor (VEGF) and CD44(13). With this background, we set to further study the biology of RU/RR cells, with the question whether RU cells can acquire tumorigenic potential and behave like RR cells upon oxidative stress.

One of the key findings of this study is that RU cells derived from ALK+ALCL can be induced to convert to RR cells upon oxidative challenge. Since our previous publications and current study indicated that RR cells are more clonogenic/tumorigenic, chemoresistant, and enhanced sphere-forming ability than RU cells (20, 21), the finding in this study represents a biological process of CSC plasticity or “acquired cancer stemness”, a concept that has been well-documented in a number of studies (9-11, 40). In fact, oxidative stress or other adversities has been shown related with CSC plasticity or “acquired cancer stemness” in some studies (10, 40-42). For example, Saijo *et al* reported that oxidative stress can induce the dedifferentiation of lung cancer non-CSCs into CSCs under oxidative stress through activating the transcription factor Homeobox A5 (HOXA5) and upregulating Sox2 expression (43). Hypoxia stress, an inducer of endogenous oxidative stress (36), also promotes the self-renewal capacity and enriches the CD133+ glioma stem cells population through activating PI3K/AKT and ERK1/2 pathways, whereas inhibition of PI3K/AKT or ERK1/2 significantly abrogates the CD133 expansion induced by hypoxia challenge (14). To our knowledge, the concept of CSC plasticity or “acquired cancer stemness” were mostly investigated in solid cancer models, studies in haematological malignancies are extremely few. We believe that data from this study supports the existence and molecular mechanisms of tumor plasticity induced by oxidative stress in haematological neoplasm – ALK+ALCL.

To the best of our knowledge, the study models for CSC plasticity or “acquired cancer stemness” are extremely few, and most of the studies of “acquired cancer stemness” have focused on either the changes of expression levels of stem cell surface markers

(e.g. CD133 and CD44) or the percentages of side population cells, a small fraction of cells that are believed to be CSCs (22, 40, 41, 44-47). With literature search, we only found one recent publication in which the authors used a colorectal cancer cell model which harbors Wnt reporter with GFP as single readout (47). Specifically, the authors found that the Wnt reporter unresponsive colorectal cancer cells are able to convert to reporter responsive cells, which carry more stem-like features, upon the activation of Wnt pathway by hepatocyte growth factor (HGF) (47). We also believe the RU/RR model presented in our study is also a good tool for studying CSC plasticity, as the dynamic conversion of RU to RR cells can be simply detected by analyzing the expression of GFP and luciferase. In brief, we believe our RU/RR model is an easy and effective tool for studying CSC plasticity or “acquired cancer stemness”.

While the phenomenon that RU cells convert to RR cells is not restricted to ALK+ALCL cell lines. Our lab recently have published that RU cells derived from two types of solid cancers, including ER+ breast cancer cell lines and esophagus squamous cancer cells, can also be induced to convert to RR cells upon oxidative challenge (22, 48). Gopal *et al* reported that Sox2 is implicated in the RU to RR cells conversion in ER+ breast cancer cells, but the detailed molecular mechanisms were not investigated (22). As for esophagus squamous cancer model, the activated PI3K/AKT/MYC is responsible for the RU to RR cells conversion induced by oxidative stress(48). Unlike ER+ breast cancer and the esophagus squamous cancer models, in the current study we found that it is the active Wnt/ $\beta$ -catenin/MYC/Sox2 axis that contributes to the RU to RR cells conversion in ALK+ALCL cell model. These studies have indicated that RU to RR cells

conversion is a universal phenomenon, but the underlying molecular mechanisms occur in a cellular context-dependent manner.

It has been previously revealed that oxidative stress (e.g. H<sub>2</sub>O<sub>2</sub>) can activate a number of molecules and cellular signaling pathways (e.g. PI3K/AKT, MAPK/ERK, Wnt/ $\beta$ -catenin, and STAT3) (35), of which Wnt/ $\beta$ -catenin is one of the most well-known pathways regulating cell pluripotency and differentiation (12). Funato *et al* reported that ROS activates the Wnt/ $\beta$ -catenin pathway by stabilizing  $\beta$ -catenin and interrupting the interaction between dishevelled (Dvl) and nucleoredoxin (NRX), a strong inhibitor of Wnt/ $\beta$ -catenin signaling (49). Keeping in line with this report, we also observed the stabilized  $\beta$ -catenin protein in the converted RR cells, as well as the RR cells upon H<sub>2</sub>O<sub>2</sub> re-challenge. The stabilized  $\beta$ -catenin protein subsequently upregulates its downstream targets, including MYC. Our previous study suggested that the high level of MYC promotes Sox2 DNA binding and its transcriptional activity, and the transcriptionally active Sox2 in turn further potentiates the expression/activation of Wnt/ $\beta$ -catenin pathway (21). Indeed, in this study we found the potentiated Sox2-DNA binding and upregulated expression of Sox2 downstream targets, such as *CTNNB1* and *WNT2B*, in the converted RR cells, as compared to native RU cells. Results from current study further supported our RR cells model in which Wnt/ $\beta$ -catenin/MYC axis drives Sox2 transcriptional activity, which thereafter potentiates the Wnt/ $\beta$ -catenin activity, inducing a positive forward loop (21). Nevertheless, oxidative stress has also been shown to be critical for maintaining the active status of NPM-ALK kinase in ALK+ALCL (50), as inhibition of ROS generation by using a pharmacological

inhibitor—nordihydroguaiaretic acid (NDGA) led to the decreased activation of NPM-ALK, as well as its downstream molecules, including STAT3, AKT and ERK1/2 (50). In our study, the activation status/expression level of NPM-ALK and STAT3 in both RU and RR cells derived from SupM2 show slight or no changes upon H<sub>2</sub>O<sub>2</sub> re-challenge (**Figure 4.3A**). This conflicting result may be caused by different experimental protocols applied. Specifically, we created a chronic oxidative circumstance by using a low dose of H<sub>2</sub>O<sub>2</sub> (0.3 mM) in our experimental model, while the authors of the report discussed above transiently subjected ALK+ALCL cells with high dose (1 mM) of H<sub>2</sub>O<sub>2</sub> (for 1 hour) (50). Of note, we did find the robustly activated ERK1/2 after H<sub>2</sub>O<sub>2</sub> re-challenge in both RU and RR cells (**Figure 4.3A**). Given that pERK1/2 are known to positively regulate the phosphorylation and stabilization of MYC protein (31, 51), it is highly likely that pERK1/2 are involved in the RU to RR cells conversion induced by oxidative stress in this context. In addition to this, our preliminary data also suggested that ERK1/2 is preferentially activated in RR cells to RU cells, and inhibition of ERK1/2 activity by MEK inhibitor U0126 in RR cells dramatically decreased the expression levels of MYC and Sox2, along with the significantly decreased SRR2 luciferase activity (**Figure 4.5A-C**). Nevertheless, further studies are necessary to unearth the biological roles of active ERK1/2 in the RU to RR cells conversion in ALK+ALCL.

Our data also suggested that pharmacological inhibition of MYC or its upregulator –  $\beta$ -catenin can significantly abrogate the RU to RR cells conversion induced by oxidative stress, furthering highlighting the biological significance of  $\beta$ -catenin and MYC in our RR cells model. In addition, although Sox2 expression is not appreciably altered in RU

cells derived from SupM2 upon H<sub>2</sub>O<sub>2</sub> re-challenge, siRNA knockdown of Sox2 significantly abolished the RU to RR cells conversion. Correlating well with this data, we found that Sox2 in the converted RR cells indeed bind DNA more efficiently and has increased transcriptional activity, as compared to native RU cells. Regarding the transcriptional activity of Sox2 in our experimental model, there is another possibility which is Sox2 being more phosphorylated or only phosphorylated in RR cells and the converted RR cells, instead of RU cells; because phosphorylation of Sox2 is reported to be essential for Sox2 transcriptional activity and stemness features in mouse embryonic stem cells (mESCs) and CSCs (52-54). For instance, Sox2 phosphorylated by AKT1 at threonine 118 (T118) is essential for Sox2 protein stabilization and its transcriptional activity to promote the pluripotent state of mESCs, while mESCs harboring mutated Sox2<sup>T118A</sup> has significantly attenuated pluripotency, as compared to cells transfected with wild-type Sox2 (52, 54). In cancer stem-like lung squamous carcinoma cells, protein kinase C  $\alpha$  (PKC $\alpha$ ) has been reported to interact directly and phosphorylate Sox2 at Threonine 118 which subsequently enhances the hedgehog pathway to maintain a cancer stem-like phenotype (53). However, due to the lack of commercial antibody against human phosphorylated Sox2, phosphorylation of Sox2 in human cancer is extremely poorly understood. It will be of interest and value for an in-depth understanding of the cell biology of RU, RR, and the converted RR cells by investigating the phosphorylation status of Sox2 in these cells.

In addition, STAT1 is reported to be a tumor suppressor in ALK+ALCL (6). We were curious whether STAT1 is involved in RU/RR dichotomy or the RU to RR cells conversion induced by oxidative stress. However, data from this study suggested that

STAT1 is not consistently preferentially activated in either RU or RR cells from the two cell lines we utilized in our study, indicating that the activated STAT1 might not be an important regulator of the RU/RR dichotomy. Nevertheless, we observed that STAT1 is activated in RU and RR cells derived from SupM2 with H<sub>2</sub>O<sub>2</sub> transient exposure and re-challenge treatment (**Figure 4.6A and 4.6C**), in keeping with a previous report which showed that oxidative stress activates STAT1 in rat basilar arteries (55). The activated STAT1 has been shown to suppress MYC expression in some cell models (32, 33). In line with this, we also observed that STAT1 downregulates MYC expression in ALK+ALCL cell lines using Tet on-inducible system (**Figure 4.6D**). Of note, MYC expression is upregulated in both RU and RR cells upon H<sub>2</sub>O<sub>2</sub> re-challenge, despite that STAT1 is also activated in this biological process. This may be explained by that oxidative stress-induced STAT1 activation is not sufficient to antagonize the oxidative stress-activated Wnt/ $\beta$ -catenin pathway that upregulates MYC expression in our cell models. Nevertheless, it will be of interest to investigate the biological role of STAT1 in the RU to RR cells conversion induced by oxidative stress.

In summary, our study has demonstrated a novel experimental model in which acquired tumorigenic potential upon oxidative stress was shown in ALK+ALCL, and highlighted the significance of the Wnt/ $\beta$ -catenin/MYC/Sox2 axis in this biological process.

#### 4.5 References

1. Ferreri AJ, Govi S, Pileri SA, Savage KJ. Anaplastic large cell lymphoma, ALK-positive. *Crit Rev Oncol Hematol*. 2012;83(2):293-302.

2. Piccaluga PP, Gazzola A, Mannu C, Agostinelli C, Bacci F, Sabbatini E, et al. Pathobiology of anaplastic large cell lymphoma. *Adv Hematol*. 2010;345053.
3. Amin HM, Lai R. Pathobiology of ALK+ anaplastic large-cell lymphoma. *Blood*. 2007;110(7):2259-67.
4. Amin HM, McDonnell TJ, Ma Y, Lin Q, Fujio Y, Kunisada K, et al. Selective inhibition of STAT3 induces apoptosis and G(1) cell cycle arrest in ALK-positive anaplastic large cell lymphoma. *Oncogene*. 2004;23(32):5426-34.
5. Raetz EA, Perkins SL, Carlson MA, Schooler KP, Carroll WL, Virshup DM. The nucleophosmin-anaplastic lymphoma kinase fusion protein induces c-Myc expression in pediatric anaplastic large cell lymphomas. *The American journal of pathology*. 2002;161(3):875-83.
6. Wu C, Molavi O, Zhang H, Gupta N, Alshareef A, Bone KM, et al. STAT1 is phosphorylated and downregulated by the oncogenic tyrosine kinase NPM-ALK in ALK-positive anaplastic large-cell lymphoma. *Blood*. 2015;126(3):336-45.
7. Han Y, Amin HM, Frantz C, Franko B, Lee J, Lin Q, et al. Restoration of shp1 expression by 5-AZA-2'-deoxycytidine is associated with downregulation of JAK3/STAT3 signaling in ALK-positive anaplastic large cell lymphoma. *Leukemia*. 2006;20(9):1602-9.
8. Zhang Q, Wang HY, Liu X, Wasik MA. STAT5A is epigenetically silenced by the tyrosine kinase NPM1-ALK and acts as a tumor suppressor by reciprocally inhibiting NPM1-ALK expression. *Nature medicine*. 2007;13(11):1341-8.
9. Cabrera MC, Hollingsworth RE, Hurt EM. Cancer stem cell plasticity and tumor hierarchy. *World J Stem Cells*. 2015;7(1):27-36.



10. Tang DG. Understanding cancer stem cell heterogeneity and plasticity. *Cell research*. 2012;22(3):457-72.
11. Meacham CE, Morrison SJ. Tumour heterogeneity and cancer cell plasticity. *Nature*. 2013;501(7467):328-37.
12. Oren O, Smith BD. Eliminating Cancer Stem Cells by Targeting Embryonic Signaling Pathways. *Stem cell reviews*. 2016.
13. Mahalingaiah PK, Singh KP. Chronic oxidative stress increases growth and tumorigenic potential of MCF-7 breast cancer cells. *PloS one*. 2014;9(1):e87371.
14. Soeda A, Park M, Lee D, Mintz A, Androutsellis-Theotokis A, McKay RD, et al. Hypoxia promotes expansion of the CD133-positive glioma stem cells through activation of HIF-1alpha. *Oncogene*. 2009;28(45):3949-59.
15. Kemper K, de Goeje PL, Peeper DS, van Amerongen R. Phenotype switching: tumor cell plasticity as a resistance mechanism and target for therapy. *Cancer research*. 2014;74(21):5937-41.
16. Chen W, Dong J, Haiech J, Kilhoffer MC, Zeniou M. Cancer Stem Cell Quiescence and Plasticity as Major Challenges in Cancer Therapy. *Stem Cells Int*. 2016;2016:1740936.
17. Doherty MR, Smigiel JM, Junk DJ, Jackson MW. Cancer Stem Cell Plasticity Drives Therapeutic Resistance. *Cancers*. 2016;8(1).
18. Wu F, Zhang J, Wang P, Ye X, Jung K, Bone KM, et al. Identification of two novel phenotypically distinct breast cancer cell subsets based on Sox2 transcription activity. *Cellular signalling*. 2012;24(11):1989-98.

19. Zhang HF, Wu C, Alshareef A, Gupta N, Zhao Q, Xu XE, et al. The PI3K/AKT/c-MYC axis promotes the acquisition of cancer stem-like features in esophageal squamous cell carcinoma. *Stem cells*. 2016.
20. Gelebart P, Hegazy SA, Wang P, Bone KM, Anand M, Sharon D, et al. Aberrant expression and biological significance of Sox2, an embryonic stem cell transcriptional factor, in ALK-positive anaplastic large cell lymphoma. *Blood Cancer J*. 2012;2:e82.
21. Wu C, Zhang HF, Gupta N, Alshareef A, Wang Q, Huang YH, et al. A positive feedback loop involving the Wnt/beta-catenin/MYC/Sox2 axis defines a highly tumorigenic cell subpopulation in ALK-positive anaplastic large cell lymphoma. *Journal of hematology & oncology*. 2016;9(1):120.
22. Gopal K, Gupta N, Zhang H, Alshareef A, Alqahtani H, Bigras G, et al. Oxidative stress induces the acquisition of cancer stem-like phenotype in breast cancer detectable by using a Sox2 regulatory region-2 (SRR2) reporter. *Oncotarget*. 2016;7(3):3111-27.
23. Zmijewski JW, Banerjee S, Bae H, Friggeri A, Lazarowski ER, Abraham E. Exposure to hydrogen peroxide induces oxidation and activation of AMP-activated protein kinase. *The Journal of biological chemistry*. 2010;285(43):33154-64.
24. Reliene R, Fischer E, Schiestl RH. Effect of N-acetyl cysteine on oxidative DNA damage and the frequency of DNA deletions in atm-deficient mice. *Cancer research*. 2004;64(15):5148-53.
25. Marampon F, Ciccarelli C, Zani BM. Down-regulation of c-Myc following MEK/ERK inhibition halts the expression of malignant phenotype in rhabdomyosarcoma and in non muscle-derived human tumors. *Molecular cancer*. 2006;5:31.

26. Wang H, Chauhan J, Hu A, Pendleton K, Yap JL, Sabato PE, et al. Disruption of Myc-Max heterodimerization with improved cell-penetrating analogs of the small molecule 10074-G5. *Oncotarget*. 2013;4(6):936-47.
27. Zhang J, Gill AJ, Issacs JD, Atmore B, Johns A, Delbridge LW, et al. The Wnt/beta-catenin pathway drives increased cyclin D1 levels in lymph node metastasis in papillary thyroid cancer. *Human pathology*. 2012;43(7):1044-50.
28. Gaitanaki C, Konstantina S, Chrysa S, Beis I. Oxidative stress stimulates multiple MAPK signalling pathways and phosphorylation of the small HSP27 in the perfused amphibian heart. *J Exp Biol*. 2003;206(Pt 16):2759-69.
29. Zhang L, Jope RS. Oxidative stress differentially modulates phosphorylation of ERK, p38 and CREB induced by NGF or EGF in PC12 cells. *Neurobiol Aging*. 1999;20(3):271-8.
30. Tsai WB, Aiba I, Long Y, Lin HK, Feun L, Savaraj N, et al. Activation of Ras/PI3K/ERK pathway induces c-Myc stabilization to upregulate argininosuccinate synthetase, leading to arginine deiminase resistance in melanoma cells. *Cancer research*. 2012;72(10):2622-33.
31. Sears R, Nuckolls F, Haura E, Taya Y, Tamai K, Nevins JR. Multiple Ras-dependent phosphorylation pathways regulate Myc protein stability. *Genes & development*. 2000;14(19):2501-14.
32. Dimberg A, Karlberg I, Nilsson K, Oberg F. Ser727/Tyr701-phosphorylated Stat1 is required for the regulation of c-Myc, cyclins, and p27Kip1 associated with ATRA-induced G0/G1 arrest of U-937 cells. *Blood*. 2003;102(1):254-61.

33. Ramana CV, Grammatikakis N, Chernov M, Nguyen H, Goh KC, Williams BR, et al. Regulation of c-myc expression by IFN-gamma through Stat1-dependent and -independent pathways. *The EMBO journal*. 2000;19(2):263-72.
34. Reuter S, Gupta SC, Chaturvedi MM, Aggarwal BB. Oxidative stress, inflammation, and cancer: how are they linked? *Free radical biology & medicine*. 2010;49(11):1603-16.
35. Sosa V, Moline T, Somoza R, Paciucci R, Kondoh H, ME LL. Oxidative stress and cancer: an overview. *Ageing research reviews*. 2013;12(1):376-90.
36. Klaunig JE, Kamendulis LM, Hocevar BA. Oxidative stress and oxidative damage in carcinogenesis. *Toxicologic pathology*. 2010;38(1):96-109.
37. Janssen-Heininger YM, Mossman BT, Heintz NH, Forman HJ, Kalyanaraman B, Finkel T, et al. Redox-based regulation of signal transduction: principles, pitfalls, and promises. *Free radical biology & medicine*. 2008;45(1):1-17.
38. Gorrini C, Harris IS, Mak TW. Modulation of oxidative stress as an anticancer strategy. *Nature reviews Drug discovery*. 2013;12(12):931-47.
39. Waris G, Ahsan H. Reactive oxygen species: role in the development of cancer and various chronic conditions. *Journal of carcinogenesis*. 2006;5:14.
40. Molina JR, Hayashi Y, Stephens C, Georgescu MM. Invasive glioblastoma cells acquire stemness and increased Akt activation. *Neoplasia*. 2010;12(6):453-63.
41. El Khoury F, Corcos L, Durand S, Simon B, Le Jossic-Corcos C. Acquisition of anticancer drug resistance is partially associated with cancer stemness in human colon cancer cells. *International journal of oncology*. 2016.

42. Zhou M, Hou Y, Yang G, Zhang H, Tu G, Du YE, et al. LncRNA-Hh Strengthen Cancer Stem Cells Generation in Twist-Positive Breast Cancer via Activation of Hedgehog Signaling Pathway. *Stem cells*. 2016;34(1):55-66.
43. Saijo H, Hirohashi Y, Torigoe T, Horibe R, Takaya A, Murai A, et al. Plasticity of lung cancer stem-like cells is regulated by the transcription factor HOXA5 that is induced by oxidative stress. *Oncotarget*. 2016.
44. Das B, Tsuchida R, Malkin D, Koren G, Baruchel S, Yeger H. Hypoxia enhances tumor stemness by increasing the invasive and tumorigenic side population fraction. *Stem cells*. 2008;26(7):1818-30.
45. Hu X, Ghisolfi L, Keates AC, Zhang J, Xiang S, Lee DK, et al. Induction of cancer cell stemness by chemotherapy. *Cell cycle*. 2012;11(14):2691-8.
46. Ghisolfi L, Keates AC, Hu X, Lee DK, Li CJ. Ionizing radiation induces stemness in cancer cells. *PloS one*. 2012;7(8):e43628.
47. Vermeulen L, De Sousa EMF, van der Heijden M, Cameron K, de Jong JH, Borovski T, et al. Wnt activity defines colon cancer stem cells and is regulated by the microenvironment. *Nature cell biology*. 2010;12(5):468-76.
48. Zhang HF, Wu C, Alshareef A, Gupta N, Zhao Q, Xu XE, et al. The PI3K/AKT/c-MYC Axis Promotes the Acquisition of Cancer Stem-Like Features in Esophageal Squamous Cell Carcinoma. *Stem cells*. 2016;34(8):2040-51.
49. Funato Y, Michiue T, Asashima M, Miki H. The thioredoxin-related redox-regulating protein nucleoredoxin inhibits Wnt-beta-catenin signalling through dishevelled. *Nature cell biology*. 2006;8(5):501-8.

50. Thornber K, Colomba A, Ceccato L, Delsol G, Payraastre B, Gaits-Iacovoni F. Reactive oxygen species and lipoxygenases regulate the oncogenicity of NPM-ALK-positive anaplastic large cell lymphomas. *Oncogene*. 2009;28(29):2690-6.
51. Sears R, Leone G, DeGregori J, Nevins JR. Ras enhances Myc protein stability. *Molecular cell*. 1999;3(2):169-79.
52. Fang L, Zhang L, Wei W, Jin X, Wang P, Tong Y, et al. A methylation-phosphorylation switch determines Sox2 stability and function in ESC maintenance or differentiation. *Molecular cell*. 2014;55(4):537-51.
53. Justilien V, Walsh MP, Ali SA, Thompson EA, Murray NR, Fields AP. The PRKCI and SOX2 oncogenes are coamplified and cooperate to activate Hedgehog signaling in lung squamous cell carcinoma. *Cancer cell*. 2014;25(2):139-51.
54. Jeong CH, Cho YY, Kim MO, Kim SH, Cho EJ, Lee SY, et al. Phosphorylation of Sox2 cooperates in reprogramming to pluripotent stem cells. *Stem cells*. 2010;28(12):2141-50.
55. Osuka K, Watanabe Y, Usuda N, Atsuzawa K, Wakabayashi T, Takayasu M. Oxidative stress activates STAT1 in basilar arteries after subarachnoid hemorrhage. *Brain research*. 2010;1332:12-9.

## CHAPTER 5

### General Discussion and Conclusions

---

## 5.1 Thesis overview

In this thesis, I have further investigated the molecular mechanisms underlining the pathobiology of ALK+ALCL by demonstrating deregulated proteins or signaling pathways directly or indirectly related with NPM-ALK which is the key oncogenic driver in this malignance (1). In Chapter 2, I presented that the expression of STAT1 is decreased in ALK+ALCL because of NPM-ALK that induces the phosphorylation of STAT1 at Y701 and thereby promotes STAT1 degradation in a STAT3-dependent proteasome manner (2). In Chapter 3, I presented the molecular mechanisms underlining the dichotomy of two distinct cell populations derived from ALK+ALCL cell lines, namely RU and RR cells, based on their differential responsiveness to a Sox2 reporter – SRR2. In this study, I found that NPM-ALK/STAT3 is involved in the RU/RR dichotomy, as NPM-ALK/STAT3 provides the basal expression levels of MYC and Sox2 in both RU and RR cells. However, the NPM-ALK/STAT3 axis alone does not account for the distinct biological and biochemical differences between RU and RR cells, because RU and RR cells exhibit a similar expression/activation of NPM-ALK/STAT3 (3). Briefly, in this study I found that the positive loop involving Wnt/ $\beta$ -catenin/MYC/Sox2 axis defines the biochemical features of RR cells that carry high tumorigenicity and chemoresistance. In Chapter 4, I showed that RU cells derived from ALK+ALCL can be induced to convert to RR cells by oxidative stress, a biological process known as “acquired tumorigenic potential” or tumor plasticity. In this study, I found that the converted RR cells share similar biological functions and biochemical features with native RR cells; moreover, increased expression/activity of Wnt/ $\beta$ -



catenin/MYC/Sox2 axis is required for the RU to RR cells conversion induced by oxidative stress.

## **5.2 STAT1 in ALK+ALCL**

STAT1 has been widely studied in a number of cancer models, including breast cancer (4-6), esophagus squamous cancer (7, 8), melanoma (9, 10), and T-cell leukemia (11, 12). Intriguingly, STAT1 serves as either a tumor suppressor or a tumor promoter in different types of cancer or even in the same type of cancer of different disease stages, indicating the importance of cellular context in determining the biological roles of STAT1 in cancer (13-17).

The downregulation of STAT1 expression in cancer cells has been reported in a few studies (7, 8, 18, 19); however, how STAT1 expression is decreased in cancer remains poorly studied. In this study, using immunohistochemical staining, I demonstrated that STAT1 expression is decreased/lost in 7/7 ALK+ALCL primary tumor samples by using immunohistochemical staining, while STAT1 expression is relatively high in 5/5 ALK-ALCL (2). One of the limitations of this study is the very small number of primary patient samples used. It would be more convincing to include a large cohort of primary tumor cases in this study, and it is also of interest to study whether the expression level of STAT1 correlates with disease progression in ALK+ALCL patients. Regarding this, the Lai lab previously published that the high expression of STAT1 correlates with favourable prognosis in esophagus squamous carcinoma patients (n=131) (7).

Surprisingly, NPM-ALK is directly implicated in the downregulation of STAT1 in ALK+ALCL, as it promotes the phosphorylation of STAT1 at Y701, an active form of STAT1, and facilitates its degradation in ubiquitin-proteasome pathway (2). A recent study has indicated that phosphorylation of STAT1 at Y701, being the major form of ubiquitinated STAT1 induced by IFNs, is rapidly degraded in ubiquitin-proteasome pathway in 293T cells (20). My data also suggests that STAT3 is required in this biological process, despite the underlining mechanism being not investigated (2). There is evidence showing that the E3 ubiquitin ligase – MDM2 is the mediator of STAT3 in downregulating the tumor suppressor p53 in ubiquitin-dependent proteasome pathway in colorectal cancer and prostate cancer (21, 22). Identification of the mediator of NPM-ALK/STAT3–induced STAT1 downregulation in ALK+ALCL would provide more details for the in-depth understanding of STAT3/STAT1 interaction.

I have also shown that STAT1 functions as a potent tumor suppressor, if its overexpressed to a relatively high level, in ALK+ALCL *in vitro* and *in vivo* (2). Consistent with other reports, activation of STAT1 attenuates the STAT3 transcriptional activity by decreasing STAT3 DNA binding/downstream targets and increasing the ratio of STAT1/STAT3 heterodimers (23). Of note, in my study, it would be helpful to further understand the biological functions of STAT1 in ALK+ALCL by identifying the gene expression profiles upon STAT1 overexpression.

### 5.3 The RU/RR dichotomy in ALK+ALCL

The concept of intra-tumor heterogeneity has been well documented in a few recent reviews (24-28), while our understanding of intra-tumor heterogeneity in haematological neoplasms remains poor. Lai lab previously revealed two distinct cell populations in ALK+ALCL cell lines using a Sox2 reporter-SRR2 (3). The cells responsive to the reporter (RR) cells are found to be more invasive, tumorigenic and chemoresistant than cells unresponsive to the reporter (RU) (3). A recent literature reported that the CSCs derived from ALK+ALCL cell lines and patient samples, identified by side population technique, harbor relatively high protein level of NPM-ALK and ABCG2, a cell surface drug transporter, as compared to the major cell population (29). I firstly tested whether RR cells are enriched with these side population cells by using the side population technique. However, I was unable to detect these small side population cells in both RU and RR cells, and this has been discussed in section 3.4 of Chapter 3. Considering that RR cells share some cancer stem-like phenotypes (e.g. chemoresistance and sphere-forming ability), I then tested whether RR cells share biochemical features with these CSCs derived from ALK+ALCL cell lines identified by the above authors, such as the expression level of NPM-ALK and ABCG2 (29). However, my data suggests that RU and RR cells express almost identical level of NPM-ALK (in protein level) and ABCG2 (in mRNA level). In brief, my data suggests that RR cells have different biochemical features with the tumor-propagating cells identified by the side population assay as reported by Moti *et al*, further indicating the complexity of ALK+ALCL intra-tumor heterogeneity (25).

My study presented in Chapter 3 unearths that MYC is a key player in the RU/RR dichotomy. Specifically, as a result of the highly active Wnt/ $\beta$ -catenin pathway, RR cells express a higher level of MYC than RU cells, and the high level of MYC promotes Sox2 DNA binding and its transcriptional activity. The transcriptionally active Sox2 enhances the activation of Wnt/ $\beta$ -catenin pathway, which thereafter increases the expression of MYC, thus forming a positive forward loop. My data also suggests that modulation of the Wnt/ $\beta$ -catenin pathway can influence SRR2 reporter responsiveness in RU cells, as evidenced by that in the transwell experiment RU cells can convert to “RR-like” cells when co-cultured with RR cells which express a relative higher level of Wnt ligands, such as Wnt2B. Regarding the transwell experiment presented in Chapter 3, one may ask why RU cells are not able to convert to RR cells in the cultured ALK+ALCL cells before sorting RU and RR cells. I do consider that RR cells only account for a small percentage of whole cell populations, and the cytokines secreted by RR cells (e.g. Wnt2B) are much diluted in the cultured medium, thus the conversion of RU cells to “RR-like” induced by these cytokines is inappreciable. This notion has been supported by my result that RU cells are not able to convert to RR cells when co-cultured with parental ALK+ALCL cells or diluted RR cells (e.g. The dilution of RR/RU=1:10).

Regarding the phosphorylation status of Sox2 in RU and RR cells, I speculate that Sox2 is only phosphorylated or more Sox2 is phosphorylated in RR cells in comparison to RU cells, as Sox2 phosphorylation is known to be essential for maintaining stemness in embryonic stem cells and CSCs (30-33). Sox2 phosphorylation in cancer cells is poorly studied because of the lack of commercial and reliable antibody against human phosphorylated Sox2. The Lai lab previously used mass spectrometry assay and

identified two potential phosphorylation sites of Sox2, Threonine 116 and Threonine 118, which only exist in RR cells derived from ER+ breast cancer cell line MCF-7 (Wu F, personal communication, Sept, 2012). It would be of interest to perform the similar study in RU and RR cells derived from ALK+ALCL, and further studies are needed to investigate the phosphorylation status and residues of Sox2 in the RU/RR dichotomy for an in-depth understanding of the biology of RU and RR cells.

In this study, I also observed that RU cells with overexpressed MYC are not exactly RR cells, despite that RU cells with MYC overexpression have demonstrated as comparable chemoresistance and tumorigenicity as RR cells do. As shown in Chapter 3, RU cells stably transfected with *MYC* still have significantly lower SRR2 reporter activity than RR cells. This indirectly suggests that additional factors are required in RU cells to fully drive SRR2 reporter responsiveness.

Another interesting observation in my experience is that RR cells automatically lose SRR2 reporter activity to become “RU-like” cells in the long term cell culture condition. Specifically, in regular cell culture condition, RR cells derived from SupM2 and Karpas 299 with initial purity of >95% GFP-positive cells, would gradually lose GFP-positive cells and eventually reach a stable state containing ~40% and ~10% GFP-positive cells, respectively, in 20 weeks. In contrast, RU cells, the GFP-negative cells, always remain in a relatively stable state. This phenomenon reveals that RR cells, a more tumorigenic and cancer stem-like cell population, would automatically differentiate to a less tumorigenic or cancer stem-like state, supporting the CSC model in which CSCs are capable to differentiate into non-CSCs (25). Of note, in my study, I cannot name RR cells as CSC cells because of the lack of serial transplantation assay, which is the gold

standard assay for identifying CSCs (34). Therefore, to compare the tumor-initiating ability of RU and RR cells, the serial transplantation assay should be performed in immunodeficient mice, which is also my future study plan.

#### **5.4 Oxidative stress-induced tumorigenic potential in ALK+ALCL**

“Acquired cancer stemness” or CSC plasticity is a popular concept that has been raised in recent years (25, 27, 35, 36). It is believed that the CSC phenotype is a dynamic state that can be acquired by non-stem cells if appropriate stimuli and microenvironment are present (9). For instance, it has been observed that a subset of transformed human mammary epithelial cells spontaneously de-differentiate into stem-like cells both *in vitro* and *in vivo* (37). In another study, fludarabine was used to induce the non-side population cells derived from chronic lymphocytic leukemia to become side population cells which are shown to be more chemoresistant (38). CSC plasticity has been postulated to be a major mechanism to explain how cancer cells develop resistance to chemotherapy, and ultimately, to contribute to cancer treatment failure (36, 39, 40).

However, due to the lack of good cell models, the exact molecular mechanisms underlying “acquired cancer stemness” or CSC plasticity are not well-understood, especially in haematological malignancies. I believe the RU/RR cell model is a good tool for studying tumor plasticity. In Chapter 4, I showed that RU cells can be induced to convert to RR cells upon oxidative stress. Further evidence showed that the converted RR cells share similar biological functions and biochemical features with native RR cells.

Although oxidative stress-induced “acquisition of stemness” has been recently reported in ER+ breast cancer cell lines, patient samples, and esophagus squamous cancer cells, the molecular mechanisms underlined were completely distinct (41, 42). In my model, I found the active Wnt/ $\beta$ -catenin/MYC/Sox2 axis is responsible for the RU/RR conversion induced by oxidative stress.

However, I also observed the ERK1/2 is highly active in both RU and RR cells upon H<sub>2</sub>O<sub>2</sub> re-challenge. Although the biological role of active ERK1/2 in the RU to RR cells conversion induced by oxidative stress is not investigated in my study, it is likely that active ERK1/2 partially contributes to this conversion, as active ERK1/2 is shown to phosphorylate and stabilize MYC in various cell models (43-46). My data also suggests that ERK1/2 is preferentially activated in RR cells and inhibition of ERK1/2 activity by using MEK inhibitor U0126 in RR cells dramatically decreased the MYC protein level and the SRR2 luciferase activity, suggesting the involvement of active ERK1/2 in the RU/RR dichotomy (**Figure 4.5**). Further studies are required to understand the biological roles of active ERK1/2 in the RU to RR cells conversion.

Another interesting question in this study is that whether Sox2 is phosphorylated in the converted RR cells, and what kinase(s) is involved here to interact and phosphorylate Sox2. As indicated in a number of reports, phosphorylated Sox2 is implicated in maintaining stemness in embryonic stem cells and CSCs (30-33). To my knowledge, there is no literature so far reporting the relationship of phosphorylated Sox2 and oxidative stress in either ESCs or cancer cells models. It will be of interest to delineate the phosphorylation status of Sox2 in the converted RR cells induced by oxidative stress, with comparison to RU and native RR cells.

In addition to oxidative stress, hypoxia stress also appears to be a good tool to study tumor plasticity using RU/RR cells model. Hypoxia stress, a specific tumor microenvironment caused by low oxygen supplements (47), has been reported to induce cancer stemness in a wide range type of human cancer and this notion has been well reviewed in some recent literature (47-50). Whether hypoxia challenge also induces RU to RR cells conversion needs further investigation.

### **5.5 STAT1 and the RU/RR dichotomy**

As shown in Chapter 2, STAT1 is a potent tumor suppressor in ALK+ALCL. Overexpression of STAT1 induces cell cycle-arrest and cell apoptosis at least by downregulating STAT3 downstream targets, including Survivin, Bcl2 and MYC (**Figure 2.5 and Figure 4.6C**). Initially I also tested whether STAT1 is differentially expressed or activated in RU and RR cells, thus partially contributing to the RU/RR dichotomy. However, the Western blotting results suggested that RU and RR cells derived from SupM2 and Karaps 299 express similar levels of total STAT1, with inconsistent patterns of active STAT1 level between the two cell subsets (**Figure 4.6A-B**). This result indicates that the RU/RR dichotomy is not attributed to the different level of active STAT1 in the two cell subsets. Notably, the biological function of STAT1 is studied in ALK+ALCL cells as a whole cell population in Chapter 2. It is reasonable to propose that overexpression of STAT1 may not be able to induce as sufficient cell apoptosis or cell cycle-arrest in RR cells as it does in RU cells, because RR cells carry more cancer stem-like features including chemoresistance and sphere-forming ability. To support this, further studies are needed to compare the sensitivity of RU and RR cells to STAT1



overexpression-induced cell apoptosis or cell cycle-arrest. Of note, whether overexpression of STAT1 can diminish the biological or biochemical features of RR cells is another interesting question. To my knowledge, the biological role of STAT1 in cancer stem cells has not been investigated yet.

In addition, I observed that STAT1 is activated in both RU and RR cells derived from SupM2 upon H<sub>2</sub>O<sub>2</sub> re-challenge (**Figure 4.6C**). The active STAT1 has been shown to suppress MYC expression in some cell models (51, 52). In keeping with this notion, I also found that constitutively active STAT1 downregulates MYC expression in Tet on-inducible SupM2-STAT1C cells (**Figure 4.6D**). However, the active STAT1 stimulated by oxidative re-challenge was not able to downregulate MYC expression in RU cells upon H<sub>2</sub>O<sub>2</sub> re-challenge, this is probably because of the oxidative stress-activated Wnt/ $\beta$ -catenin pathway which in contrast promotes MYC expression and counteracts the activated STAT1 pathway.

## **5.6 Conclusions and future directions**

Overall, my study, firstly, has revealed a novel mechanism of downregulation of STAT1 by NPM-ALK in STAT3-dependent proteasome pathway, representing a novel mechanism by which NPM-ALK exerts its oncogenic role in ALK+ALCL. It is of paramount interest to study whether other tyrosine kinases have similar effects on STAT1 in other types of cancer models. STAT1 functions as a potent tumor suppressor in ALK+ALCL if it is overexpressed to a relatively high level. The interplay between STAT1 and STAT3 has also been well demonstrated in my study. In brief, this study

has revealed that STAT1 and STAT3 act as Ying and Yang in oncogenesis in ALK+ALCL cell model, providing insight into the functional interaction of STAT1/STAT3 in cancer. My study has also shed important insight on that activating STAT1 signaling would be an attractive therapeutic strategy in treating ALK+ALCL, even potentially other types of cancer where STAT3 is constitutively activated. Secondly, my study has unearthed the biochemical features of a cancer stem-like subpopulation in ALK+ALCL. Specifically, the positive forward loop involving Wnt/ $\beta$ -catenin/MYC/Sox2 axis defines this cancer stem-like cell subpopulation. This study has revealed promising therapeutic targets for these cancer stem-like cells in ALK+ALCL by targeting Wnt/ $\beta$ -catenin/MYC/Sox2 axis. Specifically, doxorubicin, adjuvanted with Wnt/ $\beta$ -catenin inhibitor or MYC inhibitor, can be potentially applied to ALK+ALCL patients who develop chemoresistance and tumor relapses. Lastly, oxidative stress has been shown to potentiate the tumorigenicity of ALK+ALCL, in which the active Wnt/ $\beta$ -catenin/MYC/Sox2 axis is required. This study has supported the notion of CSC plasticity or “acquired cancer stemness” in haematopoietic cancer. My study has provided evidence that “acquired cancer stemness” can be achieved in haematopoietic cancer model by oxidative stress. The biological process of “acquired cancer stemness” can be easily studied by using the RU/RR cells model, as the SRR2 reporter responsiveness is a useful approach to identify and quantify cancer stemness. I believe the RU/RR cells model is a good model that can be applied to other types of cancer for identifying cancer stem-like cell populations or studying “acquired cancer stemness”.

The future study involves evaluation of the expression of STAT1 and MYC being as prognostic markers for ALK+ALCL disease. Furthermore, *in vivo* studies are warranted

to investigate the feasibility of the novel therapeutic targets, including activation of STAT1 and targeting Wnt/ $\beta$ -catenin/MYC/Sox2 axis, in mouse models mimicking human ALK+ALCL disease or patient-derived xenograft model.

In general, I believe the studies from this thesis have furthered the understanding of the pathobiology of ALK+ALCL cells and shed light on the complexity of intra-tumor heterogeneity and tumor plasticity in this haematological malignancy.

## 5.7 References

1. Kinney MC, Higgins RA, Medina EA. Anaplastic large cell lymphoma: twenty-five years of discovery. *Archives of pathology & laboratory medicine*. 2011;135(1):19-43.
2. Wu C, Molavi O, Zhang H, Gupta N, Alshareef A, Bone KM, et al. STAT1 is phosphorylated and downregulated by the oncogenic tyrosine kinase NPM-ALK in ALK-positive anaplastic large-cell lymphoma. *Blood*. 2015;126(3):336-45.
3. Gelebart P, Hegazy SA, Wang P, Bone KM, Anand M, Sharon D, et al. Aberrant expression and biological significance of Sox2, an embryonic stem cell transcriptional factor, in ALK-positive anaplastic large cell lymphoma. *Blood Cancer J*. 2012;2:e82.
4. Koromilas AE, Sexl V. The tumor suppressor function of STAT1 in breast cancer. *Jak-Stat*. 2013;2(2):e23353.
5. Khodarev N, Ahmad R, Rajabi H, Pitroda S, Kufe T, McClary C, et al. Cooperativity of the MUC1 oncoprotein and STAT1 pathway in poor prognosis human breast cancer. *Oncogene*. 2010;29(6):920-9.

6. Han W, Carpenter RL, Cao X, Lo HW. STAT1 gene expression is enhanced by nuclear EGFR and HER2 via cooperation with STAT3. *Mol Carcinog.* 2013;52(12):959-69.
7. Zhang Y, Molavi O, Su M, Lai R. The clinical and biological significance of STAT1 in esophageal squamous cell carcinoma. *BMC cancer.* 2014;14:791.
8. Kaganoi J, Watanabe G, Okabe M, Nagatani S, Kawabe A, Shimada Y, et al. STAT1 activation-induced apoptosis of esophageal squamous cell carcinoma cells in vivo. *Annals of surgical oncology.* 2007;14(4):1405-15.
9. Kortylewski M, Komyod W, Kauffmann ME, Bosserhoff A, Heinrich PC, Behrmann I. Interferon-gamma-mediated growth regulation of melanoma cells: involvement of STAT1-dependent and STAT1-independent signals. *The Journal of investigative dermatology.* 2004;122(2):414-22.
10. Schmitt MJ, Philippidou D, Reinsbach SE, Margue C, Wienecke-Baldacchino A, Nashan D, et al. Interferon-gamma-induced activation of Signal Transducer and Activator of Transcription 1 (STAT1) up-regulates the tumor suppressing microRNA-29 family in melanoma cells. *Cell communication and signaling : CCS.* 2012;10(1):41.
11. Sanda T, Tyner JW, Gutierrez A, Ngo VN, Glover J, Chang BH, et al. TYK2-STAT1-BCL2 pathway dependence in T-cell acute lymphoblastic leukemia. *Cancer discovery.* 2013;3(5):564-77.
12. Battle TE, Frank DA. STAT1 mediates differentiation of chronic lymphocytic leukemia cells in response to Bryostatins. *Blood.* 2003;102(8):3016-24.
13. Meissl K, Macho-Maschler S, Muller M, Strobl B. The good and the bad faces of STAT1 in solid tumours. *Cytokine.* 2015.

14. Kovacic B, Stoiber D, Moriggl R, Weisz E, Ott RG, Kreibich R, et al. STAT1 acts as a tumor promoter for leukemia development. *Cancer cell*. 2006;10(1):77-87.
15. Avalle L, Pensa S, Regis G, Novelli F, Poli V. STAT1 and STAT3 in tumorigenesis: A matter of balance. *Jak-Stat*. 2012;1(2):65-72.
16. Schultz J, Koczan D, Schmitz U, Ibrahim SM, Pilch D, Landsberg J, et al. Tumor-promoting role of signal transducer and activator of transcription (Stat)1 in late-stage melanoma growth. *Clinical & experimental metastasis*. 2010;27(3):133-40.
17. Regis G, Pensa S, Boselli D, Novelli F, Poli V. Ups and downs: the STAT1:STAT3 seesaw of Interferon and gp130 receptor signalling. *Semin Cell Dev Biol*. 2008;19(4):351-9.
18. Xi S, Dyer KF, Kimak M, Zhang Q, Gooding WE, Chaillet JR, et al. Decreased STAT1 expression by promoter methylation in squamous cell carcinogenesis. *Journal of the National Cancer Institute*. 2006;98(3):181-9.
19. Sun WH, Pabon C, Alsayed Y, Huang PP, Jandeska S, Uddin S, et al. Interferon-alpha resistance in a cutaneous T-cell lymphoma cell line is associated with lack of STAT1 expression. *Blood*. 1998;91(2):570-6.
20. Ren Y, Zhao P, Liu J, Yuan Y, Cheng Q, Zuo Y, et al. Deubiquitinase USP2a Sustains Interferons Antiviral Activity by Restricting Ubiquitination of Activated STAT1 in the Nucleus. *PLoS pathogens*. 2016;12(7):e1005764.
21. Yu H, Yue X, Zhao Y, Li X, Wu L, Zhang C, et al. LIF negatively regulates tumour-suppressor p53 through Stat3/ID1/MDM2 in colorectal cancers. *Nature communications*. 2014;5:5218.

22. Pencik J, Schleder M, Gruber W, Unger C, Walker SM, Chalaris A, et al. STAT3 regulated ARF expression suppresses prostate cancer metastasis. *Nature communications*. 2015;6:7736.
23. Dimberg LY, Dimberg A, Ivarsson K, Fryknas M, Rickardson L, Tobin G, et al. Stat1 activation attenuates IL-6 induced Stat3 activity but does not alter apoptosis sensitivity in multiple myeloma. *BMC cancer*. 2012;12:318.
24. Fisher R, Puztai L, Swanton C. Cancer heterogeneity: implications for targeted therapeutics. *British journal of cancer*. 2013;108(3):479-85.
25. Cabrera MC, Hollingsworth RE, Hurt EM. Cancer stem cell plasticity and tumor hierarchy. *World journal of stem cells*. 2015;7(1):27-36.
26. Visvader JE. Cells of origin in cancer. *Nature*. 2011;469(7330):314-22.
27. Meacham CE, Morrison SJ. Tumour heterogeneity and cancer cell plasticity. *Nature*. 2013;501(7467):328-37.
28. Tang DG. Understanding cancer stem cell heterogeneity and plasticity. *Cell research*. 2012;22(3):457-72.
29. Moti N, Malcolm T, Hamoudi R, Mian S, Garland G, Hook CE, et al. Anaplastic large cell lymphoma-propagating cells are detectable by side population analysis and possess an expression profile reflective of a primitive origin. *Oncogene*. 2015;34(14):1843-52.
30. Ouyang J, Yu W, Liu J, Zhang N, Florens L, Chen J, et al. Cyclin-dependent kinase-mediated Sox2 phosphorylation enhances the ability of Sox2 to establish the pluripotent state. *The Journal of biological chemistry*. 2015;290(37):22782-94.

31. Fang L, Zhang L, Wei W, Jin X, Wang P, Tong Y, et al. A methylation-phosphorylation switch determines Sox2 stability and function in ESC maintenance or differentiation. *Molecular cell*. 2014;55(4):537-51.
32. Justilien V, Walsh MP, Ali SA, Thompson EA, Murray NR, Fields AP. The PRKCI and SOX2 oncogenes are coamplified and cooperate to activate Hedgehog signaling in lung squamous cell carcinoma. *Cancer cell*. 2014;25(2):139-51.
33. Jeong CH, Cho YY, Kim MO, Kim SH, Cho EJ, Lee SY, et al. Phosphorylation of Sox2 cooperates in reprogramming to pluripotent stem cells. *Stem cells*. 2010;28(12):2141-50.
34. Han L, Shi S, Gong T, Zhang Z, Sun X. Cancer stem cells: therapeutic implications and perspectives in cancer therapy. *Acta Pharmaceutica Sinica B*. 2013;3(2):65-75.
35. Vicente-Duenas C, Gutierrez de Diego J, Rodriguez FD, Jimenez R, Cobaleda C. The role of cellular plasticity in cancer development. *Curr Med Chem*. 2009;16(28):3676-85.
36. Chen W, Dong J, Haiech J, Kilhoffer MC, Zeniou M. Cancer Stem Cell Quiescence and Plasticity as Major Challenges in Cancer Therapy. *Stem Cells Int*. 2016;2016:1740936.
37. Chaffer CL, Brueckmann I, Scheel C, Kaestli AJ, Wiggins PA, Rodrigues LO, et al. Normal and neoplastic nonstem cells can spontaneously convert to a stem-like state. *Proceedings of the National Academy of Sciences of the United States of America*. 2011;108(19):7950-5.

38. Gross E, L'Faqihi-Olive FE, Ysebaert L, Brassac M, Struski S, Kheirallah S, et al. B-chronic lymphocytic leukemia chemoresistance involves innate and acquired leukemic side population cells. *Leukemia*. 2010;24(11):1885-92.
39. Kemper K, de Goeje PL, Peeper DS, van Amerongen R. Phenotype switching: tumor cell plasticity as a resistance mechanism and target for therapy. *Cancer research*. 2014;74(21):5937-41.
40. Doherty MR, Smigiel JM, Junk DJ, Jackson MW. Cancer Stem Cell Plasticity Drives Therapeutic Resistance. *Cancers*. 2016;8(1).
41. Gopal K, Gupta N, Zhang H, Alshareef A, Alqahtani H, Bigras G, et al. Oxidative stress induces the acquisition of cancer stem-like phenotype in breast cancer detectable by using a Sox2 regulatory region-2 (SRR2) reporter. *Oncotarget*. 2016;7(3):3111-27.
42. Zhang HF, Wu C, Alshareef A, Gupta N, Zhao Q, Xu XE, et al. The PI3K/AKT/c-MYC axis promotes the acquisition of cancer stem-like features in esophageal squamous cell carcinoma. *Stem cells*. 2016.
43. Wang Z, Ge L, Wang M, Carr BI. Phosphorylation regulates Myc expression via prolonged activation of the mitogen-activated protein kinase pathway. *Journal of cellular physiology*. 2006;208(1):133-40.
44. Tsai WB, Aiba I, Long Y, Lin HK, Feun L, Savaraj N, et al. Activation of Ras/PI3K/ERK pathway induces c-Myc stabilization to upregulate argininosuccinate synthetase, leading to arginine deiminase resistance in melanoma cells. *Cancer research*. 2012;72(10):2622-33.



45. Sears R, Nuckolls F, Haura E, Taya Y, Tamai K, Nevins JR. Multiple Ras-dependent phosphorylation pathways regulate Myc protein stability. *Genes & development*. 2000;14(19):2501-14.
46. Marampon F, Ciccarelli C, Zani BM. Down-regulation of c-Myc following MEK/ERK inhibition halts the expression of malignant phenotype in rhabdomyosarcoma and in non muscle-derived human tumors. *Molecular cancer*. 2006;5:31.
47. Yun Z, Lin Q. Hypoxia and regulation of cancer cell stemness. *Advances in experimental medicine and biology*. 2014;772:41-53.
48. Carnero A, Leonart M. The hypoxic microenvironment: A determinant of cancer stem cell evolution. *BioEssays : news and reviews in molecular, cellular and developmental biology*. 2016;38 Suppl 1:S65-74.
49. Plaks V, Kong N, Werb Z. The cancer stem cell niche: how essential is the niche in regulating stemness of tumor cells? *Cell stem cell*. 2015;16(3):225-38.
50. Keith B, Simon MC. Hypoxia-inducible factors, stem cells, and cancer. *Cell*. 2007;129(3):465-72.
51. Dimberg A, Karlberg I, Nilsson K, Oberg F. Ser727/Tyr701-phosphorylated Stat1 is required for the regulation of c-Myc, cyclins, and p27Kip1 associated with ATRA-induced G0/G1 arrest of U-937 cells. *Blood*. 2003;102(1):254-61.
52. Ramana CV, Grammatikakis N, Chernov M, Nguyen H, Goh KC, Williams BR, et al. Regulation of c-myc expression by IFN-gamma through Stat1-dependent and -independent pathways. *The EMBO journal*. 2000;19(2):263-72.

## **Bibliography**

Abril E, Real LM, Serrano A, Jimenez P, Garcia A, Canton J, et al. Unresponsiveness to interferon associated with STAT1 protein deficiency in a gastric adenocarcinoma cell line. *Cancer immunology, immunotherapy* : CII. 1998;47(2):113-20.

Afkarian M, Sedy JR, Yang J, Jacobson NG, Cereb N, Yang SY, et al. T-bet is a STAT1-induced regulator of IL-12R expression in naive CD4<sup>+</sup> T cells. *Nat Immunol*. 2002;3(6):549-57.

Aisner DL, Nguyen TT, Paskulin DD, Le AT, Haney J, Schulte N, et al. ROS1 and ALK fusions in colorectal cancer, with evidence of intratumoral heterogeneity for molecular drivers. *Molecular cancer research* : MCR. 2014;12(1):111-8.

Akita H, Marquardt JU, Durkin ME, Kitade M, Seo D, Conner EA, et al. MYC activates stem-like cell potential in hepatocarcinoma by a p53-dependent mechanism. *Cancer research*. 2014;74(20):5903-13.

Alzona M, Jack HM, Fisher RI, Ellis TM. CD30 defines a subset of activated human T cells that produce IFN-gamma and IL-5 and exhibit enhanced B cell helper activity. *J Immunol*. 1994;153(7):2861-7.

Amaya CN, Bryan BA. Enrichment of the embryonic stem cell reprogramming factors Oct4, Nanog, Myc, and Sox2 in benign and malignant vascular tumors. *BMC Clin Pathol*. 2015;15:18.

Amin HM, Lai R. Pathobiology of ALK+ anaplastic large-cell lymphoma. *Blood*. 2007;110(7):2259-67.

Amin HM, Lin Q, Lai R. Jak3 contributes to the activation of ALK and Stat3 in ALK(+) anaplastic large cell lymphoma. *Laboratory investigation; a journal of technical methods and pathology*. 2006;86(4):417-9; author reply 20-1.

Amin HM, McDonnell TJ, Ma Y, Lin Q, Fujio Y, Kunisada K, et al. Selective inhibition of STAT3 induces apoptosis and G(1) cell cycle arrest in ALK-positive anaplastic large cell lymphoma. *Oncogene*. 2004;23(32):5426-34.

Amin HM, McDonnell TJ, Ma Y, Lin Q, Fujio Y, Kunisada K, et al. Selective inhibition of STAT3 induces apoptosis and G(1) cell cycle arrest in ALK-positive anaplastic large cell lymphoma. *Oncogene*. 2004;23(32):5426-34.

Amin HM, Medeiros LJ, Ma Y, Feretzaki M, Das P, Leventaki V, et al. Inhibition of JAK3 induces apoptosis and decreases anaplastic lymphoma kinase activity in anaplastic large cell lymphoma. *Oncogene*. 2003;22(35):5399-407.

Anand M, Lai R, Gelebart P. beta-catenin is constitutively active and increases STAT3 expression/activation in anaplastic lymphoma kinase-positive anaplastic large cell lymphoma. *Haematologica*. 2011;96(2):253-61.

Anastas JN, Moon RT. WNT signalling pathways as therapeutic targets in cancer. *Nature reviews Cancer*. 2013;13(1):11-26.

Arif K, Hussain I, Rea C, El-Sheemy M. The role of Nanog expression in

tamoxifen-resistant breast cancer cells. *OncoTargets and therapy*. 2015;8:1327-34.

Avalle L, Pensa S, Regis G, Novelli F, Poli V. STAT1 and STAT3 in tumorigenesis: A matter of balance. *Jak-Stat*. 2012;1(2):65-72.

Babchia N, Calipel A, Mouriaux F, Faussat AM, Mascarelli F. The PI3K/Akt and mTOR/P70S6K signaling pathways in human uveal melanoma cells: interaction with B-Raf/ERK. *Investigative ophthalmology & visual science*. 2010;51(1):421-9.

Bai RY, Dieter P, Peschel C, Morris SW, Duyster J. Nucleophosmin-anaplastic lymphoma kinase of large-cell anaplastic lymphoma is a constitutively active tyrosine kinase that utilizes phospholipase C-gamma to mediate its mitogenicity. *Molecular and cellular biology*. 1998;18(12):6951-61.

Baker VV, Borst MP, Dixon D, Hatch KD, Shingleton HM, Miller D. c-myc amplification in ovarian cancer. *Gynecologic oncology*. 1990;38(3):340-2.

Bard JD, Gelebart P, Anand M, Amin HM, Lai R. Aberrant expression of IL-22 receptor 1 and autocrine IL-22 stimulation contribute to tumorigenicity in ALK+ anaplastic large cell lymphoma. *Leukemia*. 2008;22(8):1595-603.

Basso K, Dalla-Favera R. Germinal centres and B cell lymphomagenesis. *Nature reviews Immunology*. 2015;15(3):172-84.

Basu-Roy U, Bayin NS, Rattanakorn K, Han E, Placantonakis DG, Mansukhani A, et al. Sox2 antagonizes the Hippo pathway to maintain stemness in cancer

cells. *Nature communications*. 2015;6:6411.

Battle TE, Frank DA. STAT1 mediates differentiation of chronic lymphocytic leukemia cells in response to Bryostatins. *Blood*. 2003;102(8):3016-24.

Bellei B, Pacchiarotti A, Perez M, Faraggiana T. Frequent beta-catenin overexpression without exon 3 mutation in cutaneous lymphomas. *Modern pathology : an official journal of the United States and Canadian Academy of Pathology, Inc*. 2004;17(10):1275-81.

Beltran H. The N-myc Oncogene: Maximizing its Targets, Regulation, and Therapeutic Potential. *Molecular cancer research : MCR*. 2014;12(6):815-22.

Benharroch D, Meguerian-Bedoyan Z, Lamant L, Amin C, Brugieres L, Terrier-Lacombe MJ, et al. ALK-positive lymphoma: a single disease with a broad spectrum of morphology. *Blood*. 1998;91(6):2076-84.

Bernabei P, Coccia EM, Rigamonti L, Bosticardo M, Forni G, Pestka S, et al. Interferon-gamma receptor 2 expression as the deciding factor in human T, B, and myeloid cell proliferation or death. *Journal of leukocyte biology*. 2001;70(6):950-60.

Bhattacharya S, Ray RM, Johnson LR. STAT3-mediated transcription of Bcl-2, Mcl-1 and c-IAP2 prevents apoptosis in polyamine-depleted cells. *The Biochemical journal*. 2005;392(Pt 2):335-44.

Bilsland JG, Wheeldon A, Mead A, Znamenskiy P, Almond S, Waters KA, et al.

Behavioral and neurochemical alterations in mice deficient in anaplastic lymphoma kinase suggest therapeutic potential for psychiatric indications. *Neuropsychopharmacology*. 2008;33(3):685-700.

Blank U, Karlsson G, Karlsson S. Signaling pathways governing stem-cell fate. *Blood*. 2008;111(2):492-503.

Bluyssen HA, Rastmanesh MM, Tilburgs C, Jie K, Wesseling S, Goumans MJ, et al. IFN gamma-dependent SOCS3 expression inhibits IL-6-induced STAT3 phosphorylation and differentially affects IL-6 mediated transcriptional responses in endothelial cells. *American journal of physiology Cell physiology*. 2010;299(2):C354-62.

Boesch M, Zeimet AG, Reimer D, Schmidt S, Gastl G, Parson W, et al. The side population of ovarian cancer cells defines a heterogeneous compartment exhibiting stem cell characteristics. *Oncotarget*. 2014;5(16):7027-39.

Bonnet D, Dick JE. Human acute myeloid leukemia is organized as a hierarchy that originates from a primitive hematopoietic cell. *Nature medicine*. 1997;3(7):730-7.

Bonzheim I, Geissinger E, Roth S, Zettl A, Marx A, Rosenwald A, et al. Anaplastic large cell lymphomas lack the expression of T-cell receptor molecules or molecules of proximal T-cell receptor signaling. *Blood*. 2004;104(10):3358-60.

Borovski T, De Sousa EMF, Vermeulen L, Medema JP. Cancer stem cell niche:

the place to be. *Cancer research*. 2011;71(3):634-9.

Boudny V, Dusek L, Adamkova L, Chumchalova J, Kocak I, Fait V, et al. Lack of STAT 1 phosphorylation at TYR 701 by IFN $\gamma$  correlates with disease outcome in melanoma patients. *Neoplasma*. 2005;52(4):330-7.

Bowden ET, Stoica GE, Wellstein A. Anti-apoptotic signaling of pleiotrophin through its receptor, anaplastic lymphoma kinase. *The Journal of biological chemistry*. 2002;277(39):35862-8.

Bowman T, Garcia R, Turkson J, Jove R. STATs in oncogenesis. *Oncogene*. 2000;19(21):2474-88.

Bowman T, Garcia R, Turkson J, Jove R. STATs in oncogenesis. *Oncogene*. 2000;19(21):2474-88.

Box JK, Paquet N, Adams MN, Boucher D, Bolderson E, O'Byrne KJ, et al. Nucleophosmin: from structure and function to disease development. *BMC molecular biology*. 2016;17(1):19.

Britton KM, Kirby JA, Lennard TW, Meeson AP. Cancer stem cells and side population cells in breast cancer and metastasis. *Cancers*. 2011;3(2):2106-30.

Buettner R, Mora LB, Jove R. Activated STAT signaling in human tumors provides novel molecular targets for therapeutic intervention. *Clinical cancer research : an official journal of the American Association for Cancer Research*. 2002;8(4):945-54.

Cabrera MC, Hollingsworth RE, Hurt EM. Cancer stem cell plasticity and tumor hierarchy. *World journal of stem cells*. 2015;7(1):27-36.

Carnero A, Leonart M. The hypoxic microenvironment: A determinant of cancer stem cell evolution. *BioEssays : news and reviews in molecular, cellular and developmental biology*. 2016;38 Suppl 1:S65-74.

Carpenter RL, Lo HW. STAT3 Target Genes Relevant to Human Cancers. *Cancers*. 2014;6(2):897-925.

Casey SC, Tong L, Li Y, Do R, Walz S, Fitzgerald KN, et al. MYC regulates the antitumor immune response through CD47 and PD-L1. *Science*. 2016;352(6282):227-31.

Ceccon M, Mologni L, Bisson W, Scapozza L, Gambacorti-Passerini C. Crizotinib-resistant NPM-ALK mutants confer differential sensitivity to unrelated Alk inhibitors. *Molecular cancer research : MCR*. 2013;11(2):122-32.

Chaffer CL, Brueckmann I, Scheel C, Kaestli AJ, Wiggins PA, Rodrigues LO, et al. Normal and neoplastic nonstem cells can spontaneously convert to a stem-like state. *Proceedings of the National Academy of Sciences of the United States of America*. 2011;108(19):7950-5.

Chan SR, Vermi W, Luo J, Lucini L, Rickert C, Fowler AM, et al. STAT1-deficient mice spontaneously develop estrogen receptor alpha-positive luminal mammary carcinomas. *Breast cancer research : BCR*. 2012;14(1):R16.



Chang F, Steelman LS, Lee JT, Shelton JG, Navolanic PM, Blalock WL, et al. Signal transduction mediated by the Ras/Raf/MEK/ERK pathway from cytokine receptors to transcription factors: potential targeting for therapeutic intervention. *Leukemia*. 2003;17(7):1263-93.

Chen D, Dou QP. The ubiquitin-proteasome system as a prospective molecular target for cancer treatment and prevention. *Current protein & peptide science*. 2010;11(6):459-70.

Chen S, Xu Y, Chen Y, Li X, Mou W, Wang L, et al. SOX2 gene regulates the transcriptional network of oncogenes and affects tumorigenesis of human lung cancer cells. *PloS one*. 2012;7(5):e36326.

Chen S, Xu Y, Chen Y, Li X, Mou W, Wang L, et al. SOX2 gene regulates the transcriptional network of oncogenes and affects tumorigenesis of human lung cancer cells. *PloS one*. 2012;7(5):e36326.

Chen W, Dong J, Haiech J, Kilhoffer MC, Zeniou M. Cancer Stem Cell Quiescence and Plasticity as Major Challenges in Cancer Therapy. *Stem Cells Int*. 2016;2016:1740936.

Chen Y, Shi L, Zhang L, Li R, Liang J, Yu W, et al. The molecular mechanism governing the oncogenic potential of SOX2 in breast cancer. *The Journal of biological chemistry*. 2008;283(26):17969-78.

Chen Y, Takita J, Choi YL, Kato M, Ohira M, Sanada M, et al. Oncogenic

mutations of ALK kinase in neuroblastoma. *Nature*. 2008;455(7215):971-4.

Chen YQ. [Frequency on N-ras as a transforming gene, DNA rearrangement and amplification, and over-expression of C-myc in human primary hepatic cancer]. *Zhonghua yi xue za zhi*. 1987;67(4):197-9, 14.

Chiarle R, Gong JZ, Guasparri I, Pesci A, Cai J, Liu J, et al. NPM-ALK transgenic mice spontaneously develop T-cell lymphomas and plasma cell tumors. *Blood*. 2003;101(5):1919-27.

Chiarle R, Simmons WJ, Cai H, Dhall G, Zamo A, Raz R, et al. Stat3 is required for ALK-mediated lymphomagenesis and provides a possible therapeutic target. *Nature medicine*. 2005;11(6):623-9.

Chiarle R, Voena C, Ambrogio C, Piva R, Inghirami G. The anaplastic lymphoma kinase in the pathogenesis of cancer. *Nature reviews Cancer*. 2008;8(1):11-23.

Choi EA, Lei H, Maron DJ, Wilson JM, Barsoum J, Fraker DL, et al. Stat1-dependent induction of tumor necrosis factor-related apoptosis-inducing ligand and the cell-surface death signaling pathway by interferon beta in human cancer cells. *Cancer research*. 2003;63(17):5299-307.

Christgen M, Ballmaier M, Lehmann U, Kreipe H. Detection of putative cancer stem cells of the side population phenotype in human tumor cell cultures. *Methods in molecular biology*. 2012;878:201-15.

Colombo E, Bonetti P, Lazzerini Denchi E, Martinelli P, Zamponi R, Marine JC, et

al. Nucleophosmin is required for DNA integrity and p19Arf protein stability. *Molecular and cellular biology*. 2005;25(20):8874-86.

Coluccia AM, Vacca A, Dunach M, Mologni L, Redaelli S, Bustos VH, et al. Bcr-Abl stabilizes beta-catenin in chronic myeloid leukemia through its tyrosine phosphorylation. *The EMBO journal*. 2007;26(5):1456-66.

Crockett DK, Lin Z, Elenitoba-Johnson KS, Lim MS. Identification of NPM-ALK interacting proteins by tandem mass spectrometry. *Oncogene*. 2004;23(15):2617-29.

Dai X, Sayama K, Yamasaki K, Tohyama M, Shirakata Y, Hanakawa Y, et al. SOCS1-negative feedback of STAT1 activation is a key pathway in the dsRNA-induced innate immune response of human keratinocytes. *The Journal of investigative dermatology*. 2006;126(7):1574-81.

Dang CV. c-Myc target genes involved in cell growth, apoptosis, and metabolism. *Molecular and cellular biology*. 1999;19(1):1-11.

Dang CV. MYC on the path to cancer. *Cell*. 2012;149(1):22-35.

Dang CV. MYC, metabolism, cell growth, and tumorigenesis. *Cold Spring Harbor perspectives in medicine*. 2013;3(8).

Das B, Tsuchida R, Malkin D, Koren G, Baruchel S, Yeger H. Hypoxia enhances tumor stemness by increasing the invasive and tumorigenic side population fraction. *Stem cells*. 2008;26(7):1818-30.

Das TP, Suman S, Alatassi H, Ankem MK, Damodaran C. Inhibition of AKT promotes FOXO3a-dependent apoptosis in prostate cancer. *Cell death & disease*. 2016;7:e2111.

Datta SR, Dudek H, Tao X, Masters S, Fu H, Gotoh Y, et al. Akt phosphorylation of BAD couples survival signals to the cell-intrinsic death machinery. *Cell*. 1997;91(2):231-41.

Dayem AA, Choi HY, Kim JH, Cho SG. Role of oxidative stress in stem, cancer, and cancer stem cells. *Cancers*. 2010;2(2):859-84.

de Beca FF, Caetano P, Gerhard R, Alvarenga CA, Gomes M, Paredes J, et al. Cancer stem cells markers CD44, CD24 and ALDH1 in breast cancer special histological types. *Journal of clinical pathology*. 2013;66(3):187-91.

Dean M. ABC transporters, drug resistance, and cancer stem cells. *J Mammary Gland Biol Neoplasia*. 2009;14(1):3-9.

Decker T, Muller M, Stockinger S. The yin and yang of type I interferon activity in bacterial infection. *Nature reviews Immunology*. 2005;5(9):675-87.

Demoulin JB, Uyttenhove C, Van Roost E, DeLestre B, Donckers D, Van Snick J, et al. A single tyrosine of the interleukin-9 (IL-9) receptor is required for STAT activation, antiapoptotic activity, and growth regulation by IL-9. *Molecular and cellular biology*. 1996;16(9):4710-6.

DePinho RA, Hatton KS, Tesfaye A, Yancopoulos GD, Alt FW. The human myc

gene family: structure and activity of L-myc and an L-myc pseudogene. *Genes & development*. 1987;1(10):1311-26.

Dhillon AS, Hagan S, Rath O, Kolch W. MAP kinase signalling pathways in cancer. *Oncogene*. 2007;26(22):3279-90.

Diehn M, Cho RW, Lobo NA, Kalisky T, Dorie MJ, Kulp AN, et al. Association of reactive oxygen species levels and radioresistance in cancer stem cells. *Nature*. 2009;458(7239):780-3.

Dien Bard J, Gelebart P, Anand M, Zak Z, Hegazy SA, Amin HM, et al. IL-21 contributes to JAK3/STAT3 activation and promotes cell growth in ALK-positive anaplastic large cell lymphoma. *The American journal of pathology*. 2009;175(2):825-34.

Dimberg A, Karlberg I, Nilsson K, Oberg F. Ser727/Tyr701-phosphorylated Stat1 is required for the regulation of c-Myc, cyclins, and p27Kip1 associated with ATRA-induced G0/G1 arrest of U-937 cells. *Blood*. 2003;102(1):254-61.

Dimberg A, Karlberg I, Nilsson K, Oberg F. Ser727/Tyr701-phosphorylated Stat1 is required for the regulation of c-Myc, cyclins, and p27Kip1 associated with ATRA-induced G0/G1 arrest of U-937 cells. *Blood*. 2003;102(1):254-61.

Dimberg LY, Dimberg A, Ivarsson K, Fryknas M, Rickardson L, Tobin G, et al. Stat1 activation attenuates IL-6 induced Stat3 activity but does not alter apoptosis sensitivity in multiple myeloma. *BMC cancer*. 2012;12:318.

Ding XW, Wu JH, Jiang CP. ABCG2: a potential marker of stem cells and novel target in stem cell and cancer therapy. *Life sciences*. 2010;86(17-18):631-7.

Doherty MR, Smigiel JM, Junk DJ, Jackson MW. Cancer Stem Cell Plasticity Drives Therapeutic Resistance. *Cancers*. 2016;8(1).

Doherty MR, Smigiel JM, Junk DJ, Jackson MW. Cancer Stem Cell Plasticity Drives Therapeutic Resistance. *Cancers*. 2016;8(1).

Drexler HG, Gignac SM, von Wasielewski R, Werner M, Dirks WG. Pathobiology of NPM-ALK and variant fusion genes in anaplastic large cell lymphoma and other lymphomas. *Leukemia*. 2000;14(9):1533-59.

Duchartre Y, Kim YM, Kahn M. The Wnt signaling pathway in cancer. *Critical reviews in oncology/hematology*. 2016;99:141-9.

Dunn GP, Sheehan KC, Old LJ, Schreiber RD. IFN unresponsiveness in LNCaP cells due to the lack of JAK1 gene expression. *Cancer research*. 2005;65(8):3447-53.

El Khoury F, Corcos L, Durand S, Simon B, Le Jossic-Corcos C. Acquisition of anticancer drug resistance is partially associated with cancer stemness in human colon cancer cells. *International journal of oncology*. 2016.

Falini B, Mecucci C, Tiacci E, Alcalay M, Rosati R, Pasqualucci L, et al. Cytoplasmic nucleophosmin in acute myelogenous leukemia with a normal karyotype. *The New England journal of medicine*. 2005;352(3):254-66.

Fanale MA, Horwitz SM, Forero-Torres A, Bartlett NL, Advani RH, Pro B, et al. Brentuximab vedotin in the front-line treatment of patients with CD30+ peripheral T-cell lymphomas: results of a phase I study. *Journal of clinical oncology : official journal of the American Society of Clinical Oncology*. 2014;32(28):3137-43.

Fang L, Zhang L, Wei W, Jin X, Wang P, Tong Y, et al. A methylation-phosphorylation switch determines Sox2 stability and function in ESC maintenance or differentiation. *Molecular cell*. 2014;55(4):537-51.

Farina F, Gambacorti-Passerini C. ALK inhibitors for clinical use in cancer therapy. *Front Biosci (Elite Ed)*. 2016;8:46-60.

Farrell AS, Sears RC. MYC degradation. *Cold Spring Harbor perspectives in medicine*. 2014;4(3).

Felgar RE, Salhany KE, Macon WR, Pietra GG, Kinney MC. The expression of TIA-1+ cytolytic-type granules and other cytolytic lymphocyte-associated markers in CD30+ anaplastic large cell lymphomas (ALCL): correlation with morphology, immunophenotype, ultrastructure, and clinical features. *Human pathology*. 1999;30(2):228-36.

Felsher DW. MYC Inactivation Elicits Oncogene Addiction through Both Tumor Cell-Intrinsic and Host-Dependent Mechanisms. *Genes & cancer*. 2010;1(6):597-604.

Fenghao X, Saxon A, Nguyen A, Ke Z, Diaz-Sanchez D, Nel A. Interleukin 4

activates a signal transducer and activator of transcription (Stat) protein which interacts with an interferon-gamma activation site-like sequence upstream of the I epsilon exon in a human B cell line. Evidence for the involvement of Janus kinase 3 and interleukin-4 Stat. *The Journal of clinical investigation*. 1995;96(2):907-14.

Ferreri AJ, Govi S, Pileri SA, Savage KJ. Anaplastic large cell lymphoma, ALK-positive. *Crit Rev Oncol Hematol*. 2012;83(2):293-302.

Fisher R, Puzstai L, Swanton C. Cancer heterogeneity: implications for targeted therapeutics. *British journal of cancer*. 2013;108(3):479-85.

Fodde R, Brabletz T. Wnt/beta-catenin signaling in cancer stemness and malignant behavior. *Current opinion in cell biology*. 2007;19(2):150-8.

Foss HD, Anagnostopoulos I, Araujo I, Assaf C, Demel G, Kummer JA, et al. Anaplastic large-cell lymphomas of T-cell and null-cell phenotype express cytotoxic molecules. *Blood*. 1996;88(10):4005-11.

Foss HD, Demel G, Anagnostopoulos I, Araujo I, Hummel M, Stein H. Uniform expression of cytotoxic molecules in anaplastic large cell lymphoma of null/T cell phenotype and in cell lines derived from anaplastic large cell lymphoma. *Pathobiology*. 1997;65(2):83-90.

Fujiwara D, Kato K, Nohara S, Iwanuma Y, Kajiyama Y. The usefulness of three-dimensional cell culture in induction of cancer stem cells from esophageal



squamous cell carcinoma cell lines. *Biochemical and biophysical research communications*. 2013;434(4):773-8.

Fulda S, Debatin KM. IFN $\gamma$  sensitizes for apoptosis by upregulating caspase-8 expression through the Stat1 pathway. *Oncogene*. 2002;21(15):2295-308.

Funa K, Steinholtz L, Nou E, Bergh J. Increased expression of N-myc in human small cell lung cancer biopsies predicts lack of response to chemotherapy and poor prognosis. *American journal of clinical pathology*. 1987;88(2):216-20.

Funato Y, Michiue T, Asashima M, Miki H. The thioredoxin-related redox-regulating protein nucleoredoxin inhibits Wnt-beta-catenin signalling through dishevelled. *Nature cell biology*. 2006;8(5):501-8.

Gabay M, Li Y, Felsher DW. MYC activation is a hallmark of cancer initiation and maintenance. *Cold Spring Harbor perspectives in medicine*. 2014;4(6).

Gaitanaki C, Konstantina S, Chrysa S, Beis I. Oxidative stress stimulates multiple MAPK signalling pathways and phosphorylation of the small HSP27 in the perfused amphibian heart. *J Exp Biol*. 2003;206(Pt 16):2759-69.

Gaietta A, Gunby RH, Redaelli S, Stano P, Carniti C, Bachi A, et al. NPM/ALK binds and phosphorylates the RNA/DNA-binding protein PSF in anaplastic large-cell lymphoma. *Blood*. 2007;110(7):2600-9.

Galkin AV, Melnick JS, Kim S, Hood TL, Li N, Li L, et al. Identification of NVP-

TAE684, a potent, selective, and efficacious inhibitor of NPM-ALK. Proceedings of the National Academy of Sciences of the United States of America. 2007;104(1):270-5.

Gao C, Mi Z, Guo H, Kuo PC. Osteopontin regulates ubiquitin-dependent degradation of Stat1 in murine mammary epithelial tumor cells. Neoplasia. 2007;9(9):699-706.

Gao H, Teng C, Huang W, Peng J, Wang C. SOX2 Promotes the Epithelial to Mesenchymal Transition of Esophageal Squamous Cells by Modulating Slug Expression through the Activation of STAT3/HIF-alpha Signaling. International journal of molecular sciences. 2015;16(9):21643-57.

Gao J, Yin M, Zhu Y, Gu L, Zhang Y, Li Q, et al. Prognostic significance and therapeutic potential of the activation of anaplastic lymphoma kinase/protein kinase B/mammalian target of rapamycin signaling pathway in anaplastic large cell lymphoma. BMC cancer. 2013;13:471.

Gelebart P, Anand M, Armanious H, Peters AC, Dien Bard J, Amin HM, et al. Constitutive activation of the Wnt canonical pathway in mantle cell lymphoma. Blood. 2008;112(13):5171-9.

Gelebart P, Hegazy SA, Wang P, Bone KM, Anand M, Sharon D, et al. Aberrant expression and biological significance of Sox2, an embryonic stem cell transcriptional factor, in ALK-positive anaplastic large cell lymphoma. Blood

Cancer J. 2012;2:e82.

Gen Y, Yasui K, Nishikawa T, Yoshikawa T. SOX2 promotes tumor growth of esophageal squamous cell carcinoma through the AKT/mammalian target of rapamycin complex 1 signaling pathway. *Cancer science*. 2013;104(7):810-6.

George SK, Vishwamitra D, Manshoury R, Shi P, Amin HM. The ALK inhibitor ASP3026 eradicates NPM-ALK(+) T-cell anaplastic large-cell lymphoma in vitro and in a systemic xenograft lymphoma model. *Oncotarget*. 2014;5(14):5750-63.

Ghisolfi L, Keates AC, Hu X, Lee DK, Li CJ. Ionizing radiation induces stemness in cancer cells. *PloS one*. 2012;7(8):e43628.

Giambra V, Jenkins CE, Lam SH, Hoofd C, Belmonte M, Wang X, et al. Leukemia stem cells in T-ALL require active Hif1alpha and Wnt signaling. *Blood*. 2015;125(25):3917-27.

Giuriato S, Foisseau M, Dejean E, Felsher DW, Al Saati T, Demur C, et al. Conditional TPM3-ALK and NPM-ALK transgenic mice develop reversible ALK-positive early B-cell lymphoma/leukemia. *Blood*. 2010;115(20):4061-70.

Giuriato S, Turner SD. Twenty years of modelling NPM-ALK-induced lymphomagenesis. *Frontiers in bioscience*. 2015;7:236-47.

Gogineni SK, Shah HO, Chester M, Lin JH, Garrison M, Alidina A, et al. Variant complex translocations involving chromosomes 1, 9, 9, 15 and 17 in acute promyelocytic leukemia without RAR alpha/PML gene fusion rearrangement.

Leukemia. 1997;11(4):514-8.

Golebiewska A, Brons NH, Bjerkvig R, Niclou SP. Critical appraisal of the side population assay in stem cell and cancer stem cell research. *Cell stem cell*. 2011;8(2):136-47.

Gopal K, Gupta N, Zhang H, Alshareef A, Alqahtani H, Bigras G, et al. Oxidative stress induces the acquisition of cancer stem-like phenotype in breast cancer detectable by using a Sox2 regulatory region-2 (SRR2) reporter. *Oncotarget*. 2016;7(3):3111-27.

Gordon A, Conlon C, Collin J, Peto T, Gray D, Hands L, et al. An eight year experience of conservative management for aortic graft sepsis. *European journal of vascular surgery*. 1994;8(5):611-6.

Gorrini C, Harris IS, Mak TW. Modulation of oxidative stress as an anticancer strategy. *Nature reviews Drug discovery*. 2013;12(12):931-47.

Gorrini C, Harris IS, Mak TW. Modulation of oxidative stress as an anticancer strategy. *Nature reviews Drug discovery*. 2013;12(12):931-47.

Greenland C, Dastugue N, Touriol C, Lamant L, Delsol G, Brousset P. Anaplastic large cell lymphoma with the t(2;5)(p23;q35) NPM/ALK chromosomal translocation and duplication of the short arm of the non-translocated chromosome 2 involving the full length of the ALK gene. *Journal of clinical pathology*. 2001;54(2):152-4.

Gregory MA, Hann SR. c-Myc proteolysis by the ubiquitin-proteasome pathway: stabilization of c-Myc in Burkitt's lymphoma cells. *Molecular and cellular biology*. 2000;20(7):2423-35.

Grisendi S, Mecucci C, Falini B, Pandolfi PP. Nucleophosmin and cancer. *Nature reviews Cancer*. 2006;6(7):493-505.

Gritsko T, Williams A, Turkson J, Kaneko S, Bowman T, Huang M, et al. Persistent activation of stat3 signaling induces survivin gene expression and confers resistance to apoptosis in human breast cancer cells. *Clinical cancer research : an official journal of the American Association for Cancer Research*. 2006;12(1):11-9.

Gross E, L'Faqihi-Olive FE, Ysebaert L, Brassac M, Struski S, Kheirallah S, et al. B-chronic lymphocytic leukemia chemoresistance involves innate and acquired leukemic side population cells. *Leukemia*. 2010;24(11):1885-92.

Guan J, Umapathy G, Yamazaki Y, Wolfstetter G, Mendoza P, Pfeifer K, et al. FAM150A and FAM150B are activating ligands for anaplastic lymphoma kinase. *eLife*. 2015;4:e09811.

Guzzo C, Che Mat NF, Gee K. Interleukin-27 induces a STAT1/3- and NF-kappaB-dependent proinflammatory cytokine profile in human monocytes. *The Journal of biological chemistry*. 2010;285(32):24404-11.

Hadjimichael C, Chanoumidou K, Papadopoulou N, Arampatzi P, Papamatheakis

J, Kretsovali A. Common stemness regulators of embryonic and cancer stem cells. *World journal of stem cells*. 2015;7(9):1150-84.

Hallberg B, Palmer RH. Mechanistic insight into ALK receptor tyrosine kinase in human cancer biology. *Nature reviews Cancer*. 2013;13(10):685-700.

Han L, Shi S, Gong T, Zhang Z, Sun X. Cancer stem cells: therapeutic implications and perspectives in cancer therapy. *Acta Pharmaceutica Sinica B*. 2013;3(2):65-75.

Han L, Shi S, Gong T, Zhang Z, Sun X. Cancer stem cells: therapeutic implications and perspectives in cancer therapy. *Acta Pharmaceutica Sinica B*. 2013;3(2):65-75.

Han W, Carpenter RL, Cao X, Lo HW. STAT1 gene expression is enhanced by nuclear EGFR and HER2 via cooperation with STAT3. *Mol Carcinog*. 2013;52(12):959-69.

Han X, Fang X, Lou X, Hua D, Ding W, Foltz G, et al. Silencing SOX2 induced mesenchymal-epithelial transition and its expression predicts liver and lymph node metastasis of CRC patients. *PloS one*. 2012;7(8):e41335.

Han Y, Amin HM, Franko B, Frantz C, Shi X, Lai R. Loss of SHP1 enhances JAK3/STAT3 signaling and decreases proteasome degradation of JAK3 and NPM-ALK in ALK+ anaplastic large-cell lymphoma. *Blood*. 2006;108(8):2796-803.

Han Y, Amin HM, Frantz C, Franko B, Lee J, Lin Q, et al. Restoration of shp1 expression by 5-AZA-2'-deoxycytidine is associated with downregulation of JAK3/STAT3 signaling in ALK-positive anaplastic large cell lymphoma. *Leukemia*. 2006;20(9):1602-9.

Hansel DE, Platt E, Orloff M, Harwalker J, Sethu S, Hicks JL, et al. Mammalian target of rapamycin (mTOR) regulates cellular proliferation and tumor growth in urothelial carcinoma. *The American journal of pathology*. 2010;176(6):3062-72.

Hapgood G, Savage KJ. The biology and management of systemic anaplastic large cell lymphoma. *Blood*. 2015;126(1):17-25.

Hassler MR, Pulverer W, Lakshminarasimhan R, Redl E, Hacker J, Garland GD, et al. Insights into the Pathogenesis of Anaplastic Large-Cell Lymphoma through Genome-wide DNA Methylation Profiling. *Cell reports*. 2016;17(2):596-608.

Hecht JL, Aster JC. Molecular biology of Burkitt's lymphoma. *Journal of clinical oncology : official journal of the American Society of Clinical Oncology*. 2000;18(21):3707-21.

Hegazy SA, Alshareef A, Gelebart P, Anand M, Armanious H, Ingham RJ, et al. Disheveled proteins promote cell growth and tumorigenicity in ALK-positive anaplastic large cell lymphoma. *Cellular signalling*. 2013;25(1):295-307.

Hemmings BA, Restuccia DF. PI3K-PKB/Akt pathway. *Cold Spring Harbor perspectives in biology*. 2012;4(9):a011189.

Herreros-Villanueva M, Zhang JS, Koenig A, Abel EV, Smyrk TC, Bamlet WR, et al. SOX2 promotes dedifferentiation and imparts stem cell-like features to pancreatic cancer cells. *Oncogenesis*. 2013;2:e61.

Heuser M, Sly LM, Argiropoulos B, Kuchenbauer F, Lai C, Weng A, et al. Modeling the functional heterogeneity of leukemia stem cells: role of STAT5 in leukemia stem cell self-renewal. *Blood*. 2009;114(19):3983-93.

Ho HH, Ivashkiv LB. Role of STAT3 in type I interferon responses. Negative regulation of STAT1-dependent inflammatory gene activation. *The Journal of biological chemistry*. 2006;281(20):14111-8.

Ho MM, Ng AV, Lam S, Hung JY. Side population in human lung cancer cell lines and tumors is enriched with stem-like cancer cells. *Cancer research*. 2007;67(10):4827-33.

Hong F, Jaruga B, Kim WH, Radaeva S, El-Assal ON, Tian Z, et al. Opposing roles of STAT1 and STAT3 in T cell-mediated hepatitis: regulation by SOCS. *Journal of Clinical Investigation*. 2002;110(10):1503-13.

Honorat JF, Ragab A, Lamant L, Delsol G, Ragab-Thomas J. SHP1 tyrosine phosphatase negatively regulates NPM-ALK tyrosine kinase signaling. *Blood*. 2006;107(10):4130-8.

Hu X, Ghisolfi L, Keates AC, Zhang J, Xiang S, Lee DK, et al. Induction of cancer cell stemness by chemotherapy. *Cell cycle*. 2012;11(14):2691-8.



Hu Y, Chen Y, Douglas L, Li S. beta-Catenin is essential for survival of leukemic stem cells insensitive to kinase inhibition in mice with BCR-ABL-induced chronic myeloid leukemia. *Leukemia*. 2009;23(1):109-16.

Huang B, Huang YJ, Yao ZJ, Chen X, Guo SJ, Mao XP, et al. Cancer stem cell-like side population cells in clear cell renal cell carcinoma cell line 769P. *PLoS one*. 2013;8(7):e68293.

Hurlin PJ. N-Myc functions in transcription and development. *Birth defects research Part C, Embryo today : reviews*. 2005;75(4):340-52.

Jager R, Hahne J, Jacob A, Egert A, Schenkel J, Wernert N, et al. Mice transgenic for NPM-ALK develop non-Hodgkin lymphomas. *Anticancer research*. 2005;25(5):3191-6.

Jang GB, Hong IS, Kim RJ, Lee SY, Park SJ, Lee ES, et al. Wnt/beta-Catenin Small-Molecule Inhibitor CWP232228 Preferentially Inhibits the Growth of Breast Cancer Stem-like Cells. *Cancer research*. 2015;75(8):1691-702.

Jang GB, Kim JY, Cho SD, Park KS, Jung JY, Lee HY, et al. Blockade of Wnt/beta-catenin signaling suppresses breast cancer metastasis by inhibiting CSC-like phenotype. *Scientific reports*. 2015;5:12465.

Jang GB, Kim JY, Cho SD, Park KS, Jung JY, Lee HY, et al. Blockade of Wnt/beta-catenin signaling suppresses breast cancer metastasis by inhibiting CSC-like phenotype. *Scientific reports*. 2015;5:12465.

Janssen-Heininger YM, Mossman BT, Heintz NH, Forman HJ, Kalyanaraman B, Finkel T, et al. Redox-based regulation of signal transduction: principles, pitfalls, and promises. *Free radical biology & medicine*. 2008;45(1):1-17.

Jeong CH, Cho YY, Kim MO, Kim SH, Cho EJ, Lee SY, et al. Phosphorylation of Sox2 cooperates in reprogramming to pluripotent stem cells. *Stem cells*. 2010;28(12):2141-50.

Johnston PA, Grandis JR. STAT3 signaling: anticancer strategies and challenges. *Molecular interventions*. 2011;11(1):18-26.

Juan J, Muraguchi T, Iezza G, Sears RC, McMahon M. Diminished WNT -> beta-catenin -> c-MYC signaling is a barrier for malignant progression of BRAFV600E-induced lung tumors. *Genes & development*. 2014;28(6):561-75.

Jung K, Gupta N, Wang P, Lewis JT, Gopal K, Wu F, et al. Triple negative breast cancers comprise a highly tumorigenic cell subpopulation detectable by its high responsiveness to a Sox2 regulatory region 2 (SRR2) reporter. *Oncotarget*. 2015;6(12):10366-73.

Justilien V, Walsh MP, Ali SA, Thompson EA, Murray NR, Fields AP. The PRKCI and SOX2 oncogenes are coamplified and cooperate to activate Hedgehog signaling in lung squamous cell carcinoma. *Cancer cell*. 2014;25(2):139-51.

Kaganoi J, Watanabe G, Okabe M, Nagatani S, Kawabe A, Shimada Y, et al. STAT1 activation-induced apoptosis of esophageal squamous cell carcinoma

cells in vivo. *Annals of surgical oncology*. 2007;14(4):1405-15.

Kamachi Y, Kondoh H. Sox proteins: regulators of cell fate specification and differentiation. *Development*. 2013;140(20):4129-44.

Kaplan DH, Shankaran V, Dighe AS, Stockert E, Aguet M, Old LJ, et al. Demonstration of an interferon gamma-dependent tumor surveillance system in immunocompetent mice. *Proceedings of the National Academy of Sciences of the United States of America*. 1998;95(13):7556-61.

Karagiannis P, Eto K. Ten years of induced pluripotency: from basic mechanisms to therapeutic applications. *Development*. 2016;143(12):2039-43.

Kawano T, Morioka M, Yano S, Hamada J, Ushio Y, Miyamoto E, et al. Decreased akt activity is associated with activation of forkhead transcription factor after transient forebrain ischemia in gerbil hippocampus. *Journal of cerebral blood flow and metabolism: official journal of the International Society of Cerebral Blood Flow and Metabolism*. 2002;22(8):926-34.

Kazandjian D, Blumenthal GM, Chen HY, He K, Patel M, Justice R, et al. FDA approval summary: crizotinib for the treatment of metastatic non-small cell lung cancer with anaplastic lymphoma kinase rearrangements. *The oncologist*. 2014;19(10):e5-11.

Keith B, Simon MC. Hypoxia-inducible factors, stem cells, and cancer. *Cell*. 2007;129(3):465-72.

Kemper K, de Goeje PL, Peeper DS, van Amerongen R. Phenotype switching: tumor cell plasticity as a resistance mechanism and target for therapy. *Cancer research*. 2014;74(21):5937-41.

Kesler MV, Paranjape GS, Asplund SL, McKenna RW, Jamal S, Kroft SH. Anaplastic large cell lymphoma: a flow cytometric analysis of 29 cases. *American journal of clinical pathology*. 2007;128(2):314-22.

Khodarev N, Ahmad R, Rajabi H, Pitroda S, Kufe T, McClary C, et al. Cooperativity of the MUC1 oncoprotein and STAT1 pathway in poor prognosis human breast cancer. *Oncogene*. 2010;29(6):920-9.

Khoury JD, Medeiros LJ, Rassidakis GZ, Yared MA, Tsioli P, Leventaki V, et al. Differential expression and clinical significance of tyrosine-phosphorylated STAT3 in ALK+ and ALK- anaplastic large cell lymphoma. *Clinical cancer research*. 2003; 9(10 Pt 1):3692-9.

Kim HS, Lee MS. STAT1 as a key modulator of cell death. *Cellular signalling*. 2007;19(3):454-65.

Kim J, Orkin SH. Embryonic stem cell-specific signatures in cancer: insights into genomic regulatory networks and implications for medicine. *Genome Med*. 2011;3(11):75.

Kim MH, Kim H. Oncogenes and tumor suppressors regulate glutamine metabolism in cancer cells. *Journal of cancer prevention*. 2013;18(3):221-6.

Kim TK, Maniatis T. Regulation of interferon-gamma-activated STAT1 by the ubiquitin-proteasome pathway. *Science*. 1996;273(5282):1717-9.

Kinney MC, Collins RD, Greer JP, Whitlock JA, Sioutos N, Kadin ME. A small-cell-predominant variant of primary Ki-1 (CD30)+ T-cell lymphoma. *The American journal of surgical pathology*. 1993;17(9):859-68.

Kinney MC, Higgins RA, Medina EA. Anaplastic large cell lymphoma: twenty-five years of discovery. *Archives of pathology & laboratory medicine*. 2011;135(1):19-43.

Kirken RA, Rui H, Malabarba MG, Howard OM, Kawamura M, O'Shea JJ, et al. Activation of JAK3, but not JAK1, is critical for IL-2-induced proliferation and STAT5 recruitment by a COOH-terminal region of the IL-2 receptor beta-chain. *Cytokine*. 1995;7(7):689-700.

Klaunig JE, Kamendulis LM, Hocevar BA. Oxidative stress and oxidative damage in carcinogenesis. *Toxicologic pathology*. 2010;38(1):96-109.

Klempner SJ, Cohen DW, Costa DB. ALK translocation in non-small cell lung cancer with adenocarcinoma and squamous cell carcinoma markers. *Journal of thoracic oncology : official publication of the International Association for the Study of Lung Cancer*. 2011;6(8):1439-40.

Koromilas AE, Sexl V. The tumor suppressor function of STAT1 in breast cancer. *Jak-Stat*. 2013;2(2):e23353.

Kortylewski M, Komyod W, Kauffmann ME, Bosserhoff A, Heinrich PC, Behrmann I. Interferon-gamma-mediated growth regulation of melanoma cells: involvement of STAT1-dependent and STAT1-independent signals. *The Journal of investigative dermatology*. 2004;122(2):414-22.

Kortylewski M, Kujawski M, Wang T, Wei S, Zhang S, Pilon-Thomas S, et al. Inhibiting Stat3 signaling in the hematopoietic system elicits multicomponent antitumor immunity. *Nature medicine*. 2005;11(12):1314-21.

Kothari S, Ud-Din N, Lisi M, Coyle T. Crizotinib in anaplastic lymphoma kinase-positive anaplastic large cell lymphoma in the setting of renal insufficiency: a case report. *Journal of medical case reports*. 2016;10:176.

Kovacic B, Stoiber D, Moriggl R, Weisz E, Ott RG, Kreibich R, et al. STAT1 acts as a tumor promoter for leukemia development. *Cancer cell*. 2006;10(1):77-87.

Kovarik J, Boudny V, Kocak I, Lauerova L, Fait V, Vagundova M. Malignant melanoma associates with deficient IFN-induced STAT 1 phosphorylation. *International journal of molecular medicine*. 2003;12(3):335-40.

Koyama-Nasu R, Haruta R, Nasu-Nishimura Y, Taniue K, Katou Y, Shirahige K, et al. The pleiotrophin-ALK axis is required for tumorigenicity of glioblastoma stem cells. *Oncogene*. 2014;33(17):2236-44.

Kramer MH, Hermans J, Wijburg E, Philippo K, Geelen E, van Krieken JH, et al. Clinical relevance of BCL2, BCL6, and MYC rearrangements in diffuse large B-

cell lymphoma. *Blood*. 1998;92(9):3152-62.

Krenacs L, Wellmann A, Sorbara L, Himmelmann AW, Bagdi E, Jaffe ES, et al. Cytotoxic cell antigen expression in anaplastic large cell lymphomas of T- and null-cell type and Hodgkin's disease: evidence for distinct cellular origin. *Blood*. 1997;89(3):980-9.

Kress TR, Sabo A, Amati B. MYC: connecting selective transcriptional control to global RNA production. *Nature reviews Cancer*. 2015;15(10):593-607.

Kwan KY, Shen J, Corey DP. C-MYC transcriptionally amplifies SOX2 target genes to regulate self-renewal in multipotent otic progenitor cells. *Stem cell reports*. 2015;4(1):47-60.

Lai R, Ingham RJ. The pathobiology of the oncogenic tyrosine kinase NPM-ALK: a brief update. *Therapeutic advances in hematology*. 2013;4(2):119-31.

Laimer K, Spizzo G, Obrist P, Gastl G, Brunhuber T, Schafer G, et al. STAT1 activation in squamous cell cancer of the oral cavity: a potential predictive marker of response to adjuvant chemotherapy. *Cancer*. 2007;110(2):326-33.

Lamant L, Pulford K, Bischof D, Morris SW, Mason DY, Delsol G, et al. Expression of the ALK tyrosine kinase gene in neuroblastoma. *Am J Pathol*. 2000;156(5):1711-21.

Lange K, Uckert W, Blankenstein T, Nadrowitz R, Bittner C, Renauld JC, et al. Overexpression of NPM-ALK induces different types of malignant lymphomas in

IL-9 transgenic mice. *Oncogene*. 2003;22(4):517-27.

Laplante M, Sabatini DM. mTOR signaling in growth control and disease. *Cell*. 2012;149(2):274-93.

Lawrence DW, Kornbluth J. E3 ubiquitin ligase NKLAM ubiquitinates STAT1 and positively regulates STAT1-mediated transcriptional activity. *Cellular signalling*. 2016;28(12):1833-41.

Lee HH, Norris A, Weiss JB, Frasch M. Jelly belly protein activates the receptor tyrosine kinase Alk to specify visceral muscle pioneers. *Nature*. 2003;425(6957):507-12.

Leis O, Eguiara A, Lopez-Arribillaga E, Alberdi MJ, Hernandez-Garcia S, Elorriaga K, et al. Sox2 expression in breast tumours and activation in breast cancer stem cells. *Oncogene*. 2012;31(11):1354-65.

Li L, Neaves WB. Normal stem cells and cancer stem cells: the niche matters. *Cancer research*. 2006;66(9):4553-7.

Li S, Lin P, Young KH, Kanagal-Shamanna R, Yin CC, Medeiros LJ. MYC/BCL2 double-hit high-grade B-cell lymphoma. *Advances in anatomic pathology*. 2013;20(5):315-26.

Li X, Xu Y, Chen Y, Chen S, Jia X, Sun T, et al. SOX2 promotes tumor metastasis by stimulating epithelial-to-mesenchymal transition via regulation of WNT/beta-catenin signal network. *Cancer letters*. 2013;336(2):379-89.



Lighvani AA, Frucht DM, Jankovic D, Yamane H, Aliberti J, Hissong BD, et al. T-bet is rapidly induced by interferon-gamma in lymphoid and myeloid cells. *Proceedings of the National Academy of Sciences of the United States of America*. 2001;98(26):15137-42.

Lin CY, Loven J, Rahl PB, Paranal RM, Burge CB, Bradner JE, et al. Transcriptional amplification in tumor cells with elevated c-Myc. *Cell*. 2012;151(1):56-67.

Lin CY, Tan BC, Liu H, Shih CJ, Chien KY, Lin CL, et al. Dephosphorylation of nucleophosmin by PP1beta facilitates pRB binding and consequent E2F1-dependent DNA repair. *Molecular biology of the cell*. 2010;21(24):4409-17.

Little CD, Nau MM, Carney DN, Gazdar AF, Minna JD. Amplification and expression of the c-myc oncogene in human lung cancer cell lines. *Nature*. 1983;306(5939):194-6.

Lu YX, Yuan L, Xue XL, Zhou M, Liu Y, Zhang C, et al. Regulation of colorectal carcinoma stemness, growth, and metastasis by an miR-200c-Sox2-negative feedback loop mechanism. *Clinical cancer research : an official journal of the American Association for Cancer Research*. 2014;20(10):2631-42.

Luis TC, Naber BA, Roozen PP, Brugman MH, de Haas EF, Ghazvini M, et al. Canonical wnt signaling regulates hematopoiesis in a dosage-dependent fashion. *Cell stem cell*. 2011;9(4):345-56.

MacDonald BT, Tamai K, He X. Wnt/beta-catenin signaling: components, mechanisms, and diseases. *Developmental cell*. 2009;17(1):9-26.

Maes B, Vanhentenrijk V, Wlodarska I, Cools J, Peeters B, Marynen P, et al. The NPM-ALK and the ATIC-ALK fusion genes can be detected in non-neoplastic cells. *The American journal of pathology*. 2001;158(6):2185-93.

Mahalingaiah PK, Singh KP. Chronic oxidative stress increases growth and tumorigenic potential of MCF-7 breast cancer cells. *PloS one*. 2014;9(1):e87371.

Malabarba MG, Rui H, Deutsch HH, Chung J, Kalthoff FS, Farrar WL, et al. Interleukin-13 is a potent activator of JAK3 and STAT6 in cells expressing interleukin-2 receptor-gamma and interleukin-4 receptor-alpha. *The Biochemical journal*. 1996;319 ( Pt 3):865-72.

Malcolm TI, Villarese P, Fairbairn CJ, Lamant L, Trinquand A, Hook CE, et al. Anaplastic large cell lymphoma arises in thymocytes and requires transient TCR expression for thymic egress. *Nature communications*. 2016;7:10087.

Marampon F, Ciccarelli C, Zani BM. Down-regulation of c-Myc following MEK/ERK inhibition halts the expression of malignant phenotype in rhabdomyosarcoma and in non-muscle-derived human tumors. *Molecular cancer*. 2006;5:31.

Marusyk A, Almendro V, Polyak K. Intra-tumour heterogeneity: a looking glass for cancer? *Nature reviews Cancer*. 2012;12(5):323-34.

Marzec M, Kasprzycka M, Liu X, Raghunath PN, Wlodarski P, Wasik MA. Oncogenic tyrosine kinase NPM/ALK induces activation of the MEK/ERK signaling pathway independently of c-Raf. *Oncogene*. 2007;26(6):813-21.

Mathivet T, Mazot P, Vigny M. In contrast to agonist monoclonal antibodies, both C-terminal truncated form and full length form of Pleiotrophin failed to activate vertebrate ALK (anaplastic lymphoma kinase)? *Cellular signalling*. 2007;19(12):2434-43.

McCauley HA, Guasch G. Serial orthotopic transplantation of epithelial tumors in single-cell suspension. *Methods in molecular biology*. 2013;1035:231-45.

McCubrey JA, Steelman LS, Chappell WH, Abrams SL, Wong EW, Chang F, et al. Roles of the Raf/MEK/ERK pathway in cell growth, malignant transformation and drug resistance. *Biochimica et biophysica acta*. 2007;1773(8):1263-84.

McDonnell SR, Hwang SR, Basrur V, Conlon KP, Fermin D, Wey E, et al. NPM-ALK signals through glycogen synthase kinase 3beta to promote oncogenesis. *Oncogene*. 2012;31(32):3733-40.

Meacham CE, Morrison SJ. Tumour heterogeneity and cancer cell plasticity. *Nature*. 2013;501(7467):328-37.

Medeiros LJ, Elenitoba-Johnson KS. Anaplastic Large Cell Lymphoma. *American journal of clinical pathology*. 2007;127(5):707-22.

Meissl K, Macho-Maschler S, Muller M, Strobl B. The good and the bad faces of

STAT1 in solid tumours. *Cytokine*. 2015.

Meraz MA, White JM, Sheehan KC, Bach EA, Rodig SJ, Dighe AS, et al. Targeted disruption of the Stat1 gene in mice reveals unexpected physiologic specificity in the JAK-STAT signaling pathway. *Cell*. 1996;84(3):431-42.

Merkel O, Hamacher F, Sifft E, Kenner L, Greil R. Novel therapeutic options in anaplastic large cell lymphoma: molecular targets and immunological tools. *Molecular cancer therapeutics*. 2011;10(7):1127-36.

Merkel O, Kenner L, Turner SD. Stem cell hunt in NHL. *Oncoscience*. 2015;2(10):809-10.

Miller DM, Thomas SD, Islam A, Muench D, Sedoris K. c-Myc and cancer metabolism. *Clinical cancer research : an official journal of the American Association for Cancer Research*. 2012;18(20):5546-53.

Miura Y, Tsujioka T, Nishimura Y, Sakaguchi H, Maeda M, Hayashi H, et al. TRAIL expression up-regulated by interferon-gamma via phosphorylation of STAT1 induces myeloma cell death. *Anticancer research*. 2006;26(6B):4115-24.

Molina JR, Hayashi Y, Stephens C, Georgescu MM. Invasive glioblastoma cells acquire stemness and increased Akt activation. *Neoplasia*. 2010;12(6):453-63.

Moog-Lutz C, Degoutin J, Gouzi JY, Frobert Y, Brunet-de Carvalho N, Bureau J, et al. Activation and inhibition of anaplastic lymphoma kinase receptor tyrosine kinase by monoclonal antibodies and absence of agonist activity of pleiotrophin.

The Journal of biological chemistry. 2005;280(28):26039-48.

Moon RT, Kohn AD, De Ferrari GV, Kaykas A. WNT and beta-catenin signalling: diseases and therapies. Nature reviews Genetics. 2004;5(9):691-701.

Mora J, Filippa DA, Thaler HT, Polyak T, Cranor ML, Wollner N. Large cell non-Hodgkin lymphoma of childhood: Analysis of 78 consecutive patients enrolled in 2 consecutive protocols at the Memorial Sloan-Kettering Cancer Center. Cancer. 2000;88(1):186-97.

Morris SW, Kirstein MN, Valentine MB, Dittmer KG, Shapiro DN, Saltman DL, et al. Fusion of a kinase gene, ALK, to a nucleolar protein gene, NPM, in non-Hodgkin's lymphoma. Science. 1994;263(5151):1281-4.

Morrissey PA, Quinn PB, Sheehy PJ. Newer aspects of micronutrients in chronic disease: vitamin E. The Proceedings of the Nutrition Society. 1994;53(3):571-82.

Mosse YP, Lim MS, Voss SD, Wilner K, Ruffner K, Laliberte J, et al. Safety and activity of crizotinib for paediatric patients with refractory solid tumours or anaplastic large-cell lymphoma: a Children's Oncology Group phase 1 consortium study. The Lancet Oncology. 2013;14(6):472-80.

Moti N, Malcolm T, Hamoudi R, Mian S, Garland G, Hook CE, et al. Anaplastic large cell lymphoma-propagating cells are detectable by side population analysis and possess an expression profile reflective of a primitive origin. Oncogene. 2015;34(14):1843-52.

Moumen M, Chiche A, Decraene C, Petit V, Gandarillas A, Deugnier MA, et al. Myc is required for beta-catenin-mediated mammary stem cell amplification and tumorigenesis. *Molecular cancer*. 2013;12(1):132.

Murga-Zamalloa CA, Mendoza-Reinoso V, Sahasrabudhe AA, Rolland D, Hwang SR, McDonnell SR, et al. NPM-ALK phosphorylates WASp Y102 and contributes to oncogenesis of anaplastic large cell lymphoma. *Oncogene*. 2016.

Murray PB, Lax I, Reshetnyak A, Ligon GF, Lillquist JS, Natoli EJ, Jr., et al. Heparin is an activating ligand of the orphan receptor tyrosine kinase ALK. *Sci Signal*. 2015;8(360):ra6.

Myers SA, Peddada S, Chatterjee N, Friedrich T, Tomoda K, Krings G, et al. SOX2 O-GlcNAcylation alters its protein-protein interactions and genomic occupancy to modulate gene expression in pluripotent cells. *eLife*. 2016;5:e10647.

Nakamura S, Shiota M, Nakagawa A, Yatabe Y, Kojima M, Motoori T, et al. Anaplastic large cell lymphoma: a distinct molecular pathologic entity: a reappraisal with special reference to p80(NPM/ALK) expression. *The American journal of surgical pathology*. 1997;21(12):1420-32.

Nath S, Mukherjee P. MUC1: a multifaceted oncoprotein with a key role in cancer progression. *Trends Mol Med*. 2014;20(6):332-42.

Neumann J, Bahr F, Horst D, Kriegl L, Engel J, Luque RM, et al. SOX2

expression correlates with lymph-node metastases and distant spread in right-sided colon cancer. *BMC cancer*. 2011;11:518.

Nie Z, Hu G, Wei G, Cui K, Yamane A, Resch W, et al. c-Myc is a universal amplifier of expressed genes in lymphocytes and embryonic stem cells. *Cell*. 2012;151(1):68-79.

Nieborowska-Skorska M, Slupianek A, Xue L, Zhang Q, Raghunath PN, Hoser G, et al. Role of signal transducer and activator of transcription 5 in nucleophosmin/ anaplastic lymphoma kinase-mediated malignant transformation of lymphoid cells. *Cancer research*. 2001;61(17):6517-23.

Ning Y, Riggins RB, Mulla JE, Chung H, Zwart A, Clarke R. IFN $\gamma$  restores breast cancer sensitivity to fulvestrant by regulating STAT1, IFN regulatory factor 1, NF- $\kappa$ B, BCL2 family members, and signaling to caspase-dependent apoptosis. *Molecular cancer therapeutics*. 2010;9(5):1274-85.

Nishikawa S, Goldstein RA, Nierras CR. The promise of human induced pluripotent stem cells for research and therapy. *Nature reviews Molecular cell biology*. 2008;9(9):725-9.

O'Brien CA, Kreso A, Dick JE. Cancer stem cells in solid tumors: an overview. *Seminars in radiation oncology*. 2009;19(2):71-7.

O'Brien CA, Kreso A, Jamieson CH. Cancer stem cells and self-renewal. *Clinical cancer research : an official journal of the American Association for Cancer*

Research. 2010;16(12):3113-20.

Oren O, Smith BD. Eliminating Cancer Stem Cells by Targeting Embryonic Signaling Pathways. Stem cell reviews. 2016.

Ortmann RA, Cheng T, Visconti R, Frucht DM, O'Shea JJ. Janus kinases and signal transducers and activators of transcription: their roles in cytokine signaling, development and immunoregulation. Arthritis research. 2000;2(1):16-32.

Oskarsson T, Batlle E, Massague J. Metastatic stem cells: sources, niches, and vital pathways. Cell stem cell. 2014;14(3):306-21.

Osuka K, Watanabe Y, Usuda N, Atsuzawa K, Wakabayashi T, Takayasu M. Oxidative stress activates STAT1 in basilar arteries after subarachnoid hemorrhage. Brain research. 2010;1332:12-9.

Ou SH, Bartlett CH, Mino-Kenudson M, Cui J, Iafrate AJ. Crizotinib for the treatment of ALK-rearranged non-small cell lung cancer: a success story to usher in the second decade of molecular targeted therapy in oncology. The oncologist. 2012;17(11):1351-75.

Ouyang J, Yu W, Liu J, Zhang N, Florens L, Chen J, et al. Cyclin-dependent kinase-mediated Sox2 phosphorylation enhances the ability of Sox2 to establish the pluripotent state. The Journal of biological chemistry. 2015;290(37):22782-94.



Pan XN, Chen JJ, Wang LX, Xiao RZ, Liu LL, Fang ZG, et al. Inhibition of c-Myc overcomes cytotoxic drug resistance in acute myeloid leukemia cells by promoting differentiation. *PLoS one*. 2014;9(8):e105381.

Pansky A, Hildebrand P, Fasler-Kan E, Baselgia L, Ketterer S, Beglinger C, et al. Defective Jak-STAT signal transduction pathway in melanoma cells resistant to growth inhibition by interferon-alpha. *International journal of cancer*. 2000;85(5):720-5.

Park JB, Lee CS, Jang JH, Ghim J, Kim YJ, You S, et al. Phospholipase signalling networks in cancer. *Nature reviews Cancer*. 2012;12(11):782-92.

Patel JH, Loboda AP, Showe MK, Showe LC, McMahon SB. Analysis of genomic targets reveals complex functions of MYC. *Nature reviews Cancer*. 2004;4(7):562-8.

Pearson JD, Lee JK, Bacani JT, Lai R, Ingham RJ. NPM-ALK: The Prototypic Member of a Family of Oncogenic Fusion Tyrosine Kinases. *J Signal Transduct*. 2012;2012:123253.

Pelengaris S, Khan M, Evan G. c-MYC: more than just a matter of life and death. *Nature reviews Cancer*. 2002;2(10):764-76.

Pencik J, Schleder M, Gruber W, Unger C, Walker SM, Chalaris A, et al. STAT3 regulated ARF expression suppresses prostate cancer metastasis. *Nature communications*. 2015;6:7736.

Perna D, Faga G, Verrecchia A, Gorski MM, Barozzi I, Narang V, et al. Genome-wide mapping of Myc binding and gene regulation in serum-stimulated fibroblasts. *Oncogene*. 2012;31(13):1695-709.

Piccaluga PP, Gazzola A, Mannu C, Agostinelli C, Bacci F, Sabattini E, et al. Pathobiology of anaplastic large cell lymphoma. *Adv Hematol*. 2010:345053.

Pileri S, Falini B, Delsol G, Stein H, Baglioni P, Poggi S, et al. Lymphohistiocytic T-cell lymphoma (anaplastic large cell lymphoma CD30+/Ki-1 + with a high content of reactive histiocytes). *Histopathology*. 1990;16(4):383-91.

Piva M, Domenici G, Iriundo O, Rabano M, Simoes BM, Comaills V, et al. Sox2 promotes tamoxifen resistance in breast cancer cells. *EMBO molecular medicine*. 2014;6(1):66-79.

Piva R, Agnelli L, Pellegrino E, Todoerti K, Grosso V, Tamagno I, et al. Gene expression profiling uncovers molecular classifiers for the recognition of anaplastic large-cell lymphoma within peripheral T-cell neoplasms. *Journal of clinical oncology : official journal of the American Society of Clinical Oncology*. 2010;28(9):1583-90.

Plaks V, Kong N, Werb Z. The cancer stem cell niche: how essential is the niche in regulating stemness of tumor cells? *Cell stem cell*. 2015;16(3):225-38.

Qi D, Wang Q, Yu M, Lan R, Li S, Lu F. Mitotic phosphorylation of SOX2 mediated by Aurora kinase A is critical for the stem-cell like cell maintenance in

PA-1 cells. *Cell cycle*. 2016;15(15):2009-18.

Qiu L, Lai R, Lin Q, Lau E, Thomazy DM, Calame D, et al. Autocrine release of interleukin-9 promotes Jak3-dependent survival of ALK+ anaplastic large-cell lymphoma cells. *Blood*. 2006;108(7):2407-15.

Raetz EA, Perkins SL, Carlson MA, Schooler KP, Carroll WL, Virshup DM. The nucleophosmin-anaplastic lymphoma kinase fusion protein induces c-Myc expression in pediatric anaplastic large cell lymphomas. *The American journal of pathology*. 2002;161(3):875-83.

Ramana CV, Chatterjee-Kishore M, Nguyen H, Stark GR. Complex roles of Stat1 in regulating gene expression. *Oncogene*. 2000;19(21):2619-27.

Ramana CV, Grammatikakis N, Chernov M, Nguyen H, Goh KC, Williams BR, et al. Regulation of c-myc expression by IFN-gamma through Stat1-dependent and -independent pathways. *The EMBO journal*. 2000;19(2):263-72.

Regis G, Pensa S, Boselli D, Novelli F, Poli V. Ups and downs: the STAT1:STAT3 seesaw of Interferon and gp130 receptor signalling. *Semin Cell Dev Biol*. 2008;19(4):351-9.

Reliene R, Fischer E, Schiestl RH. Effect of N-acetyl cysteine on oxidative DNA damage and the frequency of DNA deletions in atm-deficient mice. *Cancer research*. 2004;64(15):5148-53.

Ren Y, Zhao P, Liu J, Yuan Y, Cheng Q, Zuo Y, et al. Deubiquitinase USP2a

Sustains Interferons Antiviral Activity by Restricting Ubiquitination of Activated STAT1 in the Nucleus. *PLoS pathogens*. 2016;12(7):e1005764.

Reshetnyak AV, Murray PB, Shi X, Mo ES, Mohanty J, Tome F, et al. Augmentor alpha and beta (FAM150) are ligands of the receptor tyrosine kinases ALK and LTK: Hierarchy and specificity of ligand-receptor interactions. *Proceedings of the National Academy of Sciences of the United States of America*. 2015;112(52):15862-7.

Reuter S, Gupta SC, Chaturvedi MM, Aggarwal BB. Oxidative stress, inflammation, and cancer: how are they linked? *Free radical biology & medicine*. 2010;49(11):1603-16.

Ricardo S, Vieira AF, Gerhard R, Leitao D, Pinto R, Cameselle-Teijeiro JF, et al. Breast cancer stem cell markers CD44, CD24 and ALDH1: expression distribution within intrinsic molecular subtype. *Journal of clinical pathology*. 2011;64(11):937-46.

Riobo NA, Lu K, Ai X, Haines GM, Emerson CP, Jr. Phosphoinositide 3-kinase and Akt are essential for Sonic Hedgehog signaling. *Proceedings of the National Academy of Sciences of the United States of America*. 2006;103(12):4505-10.

Rizzardi GP, Tambussi G, Barcellini W, Capiluppi B, Clerici E, Maestra LL, et al. Soluble CD30, tumour necrosis factor (TNF)-alpha, and TNF receptors in primary HIV-1 infection: relationship with HIV-1, RNA, clinical outcome and early

antiviral therapy. *Journal of biological regulators and homeostatic agents*. 1997;11(1-2):43-9.

Rizzino A. Concise review: The Sox2-Oct4 connection: critical players in a much larger interdependent network integrated at multiple levels. *Stem cells*. 2013;31(6):1033-9.

Roberts PJ, Der CJ. Targeting the Raf-MEK-ERK mitogen-activated protein kinase cascade for the treatment of cancer. *Oncogene*. 2007;26(22):3291-310.

Roderick JE, Tesell J, Shultz LD, Brehm MA, Greiner DL, Harris MH, et al. c-Myc inhibition prevents leukemia initiation in mice and impairs the growth of relapsed and induction failure pediatric T-ALL cells. *Blood*. 2014;123(7):1040-50.

Rodrigues AB, Zoranovic T, Ayala-Camargo A, Grewal S, Reyes-Robles T, Krasny M, et al. Activated STAT regulates growth and induces competitive interactions independently of Myc, Yorkie, Wingless and ribosome biogenesis. *Development*. 2012;139(21):4051-61.

Romashkova JA, Makarov SS. NF-kappaB is a target of AKT in anti-apoptotic PDGF signalling. *Nature*. 1999;401(6748):86-90.

Rubie H, Hartmann O, Michon J, Frappaz D, Coze C, Chastagner P, et al. N-Myc gene amplification is a major prognostic factor in localized neuroblastoma: results of the French NBL 90 study. Neuroblastoma Study Group of the Societe Francaise d'Oncologie Pediatrique. *Journal of clinical oncology : official journal of*

the American Society of Clinical Oncology. 1997;15(3):1171-82.

Saijo H, Hirohashi Y, Torigoe T, Horibe R, Takaya A, Murai A, et al. Plasticity of lung cancer stem-like cells is regulated by the transcription factor HOXA5 that is induced by oxidative stress. *Oncotarget*. 2016.

Salcido CD, Larochele A, Taylor BJ, Dunbar CE, Varticovski L. Molecular characterisation of side population cells with cancer stem cell-like characteristics in small-cell lung cancer. *British journal of cancer*. 2010;102(11):1636-44.

Sanda T, Tyner JW, Gutierrez A, Ngo VN, Glover J, Chang BH, et al. TYK2-STAT1-BCL2 pathway dependence in T-cell acute lymphoblastic leukemia. *Cancer discovery*. 2013;3(5):564-77.

Sansom OJ, Meniel VS, Muncan V, Pheesse TJ, Wilkins JA, Reed KR, et al. Myc deletion rescues Apc deficiency in the small intestine. *Nature*. 2007;446(7136):676-9.

Santini R, Pietrobono S, Pandolfi S, Montagnani V, D'Amico M, Penachioni JY, et al. SOX2 regulates self-renewal and tumorigenicity of human melanoma-initiating cells. *Oncogene*. 2014;33(38):4697-708.

Santo EE, Stroeken P, Sluis PV, Koster J, Versteeg R, Westerhout EM. FOXO3a is a major target of inactivation by PI3K/AKT signaling in aggressive neuroblastoma. *Cancer research*. 2013;73(7):2189-98.

Sarkar A, Hochedlinger K. The sox family of transcription factors: versatile

regulators of stem and progenitor cell fate. *Cell stem cell*. 2013;12(1):15-30.

Sato T, Selleri C, Young NS, Maciejewski JP. Inhibition of interferon regulatory factor-1 expression results in predominance of cell growth stimulatory effects of interferon-gamma due to phosphorylation of Stat1 and Stat3. *Blood*. 1997;90(12):4749-58.

Satoh Y, Matsumura I, Tanaka H, Ezoe S, Sugahara H, Mizuki M, et al. Roles for c-Myc in self-renewal of hematopoietic stem cells. *The Journal of biological chemistry*. 2004;279(24):24986-93.

Schlessinger J. Phospholipase Cgamma activation and phosphoinositide hydrolysis are essential for embryonal development. *Proceedings of the National Academy of Sciences of the United States of America*. 1997;94(7):2798-9.

Schmitt MJ, Philippidou D, Reinsbach SE, Margue C, Wienecke-Baldacchino A, Nashan D, et al. Interferon-gamma-induced activation of Signal Transducer and Activator of Transcription 1 (STAT1) up-regulates the tumor suppressing microRNA-29 family in melanoma cells. *Cell communication and signaling : CCS*. 2012;10(1):41.

Schroder K, Hertzog PJ, Ravasi T, Hume DA. Interferon-gamma: an overview of signals, mechanisms and functions. *Journal of leukocyte biology*. 2004;75(2):163-89.

Schultz J, Koczan D, Schmitz U, Ibrahim SM, Pilch D, Landsberg J, et al. Tumor-

promoting role of signal transducer and activator of transcription (Stat)1 in late-stage melanoma growth. *Clinical & experimental metastasis*. 2010;27(3):133-40.

Schust J, Sperl B, Hollis A, Mayer TU, Berg T. Stattic: a small-molecule inhibitor of STAT3 activation and dimerization. *Chemistry & biology*. 2006;13(11):1235-42.

Sears R, Leone G, DeGregori J, Nevins JR. Ras enhances Myc protein stability. *Molecular cell*. 1999;3(2):169-79.

Sears R, Nuckolls F, Haura E, Taya Y, Tamai K, Nevins JR. Multiple Ras-dependent phosphorylation pathways regulate Myc protein stability. *Genes & development*. 2000;14(19):2501-14.

Seigel GM, Campbell LM, Narayan M, Gonzalez-Fernandez F. Cancer stem cell characteristics in retinoblastoma. *Molecular vision*. 2005;11:729-37.

Sellier H, Rebillard A, Guette C, Barre B, Coqueret O. How should we define STAT3 as an oncogene and as a potential target for therapy? *Jak-Stat*. 2013;2(3):e24716.

Shen A, Wang L, Huang M, Sun J, Chen Y, Shen YY, et al. c-Myc alterations confer therapeutic response and acquired resistance to c-Met inhibitors in MET-addicted cancers. *Cancer research*. 2015;75(21):4548-59.

Shen Y, Devgan G, Darnell JE, Jr., Bromberg JF. Constitutively activated Stat3 protects fibroblasts from serum withdrawal and UV-induced apoptosis and antagonizes the proapoptotic effects of activated Stat1. *Proceedings of the*



National Academy of Sciences of the United States of America. 2001;98(4):1543-8.

Shi GM, Xu Y, Fan J, Zhou J, Yang XR, Qiu SJ, et al. Identification of side population cells in human hepatocellular carcinoma cell lines with stepwise metastatic potentials. *Journal of cancer research and clinical oncology*. 2008;134(11):1155-63.

Simic MG, Bergtold DS, Karam LR. Generation of oxy radicals in biosystems. *Mutation research*. 1989;214(1):3-12.

Singh RR, Cho-Vega JH, Davuluri Y, Ma S, Kasbidi F, Milito C, et al. Sonic hedgehog signaling pathway is activated in ALK-positive anaplastic large cell lymphoma. *Cancer research*. 2009;69(6):2550-8.

Singh SK, Hawkins C, Clarke ID, Squire JA, Bayani J, Hide T, et al. Identification of human brain tumour initiating cells. *Nature*. 2004;432(7015):396-401.

Singhi AD, Cimino-Mathews A, Jenkins RB, Lan F, Fink SR, Nassar H, et al. MYC gene amplification is often acquired in lethal distant breast cancer metastases of unamplified primary tumors. *Modern pathology : an official journal of the United States and Canadian Academy of Pathology, Inc*. 2012;25(3):378-87.

Sironi JJ, Ouchi T. STAT1-induced apoptosis is mediated by caspases 2, 3, and 7. *The Journal of biological chemistry*. 2004;279(6):4066-74.

Slupianek A, Nieborowska-Skorska M, Hoser G, Morrione A, Majewski M, Xue L, et al. Role of phosphatidylinositol 3-kinase-Akt pathway in nucleophosmin/anaplastic lymphoma kinase-mediated lymphomagenesis. *Cancer research*. 2001;61(5):2194-9.

Soeda A, Park M, Lee D, Mintz A, Androutsellis-Theotokis A, McKay RD, et al. Hypoxia promotes expansion of the CD133-positive glioma stem cells through activation of HIF-1alpha. *Oncogene*. 2009;28(45):3949-59.

Song G, Ouyang G, Bao S. The activation of Akt/PKB signaling pathway and cell survival. *Journal of cellular and molecular medicine*. 2005;9(1):59-71.

Soond SM, Townsend PA, Barry SP, Knight RA, Latchman DS, Stephanou A. ERK and the F-box protein betaTRCP target STAT1 for degradation. *The Journal of biological chemistry*. 2008;283(23):16077-83.

Sosa V, Moline T, Somoza R, Paciucci R, Kondoh H, ME LL. Oxidative stress and cancer: an overview. *Ageing research reviews*. 2013;12(1):376-90.

Staber PB, Vesely P, Haq N, Ott RG, Funato K, Bambach I, et al. The oncoprotein NPM-ALK of anaplastic large-cell lymphoma induces JUNB transcription via ERK1/2 and JunB translation via mTOR signaling. *Blood*. 2007;110(9):3374-83.

Stancato LF, David M, Carter-Su C, Larner AC, Pratt WB. Preassociation of STAT1 with STAT2 and STAT3 in separate signalling complexes prior to cytokine

stimulation. *The Journal of biological chemistry*. 1996;271(8):4134-7.

Stephanou A, Brar BK, Knight RA, Latchman DS. Opposing actions of STAT-1 and STAT-3 on the Bcl-2 and Bcl-x promoters. *Cell death and differentiation*. 2000;7(3):329-30.

Stine ZE, Walton ZE, Altman BJ, Hsieh AL, Dang CV. MYC, Metabolism, and Cancer. *Cancer discovery*. 2015;5(10):1024-39.

Stoica GE, Kuo A, Powers C, Bowden ET, Sale EB, Riegel AT, et al. Midkine binds to anaplastic lymphoma kinase (ALK) and acts as a growth factor for different cell types. *The Journal of biological chemistry*. 2002;277(39):35990-8.

Suhara T, Kim HS, Kirshenbaum LA, Walsh K. Suppression of Akt signaling induces Fas ligand expression: involvement of caspase and Jun kinase activation in Akt-mediated Fas ligand regulation. *Molecular and cellular biology*. 2002;22(2):680-91.

Sullivan I, Planchard D. ALK inhibitors in non-small cell lung cancer: the latest evidence and developments. *Therapeutic advances in medical oncology*. 2016;8(1):32-47.

Sun WH, Pabon C, Alsayed Y, Huang PP, Jandeska S, Uddin S, et al. Interferon-alpha resistance in a cutaneous T-cell lymphoma cell line is associated with lack of STAT1 expression. *Blood*. 1998;91(2):570-6.

Szabo SJ, Kim ST, Costa GL, Zhang X, Fathman CG, Glimcher LH. A novel

transcription factor, T-bet, directs Th1 lineage commitment. *Cell*. 2000;100(6):655-69.

Tabbo F, Barreca A, Piva R, Inghirami G. ALK Signaling and Target Therapy in Anaplastic Large Cell Lymphoma. *Frontiers in oncology*. 2012;2:41.

Tabor MH, Clay MR, Owen JH, Bradford CR, Carey TE, Wolf GT, et al. Head and neck cancer stem cells: the side population. *The Laryngoscope*. 2011;121(3):527-33.

Takahashi-Yanaga F, Kahn M. Targeting Wnt signaling: can we safely eradicate cancer stem cells? *Clinical cancer research : an official journal of the American Association for Cancer Research*. 2010;16(12):3153-62.

Tang DG. Understanding cancer stem cell heterogeneity and plasticity. *Cell research*. 2012;22(3):457-72.

ten Berge RL, Oudejans JJ, Ossenkoppele GJ, Pulford K, Willemze R, Falini B, et al. ALK expression in extranodal anaplastic large cell lymphoma favours systemic disease with (primary) nodal involvement and a good prognosis and occurs before dissemination. *Journal of clinical pathology*. 2000;53(6):445-50.

ten Berge RL, Snijdwint FG, von Mensdorff-Pouilly S, Poort-Keesom RJ, Oudejans JJ, Meijer JW, et al. MUC1 (EMA) is preferentially expressed by ALK positive anaplastic large cell lymphoma, in the normally glycosylated or only partly hypoglycosylated form. *Journal of clinical pathology*. 2001;54(12):933-9.

Thomas SJ, Snowden JA, Zeidler MP, Danson SJ. The role of JAK/STAT signalling in the pathogenesis, prognosis and treatment of solid tumours. *British journal of cancer*. 2015;113(3):365-71.

Thornber K, Colomba A, Ceccato L, Delsol G, Payrastre B, Gaits-Iacovoni F. Reactive oxygen species and lipoxygenases regulate the oncogenicity of NPM-ALK-positive anaplastic large cell lymphomas. *Oncogene*. 2009;28(29):2690-6.

Thyrell L, Arulampalam V, Hjortsberg L, Farnebo M, Grander D, Pokrovskaja Tamm K. Interferon alpha induces cell death through interference with interleukin 6 signaling and inhibition of STAT3 activity. *Experimental cell research*. 2007;313(19):4015-24.

Tian Y, Jia X, Wang S, Li Y, Zhao P, Cai D, et al. SOX2 oncogenes amplified and operate to activate AKT signaling in gastric cancer and predict immunotherapy responsiveness. *Journal of cancer research and clinical oncology*. 2014;140(7):1117-24.

Tsai WB, Aiba I, Long Y, Lin HK, Feun L, Savaraj N, et al. Activation of Ras/PI3K/ERK pathway induces c-Myc stabilization to upregulate argininosuccinate synthetase, leading to arginine deiminase resistance in melanoma cells. *Cancer research*. 2012;72(10):2622-33.

Tsai WB, Aiba I, Long Y, Lin HK, Feun L, Savaraj N, et al. Activation of Ras/PI3K/ERK pathway induces c-Myc stabilization to upregulate

argininosuccinate synthetase, leading to arginine deiminase resistance in melanoma cells. *Cancer research*. 2012;72(10):2622-33.

Turner SD, Merz H, Yeung D, Alexander DR. CD2 promoter regulated nucleophosmin-anaplastic lymphoma kinase in transgenic mice causes B lymphoid malignancy. *Anticancer research*. 2006;26(5A):3275-9.

Turner SD, Tooze R, Maclennan K, Alexander DR. Vav-promoter regulated oncogenic fusion protein NPM-ALK in transgenic mice causes B-cell lymphomas with hyperactive Jun kinase. *Oncogene*. 2003;22(49):7750-61.

Vanhaesebroeck B, Stephens L, Hawkins P. PI3K signalling: the path to discovery and understanding. *Nature reviews Molecular cell biology*. 2012;13(3):195-203.

Vassallo J, Lamant L, Brugieres L, Gaillard F, Campo E, Brousset P, et al. ALK-positive anaplastic large cell lymphoma mimicking nodular sclerosis Hodgkin's lymphoma: report of 10 cases. *The American journal of surgical pathology*. 2006;30(2):223-9.

Vega F, Medeiros LJ, Leventaki V, Atwell C, Cho-Vega JH, Tian L, et al. Activation of mammalian target of rapamycin signaling pathway contributes to tumor cell survival in anaplastic lymphoma kinase-positive anaplastic large cell lymphoma. *Cancer research*. 2006;66(13):6589-97.

Vermeulen L, De Sousa EMF, van der Heijden M, Cameron K, de Jong JH,

Borovski T, et al. Wnt activity defines colon cancer stem cells and is regulated by the microenvironment. *Nature cell biology*. 2010;12(5):468-76.

Vicente-Duenas C, Gutierrez de Diego J, Rodriguez FD, Jimenez R, Cobaleda C. The role of cellular plasticity in cancer development. *Curr Med Chem*. 2009;16(28):3676-85.

Visvader JE. Cells of origin in cancer. *Nature*. 2011;469(7330):314-22.

Voena C, Conte C, Ambrogio C, Boeri Erba E, Boccalatte F, Mohammed S, et al. The tyrosine phosphatase Shp2 interacts with NPM-ALK and regulates anaplastic lymphoma cell growth and migration. *Cancer research*. 2007;67(9):4278-86.

Vose J, Armitage J, Weisenburger D, International TCLP. International peripheral T-cell and natural killer/T-cell lymphoma study: pathology findings and clinical outcomes. *Journal of clinical oncology : official journal of the American Society of Clinical Oncology*. 2008;26(25):4124-30.

Wahara T, Fujimoto J, Wen D, Cupples R, Bucay N, Arakawa T, et al. Molecular characterization of ALK, a receptor tyrosine kinase expressed specifically in the nervous system. *Oncogene*. 1997;14(4):439-49.

Wallace GC, Dixon-Mah YN, Vandergrift WA, 3rd, Ray SK, Haar CP, Mittendorf AM, et al. Targeting oncogenic ALK and MET: a promising therapeutic strategy for glioblastoma. *Metab Brain Dis*. 2013;28(3):355-66.

Walter D, Satheesha S, Albrecht P, Bornhauser BC, D'Alessandro V, Oesch SM, et al. CD133 positive embryonal rhabdomyosarcoma stem-like cell population is enriched in rhabdospheres. *PloS one*. 2011;6(5):e19506.

Wang C, Xie J, Guo J, Manning HC, Gore JC, Guo N. Evaluation of CD44 and CD133 as cancer stem cell markers for colorectal cancer. *Oncology reports*. 2012;28(4):1301-8.

Wang F, Gao X, Barrett JW, Shao Q, Bartee E, Mohamed MR, et al. RIG-I mediates the co-induction of tumor necrosis factor and type I interferon elicited by myxoma virus in primary human macrophages. *PLoS pathogens*. 2008;4(7):e1000099.

Wang H, Chauhan J, Hu A, Pendleton K, Yap JL, Sabato PE, et al. Disruption of Myc-Max heterodimerization with improved cell-penetrating analogs of the small molecule 10074-G5. *Oncotarget*. 2013;4(6):936-47.

Wang H, Yang Y, Sharma N, Tarasova NI, Timofeeva OA, Winkler-Pickett RT, et al. STAT1 activation regulates proliferation and differentiation of renal progenitors. *Cellular signalling*. 2010;22(11):1717-26.

Wang J, Kim J, Roh M, Franco OE, Hayward SW, Wills ML, et al. Pim1 kinase synergizes with c-MYC to induce advanced prostate carcinoma. *Oncogene*. 2010;29(17):2477-87.

Wang J, Wang H, Li Z, Wu Q, Lathia JD, McLendon RE, et al. c-Myc is required



for maintenance of glioma cancer stem cells. *PloS one*. 2008;3(11):e3769.

Wang SJ, Omori N, Li F, Jin G, Zhang WR, Hamakawa Y, et al. Potentiation of Akt and suppression of caspase-9 activations by electroacupuncture after transient middle cerebral artery occlusion in rats. *Neuroscience letters*. 2002;331(2):115-8.

Wang X, Cunningham M, Zhang X, Tokarz S, Laraway B, Troxell M, et al. Phosphorylation regulates c-Myc's oncogenic activity in the mammary gland. *Cancer research*. 2011;71(3):925-36.

Wang Y, Ren Z, Tao D, Tilwalli S, Goswami R, Balabanov R. STAT1/IRF-1 signaling pathway mediates the injurious effect of interferon-gamma on oligodendrocyte progenitor cells. *Glia*. 2010;58(2):195-208.

Wang Z, Ge L, Wang M, Carr BI. Phosphorylation regulates Myc expression via prolonged activation of the mitogen-activated protein kinase pathway. *Journal of cellular physiology*. 2006;208(1):133-40.

Waris G, Ahsan H. Reactive oxygen species: role in the development of cancer and various chronic conditions. *Journal of carcinogenesis*. 2006;5:14.

Waris G, Ahsan H. Reactive oxygen species: role in the development of cancer and various chronic conditions. *Journal of carcinogenesis*. 2006;5:14.

Watanabe M, Itoh K, Togano T, Kadin ME, Watanabe T, Higashihara M, et al. Ets-1 activates overexpression of JunB and CD30 in Hodgkin's lymphoma and

anaplastic large-cell lymphoma. *The American journal of pathology*. 2012;180(2):831-8.

Watanabe M, Sasaki M, Itoh K, Higashihara M, Umezawa K, Kadin ME, et al. JunB induced by constitutive CD30-extracellular signal-regulated kinase 1/2 mitogen-activated protein kinase signaling activates the CD30 promoter in anaplastic large cell lymphoma and reed-sternberg cells of Hodgkin lymphoma. *Cancer research*. 2005;65(17):7628-34.

Wei D, Kanai M, Jia Z, Le X, Xie K. Kruppel-like factor 4 induces p27Kip1 expression in and suppresses the growth and metastasis of human pancreatic cancer cells. *Cancer research*. 2008;68(12):4631-9.

Weilemann A, Grau M, Erdmann T, Merkel O, Sobhiafshar U, Anagnostopoulos I, et al. Essential role of IRF4 and MYC signaling for survival of anaplastic large cell lymphoma. *Blood*. 2015;125(1):124-32.

Weina K, Utikal J. SOX2 and cancer: current research and its implications in the clinic. *Clinical and translational medicine*. 2014;3:19.

Wellstein A. ALK receptor activation, ligands and therapeutic targeting in glioblastoma and in other cancers. *Frontiers in oncology*. 2012;2:192.

Weng AP, Millholland JM, Yashiro-Ohtani Y, Arcangeli ML, Lau A, Wai C, et al. c-Myc is an important direct target of Notch1 in T-cell acute lymphoblastic leukemia/lymphoma. *Genes & development*. 2006;20(15):2096-109.

Wernig M, Meissner A, Foreman R, Brambrink T, Ku M, Hochedlinger K, et al. In vitro reprogramming of fibroblasts into a pluripotent ES-cell-like state. *Nature*. 2007;448(7151):318-24.

Widschwendter A, Tonko-Geymayer S, Welte T, Daxenbichler G, Marth C, Doppler W. Prognostic significance of signal transducer and activator of transcription 1 activation in breast cancer. *Clinical cancer research : an official journal of the American Association for Cancer Research*. 2002;8(10):3065-74.

Wilson A, Murphy MJ, Oskarsson T, Kaloulis K, Bettess MD, Oser GM, et al. c-Myc controls the balance between hematopoietic stem cell self-renewal and differentiation. *Genes & development*. 2004;18(22):2747-63.

Wong LH, Krauer KG, Hatzinisiriou I, Estcourt MJ, Hersey P, Tam ND, et al. Interferon-resistant human melanoma cells are deficient in ISGF3 components, STAT1, STAT2, and p48-ISGF3gamma. *The Journal of biological chemistry*. 1997;272(45):28779-85.

Wu C, Molavi O, Zhang H, Gupta N, Alshareef A, Bone KM, et al. STAT1 is phosphorylated and downregulated by the oncogenic tyrosine kinase NPM-ALK in ALK-positive anaplastic large-cell lymphoma. *Blood*. 2015;126(3):336-45.

Wu C, Zhang HF, Gupta N, Alshareef A, Wang Q, Huang YH, et al. A positive feedback loop involving the Wnt/beta-catenin/MYC/Sox2 axis defines a highly tumorigenic cell subpopulation in ALK-positive anaplastic large cell lymphoma.

Journal of hematology & oncology. 2016;9(1):120.

Wu F, Wang P, Young LC, Lai R, Li L. Proteome-wide identification of novel binding partners to the oncogenic fusion gene protein, NPM-ALK, using tandem affinity purification and mass spectrometry. The American journal of pathology. 2009;174(2):361-70.

Wu F, Zhang J, Wang P, Ye X, Jung K, Bone KM, et al. Identification of two novel phenotypically distinct breast cancer cell subsets based on Sox2 transcription activity. Cellular signalling. 2012;24(11):1989-98.

Wu J, Savooji J, Liu D. Second- and third-generation ALK inhibitors for non-small cell lung cancer. Journal of hematology & oncology. 2016;9:19.

Xi S, Dyer KF, Kimak M, Zhang Q, Gooding WE, Chaillet JR, et al. Decreased STAT1 expression by promoter methylation in squamous cell carcinogenesis. Journal of the National Cancer Institute. 2006;98(3):181-9.

Xi S, Dyer KF, Kimak M, Zhang Q, Gooding WE, Chaillet JR, et al. Decreased STAT1 expression by promoter methylation in squamous cell carcinogenesis. Journal of the National Cancer Institute. 2006;98(3):181-9.

Xi S, Dyer KF, Kimak M, Zhang Q, Gooding WE, Chaillet JR, et al. Decreased STAT1 expression by promoter methylation in squamous cell carcinogenesis. Journal of the National Cancer Institute. 2006;98(3):181-9.

Xing X, Feldman AL. Anaplastic large cell lymphomas: ALK positive, ALK

negative, and primary cutaneous. *Advances in anatomic pathology*. 2015;22(1):29-49.

Yada M, Hatakeyama S, Kamura T, Nishiyama M, Tsunematsu R, Imaki H, et al. Phosphorylation-dependent degradation of c-Myc is mediated by the F-box protein Fbw7. *The EMBO journal*. 2004;23(10):2116-25.

Yang L, Ren Y, Yu X, Qian F, Bian BS, Xiao HL, et al. ALDH1A1 defines invasive cancer stem-like cells and predicts poor prognosis in patients with esophageal squamous cell carcinoma. *Modern pathology : an official journal of the United States and Canadian Academy of Pathology, Inc*. 2014;27(5):775-83.

Yang N, Hui L, Wang Y, Yang H, Jiang X. Overexpression of SOX2 promotes migration, invasion, and epithelial-mesenchymal transition through the Wnt/beta-catenin pathway in laryngeal cancer Hep-2 cells. *Tumour biology : the journal of the International Society for Oncodevelopmental Biology and Medicine*. 2014;35(8):7965-73.

Yang Z, Augustin J, Hu J, Jiang H. Physical Interactions and Functional Coordination between the Core Subunits of Set1/Mll Complexes and the Reprogramming Factors. *PloS one*. 2015;10(12):e0145336.

Yasuda K, Torigoe T, Morita R, Kuroda T, Takahashi A, Matsuzaki J, et al. Ovarian cancer stem cells are enriched in side population and aldehyde dehydrogenase bright overlapping population. *PloS one*. 2013;8(8):e68187.

Yeung J, Esposito MT, Gandillet A, Zeisig BB, Griessinger E, Bonnet D, et al. beta-Catenin mediates the establishment and drug resistance of MLL leukemic stem cells. *Cancer cell*. 2010;18(6):606-18.

You Z, Saims D, Chen S, Zhang Z, Guttridge DC, Guan KL, et al. Wnt signaling promotes oncogenic transformation by inhibiting c-Myc-induced apoptosis. *The Journal of cell biology*. 2002;157(3):429-40.

Yu H, Lee H, Herrmann A, Buettner R, Jove R. Revisiting STAT3 signalling in cancer: new and unexpected biological functions. *Nature reviews Cancer*. 2014;14(11):736-46.

Yu H, Yue X, Zhao Y, Li X, Wu L, Zhang C, et al. LIF negatively regulates tumour-suppressor p53 through Stat3/ID1/MDM2 in colorectal cancers. *Nature communications*. 2014;5:5218.

Yuan C, Qi J, Zhao X, Gao C. Smurf1 protein negatively regulates interferon-gamma signaling through promoting STAT1 protein ubiquitination and degradation. *The Journal of biological chemistry*. 2012;287(21):17006-15.

Yun Z, Lin Q. Hypoxia and regulation of cancer cell stemness. *Advances in experimental medicine and biology*. 2014;772:41-53.

Zamo A, Chiarle R, Piva R, Howes J, Fan Y, Chilosì M, et al. Anaplastic lymphoma kinase (ALK) activates Stat3 and protects hematopoietic cells from cell death. *Oncogene*. 2002;21(7):1038-47.

Zdzalik D, Dymek B, Grygielewicz P, Gunerka P, Bujak A, Lamparska-Przybysz M, et al. Activating mutations in ALK kinase domain confer resistance to structurally unrelated ALK inhibitors in NPM-ALK-positive anaplastic large-cell lymphoma. *Journal of cancer research and clinical oncology*. 2014;140(4):589-98.

Zetter BR, Mangold U. Ubiquitin-independent degradation and its implication in cancer. *Future oncology*. 2005;1(5):567-70.

Zhang HF, Wu C, Alshareef A, Gupta N, Zhao Q, Xu XE, et al. The PI3K/AKT/c-MYC Axis Promotes the Acquisition of Cancer Stem-Like Features in Esophageal Squamous Cell Carcinoma. *Stem cells*. 2016;34(8):2040-51.

Zhang J, Gill AJ, Issacs JD, Atmore B, Johns A, Delbridge LW, et al. The Wnt/beta-catenin pathway drives increased cyclin D1 levels in lymph node metastasis in papillary thyroid cancer. *Human pathology*. 2012;43(7):1044-50.

Zhang L, Jope RS. Oxidative stress differentially modulates phosphorylation of ERK, p38 and CREB induced by NGF or EGF in PC12 cells. *Neurobiol Aging*. 1999;20(3):271-8.

Zhang Q, Raghunath PN, Xue L, Majewski M, Carpentieri DF, Odum N, et al. Multilevel dysregulation of STAT3 activation in anaplastic lymphoma kinase-positive T/null-cell lymphoma. *J Immunol*. 2002;168(1):466-74.

Zhang Q, Wang HY, Liu X, Wasik MA. STAT5A is epigenetically silenced by the

tyrosine kinase NPM1-ALK and acts as a tumor suppressor by reciprocally inhibiting NPM1-ALK expression. *Nature medicine*. 2007;13(11):1341-8.

Zhang Q, Wang HY, Marzec M, Raghunath PN, Nagasawa T, Wasik MA. STAT3- and DNA methyltransferase 1-mediated epigenetic silencing of SHP-1 tyrosine phosphatase tumor suppressor gene in malignant T lymphocytes. *Proceedings of the National Academy of Sciences of the United States of America*. 2005;102(19):6948-53.

Zhang Q, Wang HY, Woetmann A, Raghunath PN, Odum N, Wasik MA. STAT3 induces transcription of the DNA methyltransferase 1 gene (DNMT1) in malignant T lymphocytes. *Blood*. 2006;108(3):1058-64.

Zhang Q, Wei F, Wang HY, Liu X, Roy D, Xiong QB, et al. The potent oncogene NPM-ALK mediates malignant transformation of normal human CD4(+) T lymphocytes. *The American journal of pathology*. 2013;183(6):1971-80.

Zhang S, Cui W. Sox2, a key factor in the regulation of pluripotency and neural differentiation. *World journal of stem cells*. 2014;6(3):305-11.

Zhang S, Li Y, Wu Y, Shi K, Bing L, Hao J. Wnt/beta-catenin signaling pathway upregulates c-Myc expression to promote cell proliferation of P19 teratocarcinoma cells. *Anatomical record*. 2012;295(12):2104-13.

Zhang Y, Chen HX, Zhou SY, Wang SX, Zheng K, Xu DD, et al. Sp1 and c-Myc modulate drug resistance of leukemia stem cells by regulating survivin



expression through the ERK-MSK MAPK signaling pathway. *Molecular cancer*. 2015;14:56.

Zhang Y, Chen HX, Zhou SY, Wang SX, Zheng K, Xu DD, et al. Sp1 and c-Myc modulate drug resistance of leukemia stem cells by regulating survivin expression through the ERK-MSK MAPK signaling pathway. *Molecular cancer*. 2015;14:56.

Zhang Y, Molavi O, Su M, Lai R. The clinical and biological significance of STAT1 in esophageal squamous cell carcinoma. *BMC cancer*. 2014;14:791.

Zhang Y, Zhang Y, Yun H, Lai R, Su M. Correlation of STAT1 with apoptosis and cell-cycle markers in esophageal squamous cell carcinoma. *PloS one*. 2014;9(12):e113928.

Zhao C, Blum J, Chen A, Kwon HY, Jung SH, Cook JM, et al. Loss of beta-catenin impairs the renewal of normal and CML stem cells in vivo. *Cancer cell*. 2007;12(6):528-41.

Zhao D, Pan C, Sun J, Gilbert C, Drews-Elger K, Azzam DJ, et al. VEGF drives cancer-initiating stem cells through VEGFR-2/Stat3 signaling to upregulate Myc and Sox2. *Oncogene*. 2015;34(24):3107-19.

Zhao JS, Li WJ, Ge D, Zhang PJ, Li JJ, Lu CL, et al. Tumor initiating cells in esophageal squamous cell carcinomas express high levels of CD44. *PloS one*. 2011;6(6):e21419.

Zhao R, Daley GQ. From fibroblasts to iPS cells: induced pluripotency by defined factors. *Journal of cellular biochemistry*. 2008;105(4):949-55.

Zhou M, Hou Y, Yang G, Zhang H, Tu G, Du YE, et al. LncRNA-Hh Strengthen Cancer Stem Cells Generation in Twist-Positive Breast Cancer via Activation of Hedgehog Signaling Pathway. *Stem cells*. 2016;34(1):55-66.

Zhu J, Blenis J, Yuan J. Activation of PI3K/Akt and MAPK pathways regulates Myc-mediated transcription by phosphorylating and promoting the degradation of Mad1. *Proceedings of the National Academy of Sciences of the United States of America*. 2008;105(18):6584-9.

Zmijewski JW, Banerjee S, Bae H, Friggeri A, Lazarowski ER, Abraham E. Exposure to hydrogen peroxide induces oxidation and activation of AMP-activated protein kinase. *The Journal of biological chemistry*. 2010;285(43):33154-64.